Polysaccharide Materials and Sorption Studies of Chloroform and Total Trihalomethanes (TTHMs) in Aqueous Solution

A Thesis Submitted to the College of

Graduate Studies and Research

In Partial Fulfillment of the Requirements

For the Degree of Doctor of Philosophy

In the Department of Chemistry

University of Saskatchewan

Saskatoon

By

Rui Guo

Permission to Use

In presenting this thesis in partial fulfilment of the requirements for a Postgraduate degree from the University of Saskatchewan, I agree that the Libraries of this University may make it freely available for inspection. I further agree that permission for copying of this thesis in any manner, in whole or in part, for scholarly purposes may be granted by the professor or professors who supervised my thesis work or, in their absence, by the Head of the Department or the Dean of the College in which my thesis work was done. It is understood that any copying or publication or use of this thesis or parts thereof for financial gain shall not be allowed without my written permission. It is also understood that due recognition shall be given to me and to the University of Saskatchewan in any scholarly use which may be made of any material in my thesis.

Requests for permission to copy or to make other use of material in this thesis in whole or part should be addressed to:

Head of the Department of Chemistry

University of Saskatchewan

Saskatoon, Saskatchewan (S7N 5C9)

Canada

Acknowledgements

First of all, I would like to sincerely thank my supervisors, Dr. Lee D. Wilson and Dr. Lalita Bharadwaj, for all the support, mentorship, and encouragement they provided to me. In Year 2006, Dr. Lee D. Wilson accepted me as a member in his research group. Since then, he has supervised my research, guided my attitude on chemistry, and treated me like family.

I am grateful to the members of Research Committee, Dr. Richard Bowles, Dr. Steve Reid, Dr. Oon-Doo Baik, and external examiner for their valuable advices on my research work.

I would like to express my appreciation to the staff from the Saskatchewan Structural Sciences Center (SSSC), especially Mr. Ken Thoms who fixed my GC machine and helped me with IR, elemental analysis, and MS measurements, Dr. Keith Brown who coached me on NMR analysis, and Mr. Jason Maley for Raman spectroscopy.

Also, I would like to thank my previous and current group members; Mohamed Hamid Mohamed, Jae Hyuck Kwon, Dawn Pratt, Abdulla Karoyo, Louis Poon, Chen Xue, Shaguftah Younus, and Leila Dehabadi for sharing knowledge and their kind help in the lab.

I wish to acknowledge the Natural Sciences and Engineering Research Council of Canada (NSERC), the Canada Foundation for Innovation (CFI), and the University of Saskatchewan for the support of this research. I gratefully acknowledge NSERC for a Ph.D. scholarship through the NSERC CREATE-HERA program.

Finally, I would pass my deepest thanks to my loving families; my parents, my wonderful husband, and my lovely daughter for their endless love and support.

Dedication

This thesis is dedicated to my parents; Lianqiang Guo (Dad) and Fenglan Bai (Mom), my husband Zhao Zhao and my daughter Jocelyn Zhao. Thank you all for your priceless love and support and I am so lucky to have you!

ABSTRACT

In this research, a series of synthetically engineered copolymers were synthesized containing polysaccharides (*e.g.*, β-cyclodextrin and chitosan) to address the removal of trihalomethanes (THMs) from water environments. There are two main parts in this research thesis: i) the preparation and characterization of polysaccharide-based copolymers; ii) sorption studies of the copolymers with chloroform and total THMs (TTHMs) in aqueous solution.

In the first part of this thesis, grafted polyester, polyester and grafted polyamide copolymers were prepared by cross-linking β-cyclodextrin (β-CD) and chitosan (CS) with various cross-linkers, including poly (acrylic acid) (PAA), terephthaloyl (TCl), and sebacoyl chloride (SCl), respectively. The synthesized copolymer materials were characterized by Diffuse Reflectance Infrared Fourier Transform Spectroscopy (DRIFTS), Scanning Electron Microscopy (SEM), Thermogravimetric analysis (TGA), Differential scanning calorimetry (DSC), elemental (C and H) analyses, and NMR spectroscopy. Nitrogen porosimetry was used to analyze the surface area and pore structure characteristics of the copolymers and starting materials in solid state. The sorption properties of the copolymers in aqueous solution were studied using different dye probes (*e.g.*, *p*-nitrophenol and methylene blue) by UV–Vis spectrophotometry. The copolymers showed markedly varied interactions with dye probes in accordance with their composition, surface area, and pore structure characteristics. Diverse materials were afforded by variation of the synthetic conditions. The sorption isotherms were evaluated with various isotherm models (*e.g.*, Langmuir, BET, Freundlich and Sips). The Sips isotherm showed the best overall agreement with the experimental results and the sorption parameters provided estimates of the sorbent surface area

and the sorption capacity for various copolymers in aqueous solution. The copolymer sorbents display tunable physicochemical properties according to the synthetic conditions.

In the second part of this thesis, the direct aqueous injection (DAI) method with gas chromatography (GC) with electron capture or electrolytic conductivity detectors (ECD) enabled quantitative detection of chloroform and TTHMs in water. A preliminary adsorption study and kinetic study of chloroform provided the information to establish the experimental protocol for the sorption study. The sorption parameters were evaluated using the Sips model. The sorption capacity (Q_m) values of chloroform for these synthetically engineered copolymers at similar conditions ranged from 0.00335-1.70 mmol/g. The relative ordering of the Q_m values was observed: β-CD/PAA 1:5 > SCl-5 > SCl-10 ~ CP-1 > β-CD/PAA 1:10 > CP-5 > AC > β-CD/PAA 1:5 at high mixing speed. An extension of the sorption study for copolymers toward the multi-component THMs in water was carried out. The copolymers showed distinct adsorption capacities to THMs: chloroform (0.0485-0.287 mmol/g); DBCM (0.0712-0.277 mmol/g); BDCM (0.0684-0.387mmol/g); and bromoform (0.0522-1.07 mmol/g). The copolymers exhibited relatively high selectivity toward individual components of THMs due to their variable molecular size and polarizability. The copolymers showed favorable adsorption (*e.g.*, β-CD/PAA 1:5, CP-1) and each type of polysaccharide (*e.g.*, β-CD and CS) copolymers displays great potential for the removal of halomethane-based contaminants.

TABLE OF CONTENTS

LIST OF SCHEMES

LIST OF FIGURES

LIST OF TABLES

LIST OF ABBREVIATIONS

Ar…….……Argon

BDCM……..…Bromodichloromethane

BET…….……....Brunauer, Emmett, and Teller

BJH……Barret-Joyner-Halenda

CAS……Chemical Abstract Service

CD…….……Cyclodextrin

$CDCl_3$…….……Deuterated chloroform

CP-X…….....CS: PAA copolymers (X=1, 5 represents mole ratio between CS: PAA at 1:1, 1:5)

CS…….……Chitosan

DBCM……...……...Dibromochloromethane

DMSO-d6……..Perdeuterated dimethyl sulfoxide

D_2O…….Deuterium oxide

DAI…….Direct aqueous injection

DRIFTS……...Diffuse Reflectance Infrared Fourier Transform spectroscopy

DSC……..Differential scanning calorimetry

EA……Elemental analysis

GC-ECD.....Gas chromatography with electron capture or electrolytic conductivity detectors

IR……...Infrared

LLE……..……Liquid-liquid extraction

IUPAC…….International Union of Pure and Applied Chemistry

MAC……...Maximum Acceptable Concentration

M_W……..……...Molecular weight

MB……....Methylene blue

N/A……Data not available

NLLS……...Non-linear least squares

NMR…….Nuclear magnetic resonance

PAA……..poly (acrylic acid)

PNP…….Para-nitrophenol

P&T……Purge and trap capillary column

SA……..Surface area

SAPs…….Super adsorbent polymers

SCl…….Sebacoyl chloride

SCl-X……...….β-CD: SCl copolymers (X=1, 5, 10 represents mole ratio between β-CD: SCl at 1:1, 1:5, 1:10)

SEM……...Scanning electron microscopy

SSR……Sum of squares of residuals

TCl:……Terephthaloyl chloride

TCl-X……...…β-CD: TCl copolymers (X=1, 5, 10 represents mole ratio between β-CD: TCl at 1:1, 1:5, 1:10)

TGA……..Thermogravimetric analysis

THMs……..Trihalomethanes

TTHMs……Total trihalomethanes

UV-Vis.....Ultra violet-Visible

U.S. EPA.....U. S. Environmental Protection Agency

VOCs.....Volatile organic compounds

WHO.....World Health Organization

W/W…….Weight per weight

w/o……water in oil emulsion

UNITS

mg……...milligram

MHz……..Megahertz

mM.....millimolar

mm.....millimeter

nm…….nanometer

ppm…….....parts per million

ppb……parts per billion

µm.....micrometer

t.....ton

CHAPTER 1

1. Introduction

1.1. Chloroform and Total Trihalomethanes (TTHMs)

1.1.1. Introduction

Trihalomethanes (THMs) are halogen-substituted carbon compounds with a general molecular formula CHX_3, where X represents fluorine, chlorine, bromine or iodine. The most commonly found THMs in drinking water (*cf.* Scheme 1.1a) are chloroform, bromodichloromethane (BDCM), dibromochloromethane (DBCM) and bromoform, which are hereafter referred as total THMs (TTHMs).

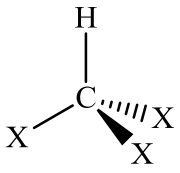

X represents either Cl, Br, or both
-Chloroform: $CHCl_3$
-Bromodichloromethane: $CHCl_2Br$
-Dibromochloromethane: $CHClBr_2$
-Bromoform: $CHBr_3$

a)

$$Cl_2 + H_2O \rightleftharpoons HOCl + HCl$$

(Hypochlorous acid)

b)

Scheme 1.1. a). Molecular structure of THMs, where X represents a halogen atom and b) the chemical reaction for water chlorination.

Chloroform is one of the most commonly occurring THMs in water. The use of chloroform was first reported in 1831 by the French chemist Eugene Soubeiran, where he prepared chloroform from acetone (2-propanone) and ethanol through the chlorination with leach powder (calcium hypochlorite)[1]. At similar time, other two scientists, Samuel Guthrie and Juetus von Liebig, also successfully and independently prepared the same compound[2]. Chloroform was

identified and chemically characterized by Jean-Baptiste Dumas[3]. The worldwide commercial production of chloroform reached about 440,000 t in 1987 and domestic production in the United States amounted to approximately 229,000 t in 1991[4] and 216,000 t in 1993[5]. Chloroform is generally used as a precursor of the chlorodifluoromethane; however, the usage of chlorodifulromethane as a refrigerant was eventually phased out under the *Montreal Protocol on Substances that Deplete the Ozone Layer*[6]. Chloroform is a common solvent in the laboratory because of its limited chemical reactivity, miscibility with most organic liquids, and relatively high volatility. Chloroform is widely applied in the pharmaceutical industry, rubber industry, and pesticide manufacturing. Chloroform has been used primarily in the production of chlorodifluoromethane as a cleaning agent and in fumigants[7]. Clinically, chloroform has been used as an analgesic, muscle relaxant, carminative, flavouring agent, preservative, bactericide, heat-transfer medium and as a counter-irritant in linaments[4]. However, its use as an anaesthetic and in proprietary medicines was quickly abandoned upon discovery of its toxicity, especially its tendency to cause fatal cardiac arrhythmia, analogous to what is now termed "sudden sniffer's death"[8].

Brominated THMs are also synthetically produced for various industrial and chemical purposes, such as laboratory reagents or as chemical intermediates for the synthesis of organic compounds, and fluids for mineral ore separation. Brominated THMs can be used as solvents for fats, waxes, resins, and flame retardant materials. Bromoform has also been used as a sedative and cough suppressant[9]. As a result, although large part of THMs is formed naturally in the environment, anthropogenic emission is also not negligible[10].

THMs result as disinfection by-products (DBPs) from drinking water chlorination. Chlorine disinfection of drinking water has been known as one the major public health achievements of the 20th century and chlorine remains the most widely used chemicals for water disinfection in North America[11]. Disinfection reduces the levels of microbes in the water supply; however, the formation of THMs increases due to the disinfection process[11] (*cf.* Scheme 1.1b). During water chlorination, gaseous chlorine (Cl_2) or liquid sodium hypochlorite (NaOCl) reagents react with water to form hypochlorous acid (*cf.* Scheme 1.1b). Hypobromous acid also forms when there is bromine present in water. Both hypochlorous and hypobromous acid are strong oxidizing agents and react with a wide variety of compounds in water as disinfectants. THMs are also formed by the reaction of hypochlorous and hypobromous acid with organic matter[12], for example, humic

acids which are the organic portion of soil formed by the decay of leaves, wood, and other plant materials are known to react with hypochlorous and hypobromous acids. The level of chloroform and brominated THMs are generally higher in chlorinated water originating from surface water compared to ground water supplies due to the higher organic content of the former[13]. Among other factors, the levels of THMs in drinking water depend upon the specific reaction conditions, such as, chlorine dosage, contact time, pH, bromide ion concentration, and organic precursor concentration in source water supplies.

Table 1.1. Physical and Chemical Properties of THMs.

Properties	**Water solubility (g/L)**	**Vapor pressure (kPa)**	**Boiling point (℃)**	**Molecular weight (g/mol)**	**Molar volume (mL/mol)**	**K_H^***
Chloroform ($CHCl_3$)	7.50-9.30 (25 ℃)	21.3 (20 ℃)	61.3	119.4	80.5	0.0367 (24 ℃)
BDCM ($CHBrCl_2$)	3.32 (30 ℃)	6.67 (20 ℃)	90.0	163.8	82.7	0.00212
DBCM ($CHBr_2Cl$)	1.05 (30 ℃)	2.00 (30 ℃)	119	208.3	85.0	0.000783 (20 ℃)
Bromoform ($CHBr_3$)	3.19 (30 ℃)	2.90 (30 ℃)	150	252.7	89.0	0.000535

[a] Henry's law constant at 25 ℃, atm•m^3/mol^6.

1.1.2. Physical and Chemical Properties of THMs

THMs are volatile organic compounds (VOCs) and some of their relevant physical and chemical properties are listed in Table 1.1. Chloroform is air- and light-sensitive, and may transform into phosgene and hydrochloric acid under photochemical conditions. It has a

characteristic odour and a burning, sweet smell. The odour threshold values of chloroform are 2.4 ppm in water and 420 mg/m^3 in air[7]. The odour threshold for bromoform in water is 0.3 ppm[7]. Chloroform evaporates quickly when exposed to air and dissolves quickly in water. Both chloroform and brominated THMs remain in air and water for long periods and can partition into groundwater through soil[9]. Hydrolysis of brominated THMs in aqueous media is very slow; where the estimated half-lives of BDCM, DBCM, and bromoform are 1000, 274, and 686 years, respectively[9, 14].

1.1.3. Environmental Levels and Human Exposure

THMs exist in all kinds of environmental media, such as air[10], water, soil[15], *etc*. In this research, the THMs in contaminated water will be of greatest concern. In coastal waters, inland rivers, lakes and groundwater, the concentrations of THMs range from several ng/L in rural and remote areas up to 100 μg/L (ppb) or more in areas directly affected by industrial sources. The concentration of chloroform in ocean environments in remote regions is typically at nanogram per litre levels. In drinking-water treated by chlorination, the concentrations are typically 10–100 ppb worldwide[8]. Based on the data received from eight provinces in Canada in 2003, the mean THM level was ~ 66 ppb in drinking water system[13]. Some systems had average values in the 400 ppb range, and some systems had maximum values in the 800 ppb range[13], which exceed the regulatory values according to Guidelines for Canadian Drinking Water Quality.

The general population can be exposed to THMs by ingesting water and food, inhaling contaminated air, and possibly through dermal contact with chlorinated water. Small amounts of chloroform[13] ranging from 1.4-3,000 μg/kg have been found in food, soft drinks, olive oil, pork, sausage, and flour products. According to estimates of mean exposure from various media, the general population is exposed to THMs principally in food, drinking water, and indoor air environments in approximately equivalent amounts[9]. Water contaminated with THMs is the major concern in this research. Except direct ingestion, the exposure to THMs, especially chloroform and BDCM, through inhalation and dermal absorption from tap water during showering and bathing is also very important. The use of swimming pools and hot tubs also can result in inhalation and dermal exposure to THMs due to the high levels of organic matter presenting in the disinfected water. The uptake of THMs from contaminated water through various pathways is a potential concern for public health.

1.1.4. Health Effect of THMs and Regulatory Limits of THMs

The negative effects of THMs have not yet been fully elucidated. Studies of human populations have indicated a slightly greater incidence of bladder and colon cancers in areas where chlorinated drinking water is consumed[11, 16]. A population-based case control analysis using Iowa birth certificate data (Jan 1, 1989-Jun 30, 1990) showed an association of waterborne chloroform in drinking water supplies with low birth weight, prematurity, and intrauterine growth retardation[17]. Possible relationships between oral exposure to various THMs and fetotoxicity[18, 19] and sperm abnormalities[20] were found in animal studies. There is some "clear evidence" of carcinogenic activity observed in both of acute and chronic animal studies using mice and rats with oral dosage of brominated THMs[9,21]. Deaths caused by central nervous system depression[9] resulting from accidental overdose (typical dose ~ 180 mg, 3-6 times per day) of orally administered bromoform were reported.

Various guideline values of THMs are regulated differently in various countries. For example, the *maximum acceptable concentration* (MAC) for THMs in drinking water by Health Canada is 100 ppb based on a locational running annual average of a minimum of quarterly samples taken at the point in the distribution system with the highest potential THM levels. The U. S. Environmental Protection Agency (EPA) has published the *Stage 1 Disinfectants-Disinfection By-products Rule* to regulate total THMs at a maximum allowable annual average level of 80 ppb and 40 ppb in Stage 2, respectively[22]. The commission of the European Communities proposed a council directive with parameter values of 40 and 15 ppb for chloroform and BDCM, respectively. The recommended value by the World Health Organization (WHO) for chloroform is 30 ppb.

As result, THMs are a global public health issue due to their wide usage and potential carcinogenic threats in the environment. The removal of THMs, especially at the contaminated sites is an important risk management strategy in addressing these environmental and public health concerns.

1.2. Adsorption

1.2.1. A Methodology for Contaminant Removal

Adsorption-based water filters have been employed as a method of water purification with a long history since ancient times from the simple Hippocratic sleeve in ancient Greece[23] to the

complicated solid block carbon and composite multimedia filter devices currently available in the global marketplace. There are three main water purification methods for the removal of chlorine, chlorine by-products, and other VOCs from drinking water: filtration, reverse osmosis and distillation. In contrast with reverse osmosis and distillation techniques, adsorption-based filtration is not strictly limited by the type or size of contaminants which can be removed[23]. Water filters may also selectively retain essential trace minerals in drinking water by chemical uptake through the adsorption process[23]. Costly and energy intensive processes such as reverse osmosis and distillation have cost disadvantages relative to less expensive adsorption processes. Common adsorbents such as activated carbon, inorganic molecular sieves, and polymeric materials represent several types of cost-efficient adsorbents.

1.2.2. Adsorption Processes

Sorption occurs when a gas or liquid molecule (sorbate) interacts with an evacuated or dry solid (sorbent), where the molecules may partition into the solid sorbent (*i.e.* absorption), or bind onto the sorbent surface (*i.e.* adsorption)[24a], as shown in Scheme 1.2. However, when gas sorbates penetrate into a solid material, it might either dissolve in the solid phase or undergo chemical transformation[24]. Adsorption, on the other hand, is a procedure based on the physical adherence or noncovalent interaction of ions and molecules onto the sorbent surface. Adsorption is the most common form of sorption used in contaminant removal, and the process will be the primary focus of this thesis research. In adsorption processes, the substance which adsorbs and accumulates onto its surface is termed the adsorbent and those species which are adsorbed are denoted as adsorbates. Based on the nature of adsorbents and adsorbates and types of interactions, the sorption process is generally classified as physisorption (characteristic of noncovalent interactions: hydrogen bonding, hydrophobic forces, van der Waals forces, π-π interactions, and electrostatic effects) or chemisorption (characteristic of covalent bonding such as metal-ligand coordination). The "seat" of the sorption site where the adsorbent and adsorbate contact each other is the surface of adsorbent[24a]. Sorption is a consequence of a reduction in surface energy so surface effects contribute to an understanding of such processes. Adsorbents are sometimes porous in nature with a large internal surface[24a], especially for nano-, meso-, and micro-porous materials. These materials possess a large *surface-to-volume* ratio and are very attractive in pharmaceutical applications, environmental remediation of aquatic environments.

Compared to the equivalent forces inside the body of the adsorbent solid, the surface atoms between two different phases (*e.g.*, liquid/solid) represent unbalanced forces, where the inward pull is greater than outward forces[24a]. To consider the thermodynamics of adsorption at the gas/solid interface, the gas was assumed to be ideal and with no intermolecular interactions[24] (refer to §1.3.4.5). As long as the pressure is not too high, nor the temperature is not too low, all gases adopt ideal behaviour[24b]. Liquid interfaces are inherently more complex than the gas/solid interface because the intermolecular interactions are no longer negligible for the liquid/solid interface. The Gibbs model is used to describe the interface of an infinitesimally thin plane between two phases[24b]. The surface excess ($\Gamma_j=n_j/A$) can be used to define the quantity of molecules in terms of moles per unit area at the ideal Gibbs interface.

A Gibbs isotherm for solid surface is described by eqn (1.1), which illustrates the relationship between the Gibbs surface and chemical potential of adsorbates[24].

$$d\gamma = -\Gamma_1 d\mu_1 - \Gamma_2 d\mu_2 \quad (1.1)$$

Hence, adsorption process tends to occur spontaneously and result in an overall decrease of the total Gibbs surface energy of the system[24]. The change in Gibbs surface energy, $\Delta G°=\gamma dA$, will increase as the surface area (dA) increases at constant temperature and pressure. Another relation, $\Delta G°=-RT\ \ln K$, shows that the adsorption energy is related to the binding affinity at equilibrium. K describes the relative binding affinity between the adsorbent and adsorbate (where R is the gas constant and T is temperature) at equilibrium conditions. Therefore, the physicochemical properties of adsorbent and adsorbate and the type of intermolecular interactions involved in the adsorption process are important in determining the overall Gibbs energy of the system.

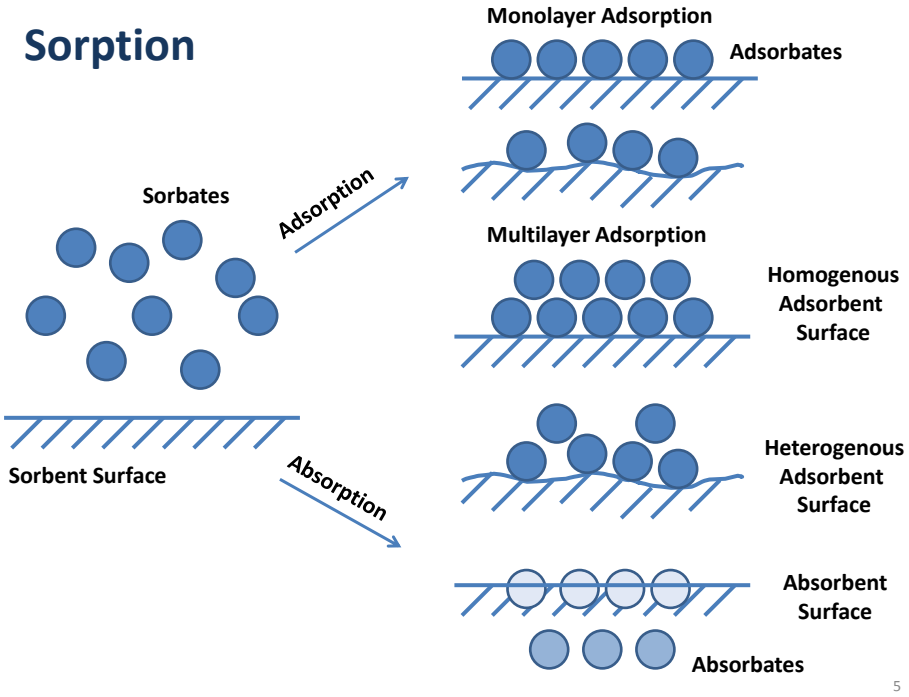

Scheme 1.2. General illustration of adsorption and absorption processes.

1.2.3. Surface Heterogeneity

According to Zettlemoyer, there are three major surface heterogeneities: physical, chemical, and induced heterogeneity[25]. Physical heterogeneities are attributed to geometrical differences in the characteristics of the surface, such as, textural properties (*e.g.*, surface area and pore structure properties), lattice imperfections, intercrystalline sites, *etc.* Chemical heterogeneities are related to different surface functional groups including impurities on the surface. Induced heterogeneities are caused by the induced energy of the first molecule after adsorption on the surface, which may cause a corresponding effect on the energy for the subsequent layer of adsorbed molecules. The interaction energy between adsorbent and adsorbate generally decreases as surface coverage (θ) increases for the process of chemisorption; however, the Gibbs energy increases as the degree of surface coverage increases for physisorption processes.

Understanding the accessible molecular surface sites (*i.e.* 1-θ) available to the adsorbates makes the study of textural properties (*i.e.* pore size and surface area) essential. According to the International Union of Pure and Applied Chemistry (IUPAC) standards, the average size of pore

diameters is classified as follows: micropores (less than 2 nm); mesopores (between 2 nm and 50 nm); macropores, size (more than 50 nm). There are numerous methods for evaluating pore textural properties (*i.e*. pore volume and size distribution) and surface area, such as microscopy, immersion calorimetry, small angle X-ray and neutron scattering, wide angle scattering, microscopy (*i.e.* TEM, SEM and STM), and mercury intrusion porosimetry[26]. These methods provide textural and physicochemical characterization of solid adsorbents by physical techniques[26]. In addition, the functional groups on the surface of adsorbents affect the physicochemical properties of materials. Thus, physical adsorption techniques are not sufficient for describing the surface and sorption properties of an adsorbent. Therefore, sorption studies of solid-gas and solid-solution isotherms are important for adequate sorbent characterization.

1.2.4. Adsorption Studies

Adsorption studies are widely used to evaluate the surface area and pore characteristics of materials using either liquid or gas probes. The process of adsorption process is represented by the following equilibrium:

$$A\ (l\ or\ g) + B\ (s) \rightleftharpoons A{\cdot}B\ (s)$$

Where A represents the adsorbate and B represents the adsorbent. The A·B complex in the equation represents the combination of the adsorbate and adsorbent. The adsorption process is reversible in the case of physisorption. Equilibrium is achieved when the rate of the forward process (adsorption) equals to the rate of the reverse process (desorption) and no further net accumulation of adsorbate onto the surface of adsorbent occurs. An understanding of the adsorption process is possible based on experimental isotherm adsorption studies.

The adsorption isotherms (solution phase will be focused in this section; gas phase refers to §1.3.4.5) are depicted as plots of the adsorbed amount of adsorbate per mass of adsorbent (Q_e; mmol/g) versus the equilibrium residual concentration of unbound adsorbate in aqueous solution (C_e). The value of Q_e is defined in eqn. (1.2) where C_o is the initial concentration of adsorbate, V is the volume of solution, and m is the mass of sorbent, as described previously.

$$Q_e = \frac{(C_0 - C_e) \times V}{m} \qquad (1.2)$$

The sorption method[27] also provides an independent estimate of the sorbent surface area (SA; m^2/g) according to eqn. (1.3).

$$SA = \frac{A_m Q_m L}{Y} \qquad (1.3)$$

where A_m represents the cross-sectional area occupied by adsorbate, Q_m is the monolayer adsorption capacity per unit mass of sorbent, L is Avogadro's number (mol^{-1}), and Y is the coverage factor which depends on the nature of the adsorbate[28].

The Freundlich, Langmuir, BET, and Sips models were used to analyze the sorption data[29-32]. The Langmuir model represents a monolayer sorption process (*cf.* Scheme 1.2) onto a homogenous surface, and the BET model describes multi-layer adsorption processes (*cf.* Scheme 1.2). The Freundlich model assumes that the sorbent surface is heterogeneous in nature (*cf.* Scheme 1.2) with an exponential distribution of active sites when an unlimited number of sorption sites are available. The Sips isotherm is a generalized isotherm model which accounts for a distribution of adsorption energies on the sorbent surface and accounts for monolayer (Langmuir) to multi-layer (Freundlich) isotherms. The Langmuir, BET, Freundlich and Sips models are respectively defined by eqns. (1.4-1.7) [29- 32].

$$Q_e = \frac{K_L Q_m C_e}{1 + K_L C_e} \qquad (1.4)$$

$$Q_e = \frac{K_{BET} Q_m C_e}{\left(1 - \frac{C_e}{C_s}\right)\left[1 + \left(K_{BET} - 1\right)\frac{C_e}{C_s}\right]} \qquad (1.5)$$

$$Q_e = K_F C_e^{\frac{1}{n}} \qquad (1.6)$$

$$Q_e = \frac{Q_m \left(K_s C_e\right)^{n_s}}{1 + \left(K_s C_s\right)^{n_s}} \qquad (1.7)$$

where K_F, K_L, K_{BET}, and K_s are the equilibrium Freundlich, Langmuir, BET, and Sips constants. C_s is the saturated aqueous solution solubility of the adsorbate, and Q_m is defined by eqn. (1.3). 1/n is the inverse of the Freundlich exponent and is a measure of the adsorption intensity.

The Freundlich model assumes there are excess available sites acting simultaneously with different Gibbs energies of sorption[29]. The model usually applies at relatively low pressure or dilute concentration. The value of 1/n is generally less than unity because sites with greater

binding energy will be occupied first and followed by more weakly bound sorption sites. Adsorptive interaction will be stronger than that for specific adsorbates with smaller values of 1/n. When 1/n is unity, the isotherm is linear and a constant Gibbs energy of sorption can be assumed for all adsorbate concentrations.

The Langmuir isotherm is a more appropriate model when there are a limited number of sorption sites with similar energies. Q_m describes the adsorption capacity of the particular sorbent and varies for each sorbent material based on the relative surface area and affinity to the adsorbate molecule. K_L is related to the binding energy of adsorption. There are several important assumptions made from the dynamic concept of adsorption equilibrium in which the rates of adsorption and desorption are equal[31]: 1) only one molecule per site can be adsorbed onto the free surface sites of adsorbent (1-θ) and saturation is reached on completion of the monolayer (θ=1); 2) the surface of a solid is composed of a two-dimensional array of energetically equivalent sites; 3) the forces (repulsive or attractive) between the adsorbed molecules are negligible in comparison to adsorbent-adsorbate interactions.

The BET theory provides an extension of the Langmuir monolayer model by using similar assumptions to represent multilayer adsorption. The first adsorbed layer is similar to that of the Langmuir model and each subsequent adsorbed molecule is assumed to be an adsorption site for second layer molecules, and occurs in a continuous multi-layer fashion as the adsorbate concentration increases.

The Sips isotherm is a relatively versatile model with several adjustable parameters where the n_s term reflects the heterogeneity of the sorbent. A unitary value of n_s infers a homogenous surface whereas a heterogeneous surface is inferred when $n_s \neq 1$. Langmuir isotherm behavior is predicted when $n_s=1$ while Freundlich behavior is predicted when $(K_s C_e)^{n_s} <<< 1$.

1.2.5. Types of Sorption Isotherms

There are several types of isotherms depending on the nature of the adsorbent/adsorbate system and the intermolecular interactions involved, as described by Brunauer et al.[33] The Brunauer, Deming, Deming and Teller (BDDT) classification has become the basis of the modern IUPAC classification system for adsorption isotherms (Fig. 1.1). Generally, there are six types of adsorption isotherms[34]: *Type I*: represents microporous adsorbent (monolayer adsorption only) with relatively small external surfaces. *Type II*: describes adsorption on non-porous or

macroporous adsorbent with strong adsorbate-adsorbent interactions (unrestricted from monolayer to multilayer adsorption). *Type III*: describes adsorption on non-porous or macroporous adsorbent with weak adsorbate/adsorbent interactions. *Types IV* and *V* are similar to *types II* and *III*, but refer to porous adsorbents. *Type VI* isotherms represent non-porous adsorbents with a homogeneous surface. The complete accumulation on a monolayer is fulfilled before adsorption onto a subsequent layer corresponding to the multilayer format.

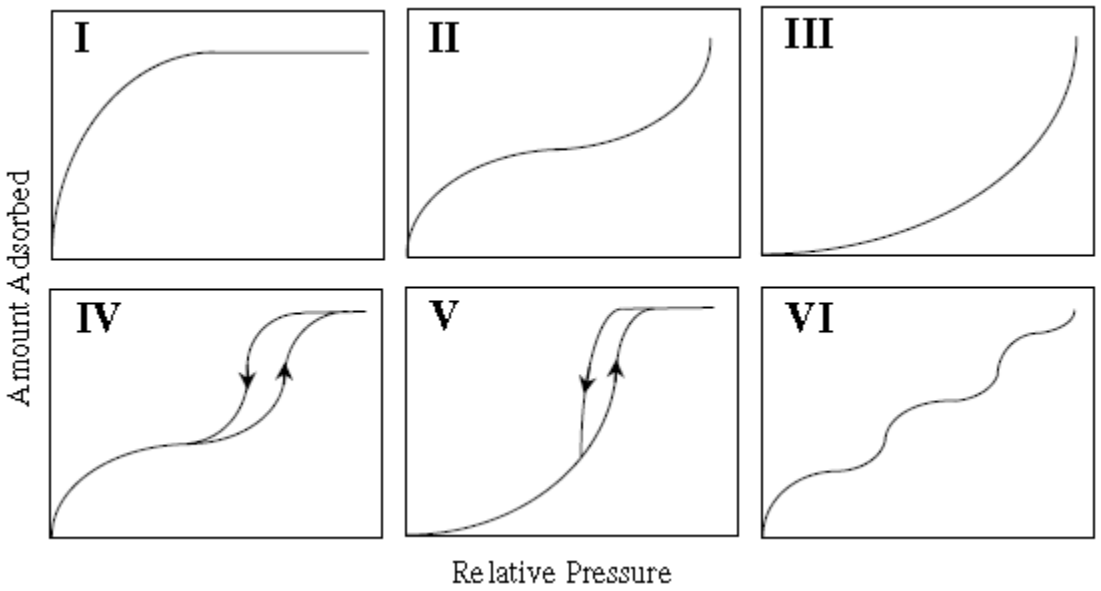

Figure 1.1. The IUPAC classification for adsorption isotherms (*Types I–VI*) with the x-axis representing the relative pressure of the fluid and the y-axis denoting amount of gas adsorbed[35]. (Figure was adapted with permission from Carmody, O.; Frost, R.; Xi, Y.; Kokot, S. *Surf. Sci.* **2007**, *601*, 2066-2076. Copyright 2007© Elsevier.)

1.2.6. Adsorption Kinetics

For further understanding of adsorption processes and their viability, kinetic studies can provide more detailed information about their temporal relationships and molecular mechanisms in addition to the overall adsorption capacity. The adsorption rate which determines the equilibrium time required for completion of the adsorption process can be established by kinetic analysis[36]. The existing mathematical models to describe adsorption kinetics are classified as

adsorption reaction models and diffusion models. Adsorption-based diffusion models were established depending on three major steps[37]: 1) diffusion across the liquid film surrounding the adsorbents; 2) diffusion in the liquid contained within the pores and/or along the pore walls; and 3) adsorption and desorption between the adsorbate and active sites. Adsorption-based reaction models, on the other hand, were developed from chemical reaction kinetics and are based on the whole process of adsorption without considering the diffusion steps. Adsorption reaction models describing the rate dominating step of physisorption processes are more widely employed to describe the kinetic process of adsorption, including pseudo-first-order and pseudo-second-order rate equations.

1.2.6.1. Pseudo-first-order Rate Equation

In 1898, Lagergren presented a first-order rate equation to describe the kinetic process of liquid-solid phase adsorption of oxalic acid and malonic acid onto charcoal[38]. The equation relies on adsorption capacity (dQ_t) relative to time change (dt). Lagergren's first-order kinetic equation was called pseudo-first order for the purpose of the differentiation from the kinetic equations based on the solution concentration[39, 40]. The equation was integrated with the boundary conditions of q_t=0 at t=0 and q_t=q_t at t=t and rearranged to eqn. (1.8)[39],

$$\ln(Q_e - Q_t) = \ln Q_e - k_1 t \qquad (1.8)$$

k_1 is the rate constant for the pseudo-first-order rate models. Q_t is the amount of adsorbate adsorbed per unit adsorbent at time t. Lagergren's kinetics equation was widely used for the adsorption of adsorbates from aqueous solution such as metal ions, dyes, and organic contaminants[41, 42].

1.2.6.2. Pseudo-second-order Rate Equation

In the 1990's, Ho presented a second-order kinetic equation to describe the adsorption of divalent metal ions onto polar functional groups of peat[43]. The main assumptions for the adsorption kinetics is that the process may be second-order, and the rate limiting step may be adsorption involving valent forces (*i.e.* chemisorption) through sharing or the exchange of electrons between adsorbents and adsorbates. Furthermore, the adsorption follows the Langmuir equation[44]. The equation can be alternatively rewritten and expressed in its integrated form by eqn. (1.9) with boundary conditions of q_t=0 at t=0 and q_t=q_t at t=t. The driving force for the

adsorption process, ($Q_e - Q_t$), is proportional to the available fraction of active unoccupied sites (1-θ)[45],

$$\frac{t}{Q_t} = \frac{1}{k_2 Q_e^2} + \frac{t}{Q_e} \qquad (1.9)$$

k_2 is the rate constant for the pseudo-second-order models. Q_t is the amount of adsorbate adsorbed per unit adsorbent at time *t*. For pseudo-second-order model, the initial adsorption rate (v_0) can be calculated as,

$$v_0 = k_2 Q_e^2 \qquad (1.10)$$

Similarly, Ho's second-order rate equation is called pseudo-second-order rate equation to distinguish kinetic equations based on adsorption capacity from concentration of solution[45]. This equation was utilized to remove metal ions, dyes, herbicides, oils, and organic substances from aqueous solutions[41, 46-48].

1.2.6.3. Weber-Morris Diffusion Model

Intraparticle diffusion equation was used for the determination of the rate-limiting step to understand the sorption mechanism expressed by eqn. (1.11)[49],

$$Q_t = k_i t^{1/2} + C \qquad (1.11)$$

where k_i is the intraparticle diffusion rate constant (mol·g^{-1}·min$^{1/2}$) and *C* is the intercept. According to eqn. (1.11), a plot of Q_t~$t^{1/2}$ should be a straight line with a slope k_i when the intraparticle diffusion is a rate-limiting step[49]. Furthermore, when the Q_t~$t^{1/2}$ plot to go through the origin (C=0), the intraparticle diffusion is the sole rate-limiting step[49]. However, in most cases, the adsorption kinetics is controlled by film diffusion and intraparticle diffusion simultaneously (C≠0).

1.3. Adsorbent Materials

1.3.1. Copolymer Materials

1.3.1.1. Introduction

Polymers are large molecules consisting of repeating units of smaller units referred to as monomers (*cf.* Scheme 1.3)[50]. The process of linking monomers together is call polymerization. There are two broad groups of polymers: synthetic polymers and biopolymers. *Synthetic polymers* are synthesized chemically by human and *biopolymers* are produced by organisms (natural polymers). Synthetic polymers are classified into two major groups based on preparation

methods: chain-growth polymers (also known as addition polymers) and step-growth polymers (also known as condensation polymers). *Chain-growth polymers* are made by adding monomers to the end of a growing chain. Chain-growth polymerization shows a preference for *head-to-tail* addition. Branching affects the physical properties of the polymer because linear unbranched chains can pack together more closely than branched chain. *Step-growth polymers* are formed by combination of molecules with reactive functional groups, by using a single monomer with two functional groups or by using two different bifunctional monomers resulting in a copolymer. *Copolymers* are made of two or more kinds of monomers. There are several types of copolymers depending on the distribution of monomers: alternating copolymers with two types of alternating monomers; block copolymers containing repeating blocks of each kind of monomer; random copolymers composed of randomly distributed monomers; graft copolymers containing branches derived from one monomer grafted onto a backbone polymeric unit. *Biodegradable polymers* are polymers which can be decomposed into small segments by enzyme-catalyzed reactions. Biodegradable polymers can be designed by incorporating a hydrolysable ester group into the polymer structure to provide "weak links" which are susceptible to enzyme-catalyzed hydrolysis.

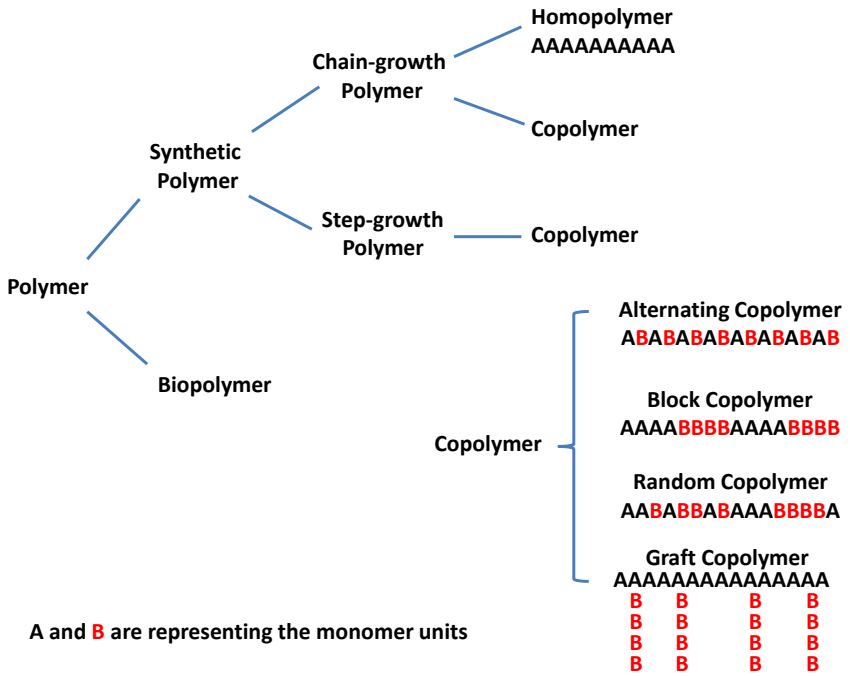

Scheme 1.3. Generalized classification of synthetic polymers and biopolymers.

1.3.1.2. Physical and Chemical Properties of Polymers

The individual chains of a polymer are associated by van der Waals and other noncovalent interactions[50]. According to the order of packed arrays of polymer chains, they are arranged from crystalline (highly ordered) to amorphous, non-crystalline (partially and randomly oriented) polymeric materials. Polymers with more ordered closely packed chains are more crystalline, relatively dense, hard, and more resistant to heat. Cross-linking of separate polymer chains results in a covalently linked network structure (*cf.* Scheme 1.4). Cross-linking prevents the polymer from being displaced when stretched and provides a relatively stable framework for the material. Therefore, density, flexibility and structural characteristics of the polymers can be controlled through the degree of cross-linking. Also the cross-linked framework of polymers may provide porous structures which can increase the surface area and adsorption sites of the polymeric network.

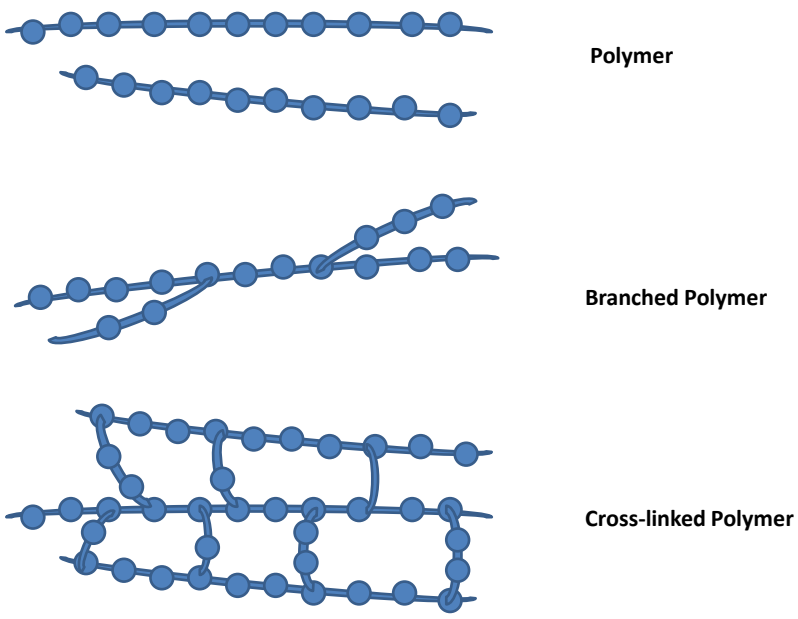

Scheme 1.4. Schematic structural arrangements of single chain polymer, branched chain polymer, and cross-linked polymer.

1.3.1.3. Cross-linkers

Cross-linker units covalently tether the structure of copolymers so that the tertiary structure of the polymeric adsorbent can be stabilized and the adsorption site is retained[51]. The choice of cross-linker depends on the nature of both cross-linker and monomer, including, the reactive groups on the units to ensure efficient cross-linking; the length and flexibility of the cross-linker for controlling the polymeric network of the copolymers and further modifying their sorption properties. Cross-linkers may or may not display attractive adsorption sites for the adsorbent *per se*, but the cross-linking domain can be modified to possess size selectivity and functionality according to the nature of cross-linkers (*e.g.*, lipophilicity, molecular size).

1.3.1.4. Super Adsorbent Polymers (SAPs)

SAPs are characterized as networks of polymer chains, which can undergo swelling and entrap large amounts of water in the polymer framework. Compared with conventional adsorbents[52], SAPs are prepared with relative ease, biodegradability, and display relatively low toxicity. These types of adsorbents possess super swelling capacity and are more versatile by virtue of their tunable pore structure and surface characteristics in aqueous solution (*cf.* Scheme 1.5).

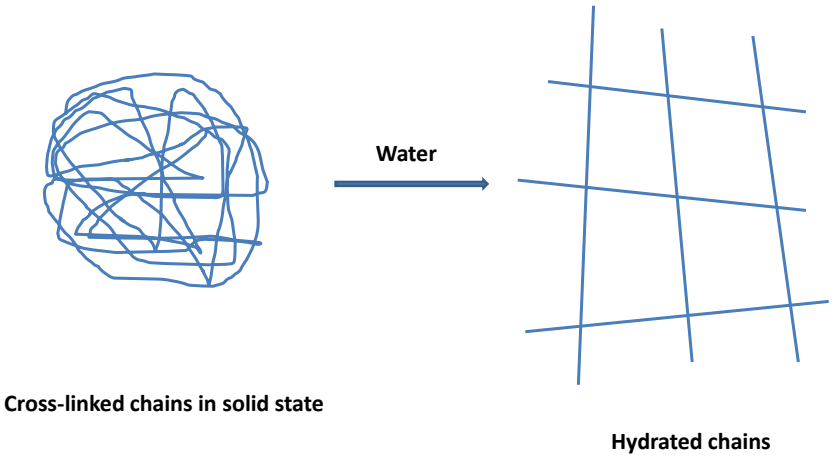

Scheme 1.5. A network of polymeric chains for SAPs in solid state and in the swollen hydrated state.

1.3.1.5. Smart Materials

Smart materials are designed materials with properties that can be significantly changed in a controlled fashion by external stimuli, such as pH, temperature, pressure, *etc.* The design of *''smart''* sorbent materials for applications of controllable sorptive uptake of contaminants is feasible through tuning of the reaction conditions (*e.g.*, stirring rate and co-monomer ratios) and the chemical nature of the cross-linkers. This approach is anticipated to afford polymeric materials with markedly different sorption characteristics according to changes in the polymer morphology, surface area, and pore structure (*i.e.* textural) properties by tuning the nature of the reactants and the reaction conditions. The sorption properties of "smart materials" are tunable with external inputs (*e.g.*, pH and temperature states of the solution), as evidenced by reversible trapping of adsorbates within the adsorbent framework.

1.3.2. Cyclodextrin-based Copolymers

1.3.2.1. Introduction

Cyclodextrins (CDs) are water soluble cyclic oligosaccharides composed of six, seven, or eight glucopyranose units linked by α-1,4-glycosidic bonds, hereafter referred to as α-, β-, and γ-cyclodextrins. CDs possess a torus-shaped macrocyclic structure with a hydrophilic exterior and a lipophilic interior (*cf*. Scheme 1.6). The lipophilic cavity of the various CDs are suitably sized for the inclusion of low to medium sized lipophilic molecules[53]; with a depth of 7.8 Å and inner macrocyclic diameters of 5.7 Å (α-CD), 7.8 Å (β-CD), 9.5 Å (γ-CD)[54,55]. CDs were recently used as potential pore templates to form microporous and nanoporous materials because of their well-defined structure, relatively low toxicity, versatility, and the ability to form inclusion complexes[56]. CDs can be used to construct copolymer frameworks by chemical cross-linking, grafting or non-covalent self-assembly[56, 57]. Although various guest molecules may favor complex formation with different CDs[58,59], β-CD is among the most widely studied because of its suitable cavity dimensions and favourable thermodynamic stability for complexing a wide range of guest molecules[53]. β-CD has limited water solubility (1.85 g/100mL) when compared with α-CD (14.5 g/100mL) and γ-CD (23.2 g/100mL). The limited water solubility of β-CD is related, in part, to the secondary hydroxyl groups which are often intramolecularly H-bonded and display variable hydration relative to nonbonded hydroxyl groups to the water medium[60]

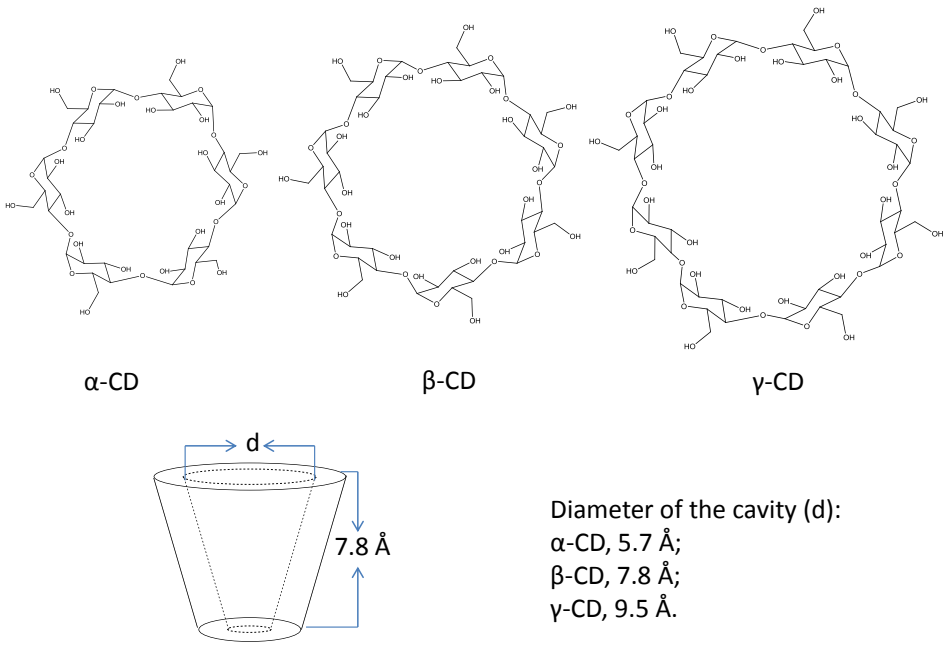

Scheme 1.6. Molecular structure of CDs and the schematic representation of the toroidal-shaped macrocycle.

1.3.2.2. β-CD/PAA Copolymers

Poly (acrylic acid) (PAA) is a soft and flexible polymer with numerous (56-68% w/w) carboxylic acid groups[61] (*cf.* Scheme 1.7a and b). PAA is hydrophilic and possesses mucoadhesive properties due to the large number of carboxylic acid groups on its surface[62]. The primary and secondary hydroxyl groups of β-CD are amenable to grafting onto the long chain of PAA as a polymeric cross-linker unit. The functional host monomer, β-CD, is attractive macrocycle for forming complexes with organic compounds (*vide supra*), so β-CD/PAA copolymers may serve as tunable supramolecular sorbents for the sequestration and immobilization of organic contaminants from aqueous solution.

β-CD/PAA copolymers were prepared with β-CD and PAA using a *water-in-oil* (w/o) micro-emulsion-evaporation method described in a previous study (*cf.* Chapter 2)[63, 64]. The formation of β-CD grafted PAA copolymers under such micro-emulsion conditions with variable cross-linking density yield copolymers with a modified hydrophile-lipophile balance (HLB) relative to that of

pristine PAA.

The polymerization procedure of forming covalent bonds between the hydroxyl groups of β-CD with the carboxylic groups of PAA results in ester bonds. The grafting of β-CD onto the chains of PAA polymer and cross-linking between the separate chains of PAA forms an extended copolymer network (*cf.* Scheme 1.7c, refers to Chapter 2). Therefore, the β-CD/PAA copolymer is a biodegradable, grafted polyester copolymer which may be prepared by step-growth polymerization.

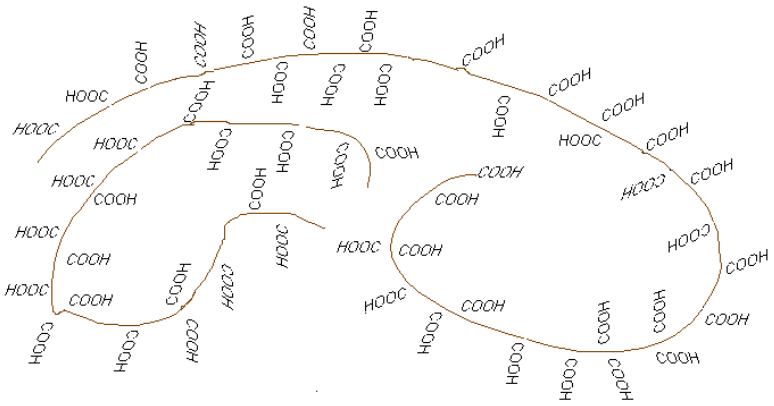

a)

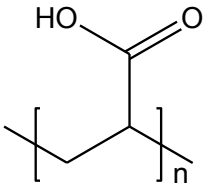

b)

c)

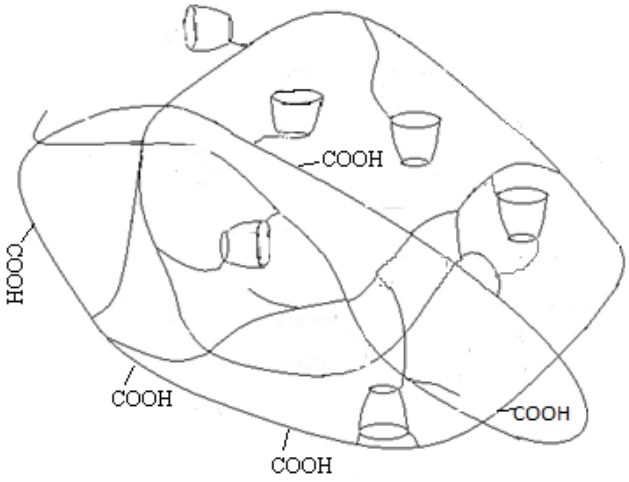

Scheme 1.7. Generalized molecular structure of PAA polymer chain a) and monomer-unit b), and c) schematic representation of a β-CD/PAA copolymer, where the toroidal-shaped units represent β-CD and the straight line segments connecting β-CD tori to PAA represent the ester linkages.

1.3.2.3. β-CD/TCl and β-CD/SCl Copolymers

Polyester copolymers were formed between β-CD and two types of acid dichlorides; terephthaloyl (TCl) and sebacoyl chloride (SCl), employing a *water-in-oil* (w/o) microemulsion-based synthesis[65, 66] (*cf.* Scheme 1.8a and b, and refer to Chapter 3). The polymerization of β-CD/TCl and β-CD/SCl copolymers involve the combination of two kinds of monomers (β-CD/TCl or β-CD/SCl) together into a *head-to-tail* addition by deprotonating β-CD to form the ester bonds between the two monomers in aqueous sodium hydroxide solution. Similarly, β-CD acts as the functional monomer for the copolymer subunit along with a cross-linker of either SCl (aliphatic) or TCl (aromatic). The β-CD/TCl and β-CD/SCl copolymers (*cf.* Scheme 1.8c) are chain-growth alternating copolymers prepared by anionic polymerization, wherein these polyester copolymers are also biodegradable. Greater cross-linking is possible at higher mole ratio of cross-linkers (TCl/SCl) and β-CD, which also results in copolymer products with more branching and random distribution of β-CD within the copolymer framework.

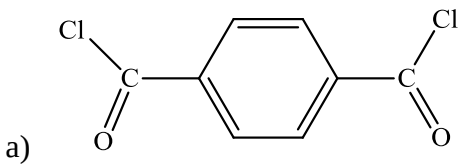

a)

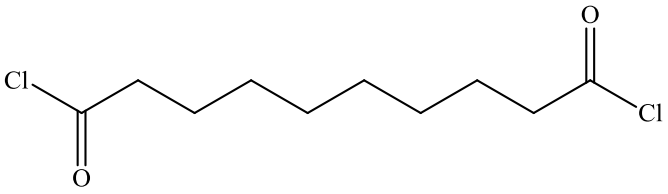

b)

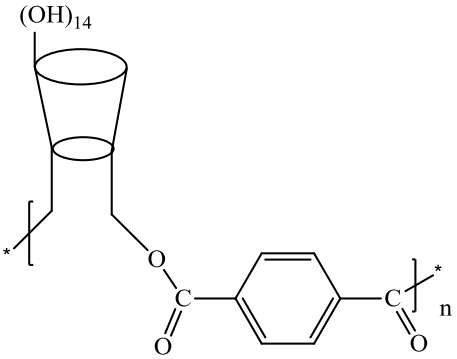

c)

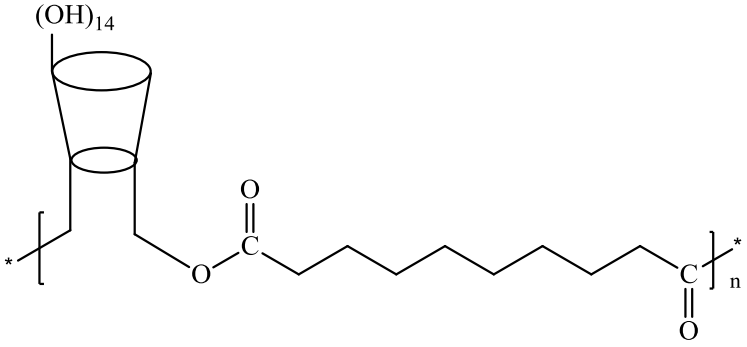

d)

Scheme 1.8. Molecular structure of cross-linkers a) TCl and b) SCl, c) β-CD/TCl copolymer, and d) β-CD/SCl copolymer.

1.3.3. Chitosan-based Copolymers

1.3.3.1. Introduction

Chitosan (CS; Scheme 1.9a) is produced industrially by the deacetylation of chitin obtained from the exoskeletons of crustaceans and the cell walls of fungi. Chitosan is widely used in

various industries due to its biocompatibility, antibacterial properties, and its relatively low cost. CS is a linear polysaccharide composed of randomly distributed β-(1→4)-linked D-glucosamine and N-acetyl-D-glucosamine units[67,68]. It has a relatively hydrophobic backbone with amine groups that are potentially available for cross-linking reactions and may serve as potential active adsorption sites (*e.g.*, electrostatic interaction, H-bonding, *etc.*). Polysaccharides such as chitosan are generally stiff polymers[67] resulting in highly extended polymer chain conformations. Therefore, CS serves as a rigid prepolymer back-bone scaffold component in the design of copolymer materials.

1.3.3.2. CS/PAA Copolymers

PAA is a soft and flexible polymer[61] which may serve as a useful cross-linker agent between the back-bone chain of CS. As the amino groups from CS are condensed together with the carboxylic groups of PAA via amide bonds, CS-PAA copolymers are formed with a pseudo "*protein-like"* structure (*cf.* Scheme 1.9b and refer to Chapter 4). The copolymers also undergo self-assembly and complexation between oppositely charged polyelectrolytes (CS and PAA) through electrostatic interactions using a solution dropping method[69, 70]. These grafted polyamide copolymers are formed by step-growth polymerization.

a)

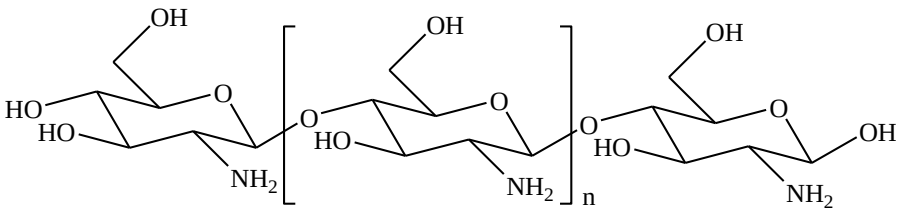

b)

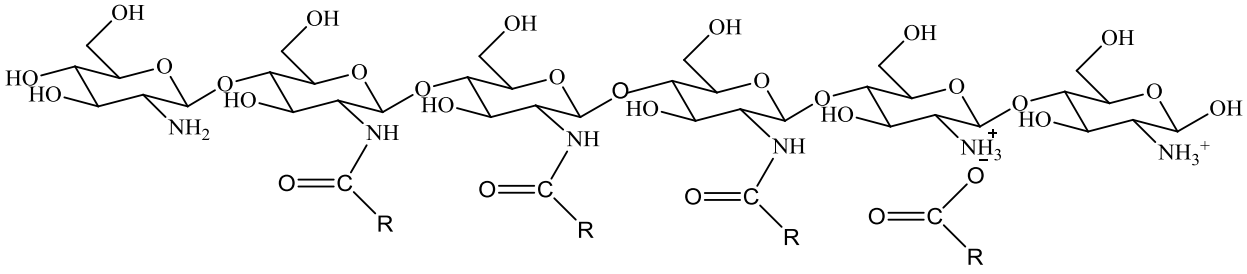

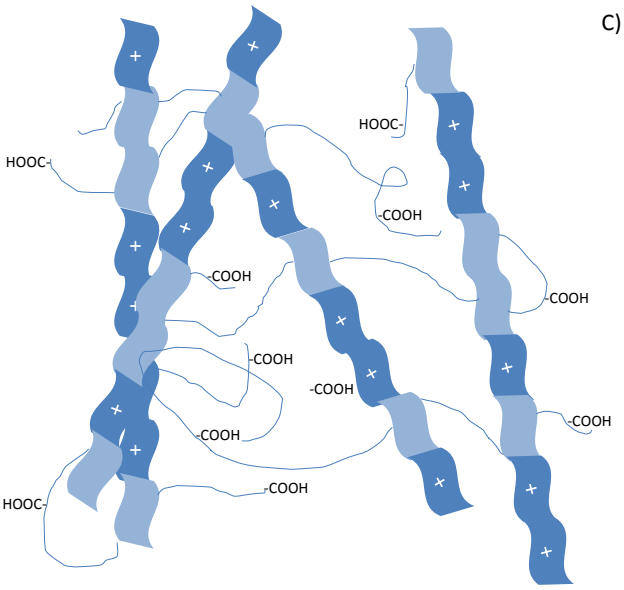

Scheme 1.9. Molecular structure of a) CS, b) synthetically engineered CS/PAA copolymers, c) the illustration of copolymer structure of cross-linked CS-PAA copolymer (*e.g.*, CP-5; refer to Chapter 4) in 2% acetic solution; Each ribbon represents one chitosan unit: light blue indicates neutral chitosan unit with amide bond after reacting with PAA and dark blue (with "+" symbols) indicates the protonation of the amine groups of chitosan.

1.3.4. Characterization of Adsorbent Materials

1.3.4.1. Introduction

Methods used for the characterization of the copolymers are grouped by using spectroscopic methods such as Diffuse Reflectance Infrared Fourier Transform Spectroscopy (DRIFTS IR), Nuclear Magnetic Resonance Spectroscopy (^{1}H NMR and ^{13}C NMR), thermogravimetry analysis (TGA), Differential scanning calorimetry (DSC), elemental analysis, and nitrogen and/or dye adsorption methods.

1.3.4.2. Spectroscopic Characterization

IR spectroscopy is a common method in copolymer characterization. The DRIFT spectra were recorded in reflectance mode (Kubelka-Munk intensity units). The theory of DRIFTS is based on the Kubelka-Munk equation for non-transmissive materials so that they can

isotropically scatter the incident light (important assumption) and provide diffuse reflectance which is quantitatively analogous to the Beer-Lambert law for transmission measurements[71, 72].

NMR spectroscopy is one of the principal techniques used to obtain physical, chemical, and structural information of compounds due to chemical shift, Zeeman effects, or the Knight shift effect on the resonant frequencies of the nuclei in the sample[73]. The method provides detailed information on the topology, dynamics and three-dimensional structure of molecules in solution and in the solid state. In this work, both ^{1}H NMR and ^{13}C NMR are employed to characterize the copolymer materials.

1.3.4.3. Thermal Analysis

TGA enables measurement of the amount and rate of change in the weight of a material as a function of temperature or time in a controlled atmosphere. Measurements of weight loss with increasing temperature can establish a weight loss curve. The technique enables characterization of materials by exhibiting weight loss or gain due to decomposition, oxidation, or dehydration. TGA shows the thermal stability, composition, moisture and volatiles content of copolymers.

DSC enables measurement of heat flow; endothermic and exothermic transitions as a function of temperature including glass transition temperature (T_g), melting, crystallization, curing and cure kinetics, onset of oxidation and heat capacity. DSC is a widely used thermal analysis technique to characterize polymers, pharmaceuticals, foods/biologicals, and organic chemicals.

1.3.4.4. Elemental Analysis

CHN elemental analysis is another materials characterization technique. The technique measures the elemental contents of carbon (C) and hydrogen (H) and nitrogen (N) by subjecting a sample to total combustion analysis. In this research, C, H contents were measured by elemental analysis. This technique offers a quantitative method to confirm the co-monomer cross-linking ratios which complements TGA results.

1.3.4.5. Nitrogen Adsorption

Gas adsorption enables characterization of the surface and pore characteristics of copolymers in solid state, such as, pore diameter, total pore volume, specific surface area, and

pore size distribution. The method involves condensing nitrogen in the pores of adsorbents and then calculating the pore volumes from the quantities of gas required to fill the pores. One drawback is that the time used for a single analysis can be on the order of hours; however, measurements can be done automatically. The pore diameter range that can be determined is from 0.3 to 300 nm, a range not completely covered by mercury intrusion porosimetry. With gas adsorption, only surface accessible pores are determined, and the cylindrical pore model is assumed in pore size distribution measurements[74]. Among various gases, such as, argon, helium, oxygen and methane, nitrogen is the probe gas most commonly used in gas porosimetry because it is inexpensive, readily obtained, inert, and well-studied in the adsorption literature[75]. The use of nitrogen as an adsorptive probe is convenient because the isothermal conditions can easily be maintained using liquid nitrogen as the cryostat. Nitrogen may adsorb at a lower relative pressure on a heterogeneous surface due to the quadrupolar interactions when compared to argon[75].

Type I, II and *IV* adsorption isotherms are commonly observed for gas adsorption (*cf.* Figure 1.1). The *Type I* isotherm is evidenced by microporous adsorbents with relatively small external surfaces, for example, activated carbon, molecular sieve zeolites and certain porous oxides. The limiting gas uptake relies on the accessible micropore volumes rather than the internal surface area[76]. The reversible *Type II* isotherm is the general type observed for non-porous or macroporous materials with strong adsorbent-adsorbate interactions. There is a point where the linear middle section of the isotherm occurs and indicates the completion of the monolayer and the start of multilayer adsorption profile[76]. The *Type II* isotherm represents the monolayer-multilayer adsorption. *Type IV* is the most commonly observed isotherm in this research (*cf.* Chapters 2-4), which show a pattern of hysteresis between the adsorption and desorption profiles associated with capillary condensation within the mesopores. The hysteresis loops appear in the multilayer range of physisorption isotherms and may vary in shape according to the different pore characteristics[76].

The BET gas adsorption method is used for the surface area estimation in spite of the over-simplified form of the model; expressed in eqn (1.12)[76]:

$$\frac{P}{n(P^0-P)} = \frac{1}{n_m C} + \frac{C-1}{n_m C} \cdot \frac{P}{P^0} \qquad \text{eqn. (1.12)}$$

Where C is the adsorption constant, n is the amount adsorbed per gram of solid adsorbent at equilibrium pressure P, n_m the amount adsorbed per gram of solid to complete layers. P_0 is the saturation pressure.

The BET surface area is suitable for analyzing *Type II* and *IV* isotherms by the following eqns (1.13) and (1.14) for the total surface area (A_s) and specific surface area (a_s), respectively.

$$A_s(BET) = n_m L a_m \qquad \text{eqn. (1.13)}$$

$$a_s(BET) = \frac{A_s(BET)}{m} \qquad \text{eqn. (1.14)}$$

The molecular cross-sectional BET area (a_m) is the average area occupied by the adsorbate molecule in the complete monolayer; m is the sorbent mass; L is Avogadro's constant.

The Barret-Joyner-Halenda (BJH) method was used to estimate the pore volume and the pore diameter from the adsorption isotherm data[77]. The BJH method used the Kelvin equation and the assumption of slit-shaped pores[77], expressed by eqn. (1.15);

$$\frac{1}{r_1} + \frac{1}{r_2} = -\frac{RT}{\sigma^{lg} v^l} ln\left(\frac{P}{P^0}\right) \qquad \text{eqn. (1.15)}$$

The expression relates the principal radii, r_1 and r_2 to the pore sites at relative pressure (P/P^0) when condensation occurs; σ^{lg} is the surface tension of the liquid condensate and v^1 is the molar volume.

The Kelvin equation was rearranged to eqn. (1.16) as follows;

$$r_K = \frac{2\sigma^{lg} v^1}{RT \ln\left(\frac{P^0}{P}\right)} \qquad \text{eqn. (1.16)}$$

Where r_k is the Kelvin radius.

The pore radius of a cylindrical pore is r_p and a correction is made for the thickness of a layer already adsorbed on the pore walls, the multilayer thickness, *t*;

$$r_P = r_K + 2t \qquad \text{eqn. (1.17)}$$

For a parallel-side slit, the slit width, d_p, is given by eqn. (1.18).

$$d_P = r_K + t \qquad \text{eqn. (1.18)}$$

1.3.4.6. Dye Sorption Method

Supplementary to the gas adsorption method, dye sorption can be used to further understand the sorbent surface area and pore structures of copolymer materials in aqueous phase. According to Giles *et al*[78-82], the method is suitable for various types of solid adsorbent materials (porous or nonporous) and relatively easy to employ. Dye sorption in solution provides insight regarding the involvement of solvent effects on the copolymer textual properties, which is not directly accessible from nitrogen adsorption studies. Dye sorption is commonly used to estimate textural

properties but may have certain limitations[83]; 1) variation of the cross-sectional area occupied by the adsorbates on the surface (A_m) may introduce errors in the SA estimation; 2) the size restriction of various dyes may limit access to the pores of porous solids; 3) potential micellization of the dye on the surface of adsorbents; 4) the quantitative accuracy was raised by Padday on the adsorption isotherms without clearly defined plateau regions[83]. Accordingly, the method is generally reliable when comparing similar materials under related experimental conditions, careful selection of dye probe, and comparable experimental conditions. The dyes chosen in this work are *p*-nitrophenol (PNP) and methylene blue (MB).

PNP (*cf.* Scheme 1.10a) is a well known organic dye molecule for studying the sorption capacity of solid adsorbents in aqueous solution due to its favorable chromophore characteristics[79,84]. PNP is a good sorptive probe because of its amphiphilic nature due to the polar functional group and its apolar organic fragment[82]. Because of its relative hydrophilicity, the molecule is water soluble and shows good sorption affinity with the surface of polar adsorbents. As well, its lipophilic aromatic ring makes PNP very attractive to non-polar molecule, *e.g.*, the internal cavity of CDs. Furthermore, PNP is a relatively small probe molecule which shows a preferable planar orientation and is more likely to be adsorbed as a vertically oriented close-packed to ensure precision in cross-sectional area estimation depending on the relative concentration of PNP and the surface properties of the adsorbents. The molecular cross-sectional area of PNP is 15.0 $Å^2$ and 25.0 $Å^2$ for close-packed arrangements in the presence and absence of solvent in the adsorbed monolayer[82], respectively. PNP has low surface-active behaviour and will not readily form three-dimensional micelles at the solid surface interface. Finally, the spectroscopic properties of PNP are conveniently observed in the visible region (yellow) and detectable by UV-Vis spectroscopy, contributing to the ease of experimental studies. All these characteristics of PNP make it a good dye probe for the measurements of sorbent surface area determinations.

MB (*cf.* Scheme 1.10b) is also a UV-Vis dye with a greater molecular size (~130 $Å^2$) than PNP[85]. Its sorption capacity is favored by controlling the pH of the solution with neutral to basic condition to reduce competition between the hydronium ion and the cation form of MB with the adsorbent.

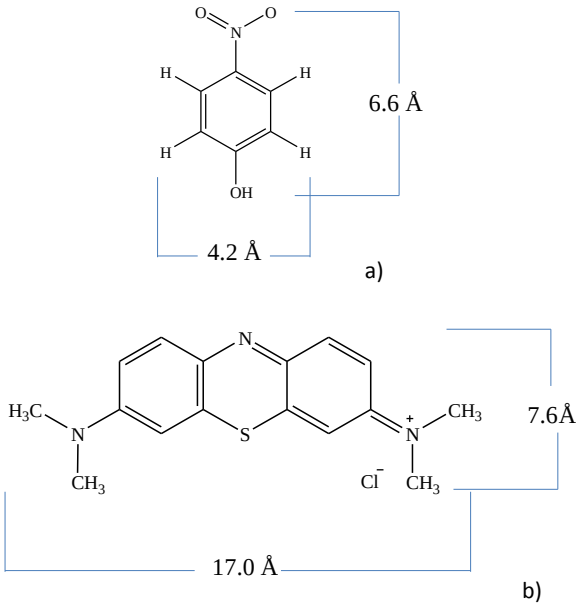

Scheme 1.10. Molecular structure of a) PNP and b) MB.

1.4. Experimental Methods for THMs Removal

1.4.1. GC-ECD

The U.S. environmental Protection Agency (U.S. EPA) has approved three analytical methods (EPA method 502.2; EPA Method 524.2 and EPA Method 551.1) (U.S EPA, 2005) for the detection of THMs. Method 502.2 uses purge and trap capillary column gas chromatography with photoionization and electron capture or electrolytic conductivity detectors (P&T/GC-ECD); Method 524.2 determines THMs using capillary column gas chromatography/mass spectrometry (GC-MS) and Method 551.1 uses liquid-liquid extraction and GC-ECD (LLE/GC-ECD). Health Canada uses a P&T, LLE and direct aqueous injection (DAI) in combination with a gas chromatography system to analyze THMs. ECD is a device for detecting atoms and molecules in a gas by the accession of electrons via electron capture ionization (Scheme 1.11). The device was invented in 1957 by Lovelock[86] and is used in gas chromatography to detect trace amounts of chemical compounds in a sample[87], especially for detecting electron-absorbing components (high electronegativity) such as halogenated compounds[16, 88, 89]. The ECD uses a radioactive beta

particle (electron) emitter in conjunction with a so-called makeup gas flowing through the detector chamber. The electron emitter typically consists a metal foil holding 10 millicuries of the radionuclide $^{63}Ni^{86}$. Nitrogen is usually used as makeup gas because of its low excitation energy, which means it is easy to remove an electron from molecular nitrogen. The electrons emitted from the electron emitter together with the makeup gas result in more free electrons. The electrons are accelerated towards a positively charged anode, generating a current and forming a background signal in the chromatogram. As the sample is carried into the detector by the carrier gas, the electron absorbing analyte molecules capture electrons and reduce the current between the collector anode and a cathode. As a result, the analyte concentration is proportional to the degree of electron capture and very sensitive to electronegative compounds.

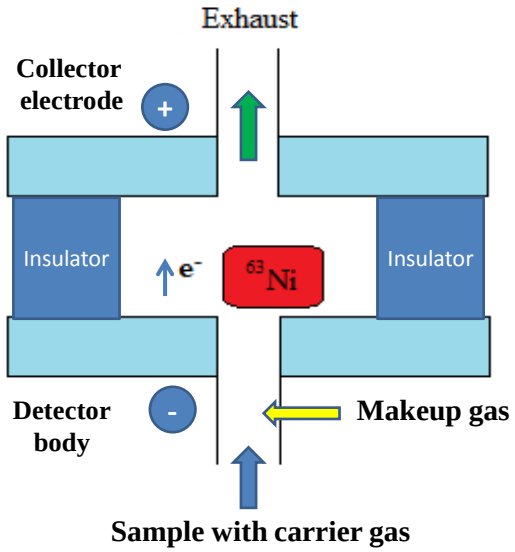

Scheme 1.11. Schematic diagram of an electron capture detector for a gas chromatograph with a ^{63}Ni radiation source.

1.4.2. Direct Aqueous Injection (DAI) method

Solvent extraction[22, 90], head space analysis[91, 92], and purge and trap[93] methods are commonly used for the detection of these highly volatile organic compounds. Compared with these methods, DAI is very convenient and time-saving since there is no additional sample preparation requirement between collection and final analysis. DAI is one of the three methods (P&T, LLE and DAI) employed by Health Canada to analyze THMs. The technique is considered reliable and provides good precision and analyte recovery[16, 88, 89]. The potential problems of DAI are: 1) water vapor may shorten the life of ECD and column; 2) the method is more suitable for relatively clean samples (*i.e.* low turbidity) because there is no initial clean-up of samples required.

1.5. Objectives of the Research

The overall objectives of this project are to design and characterize a series of synthetically engineered copolymers and to study their capacities to remove model THM compounds from laboratory water samples. Since chloroform is among the most common THM, the sorption properties of the copolymers were studied with both chloroform and a mixture of halogenated THMs in aqueous solution. The research of this thesis is divided into three major parts: 1) synthesis and characterization of copolymer sorbents; 2) sorption of chloroform with copolymers; 3) sorption of THMs with copolymers.

In the first part of the research, a series of novel copolymers (*e.g.* polyester, grafted polyester and grafted polyamide) were designed based on polysaccharide-based biomaterials, where CD and CS, as the *"green"* biomaterials for the copolymer sorbent design. The synthetically engineered copolymers were systematically designed as potentially *"smart materials"* because of their tunable physicochemical properties. The physicochemical properties of the copolymers include the textural and sorption by controlling the synthetic conditions (*e.g.*, type of linkers, co-monomer ratio, stirring rate). A comprehensive structural characterization of the copolymers was carried out using IR and NMR spectroscopy. The physicochemical properties of copolymers were performed using TGA, DSC, elemental analysis, and nitrogen/dye adsorption methods. The copolymer materials are anticipated to have tunable textural properties (*i.e.* SA, pore structure, surface area, and swellability) and surface chemistry. The sorption properties of copolymer were studied by: 1) the SA and sorption capacity estimation of the copolymers in both solid state and

aqueous solution using nitrogen and dye sorption methods, respectively; 2) the investigation of the various sorption sites on copolymers (*e.g.,* inclusion or/and interstitial sites) was carried out using adsorption and spectroscopic methods.

The second part of the research involved evaluation of the sorption capacity of the copolymer materials with chloroform in aqueous solutions using DAI method by GC-ECD. The experimental conditions and adsorption rate were evaluated using kinetic studies to further understand the adsorption processes of the copolymers and the feasibility of such materials for future field applications involving THM removal. This systematic quantitative study obtained by the DAI method provided an opportunity to evaluate this technique; it offers an efficient and relatively accurate method with a great potential for the monitoring of THMs. However, the method has not been widely applied and generally under appreciated as compared with P&T and LLE methods.

The final objective of this research was focused on the sorptive removal of chloroform and multi-component THMs from water with various copolymers. It was hypothesized that the brominated THMs adopt a similar sorption mechanism as the copolymer/chloroform systems.. The research also determined the sorption properties of chloroform with copolymers from water contaminated with various THMs. Various copolymers were hypothesized to show some preference toward different THMs because of their tunable textural and surface chemistry properties. An investigation of suitable copolymer systems will contribute to the development of materials with an improved removal efficiency for future sorption-based water treatment applications.

1.6. Organization and Scope

This PhD thesis includes the design of polysaccharide materials and their sorption studies toward chloroform along with total trihalomethanes (TTHMs) in aqueous solution. The research is divided into 7 chapters, as follows: Chapter 1 provides an introduction and context of the thesis research; Chapters 2-6 are verbatim copies of articles published in literature or manuscripts for submission; and Chapter 7 outlines the conclusions and future work. The thesis content is summarized in Table 1.2.

Table 1.2. A table of the contents and the related bibliography involved in this manuscript formed thesis.

Chapters	Bibliographic Information	Status
Chapter 1 Introduction		unpublished
Chapter 2	R. Guo; L. D. Wilson * *"Preparation and Sorption Studies of Microsphere Copolymers Containing β -Cyclodextrin and Poly(acrylic acid)"*, J. Appl. Polym. Sci. 2012, 125, 1841–1854.	Published
Chapter 3	L. D. Wilson*; R. Guo *"Preparation and Sorption Studies of Polyester Microsphere Copolymers Containing β-Cyclodextrin"* J. Colloid Interface Sci. 2012, 387(1), 250-261.	Published
Chapter 4	R. Guo, L. D. Wilson* *"Synthetically Engineered Chitosan-Based Materials and their Sorption Properties with Methylene Blue in Aqueous Solution"* J. Colloid Interface Sci. 2012, 388(1), 225-234.	Published
Chapter 5	R. Guo, L. D. Wilson*, and L. Bharadwaj *"Uptake of chloroform from water systems by synthetically engineered copolymers using a direct aqueous injection (DAI) method"* Ind. Chem. Res. Manuscript ID: ie-2013-00860b	Submitted on March 25, 2013
Chapter 6	R. Guo, L. D. Wilson*, and L. Bharadwaj *"Uptake of THMs from water systems by synthetically engineered copolymers using a direct aqueous injection (DAI) method"* Ind. Chem. Res. Manuscript ID: ie-2013-00920s	Submitted on March 31, 2013
Chapter 7 Conclusions		Unpublished

Each chapter includes a brief summary of the work and a description of how each paper relates to the stated objectives of this PhD dissertation at the beginning of the chapter.

Chapter 1 presents an introduction and overview of the PhD thesis and outlines the underlining background and the essential methodologies involved in the research.

Chapter 2 presents the design and characterization of β-CD/PAA copolymer materials. The copolymers were prepared by varying the pre-polymer ratio and stirring rate during synthesis to achieve tunable physicochemical properties. Various materials characterization methods were used to characterize the copolymers to enable selection for further study. The sorption isotherms were evaluated with various isotherm models (*e.g.*, Langmuir, BET, Freundlich and Sips) to account for their equilibrium sorption properties.

Chapter 3 presents the synthesis and characterization of CD-based polyester materials (*i.e.* β-CD/TCl and β-CD/SCl copolymers). The copolymers were prepared by the varying type of linker molecule and the cross-linking co-monomer ratio during synthesis. The nature of the potential adsorption sites were characterized studied by both dye sorption and spectroscopic methods.

Chapter 4 describes the design and characterization of chitosan-based grafted polyamide copolymers (*i.e.* CS/PAA copolymers). The copolymers were prepared by varying the prepolymer ratio during synthesis. CS was used as functional unit in comparison with β-CD based copolymers for the materials design. A sorption/desorption experiment was carried out to evaluate the utility of these copolymers as *"smart materials"* as shown by the ability to *turn on* and *turn off* dye sorption in response to external pH changes.

Chapter 5 presents the sorption properties of copolymers prepared in chapters 2-4 with chloroform in aqueous solutions. This study involved a bench sorption study, kinetic studies and the DAI-based sorption study to evaluate the sorption capacities of various adsorbents including polyester, grafted polyester, and polyamide copolymers. The results provide an understanding of the sorption mechanism of copolymers with chloroform in aqueous solution.

Chapter 6 extends the results presented in Chapter 5 by examining the sorption properties of mixtures of multi-component THMs with copolymers. The sorption capacities of THMs with the copolymers were determined using the experimental protocol and analytical method developed in Chapter 5. The sorptive selectivity of the copolymers with individual THM component species from aqueous mixtures was evaluated and described.

Chapter 7 presents a summary of the research, conclusions, and future work.

1.7. References

(1) Soubeiran, E. *Ann. chim. phys.* **1831**, *48*, 157.

(2) Liebig, J. *Annalen der Pharmacie* **1832**, *1*, 182-283.

(3) Dumas, J. *Annalen der Pharmacie* **1834**, *107*, 650-656.

(4) National Toxicology Program (1991), NTP Chemical Repository Data Sheet: Chloroform, Research Triangle Park, NC.

(5) International Trade Commission (1993), Synthetic Organic Chemicals, US Production and Sales, 77th Ed., Washington DC, US Government Printing Office, p. 3-18.

(6) Rossberg, M., et al. In *Chlorinated Hydrocarbons;* Wiley-VCH Verlag GmbH & Co. KGaA: 2000.

(7) Budavari, S., Ed.; In The Merck index: An encyclopedia of chemicals, drugs, and biologicals*;* Merck: Whitehouse Station, NJ, 1996.

(8) WHO, 1994. Chloroform (Environmental Health Criteria 163), Geneva, International Program on Chemical Safety.

(9) WHO, 1998. Trihalomethanes in Drinking-water: Background document for development of WHO Guidelines for Drinking-water Quality. .

(10) Aucott, M.; McCulloch, A.; Graedel, T.; Kleiman, G.; Midgley, P.; Li, Y. *J. Geophys. Res. - Atmos.* **1999**, *104*, 8405-8415.

(11) Calderon, R. L. *Food and Chemical Toxicology* **2000**, *38, Supplement 1*, S13-S20.

(12) Rook, J. J. *Water Treatment and Examination* **1974**, *23*, 234-243.

(13) Health Canada, 2011. Guidelines for Canadian Drinking Water Quality: Guildline Technical Document. (accessed 06/24).

(14) Mabey, D. M. **1982**, Aquatic fate process data for organic priority pollutants. *(EPA 4014-81-PB87-16909)*.

(15) Jackman, T. A.; Hughes, C. L. *Ground Water Monit. Remediat.* **2010**, *30*, 74-78.

(16) Carpi, M.; Zufall, C. *Lc Gc N. Am.* **2003**, 88-91.

(17) Kramer, M. D.; Lynch, C. F.; Isacson, P.; Hanson, J. W. *Epidemiology* **1992**, *3*, 407-413.

(18) Ruddick, J. A.; Villeneuve, D. C.; Chu, I.; Valli, V. E. *J. Environ. Sci. Health B.* **1983**, *18*, 333-349.

(19) Thompson, D. J.; Warner, S. D.; Robinson, V. B. *Toxicol. Appl. Pharmacol.* **1974**, *29*, 348-357.

(20) Klinefelter, G. R.; Suarez, J. D.; Roberts, N. L.; DeAngelo, A. B. *Reprod. Toxicol.* **1995**, *9*, 571-578.

(21) WHO; In *EHC 216: Disinfectants and Disinfectant By-products. Chapter 4. Toxicology of Disinfectant By-products*.

(22) Clesceri, L. S.; Greenberg, A. E.; Eaton, A. D. Trihalomethanes and Chlorinated Organic Solvents Standard Methods for the Examination of Water and Wastewater (APHA, AWWA and WEF) (U.S. EPA, Washiington, D. C. Method 6232, 20th ed. 1998).

(23) http://www.allaboutwater.org/filtration.html. (accessed 01/28, 2013).

(24) a) Brunauer, S. *In The adsorption of gases and vapors*; **1945**; b) Kolasinski, K. K. Surface Science: Foundations of Catalysis and Nanoscience, 3rd ed. 2012, 234-255.

(25) Zettlemoyer, A. *Chem. Rev.* **1959**, *59*, 937-981.

(26) Loiseau, A.; Launois, P.; Petit, P.; Roche, S.; Salvetat, **2006**, 485-510.

(27) Mohamed, M. H.; Wilson, L. D.; Headley, J. V. *Carbohydr. Res.* **2011**, *346*, 219-229.

(28) Giles, C. H.; Silva, A. P.; Tridevi, A. S. *J. Appl. Chem.* **1970**, *20*.

(29) Freundlich, H. M. *Phys. Chem.* **1906**, *57A*, 385-470.

(30) Langmuir, I. *J. Am. Chem. Soc.* **1918**, *40*, 1361-1403.

(31) Brunauer, S.; Emmett, P. H.; Teller, E. I. *J. Am. Chem. Soc.* **1938**, *60*, 309.

(32) Sips, R. *J. Am. Chem. Soc.* **1948**, *125*, 6452.

(33) Brunauer, S.; Deming, L.; Deming, W.; Teller, E. *J. Am. Chem. Soc.* **1940**, *62*, 1723-1732.

(34) IUPAC *Pure Applied Chemistry* **1994**, *66*, 1739.

(35) Carmody, O.; Frost, R.; Xi, Y.; Kokot, S. *Surf Sci* **2007**, *601*, 2066-2076.

(36) Qiu, H.; Lv, L.; Pan, B.; Zhang, Q.; Zhang, W.; Zhang, Q. *J. Zhejiang Univ. -SCI A* **2009**, *10*, 716-724.

(37) Lazaridis, N.; Asouhidou, D. *Water Res.* **2003**, *37*, 2875-2882.

(38) Lagergren, S. *Handlingar* **1898**, *24*, 1-39.

(39) Ho, Y. S. *Scientometrics* **2004**, *59*.

(40) Ho, Y. S.; McKay, G. *Process Saf. Environ. Prot.* **1998**, *76*.

(41) Hameed, B. H.; El-Khaiary, M. I. *J. Hazard. Mater.* **2008**, *154*.

(42) Tan, I. A. W.; Ahmad, A. L.; Hameed, B. H. *J. Hazard. Mater.* **2008**, *154*.

(43) Ho, Y. S.; McKay, G. *Chem. Eng. J.* **1998**, *70*.

(44) Ho, Y. S.; McKay, G. *Water Res.* **2000**, *34*.

(45) Ho, Y. *J. Hazard. Mater*. **2006**, *136*.

(46) Yan, G. Y.; Viraraghavan, T. *Water Res.* **2003**, *37*.

(47) Al-Asheh, S.; Banat, F.; Masad, A. *Environ. Geol.* **2004**, *45*, 1109-1117.

(48) Anirudhan, T. S.; Radhakrishnan, P. G. *J. Chem. Thermodyn.* **2008**, *40*, 702-709.

(49) Weber, W. J.; Morris, J. C. In *In Advances in water pollution research: removal of biologically resistant pollutant from waste water by adsorption.* 1962; Vol. 2, pp 231-266.

(50) Bruice, Y. P., Ed.; In *Organic Chemistry;* Pearson Education, Inc.: United State of America, 2004.

(51) Cormack, P. A. G.; Elorza, A. Z. *J. Chromatogr. B* **2004**, *804*, 173-182.

(52) Dhodapkar, R.; Borde, P.; Nandy, T. *Glob. Nest. J.* **2009**, *11*, 223-234.

(53) Inoue, Y.; Harkushi, T.; Liu, Y.; Tong, L. H.; Shen, B. J.; Jin, D. S. *J. Am. Chem. Soc.* **1993**, *115*, 475-481.

(54) Bender, M. L.; Komi yam, M. In *Cyclodextrin Chemistry;* Springer verlag.: New York, 1977.

(55) Steed, J. W.; Atwood, J. L., Eds.; In *Supramolecular Chemistry;* John Wiley & Sons, Ltd.: West Sussex, 2009.

(56) van de Manakker, F.; Vermonden, T.; van Nostrum, C. F.; Hennink, W. E. *Biomacromolecules* **2009**, *10*, 3157-3175.

(57) Jang, J. S.; Bae, J. *Macromol. Rapid Commun.* **2005**, *26*, 1320-1324.

(58) Graves, R.; Makoid, M.; Jonnalagadda, S. *J. Microencapsul.* **2005**, *22*, 661-670.

(59) Xiao, W.; Chen, W.; Zhang, J.; Li, C.; Zhuo, R.; Zhang, X. *J. Phys. Chem. B* **2011**, *115*, 13796-13802.

(60) Irie, T.; Uekama, K. *J. Pharm. Sci.* **1997**, *86*, 147-162.

(61) Li, H.; Liu, B.; Zhang, X.; Gao, C.; Shen, J.; Zou, G. *Langmuir* **1999**, *15*, 2120-2124.

(62) Park, H.; Robinson, J. R. *Pharm. Res.* **1987**, *4*, 457-464.

(63) Bibby, D. C.; Davies, N. M.; Tucker, I. G. *Int. J. Pharm.* **1999**, *187*, 243-250.

(64) Bibby, D. C.; Davies, N. M.; Tucker, I. G. *Int. J. Pharm.* **1999**, *180*, 161-168.

(65) Pariot, N.; Edwards-Levy, F.; Andry, M. C.; Levy, M. C. *Int. J. Pharm.* **2002**, *232*, 175-181.

(66) Pariot, N.; Edwards-Levy, F.; Andry, M.; Levy, M. *Int. J. Pharm.* **2000**, *211*, 19-27.

(67) Guo, R.; Wilson, L. D. *J. Colloid Interface Sci.* **2012**, *388*, 225-234.

(68) Dumitriu, S., Ed.; In *Polysaccharides: Structural Diversity and Functional Versatility.* 2005.

(69) Bernkop-Schnürch, A., Ed.; In *Oral Delivery of Macromolecular Drugs: Barriers, Strategies and Future Trends;* 2009.

(70) Wang, J.; Kuo, Y. *J. Appl. Polym. Sci.* **2008**, *107*, 2333-2342.

(71) Fanning, P. E.; Vannice, M. A. *Carbon* **1993**, *31*, 721-730.

(72) Kubelka, P.; Munk, F. *Zeit. Für Tekn. Physik.* **1931**, *12*, 593.

(73) Keeler, J., Ed.; In *Understanding NMR Spectroscopy.* 2007.

(74) Allen, T., Ed.; In *Particle size measurement;* Chapman & Hall: New York, USA, 1997.

(75) Dombrowski, R.; Hyduke, D.; Lastoskie, C. *Langmuir* **2000**, *16*, 5041-5050.

(76) Sing, K. S. W.; Everett, D. H.; Haul, R. A. W.; Moscou, L.; Pierotti, R. A.; Rouquerol, J.; Siemieniewska, T. *Pure Appl. Chem.* **1985**, *57*, 603-619.

(77) Barrett, E. P.; Joyner, L. G.; Halenda, P. P. *J. Am. Chem. Soc.* **1951**, *73*, 373-380.

(78) Giles, C.; Ahmad, M.; Dandekar, S.; McKay, R. *J. Soc. Dyers Colour.* **1962**, *78*, 120-127.

(79) Giles, C.; D'Silva, A.; Trivedi, A. *J. Appl. Chem.* **1970**, *20*, 37.

(80) Giles, C.; Duff, D. *J. Soc. Dyers Colour.* **1970**, *86*, 405.

(81) Giles, C.; Hojiwala, B.; Shah, C.; Sinclair, R. *J. Soc. Dyers Colour.* **1974**, *90*, 45-49.

(82) Giles, C.; Macewan, T.; Nakhwa, S.; Smith, D. *J. Chem. Soc.* **1960**, 3973-3993.

(83) Padday, J. F. *Ibid* **1970**, 331-337.

(84) Mohamed, M. H.; Wilson, L. D.; Headley, J. V.; Peru, K. M. *Process Saf. Environ. Prot.* **2008**, *86*, 237-243.

(85) László, K.; Podkościelny, P.; Dąbrowski, A. *Appl. Surf. Sci.* **2006**, *252*, 5752-5762.

(86) Lovelock, J. E. *J. Chromatogr. A* **1958**, *1*, 35-46.

(87) Pellizza E. D. *J. Chromatogr.* **1974**, *98*, 323-361.

(88) Nicholson, A. A.; Meresz, O.; Lemyk, B. *Anal. Chem.* **1977**, *49*, 814-819.

(89) Pfaender, F. K.; Jonas, R. B.; Stevens, A. A.; Moore, L.; Hass, J. R. *Environ. Sci. Technol.* **1978**, *12*, 438-441.

(90) Hodgeson, J. W.; Cohen, A. L. Determination of chlorination disinfection by-products and chlorinated solvents in drinking water by liquid-liquid extraction and gas chromatography with electron-capture detection. (U.S. EPA, Cincinnati, Ohio, USA, Method 551, 1990).

(91) Lovelock, J. E.; Maggs, R. J. *Nature* **1973**, *241*.

(92) Rook, J. J. *Water Treatment and Examination* **1972**, *21*.

(93) Eichelberger, J. W.; Budde, W. L. Measurement of purgeble organic compounds in water by capillary column gas chromatography/mass spectrametry (environmental monitoring systems, U. S. EPA, Method 542.2, 1990).

CHAPTER 2

Description

Chapter 2 includes a verbatim copy of an article published in January, 2012 in Journal of applied polymer science (J. Appl. Polym. Sci. **2012**, 125, 1841–1854). The paper describes the systematic methods of synthesis and characterization of β-CD/PAA copolymer materials.

Author's contribution

I carried out all of the experimental work from the synthesis to characterization of the copolymers. The solid ^{13}C NMR spectra were obtained by Abdalla Karoyo and elemental analysis result which was conducted by Ken Thomas. This work was principally supervised by Dr. Wilson. I wrote the first draft of the manuscript with assistance in the form of editing of the final manuscript from Dr. Wilson before submitting for publication. The co-authors grant permission of use of the published manuscript for this PhD thesis, and agree with the description of the roles and contributions of the authors.

Relationship of Chapter 2 to the overall objective of this project

As stated in the introduction, the first research objective was the materials design and characterization. This chapter reports the systematic design of a series of β-CD based grafted polyester copolymers by tuning the synthetic conditions (*e.g.*, pre-polymer ratio and stirring speed within the micro-emulsion synthesis). The physiochemical properties of the copolymers are anticipated to be variable according to the nature of the materials. A systematic characterization of the β-CD/PAA copolymers was described in the manuscript, including the sorption properties by gas and dye adsorption methods.

Research highlight:

A series of β-CD/PAA copolymer materials were synthesized using micro-emulsion-evaporation method to cross-link the functional unit β-CD and pre-polymer PAA. The copolymers were prepared by varying the pre-polymer ratio and stirring rate during synthesis to achieve tunable physicochemical properties. Various characterization methods, such as, ^{13}C solid NMR, FT-IR, TGA, DSC, EA, N_2 porosimetry, and dye adsorption method are involved to characterize the copolymers and for the selection of characterization method for further materials design. The sorption isotherms were evaluated with various isotherm models (*e.g.*, Langmuir, BET, Freundlich and Sips) to obtain the equilibrium sorption properties of β-CD/PAA copolymers, which is important in the sense of model-selection for further sorption study of the polysaccharide-based copolymers in this project.

2. Preparation and Sorption Studies of Microsphere Copolymers Containing β-Cyclodextrin and Poly(acrylic acid)

Rui Guo and Lee D. Wilson*

Department of Chemistry, University of Saskatchewan, 110 Science Place, Saskatoon, Saskatchewan, S7N 5C9

*Corresponding author: Tel. 1-306-966-2961, Fax. 1-306-966-4730

email: lee.wilson@usask.ca

2.1. Abstract

Microsphere polymeric materials containing β-cyclodextrin (β-CD) and poly(acrylic acid) (PAA) with tunable morphologies were prepared in order to improve their sorption characteristics in aqueous solution. The microsphere polymeric materials were prepared using a (water/oil) micro-emulsion-evaporation technique to condense β-cyclodextrin (β-CD) with PAA at various co-monomer ratios and mixing speeds. The β-CD microsphere copolymers were characterized using FT-IR, TGA, DSC, SEM, elemental (C and H) microanalyses, and solid state ^{13}C NMR spectroscopy. The sorption properties of the polymeric materials at 295 K in aqueous solution containing *p*-nitrophenol (PNP) were studied using a dye-based method using UV–Vis spectrophotometry at pH 4.6 and 10.3. The sorption isotherms of copolymer/PNP systems were evaluated with various isotherm models (*e.g.*, Langmuir, BET, Freundlich and Sips). The Sips isotherm showed the best overall agreement with the experimental results and the sorption parameters provided estimates of the sorbent surface area (12.0-331 m^2/g) and the sorption capacity (Q_m=0.359-2.20 mmol/g at pH=4.6; Q_m=0.070-0.191 mmol/g at pH=10.3) for the microsphere copolymer/PNP systems in aqueous solution. The nitrogen adsorption properties of the microporous copolymers in the solid state were obtained at 77K with BET surface areas

ranging from 0.275 to 4.47 m^2/g.

Keywords: Cyclodextrin, poly (acrylic acid), copolymers, sorbents, grafting, sorption properties, *p*-nitrophenol

2.2. Introduction

Phenolic compounds are widely used as raw materials in the chemical industry[1] and other applications including petrochemical processing, kraft pulp and paper production, and olive oil products[1, 2]. Phenolic compounds are found extensively in effluent streams and are considered as primary pollutants in waste water due to their relatively high toxicity, high biochemical oxygen demand and relatively low biodegradability[3]. The accumulation and transport of phenol-based pollutants are important environmental issues, which adversely impact aquatic ecosystems, biodiversity, and human health[1, 3, 4]. The United Nations Environment Program (UNEP) has recognized the importance of safe, clean, drinking water by making it one of the eight millennium goals to reduce the proportion of people without sustainable access by half in 2015[4]. Therefore, there is an urgent need to develop novel materials and innovative methods to address the removal of water borne phenols in contaminated aquatic environments.

Cyclodextrins (CDs) are water soluble cyclic oligosaccharides composed of six, seven, or eight glucopyranose units linked by α-1,4-glycosidic bonds; hereafter, they are referred to as α-, β-, and γ-cyclodextrin. CDs possess a torus-shaped macrocyclic structure with a hydrophilic exterior and a lipophilic interior (*cf.* Figure 2.1.a). The lipophilic cavity of the various CDs are suitably sized for the inclusion of low to medium sized lipophilic molecules[5]; with a depth of 7.8 Å and inner macrocyclic diameters of 5.7 Å (α-CD), 7.8 Å (β-CD), 9.5 Å (γ-CD). CDs were recently used as potential pore templates to form microporous and nanoporous materials because of their well-defined structure, relatively low toxicity, versatility, and the ability to form inclusion complexes[6]. CDs can be used to construct copolymer frameworks by chemical cross-linking, grafting or noncovalent self-assembly[6, 7]. In this study, β-CD was used because it forms stable inclusion complexes with a wide range of inorganic and organic guest compounds. In the case of

the latter, compounds containing benzyl and naphthyl moieties are known to form thermodynamically stable inclusion complexes in aqueous solutions[5]. The primary and secondary hydroxyl groups of β-CD are amenable to grafting onto suitable substrates such as poly(acrylic acid) (PAA), a hydrophilic mucoadhesive polymer containing numerous (56% to 68% w/w) carboxylic acid groups[8] (*cf.* Figure 2.1b and 2.1c). Copolymers derived from β-CD and PAA may serve as tunable supramolecular sorbents for the sequestration and immobilization of organic and inorganic pollutants from aqueous solution. In a previous study, CD-based microsphere polymeric materials were prepared with β-CD and PAA using a water-in-oil (w/o) micro-emulsion-evaporation method[9, 10].

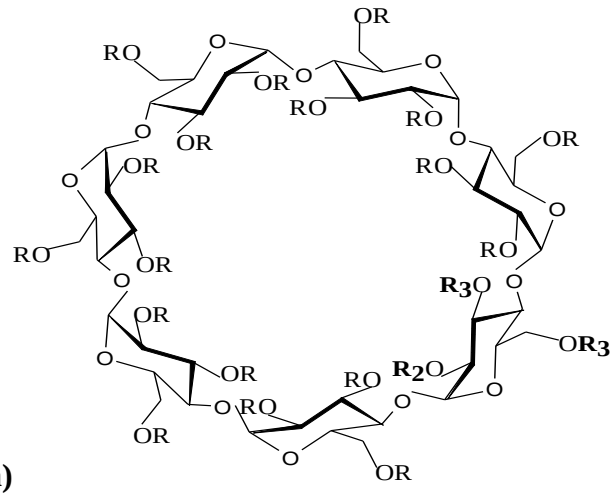

a)

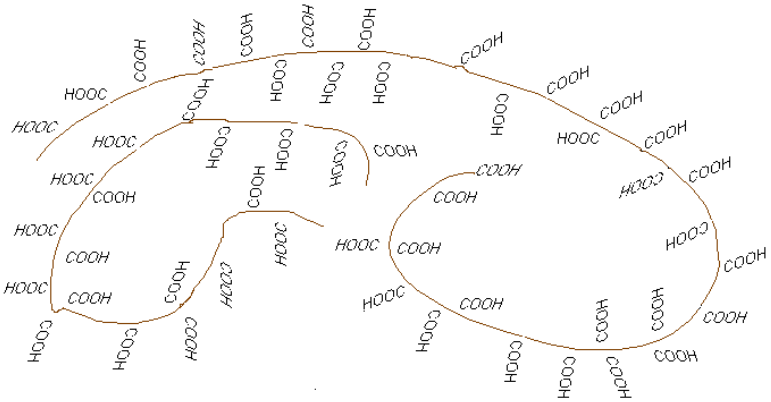

b)

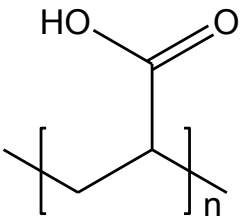

c)

Figure 2.1. Molecular structure of a) β-cyclodextrin (β-CD) where R = H at C_2-, C_3-, and C_6-OH positions. b) Folded structure of Poly (acrylic acid) (PAA), and c) PAA monomer, where n is the degree of polymerization.

The objective of this study was to prepare copolymer materials containing β-CD and PAA at various conditions (*e.g.*, stirring rate and co-monomer ratios) to evaluate changes in their physicochemical and sorption properties. This approach is anticipated to afford materials with markedly different sorption characteristics according to changes in the polymer morphology, surface area, and pore structure properties by tuning the reaction conditions. For example, the formation of β-CD grafted PAA copolymer with micro-emulsion conditions and variable crosslinking density is anticipated to yield copolymers with modified hydrophile-lipophile balance (HLB) relative to that of PAA. The surface area of the copolymer materials were characterized using N_2 adsorption and a UV-Vis dye-based sorption method in aqueous solution, respectively. The adsorbate dye (*p*-nitrophenol; PNP) was studied at variable experimental conditions (*e.g.*, pH and concentration) and the results were evaluated using various (*i.e.* Langmuir, Freundlich, BET and the Sips isotherms) models.

2.3. Experimental Methods

2.3.1. Materials

β-cyclodextrin (β-CD), poly (acrylic acid) (PAA, Mwt. 250,000 g/mol), potassium bromide and *p*-nitrophenol (PNP) were obtained from Sigma-Aldrich Canada Ltd. and used as received

without any further purification. Mineral oil (heavy) and potassium phosphate monobasic were obtained from EMD. Millipore water was used to prepare aqueous solutions. Medical grade nitrogen gas (Praxair) was used as the backfill gas for the nitrogen adsorption experiments.

2.3.2. Synthesis of Copolymer Microsphere Materials

β-CD hydrate (~ 1 g) and PAA (Mwt. 250,000 g/mol) with an accordingly variable mass ratio (1:3, 1:5, 1:10, 5:1, and 10:1; w/w) was utilized and reagent was dissolved in 50 mL water. 1:5 water/oil emulsions were used throughout this study where 250 mL mineral oil was used in two stages (*i.e.* 150 mL and 100 mL). The first portion of mineral oil (100 mL) was pre-heated to 110-120 ℃ in a 500 mL beaker. The aqueous solution was added to the second portion of mineral oil (150 mL) with stirring using a Corning stirrer (PC320) with drop-wise addition, and the mixtures were stirred at 1,100 rpm for 30 min. at ambient conditions. To prepare the copolymers at high mixing speeds, the reaction mixture was homogenized using a Power Fist rotary tool with a custom built stirring head at 13,500 rpm for an additional 10 minutes. The mixture was then added to the pre-heated 100 mL mineral oil at 110-120 ℃ with stirring at 1,100 rpm for 6 hours until the water in the mixture was evaporated. The product and oil were cooled to room temperature, centrifuged (12,000 rpm for 10 min) and the mineral oil was decanted. 25 mL diethyl ether (5×) was added to the product, and centrifuged (12,000 rpm for 2 min.) to wash away residual mineral oil from the copolymer product. The copolymer was dried at 50 ℃, crushed to fine powder, and washed in a Soxhlet extractor with diethyl ether for 24 hours. Finally the copolymer was dried in pistol dryer for 24 hours, ground, passed through a size 40 mesh (≤ 0.42 mm) particle sieve, and subsequently dried under vacuum.

2.3.3. Characterization of Copolymers

IR spectra were obtained with a Bio-RAD FTS-40 instrument and samples were analyzed in reflectance mode. Solid samples were prepared by mixing copolymers (~5 mg) with pure spectroscopic grade KBr (~50 mg) with grinding in a small mortar and pestle. The DRIFT (Diffuse

Reflectance Infrared Fourier Transform) spectra were recorded at room temperature with a resolution of 4 cm^{-1} operating in the range of 400-4000 cm^{-1}. Sixteen scans were recorded and corrected against a background spectrum of pure KBr. The DRIFT spectra were recorded in the reflectance mode (Kubelka-Munk intensity units). The elemental content (w/w; %) of carbon (C) and hydrogen (H) was measured by a Perkin-Elmer 2400 CHN Elemental Analyzer with a detection limit of $\pm 0.3\%$. Solid state ^{13}C NMR spectra with magic angle spinning (MAS) were obtained with a Varian Inova-500 operating at 125 MHz for ^{13}C. Samples were obtained with a MAS frequency of 16 kHz in 3.2 mm vespel rotors. All ^{13}C spectra were acquired under $^{1}H \rightarrow {}^{13}C$ CP (cross polarization) conditions with proton decoupling $\{^{1}H\}$, and external referencing to adamantane (δ = 38.5 ppm) at 295K. Thermal analyses of the copolymers were performed using a thermogravimetric analyzer, TGA (Q50 TA Instruments). Samples were heated in open aluminum pans at 30 °C and allowed to equilibrate for 5 min. prior to heating at a scan rate of 5 °C/min. up to 500 °C. The scan rate for DSC (Q50 TA Instruments) was set to 10 °C per min where a dry nitrogen purge gas was used to regulate the sample temperature and the furnace compartment. DSC samples were analyzed in hermetically sealed aluminum pans over a similar temperature range. Scanning electron microscopy (SEM) images were obtained with a JEOL JSM-840A micro-imager with maximum resolution of images of 6 nm. A few granules of samples were sputter coated with gold (~200 Å thickness) with an Edwards 505 gold sputter coater using argon plasma generated with 1 kV and 30 mA for 3 minutes at 7.5 millibars (mb) with Ar purging during the coating process. The resulting SEM images of the samples are illustrated with a magnification of 1,200× relative to the original image.

2.3.4. Nitrogen Adsorption

Nitrogen adsorption measurements were made using a Micromeritics ASAP 2020 (Norcross, GA) to obtain the surface area and pore structure properties with an accuracy of ±5 % for the copolymers. Approximately 1 g of sample was degassed at 550 μm Hg and ~ 70 ℃ for several hours in the sample chamber until the outgas rate became stabilized. Granular activated carbon

(GAC), alumina, and silica-alumina sieves were used to check the calibration of the instrumental parameters. The BET surface area[11] was calculated from the adsorption isotherm using 0.162 nm^2 as the surface area for nitrogen gas. The micropore surface area was obtained using a *t*-plot (de Boer method)[12, 13]. The Barret-Joyner-Halenda (BJH) method was used to estimate the pore volume and diameter from the adsorption isotherm data[14]. The BJH method uses the Kelvin equation and the assumption of slit-shaped pores[14].

2.3.5. Water Swellability of Copolymer Materials

β-CD/PAA copolymers were placed in 3 dram glass vials containing pure Millipore water and allowed to equilibrate on a horizontal shaker table for 24 h. After the adsorption period, the materials were centrifuged in a precision semi-micro centrifuge at 1550 rpm for 30 min. and the supernatant water was decanted. The copolymer materials were tamped dry with a Whatman filter paper and subsequently tested using TGA from an isothermal set point of 30 ℃ with linear heating at 5 ℃/min. up to 200 ℃. The swelling ratio was determined using the following Eqn. (2.1)[15],

$$r = \frac{m(swollen)}{m(dry)} \qquad (2.1)$$

where r is the swelling ratio, m (dry) and m (swollen) are the respective masses of the copolymer before and after equilibrating with water.

2.3.6. Copolymer Sorption Study

The pore structure properties, surface area, and sorption properties were evaluated using a dye-based UV–Vis method reported previously[16,23] where PNP served as the adsorbate dye. Fixed amounts (~10 mg) of the powdered and sieved copolymer materials were mixed with 7 mL of aqueous solution at variable dye concentration (0.2–10 mM) in 10 mM potassium phosphate monobasic buffer solution until fully equilibrated on a horizontal shaker table for 24 h. The buffers were prepared at pH 4.6 and 10.3, respectively, to study the sorption properties of PNP in its neutral and deprotonated forms. The initial concentration of PNP (C_o) was determined before and

after sorption (C_e) with the β-CD/PAA copolymers. The estimated molar absorptivity (ε) values for PNP were determined as follows: ε=9286.5 L mol^{-1} cm^{-1} (pH= 4.6; λ_{max}= 317 nm) and ε =18,478 L mol^{-1} cm^{-1} (pH =10.3; λ_{max}= 400 nm), in agreement with published values[17]. The sorption isotherms are depicted as plots of the adsorbed amount of PNP in the copolymer phase per mass of adsorbate (Q_e; mmol/g) versus the equilibrium residual concentration of unbound PNP in aqueous solution (C_e). The value of Q_e is defined by eqn. (2.2) where C_o is the initial PNP concentration, V is the volume of solution, and m is the mass of sorbent.

$$Q_e = \frac{(C_0 - C_e) \times V}{m} \qquad (2.2)$$

The dye sorption method[16] provides an independent estimate of the sorbent surface area (SA; m^2/g) in its hydrated state, according to eqn 2.3.

$$SA = \frac{A_m Q_m L}{Y} \qquad (2.3)$$

where A_m represents the cross-sectional area occupied by PNP (A_m for a "coplanar" orientation is 5.25×10^{-19} m^2/mol whereas an "orthogonal" orientation is 2.5×10^{-19} m^2/mol), Q_m is the monolayer adsorption capacity per unit mass of sorbent, L is Avogadro's number (mol^{-1}), and Y is the coverage factor (Y = 1) for PNP [18].

The Freundlich, Langmuir, BET, and Sips isotherm models were used to analyze the sorption data [19-21, 21, 22]. The Langmuir model (*cf.* eqn 2.4) represents a monolayer sorption process onto a homogenous surface whereas the BET model (*cf.* eqn 2.5) describes multi-layer adsorption processes. The Freundlich model (*cf.* eqn 2.6) assumes that the sorbent surface is heterogeneous in nature with an exponential distribution of active sites when an unlimited number of sorption sites are available. The Sips isotherm is a generalized isotherm model that accounts for a distribution of adsorption energies on the sorbent surface and accounts for monolayer (Langmuir) to multi-layer (Freundlich) isotherms. The Sips isotherm is a relatively versatile model with several adjustable parameters where the exponent (n_s) term reflects the heterogeneity of the sorbent. A value of n_s=1 infers a homogenous surface whereas a heterogeneous surface is inferred when $n_s \neq 1$. Langmuir

isotherm behavior is predicted when n_s=1, and Freundlich behavior occurs when $K_s C_e^{n_s}$ <<<1. The Langmuir, BET, Freundlich and Sips models are defined in eqns. 2.4-2.7 [19-21, 21, 22].

$$Q_e = \frac{K_L Q_m C_e}{1 + K_L C_e} \qquad (2.4)$$

$$Q_e = \frac{K_{BET} Q_m C_e}{\left(1 - \frac{C_e}{C_s}\right)\left[1 + \left(K_{BET} - 1\right)\frac{C_e}{C_s}\right]} \qquad (2.5)$$

$$Q_e = K_F C_e^{\frac{1}{n}} \qquad (2.6)$$

$$Q_e = \frac{Q_m K_s C_e^{n_s}}{1 + K_s C_e^{n_s}} \qquad (2.7)$$

where K_F, K_L, K_{BET} , and K_s are the Freundlich, Langmuir, BET, and Sips equilibrium constants. C_s is the saturated aqueous solution solubility of PNP, and Q_m is defined above in eqn. (2.3). 1/n is the inverse of the Freundlich exponent and is a measure of the adsorption intensity.

The criteria of the "*best-fit*" between the calculated isotherm and the experimental data are determined by the correlation coefficient (R^2) and the chi-square distribution (χ^2). The parameter $R^2 \sim 1$ denotes a "*best-fit*"; however, a more sensitive measure for non-linear least squares fitting involves the minimization of χ^2. χ^2 is defined by eqn. (2.8) according to the difference between the experimental ($Q_{e,i}$) and calculated ($Q_{c,i}$) sorption values toward PNP in aqueous solution

$$\chi^2 = \sum \sqrt{\frac{\left(Q_{e,i} - Q_{c,i}\right)^2}{N}} \qquad (2.8)$$

where $Q_{c,i}$ is the calculated Q_e value with an appropriate isotherm model (*cf.* eqn 2.3-2.6), and N is the number of experimental data points.

2. 4. Results and discussion

2.4.1. Synthesis of Copolymer Materials

Microsphere β-CD-PAA copolymers were prepared using variable weight ratios of β-CD to PAA (*i.e*. 1:10, 1:5, 1:3, 1:1, 5:1, and 10:1; w/w) at relatively low (1,100 rpm) and high mixing speeds (13,500 rpm), respectively. The adopted notation to represent these conditions are as follows: 10:1_135, 5:1_135 and 1:5_135 where the ratio represents the relative co-monomer mass ratio (β-CD: PAA) and the latter number designates the stirring speed, respectively. According to the different β-CD:PAA ratios, the copolymers exhibited different physical appearance, physical characteristics (*e.g*., thermal stability) and product morphology which varied from crystalline to amorphous powders. The relative mixing speed affects the morphology of the copolymers by altering the water droplet size in the micro-emulsion; thereby, affecting the surface area and pore structure properties of the microsphere copolymers. In contrast to the water soluble reactants, β-CD and PAA, the copolymer products are generally insoluble. The insolubility of copolymers in water is an important property for the design of sorbents for the study of solid-solution sorption equilibria, as outlined herein.

2.4.2. Characterization of Copolymer Materials

The FT-IR spectra for the starting materials (β-CD and PAA) and the β-CD:PAA copolymers (10:1, 5:1, 1:5 and 1:10) are shown in Figure 2.2.A. The –OH (~3400 cm^{-1}), -CH (~2900 cm^{-1}) and –C=O (~1700 cm^{-1}) stretching regions are present in the copolymer products and confirm their molecular identity. The IR spectra for the copolymers generally represent additive features of the characteristic functional groups present in the starting materials. However, each copolymer has –C=O band (~1730 cm^{-1}) due to the formation of the ester linkage between β-CD and PAA (*cf*. Fig. 2.2.A), which agrees with previous reports[23, 24]. The –C=O vibrational band is relatively broad for the copolymers as compared to β-CD, especially for the copolymers with greater PAA content (1:5 and 1:10). A possible reason may be the overlap of the IR signatures for the unreacted carboxylic groups of PAA (-COOH) and the crosslinked ester (-COOR; R= β-CD) linkages of the grafted

PAA. The carbonyl band (~ 1700 cm^{-1}) also shows a shift in frequency that varies according to the β-CD:PAA co-monomer ratio. Generally, the IR spectra of copolymers 10:1 and 5:1 tend to resemble the spectral features observed for β-CD hydrate whereas the 1:5 and 1:10 spectra tend to resemble the broad spectral features of PAA (~2900 cm^{-1}, ~1700 cm^{-1} and 1500-500 cm^{-1}). The broad features relate to the polydisperse nature of the PAA polymers and its amorphous structural characteristics. The copolymer products obtained from preparations at the various mixing speeds do not reveal any major differences amongst copolymers with similar β-CD:PAA ratios (*i.e*. 10:1 and 10:1_135, 5:1 and 5:1_135, and 1:5 and 1:5_135), as evidence in Fig. 2.2.B-D. A notable difference is the relative intensity changes of the –C=O to –OH vibration bands for the copolymers prepared at high *vs*. low speed mixing conditions, respectively. The –C=O band shows a reduced intensity for the copolymers prepared at high mixing speeds.

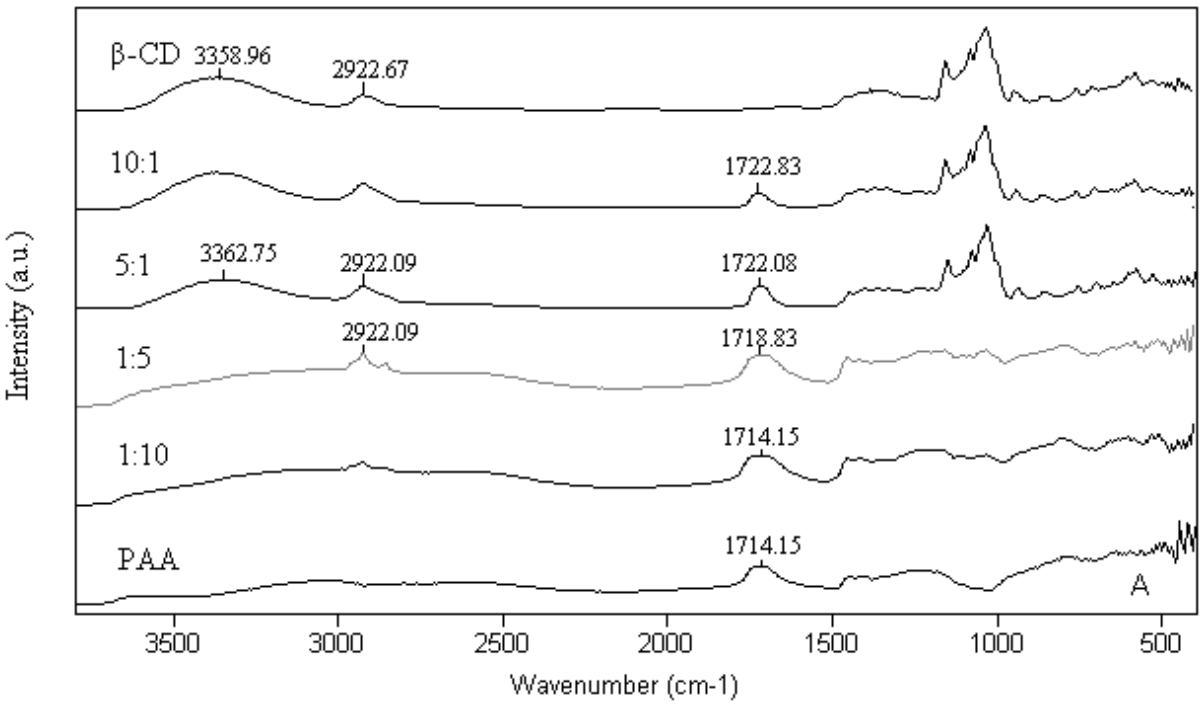

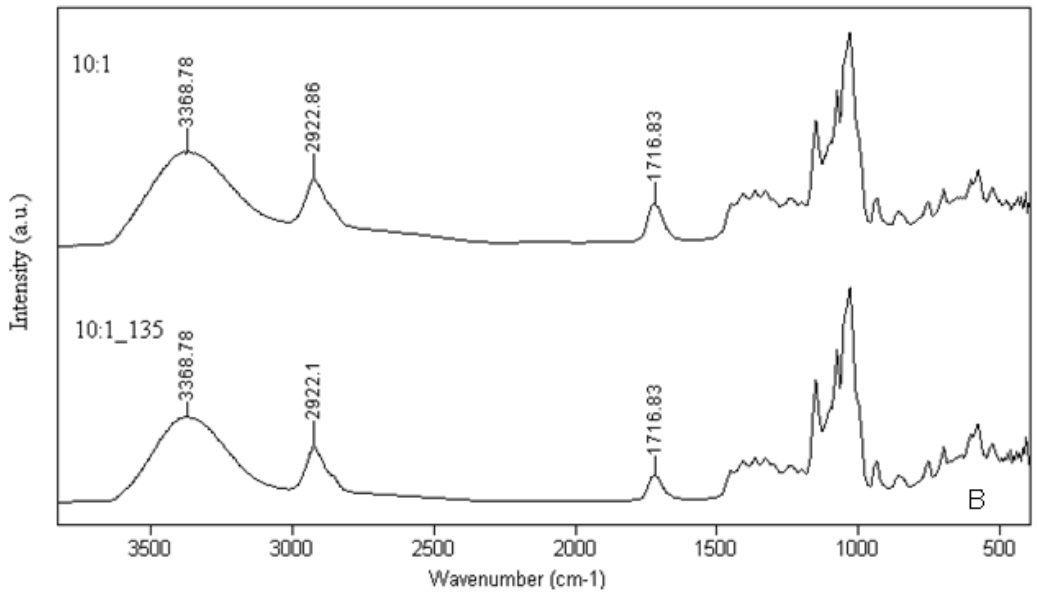
10:1
3368.78
2922.86
1716.83
10:1_135
3368.78
2922.1
1716.83
B
Intensity (a.u.)
3500
3000
2500
2000
1500
1000
500
Wavenumber (cm-1)

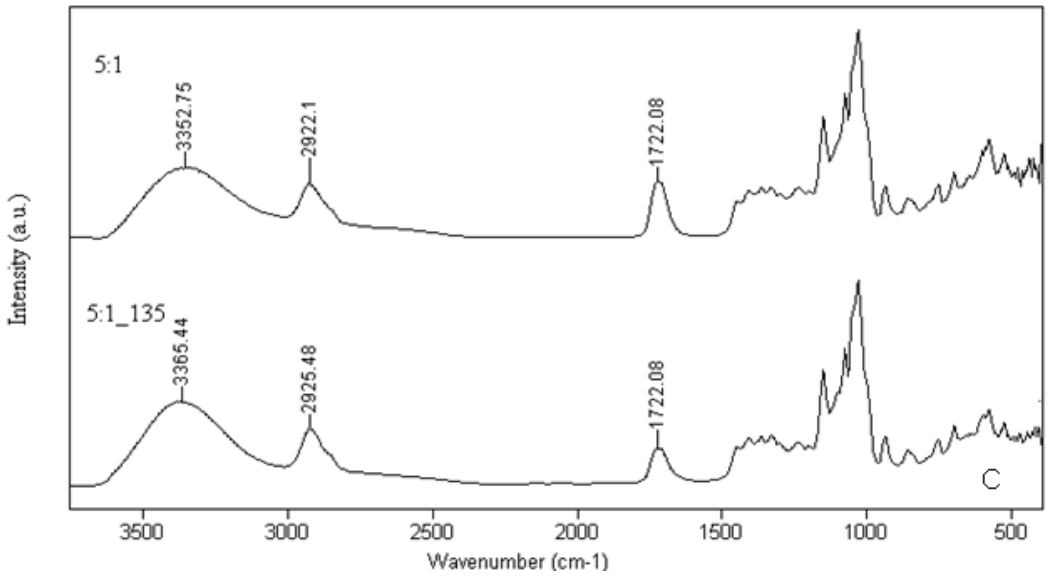
5:1
3352.75
2922.1
1722.08
5:1_135
3365.44
2925.48
1722.08
C
Intensity (a.u.)
3500
3000
2500
2000
1500
1000
500
Wavenumber (cm-1)

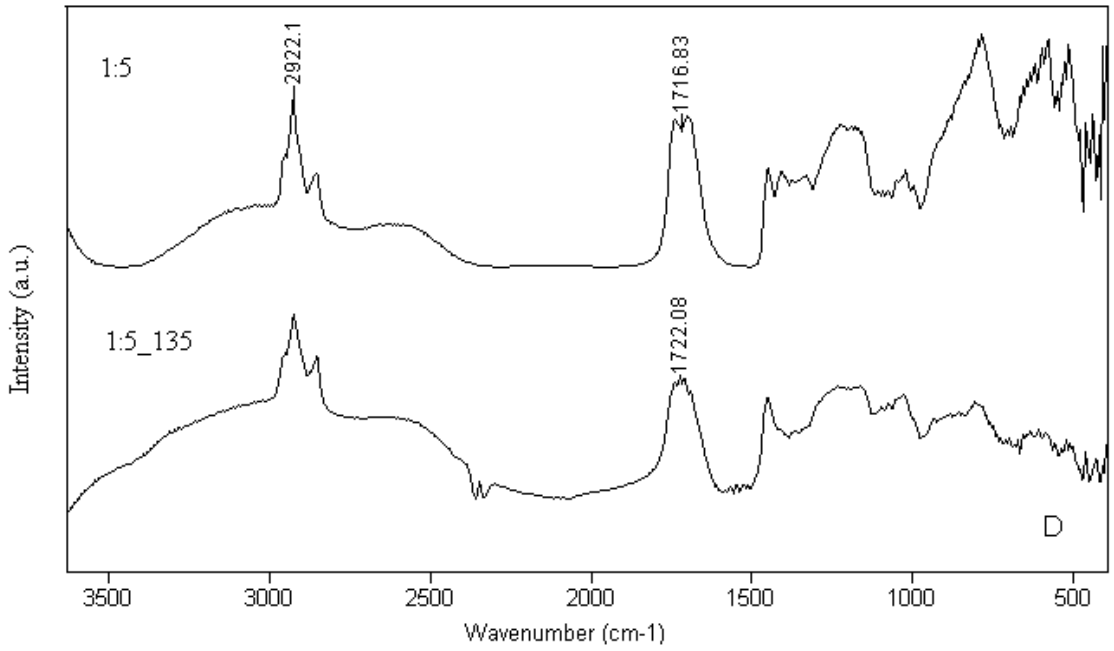

Figure 2.2. IR spectra (DRIFTS) for A). β-CD and β-CD/PAA copolymers 1:10, 1:5, 10:1, and 5:1 (w/w ratios) at room temperature. B). β-CD/PAA copolymers 10:1 and 10:1_135 using low and high mixing speeds (1,100 and 13,500rpm), respectively C). 5:1 and 5:1_135 D). 1:5 and 1:5_135.

Figure 2.3. illustrates the ^{13}C CP-MAS NMR spectra of the 5:1 and 1:5 β-CD:PAA copolymers, along with the co-monomers, β-CD hydrate and PAA. Although each glucose unit of β-CD contains six unique ^{13}C atoms per glucose residue, the spectra for the copolymers in Figure 2.3 reveal approximately four unique ^{13}C NMR lines between 60 and 110 ppm due to the overlap of some of the individual ^{13}C resonance lines, in agreement with a previous report[31]. Similar ^{13}C NMR signatures observed in Fig. 2.3. for β-CD are similarly noted for the 5:1 and 1:5 copolymer materials, especially for the copolymers with greater β-CD content. The β-CD macrocycle in copolymer materials is covalently grafted onto the PAA polymer chain as a pendant group via an ester linkage via the primary C6-OH groups of β-CD (*cf*. Fig. 2.1) because of its greater reactivity relative to the secondary (*i.e*. C2- and C3-OH) hydroxyl groups. Thus, β-CD is tethered to the

polymer chain at one or more hydroxyl groups which facilitates sufficient motional dynamics that contribute to the relatively narrow lines, as compared with other types of conventional cross-linked copolymer materials[23]. The carbonyl signature (~170-183 ppm) for the copolymer materials is attributed to the numerous carboxylic acid and ester groups along the PAA backbone. The reduced NMR intensity of the carbonyl signature for the 5:1 copolymer is attributed to a reduction in cross polarization due to esterification (-COOR) of the carboxylic acid (-COOH) groups of PAA and changes in the hydration state of the material. The presence of an adjacent H atom in the –COOH groups with variable hydration contribute to variable cross polarization transfer (H→C) dynamics. Compared to the sharp resonance lines of β-CD hydrate, the broad ^{13}C resonance lines for the aliphatic signatures (~ 15-50 ppm) of the PAA backbone are related to the variable conformations of aliphatic chain and contributions arising from the polydisperse chain length distribution of PAA. The broad resonance lines of the subunits for the β-CD:PAA copolymers illustrate the amorphous character of the materials, according to an ensemble of molecular environments due to random attachment of the co-monomers. The foregoing ^{13}C CP-MAS NMR results are consistent with grafted copolymer materials containing β-CD and PAA[10].

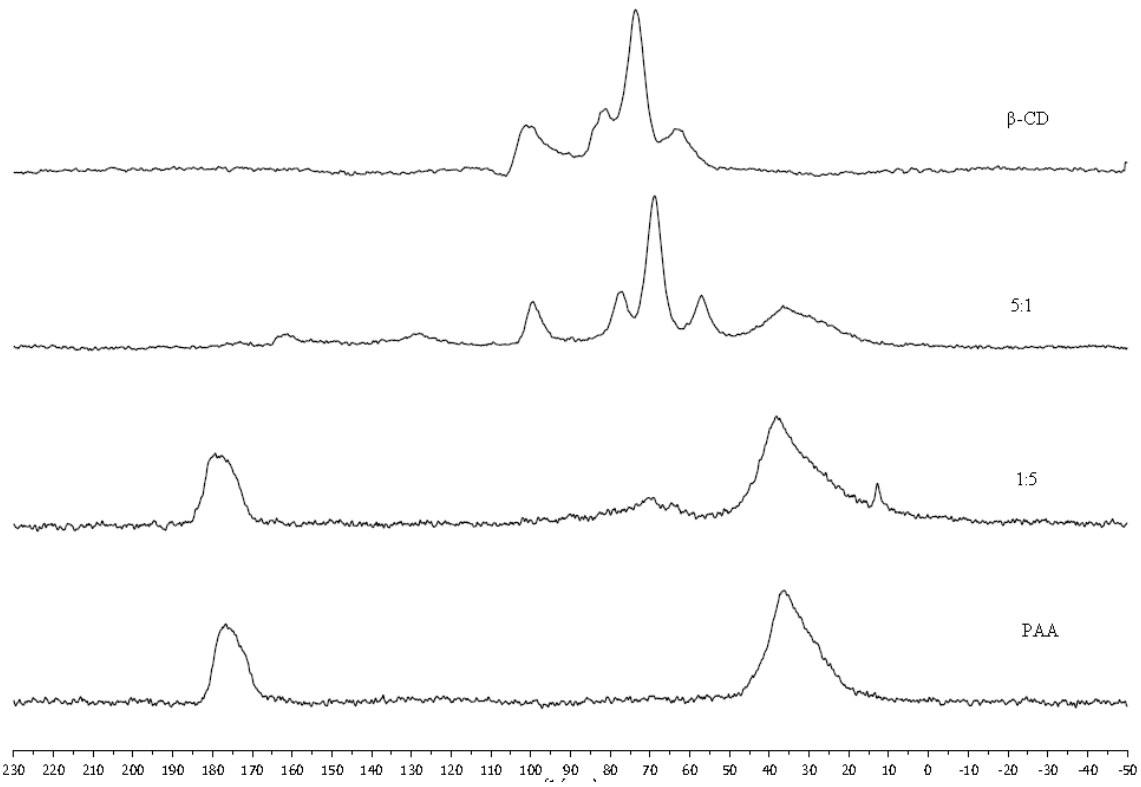

Figure 2.3. ^{13}C CP-MAS NMR spectra for β-CD, β-CD/PAA copolymers 5:1, 1:5 and PAA at 295 K.

In Fig. 2.4, the TGA results are presented as the derivative weight (mass loss/temperature) against temperature for the copolymers and co-monomers, respectively. Different thermal profiles are observed for the various copolymers as the relative monomer content is varied. Accordingly, the TGA results for the copolymers show two thermal events near 275 ℃ and 400 ℃, respectively. The mass loss corresponds to the decomposition of the respective co-monomers (*i.e*. β-CD and PAA) at their respective thermal decomposition temperatures. The relative mole ratios of β-CD and PAA were estimated by deconvolution of the thermal events of the tabulated peak areas in Table 2.1. As the β-CD composition of the copolymer increases, the area corresponding to the

thermal event ~ 275 ℃ increases. Similarly, the integrated area ~ 400 ℃ increases as the PAA content of the copolymer increases. The relative peak areas observed in Fig. 4 correlate with the observed intensity change for the IR results for each co-monomer subunit. In Figure 2.4B, the copolymers prepared at high speed conditions show greater β-CD content relative to slower mixing speed conditions (*e.g*., 5:1 and 5:1_135). Notwithstanding the presence of trace solvent residues in the copolymer sorbents, the results are in general agreement with the C and H elemental micro-analyses (*cf*. Table 2.2)[27]. Based on the IR, TGA, and the elemental micro-analyses, a greater amount of β-CD was grafted onto the PAA at higher mixing speed conditions. The higher mixing speeds produce greater internal pressure within the water droplets of the w/o micro-emulsion, and provide further support for the observed effects. The higher mixing speeds produce smaller droplets and favour the formation of such condensation reactions[16,17]. The relative offset in the grafting efficiency of β-CD onto PAA is less apparent at 10:1 *vs*. 5:1 copolymers at variable spinning speed; however, this can be related to increased steric effects as the PAA chain becomes increasingly grafted. The β-CD content of the grafted copolymer materials are observed to adopt the following order: 10:1_135 ~ 10:1 > 5:1_135 > 5:1> 1:5_135 > 1:5 > 1:10 (w/w).

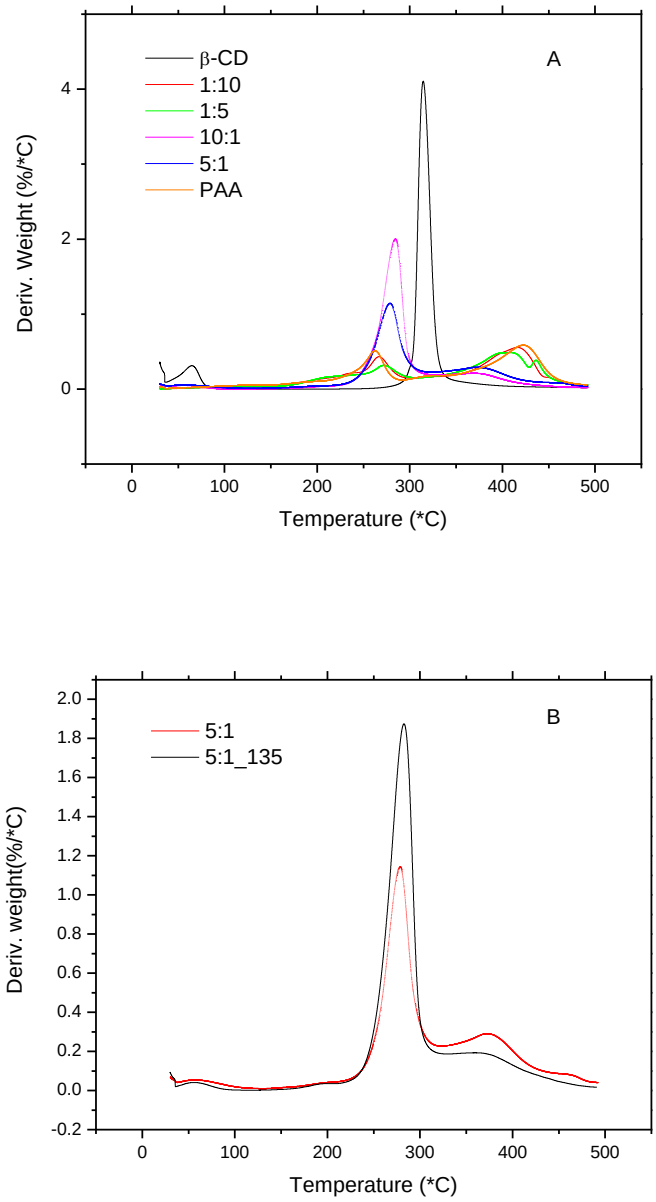

Figure 2.4. A). TGA of β-CD, PAA and β-CD/PAA copolymers 1:10, 1:5, 10:1, and 5:1 (w/w). B). β-CD/PAA copolymers 5:1 and 5:1_135 using low and high mixing speed (1,100 and 13,500rpm, respectively).

Table 2.1. Experimental[1] and calculated[2] mole ratios of β-CD to PAA.

β-CD/PAA Copolymers (w/w)	Experimental value[1] (β-CD:PAA)	Calculated value[2] (β-CD:PAA)	χ^{2a}
1:10	14:1	22:1	0.00005
1:5	42:1	44:1	0.00033
10:1	239:1	2203:1	0.00252
10:1_135	302:1	2203:1	0.00554
5:1	122:1	1101:1	0.00043
5:1_135	239:1	1101:1	0.00262

[a] χ^2, Chi-square distribution

[1]Experimental values (mole ratio) obtained from TGA deconvolution results

[2]Calculated values (mole ratio) obtained from mass ratios of β-CD/PAA from the reactants used in the synthesis

Table 2.2. Calculated elemental composition (%C and %H (w/w %)) for β-CD and PAA and elemental (C, H) analysis results for the comparison between copolymers using high (5:1, 1:5) and low (5:1_135, 1:5_135) mixing speeds, respectively.

	PAA (cal.[a])	β-CD (cal.[a])	5:1	5:1_135	1:5	1:5_135
%C	50.0	44.4	46.1	45.8	48.3	48.2
%H	5.56	6.17	7.14	6.97	6.29	6.32

[a]The calculated elemental composition was calculated based on known molecular weight and formula of the molecules.

The DSC plots shown in Figure 2.5 indicate that the copolymers have modified thermal stability relative to the co-monomers (PAA and β-CD), as anticipated for cross-linked copolymer materials. The greater temperature onset for the PAA co-monomer in the copolymer material illustrates that the thermal stability of PAA is enhanced. The grafted copolymer is anticipated to display different morphology relative to PAA because grafting of β-CD onto the –COOH surface groups will affect the packing and intermolecular interactions between adjacent copolymer chains in the solid state. The broadened thermal transitions for the copolymers and the broader ^{13}C NMR signatures provide evidence that the copolymer material is amorphous in nature. The incremental grafting of β-CD onto PAA increases the molecular weight of the copolymer and alters its thermophysical properties in a corresponding manner, as evidenced from the DSC results of Fig. 2.5.

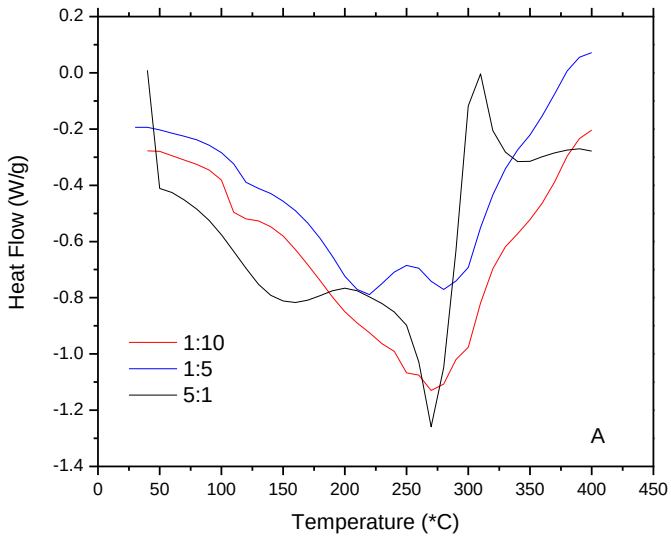

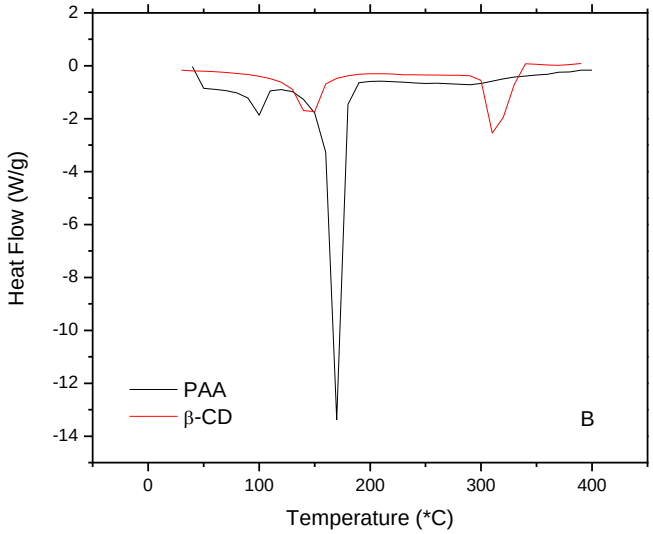

Figure 2.5. DSC thermograms of A). β-CD/PAA copolymers 1:10, 1:5, 10:1, and 5:1 (w/w) and B). β-CD and PAA in the temperature range 35-450 ℃ at a scan rate of 10 ℃/min.

2.4.3. Nitrogen Adsorption

The sorption properties of the copolymer materials in the solid state were studied by nitrogen porosimetry (*cf.* Table 2.3). Figure 2.6A-D illustrates the nitrogen adsorption-desorption isotherms β-CD/PAA copolymers and the PAA precursor. The copolymers show the hysteresis loops which represent Type IV isotherms. Type IV isotherms generally describe the monolayer-multilayer adsorption of microporous adsorbents[25]. The corresponding hysteresis loops feature parallel and almost horizontal branches (Type H1 and H3) and have been attributed to adsorption-desorption in narrow slit-like pores that are often associated with narrow pore size distributions[25]. The BET surface area estimates for 10:1 and 10:1_135 are 4.47 and 3.90 m^2/g, respectively. The copolymers with high PAA content (1:5) yielded lower BET surface area (0.275 m^2/g); whereas, the 1:3 β-CD:PAA copolymer was slightly greater (0.287 m^2/g). The magnitude of the BET estimates

obtained herein are similar in magnitude to those for 1:22 β-CD-epichlorohydrin copolymers (~0.2 m^2/g, BET)[26]. A contributing factor for the attenuated surface areas may originate from the disordered and collapsed copolymer framework in the anhydrous state, and the reduced accessibility of the micropores in the copolymer framework. At low β-CD content, the PAA copolymer forms a more densely packed framework. In contrast, copolymers with greater β-CD content may have reduced packing density which results in the formation of micropore sites, evidenced by the greater sorption of N_2 in such materials. The high speed copolymer materials (10:1_135) show attenuated sorption toward nitrogen relative to the copolymers prepared at reduced mixing speed (10:1) because of the greater crosslink density and reduced pore size of the 10:1_135 material, described above. Similarly, the highly cross-linked and dense framework structure attenuates the accessibility of nitrogen gas. Additionally, PAA is considered a "*soft material*" with significant conformational motility of the PAA backbone. This results in a fairly low BET surface area (0.376 m^2/g) in the solid state since the polymer likely adopts a collapsed micropore structure with reduced surface area, as compared to the hydrated copolymer in aqueous solution[27].

Table 2.3. N_2 porosimetry method estimates of the Surface area for the polymeric materials and their starting materials β-CD and PAA at 77K.

Sorbent materials	10:1	10:1_135	5:1	5:1_135	1:5	1:3	β-CD	PAA
Surface area[a] (m^2/g)	4.47	3.90	1.63	0.970	0.275	0.287	1.20	0.376

[a]According to N_2 porosimetry and using a linearlized BET model.

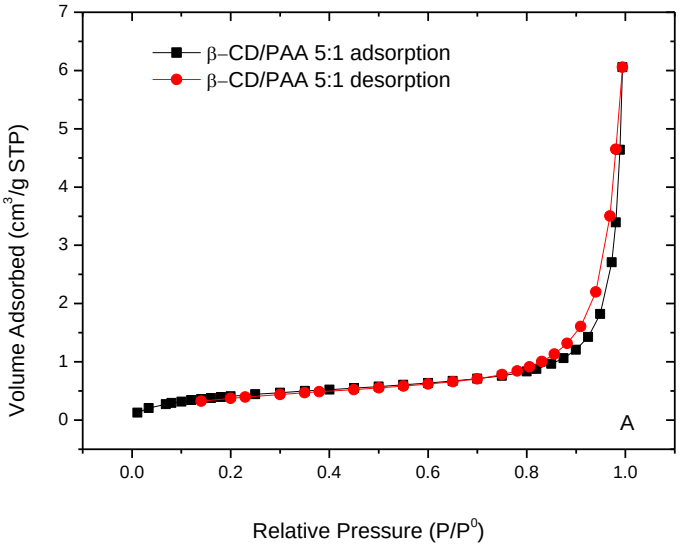
β–CD/PAA 5:1 adsorption
β–CD/PAA 5:1 desorption
Volume Adsorbed (cm3/g STP)
Relative Pressure (P/P0)
A
0
1
2
3
4
5
6
7
0.0
0.2
0.4
0.6
0.8
1.0

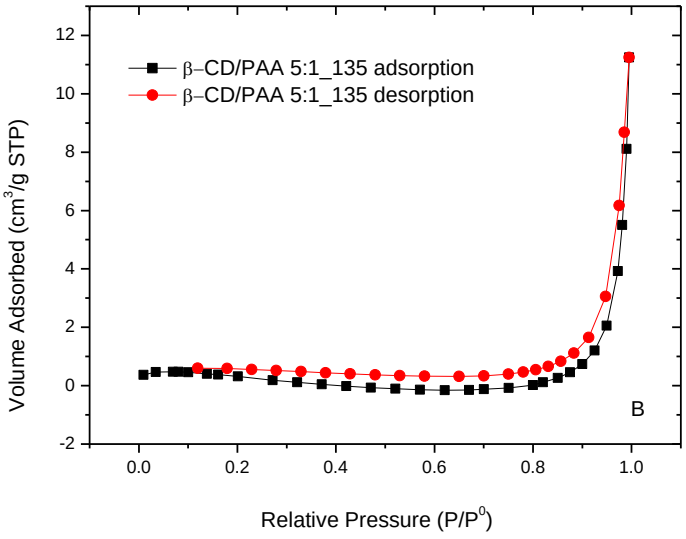
β–CD/PAA 5:1_135 adsorption
β–CD/PAA 5:1_135 desorption
Volume Adsorbed (cm3/g STP)
Relative Pressure (P/P0)
B
-2
0
2
4
6
8
10
12
0.0
0.2
0.4
0.6
0.8
1.0

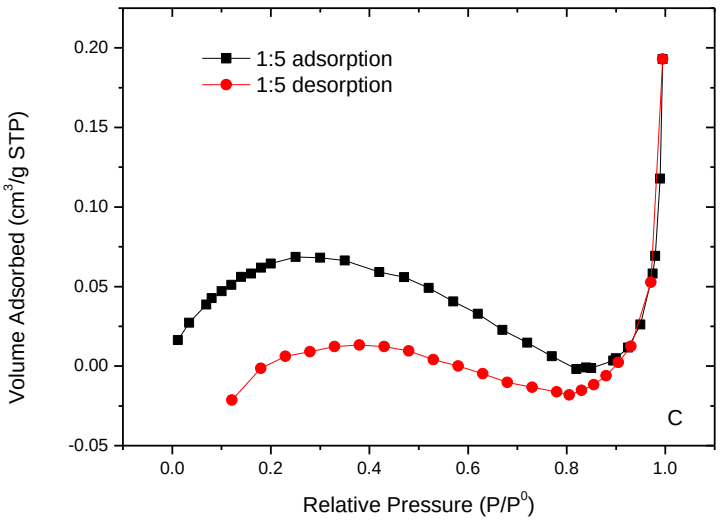

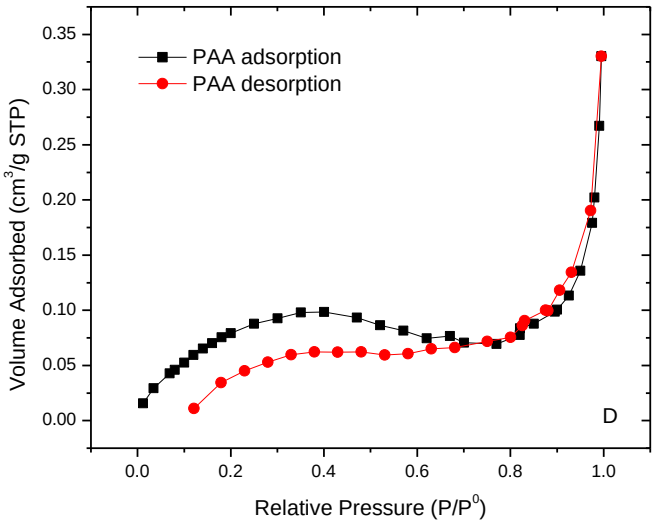

Figure 2.6. Nitrogen adsorption-desorption isotherm for β-CD/PAA copolymers materials and their starting materials A) 5:1; B) 5:1_135; C) 1:5; D) PAA using N_2 porosimetry at 77K.

2.4.4. Water Swellability Studies

The occurrence of potential swelling of the copolymer framework in aqueous solution motivated a study of the swelling property of such materials[28]. The swelling properties of the 5:1 and 1:5 β-CD:PAA copolymers were studied in water using a TGA-based method (*cf.* Fig. 2.7A -B). The copolymer with greater PAA content (1:5 β-CD:PAA) shows greater swelling than the 5:1 β-CD:PAA copolymer. The greater swelling of the 1:5 copolymer is attributed to the higher PAA content and its hydrophilic characteristics. The swelling ratio was calculated from the gravimetric loss using TGA results and eqn 2.1. After 24 hours of equilibrium swelling in deionized water, the hydrated 1:5 polymer was observed to have a swelling ratio r=59 and the 5:1 β-CD:PAA had a value of r=5. The results show that the 1:5 β-CD/PAA adsorbs ~59 times the amount of water relative to its mass. In contrast, the 5:1 β-CD/PAA copolymer adsorbs ~ 4 times its weight in water relative to its dry mass. In Fig. 2.7, the desorption temperature of water for the 5:1 β-CD:PAA copolymer is ~ 60 ℃, indicating that adsorption occurs mainly on the surface sites. In contrast, the 1:5 copolymer has a wider temperature range of desorption (~40-120 ℃) where the maximum water desorption occurs ~ 110 ℃. Water is adsorbed at both the surface and micropore framework sites of the 1:5 copolymer. The increased swelling of the copolymers with greater PAA content may result from the favourable hydration of the –COOH groups. Such hydration effects are anticipated to contribute to morphological changes and surface area effects due to swelling of the copolymer framework[28].

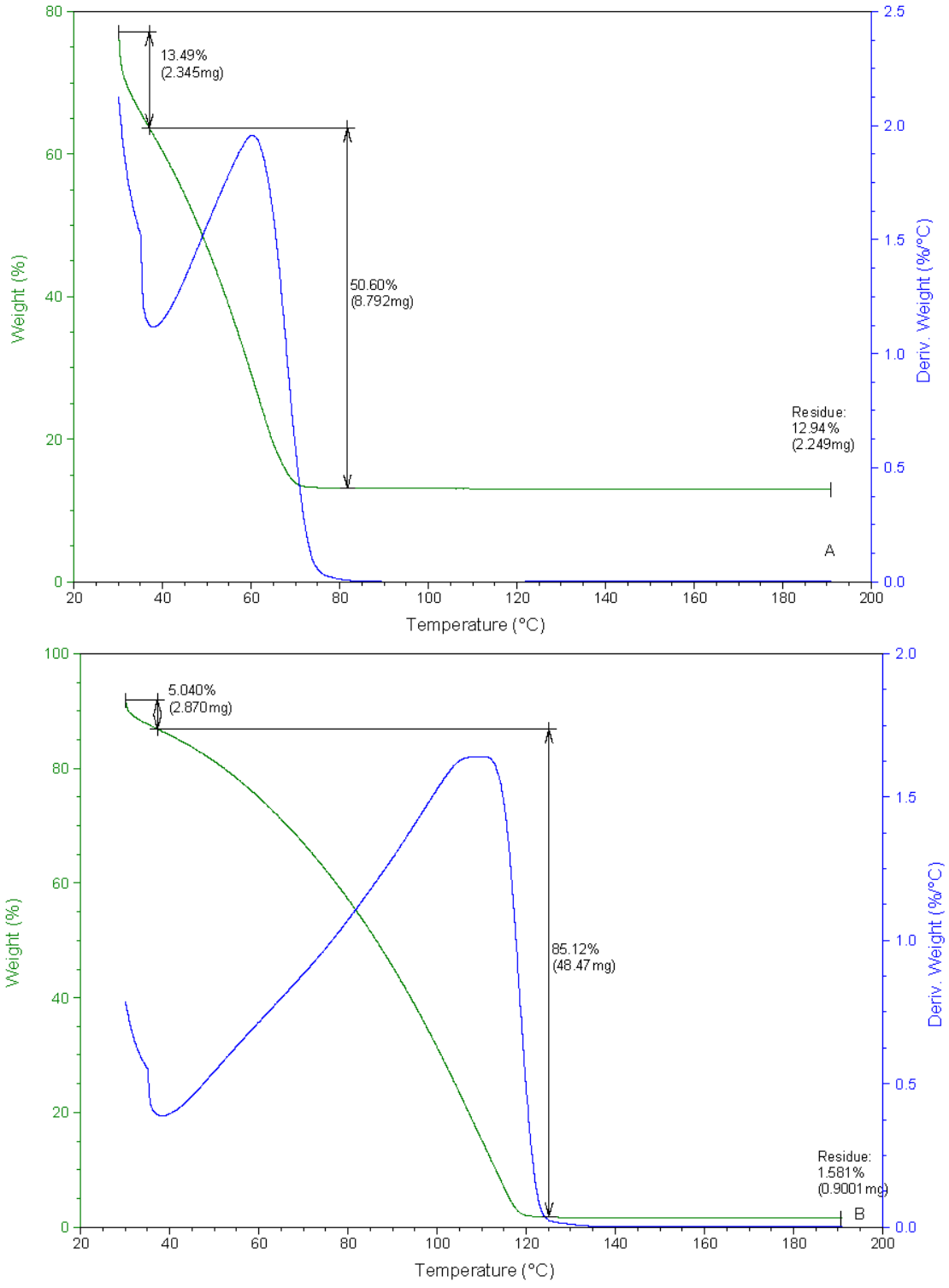

Figure 2.7. TGA of β-CD/PAA copolymers A. 5:1 and B. 1:5 (w/w) (saturated in Millipore water for 24hours) water removal.

2.4.5. Copolymer Sorption Studies

2.4.5.1. Sorption properties at pH 4.6

The sorption properties of the copolymer materials were studied at 22 ℃ with PNP as the adsorbate molecule, below and above the pK_a for PNP (pH 4.6 and 10.3), respectively, in aqueous solution. The decolouration of PNP in the supernatant solution was monitored at equilibrium in solutions containing fixed amounts of copolymer. The absorbance of PNP ranged from yellow to various levels of decolourization over the concentration range investigated at pH 4.6. At similar conditions, the inclusion of PNP by β-CD results in enhancement of the molar absorptivity of the dye in aqueous solutions. The attenuation observed in the case of the β-CD:PAA copolymer materials was related to the unique intermolecular interactions between the PAA co-monomer and PNP.

In Figure 2.8, the sorption isotherms (Q_e *vs.* C_e) are shown for the 5:1 and 1:5 β-CD:PAA copolymers at pH 4.6. In general, the magnitude of Q_e increases monotonically with increasing C_e. The isotherms for the 5:1, 1:5, 5:1_135 and 1:5_135 β-CD:PAA copolymers were analyzed by various models, described by eqns. (2.4-2.7). The *best-fit* parameters obtained from each model are listed in Table 2.4. The Langmuir model generally showed unsatisfactory fits except for the 5:1 β-CD/PAA copolymer. In contrast, the BET isotherm provides a more suitable fit to the sorption data; however, greater χ^2 values are observed (*cf.* Table 2.4). The Sips isotherm provides a good general description of the sorption behavior for each of the copolymers, and the n_s parameter provides an estimate of the surface heterogeneity. Monolayer (*i.e.* Langmuir) adsorption behavior is observed for isotherms when n_s=1, according to the Sips isotherm. The 5:1 copolymer yields a heterogeneity parameter (n_s=1) and reasonable agreement is observed with the three isotherms (Langmuir, BET and Sips); whereas, poor agreement is observed for the Freundlich model. Heterogeneous sorption sites are concluded as the value of n_s deviates from unity. In copolymer materials, heterogeneous sorption ($n_s \neq 1$) may occur because of the occurrence of inclusion and non-inclusion binding sites. In Table 2.4, the 1:5 copolymers (n_s=1.4, *cf.* Figure 2.8B), 1:5_135 (n_s=1.5) and 5:1_135 (n_s=1.2) are well-described by the Freundlich model because it accounts for

such heterogeneous adsorption processes. Over the range of dye concentrations examined, the saturation of the 1:5 β-CD:PAA copolymer is not achieved. There are multiple sorption sites if one considers the potential contribution of the β-CD (*inclusion*) sites and the PAA surface (*non-inclusion*) sites of the PAA backbone. In Figure 2.8B, the 1:5 β-CD:PAA copolymer does not show saturation of the sorption sites when C_e reaches ~10 mM. In general, the Sips isotherm model shows favorable agreement with the observed sorption results of copolymers. In addition to the heterogeneity parameter (n_s), the K_{Sips} parameter provides insight about the sorption affinity between the sorbent and PNP. The Sips isotherm was the preferred model to describe the overall sorption behavior for the systems in this study because of its versatility in describing monolayer- to multi-layer sorption phenomena, according to the overall *goodness-of-fit* observed.

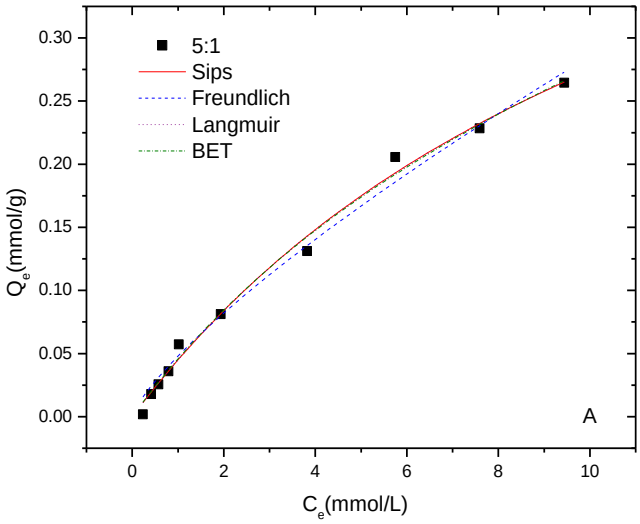

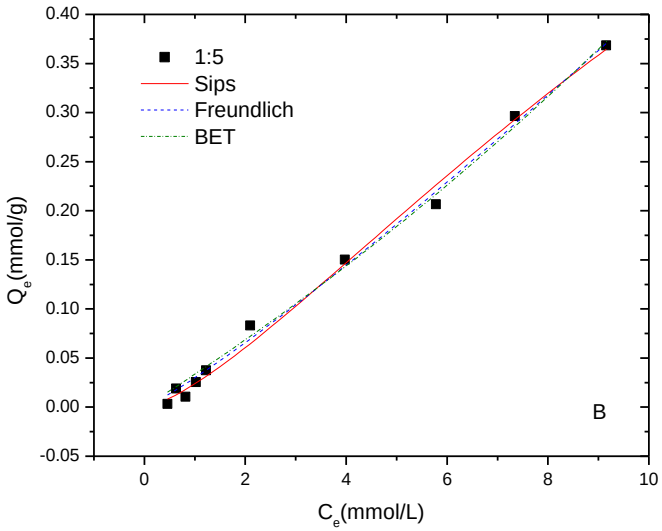

Figure 2.8. Sorption isotherm for β-CD/PAA copolymers A. 5:1 (w/w), n_s=1.0 and B. 1:5 (w/w), n_s=1.4 using various fitting models: Sips, Freundlich, Langmuir, and BET.

Figure 2.9A shows the Sips isotherm (Q_e *vs.* C_e) results for the 5:1 and 1:5 β-CD:PAA copolymer and PAA at pH 4.6. The value of Q_e increases monotonically as C_e increases. The sorption data were fit using the Sips isotherm (*cf.* Eqn. 2.7) and the "*best-fit*" sorption parameters for this model are listed in Table 2.4. In Table 2.5, the dye-based SA estimates of the copolymers were estimated using Q_m (Table 2.5) and eqn. 2.3. The values in Table 2.5 range from 54.0 m^2/g to 331 m^2/g at pH 4.6 and are two orders of magnitude greater than the BET SA values in Table 2.3.

Table 2.4. Sorption parameters obtained from the dye-based method for copolymer materials for the sorption of PNP at pH 4.6 and 295K according to various isotherm models.

Isotherm models	Parameters	5:1	5:1_135	1:5	1:5_135
Langmuir	Q_m (mmol/g)	0.632	-	-	-
	K_L (L/mmol)	0.0766	-	-	-
	R^2	0.994	-	-	-
	χ^2	0.0000700	-	-	-
BET	Q_m (mmol/g)	0.478	1.66	2.19	15.7
	K_{BET} (Lmmol/g^2)	8.29	1.87	1.55	0.186
	R^2	0.996	0.996	0.995	0.994
	χ^2	0.0182	0.0263	0.0302	0.0345
Sips	Q_m (mmol/g)	0.613	0.872	1.12	1.32
	K_{Sips} (L/mmol)	0.0809	0.0667	0.0646	0.0591
	n_s	1.0	1.2	1.4	1.5
	R^2	0.994	0.990	0.994	0.988
	χ^2	0.0000800	0.000130	0.000120	0.000230
Freundlich	K_F (mmol/g)	0.0480	0.0375	0.0299	0.0253
	1/n	0.775	0.964	1.14	1.22
	R^2	0.990	0.992	0.995	0.993
	χ^2	0.000110	0.000110	0.0000900	0.000150

This difference is attributed to the occurrence of swelling which was previously observed in urethane copolymers containing β-CD[28]. The β-CD:PAA copolymers display a relatively wide range of sorption capacities toward PNP according to the values of Q_m (0.359~2.20 mmol/g) for these conditions. The sorption properties are related to the preparative (co-monomer mole ratio and mixing speed) conditions of the copolymers and may be tuned accordingly. The values of Q_m fall in the range observed for β-CD epichlorohydrin copolymers (0.296 mmol/g)[29] and surface

modified activated carbon materials containing β-CD (2.58 mmol/g)[30]. At pH 4.6, the sorption capacity varied amongst the various β-CD/PAA the copolymers, as follows: 1:10 > 1:5 > 1:3 > 1:1 > 5:1 >10:1 (w/w). The increasing magnitude of Q_m correlates with increasing PAA content of the copolymer materials. There are several factors that contribute to the observed differences; increased number of -COOH groups of PAA favour H-bonding with PNP, and reduced grafting affects the surface area of the sorbent material[31]. The mixing speed affects the sorption properties of the copolymers (*cf.* Figure 2.9B) because greater mixing speed dramatically increases the accessible surface area as evidenced in the following trend for Q_m: 10:1_135>10:1; 5:1_135>5:1. Two factors which account for the observations are the surface accessibility of the sorption sites toward PNP and the aforementioned grafting efficiency as the mixing speed increases.

2.4.5.2. Sorption properties at pH 10.3

Figure 2.9C illustrates a comparison of the copolymer 10:1_135 sorption isotherms at pH 10.3 and 4.6 at 22 ℃. There are significant differences between the two isotherms and the "*apparent*" surface area of the copolymer materials are attenuated (SA~12.0 m^2/g to ~28.8 m^2/g) above the pK_a of PNP. The copolymers have greater sorption at pH 4.6 compared with pH 10.3 because PAA is deprotonated resulting in negatively charged surface sites. The ionization of the –COOH side groups along the polymer backbone of PAA (pK_a~4.5) undergo coulombic repulsions with the anion form of PNP (pK_a=7.14). The phenoxide form of PNP is the prevalent form at pH 10.3.

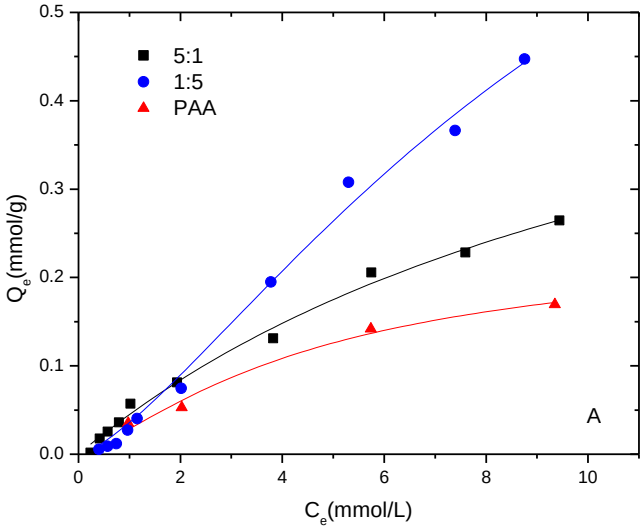
5:1
1:5
PAA
A
Q_e(mmol/g)
C_e(mmol/L)
0.0
0.1
0.2
0.3
0.4
0.5
0
2
4
6
8
10

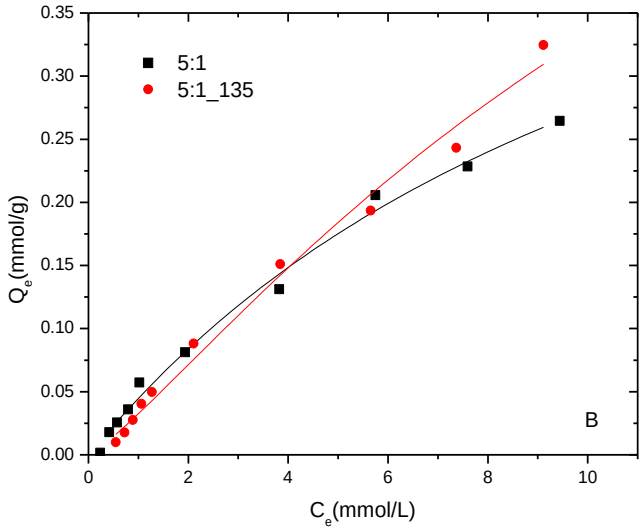
5:1
5:1_135
B
Q_e(mmol/g)
C_e(mmol/L)
0.00
0.05
0.10
0.15
0.20
0.25
0.30
0.35
0
2
4
6
8
10

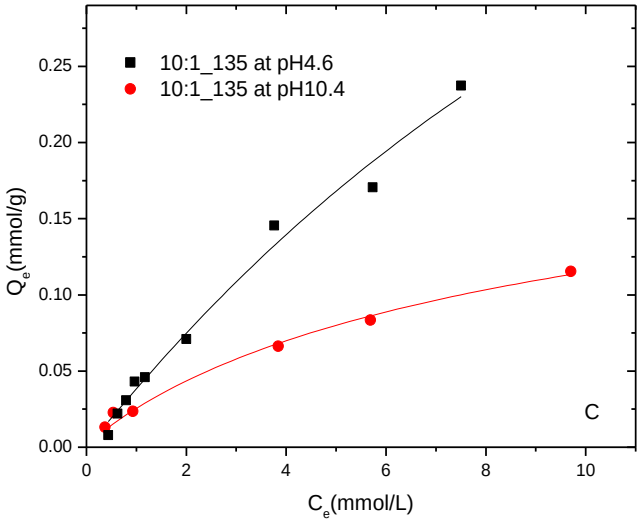

Figure 2.9. Sorption isotherm for β-CD/PAA copolymers using a fixed mass of polymer (~10 mg) and varying concentrations of PNP at 22 ℃: A. PAA and β-CD/PAA copolymers 1:5 and 5:1(w/w) at pH 4.6; B. Copolymer with various mixing speed, low speed 5:1 and high speed, 5:1_135(w/w) at pH 4.6; C. Copolymer 10:1(w/w) at pH 4.6 and pH 10.3. The best-fit results were obtained with the Sips isotherm model.

Table 2.5. Dye-based method estimates of the surface area for polymeric materials obtained for the sorption of PNP at 295 K and pH 4.6 and 10.3 and the best fit parameters (Q_m, K_{Sips} and n_s) using Sips nonlinear model.

Copolymer	pH	SA[a]	Q_m[b]	K_{Sips}[c]	n_s	χ^{2}[d]
10:1	4.6	54.0	0.359	0.185	1.3	0.00002
5:1	4.6	92.2	0.613	0.0809	1.0	0.00008
1:3	4.6	165	1.10	0.0509	1.3	0.00013
1:5	4.6	169	1.12	0.0646	1.4	0.00012
1:10	4.6	331	2.20	35.5	1.5	0.0403
10:1_135	4.6	67.1	0.447	0.129	1.2	0.0285
5:1_135	4.6	131	0.872	0.0667	1.2	0.00013
1:5_135	4.6	199	1.32	0.0591	1.5	0.00023
PAA[e]	4.6	36.2	0.240	0.216	1.3	0.00015
5:1_135	10.3	12.0	0.0701	0.277	1.2	0.00002
10:1_135	10.3	28.8	0.191	0.147	1.0	0.00003

[a] surface area, (m^2/g)

[b] Q_m, (mmol/g)

[c] K_{Sips}, (L/mmol)

[d] χ^2, Chi-square distribution

[e]PAA was test at both pH 4.6 and 10.3; however, PAA at pH 10.3 did not show any observable sorption.

In general, the copolymer materials with greater PAA contents (reduced crosslink density) and higher mixing speeds are concluded to have greater sorption capacity at pH 4.6. This is understood in terms of favorable H-bonding interactions between PNP and with the carboxylic groups along the PAA polymer backbone along with van der Waals interactions in the micropore sites of the copolymer framework. At pH 10.3, the inclusion sites are favoured since the coulombic repulsion with carboxylate groups of PAA and the phenoxide form of PNP are shielded when bound by β-CD. The enhanced binding affinity of PNP at alkaline conditions was independently observed in a recent study (*cf.* Table 2.3 in Ref. 32)[32]. The sorption of PNP by the β-CD:PAA copolymers at different pH (4.6 and 10.3) are shown in Scheme 2.1. There are two potential sorption sites on the β-CD:PAA copolymer framework when pH ≤ pK_a (PAA) due to the availability of the β-CD inclusion sites and the PAA surface domains (*non-inclusion*). The copolymers with low PAA (high β-CD) content show a monolayer adsorption with $n_s \sim 1$ indicating that the β-CD inclusion sites are independent and play a dominant role in the sorption processes (*i.e.* 5:1 copolymer). Copolymers with reduced levels of grafting show favourable sorption at the *non-inclusion* sorption sites and yield non-unitary values for the heterogeneity parameter ($n_s \neq 1$). The pH may dramatically change the framework morphology of the copolymers, especially for the copolymers with low β-CD content. At pH 10.3, pH > pK_a (PAA), and the presence of negatively charged carboxylate groups on PAA results in coulombic repulsion with the phenolate form of PNP, and the sorption capacity of the copolymer is attenuated.

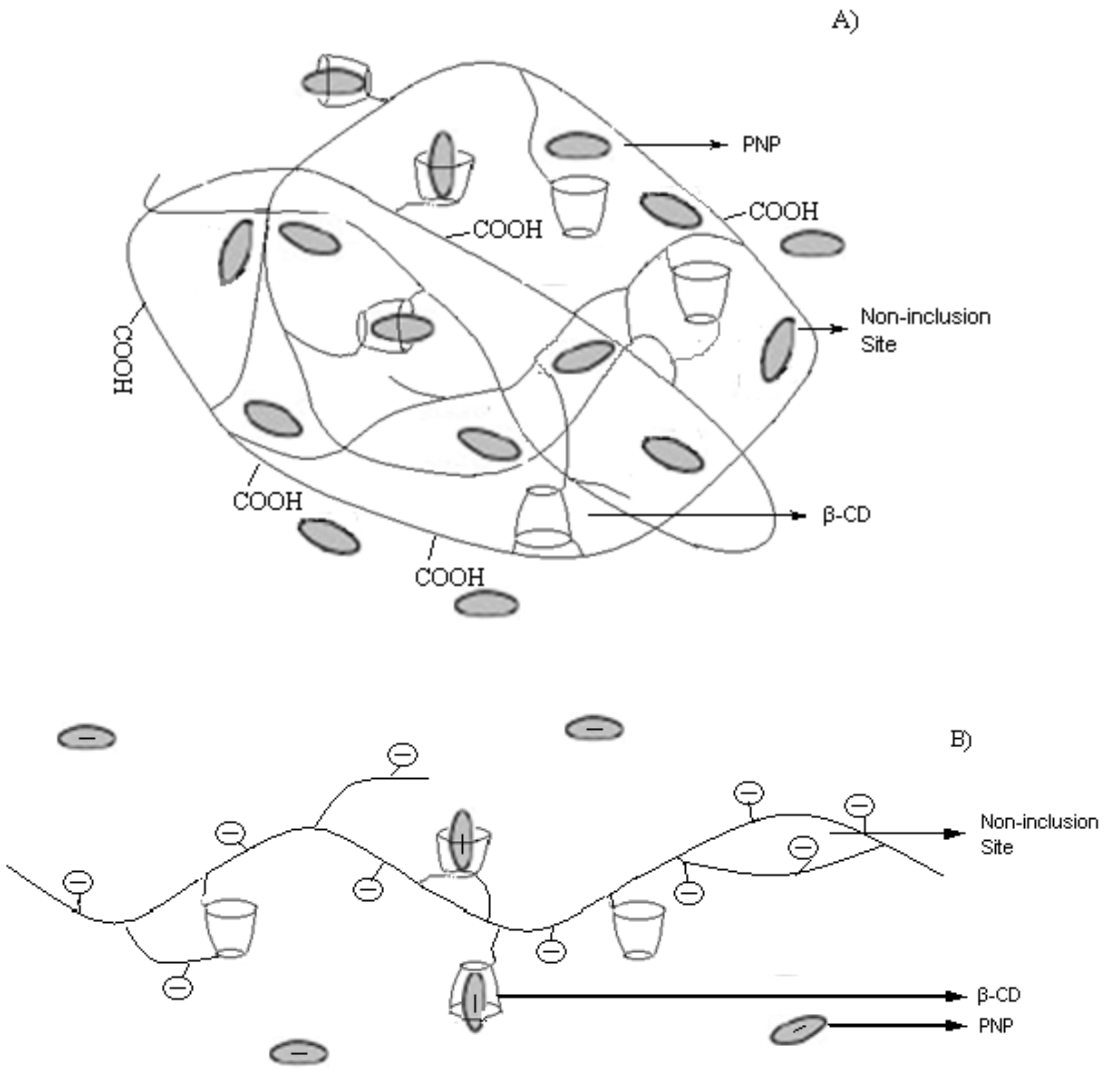

Scheme 2.1. The copolymer structure of a cross linked β-CD/PAA polymer containing an adsorbed guest molecule (oval) within the β-CD inclusion sites (tori interior) and the non-inclusion sites (tori exterior) of the PAA framework A. pH 4.6 B. pH 10.4. The straight line segments connecting the β-CD tori represent the ester linkage. The solvent has been omitted for clarity purposes.

Compared to porosimetry-based methods, the PNP-based sorption in aqueous solution provides a much greater "*apparent*" surface area for copolymer sorbents. This effect results from hydration-induced swelling of the copolymer framework in aqueous solution[27]. The dye-based method monitors changes in the absorbance of PNP related to sorption by the copolymer sorbent. The SEM images in Figure 2.10. do not show evidence of meso- or macro-porous structures in the solid state, in agreement with the gas adsorption results. The SEM results reveal a microporous material with limited pore structure characteristics. The occurrence of swelling strongly affects the accessibility of adsorptive probes in the anhydrous *vs*. hydrate states because of the hydration dependent morphology and variable sorption properties of the copolymer material.

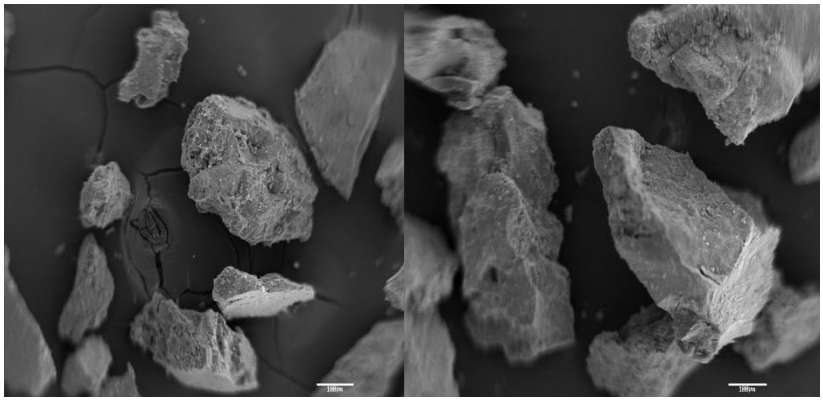

Figure 2.10. SEM image of β-CD/PAA copolymers 1:3(w/w) [Scale = 100 μm]

2.5. Conclusions

In this work, a range of copolymer materials were prepared and their sorption properties were characterized in aqueous solution with *p*-nitrophenol at 295 K and nitrogen adsorption in the solid state at 77K. The copolymers show a range of physicochemical properties characteristic of

amorphous powders to crystalline materials in the solid state, corresponding to the co-monomer ratios and the mixing speed employed in the synthesis. In aqueous solution, the copolymers display variable swelling properties in aqueous solution. The Sips model provided the best overall description of the experimental results and yield reliable estimates of the equilibrium sorption parameters in aqueous solution. At pH 4.6, the monolayer sorption capacity (Q_m) of the copolymers with PNP varied from 0.359-2.20 mmol/g. At pH 10.3, the value of Q_m for the copolymers was significantly attenuated (0.070-0.191 mmol/g) due to electrostatic repulsions between the carboxylate anion sites of PAA and the deprotonated form of PNP. The variable surface area results obtained from the solid-gas and solid-solution adsorption methods are attributed to hydration effects and swelling of the copolymer framework in solution relative to the solid state. CD-based copolymer materials with tunable physicochemical properties were prepared with variable co-monomer content and efficient uptake of organic contaminants in aqueous solution. The copolymer materials have numerous potential applications for sorption-based processes, and further studies are underway to improve their molecular recognition properties for a variety of environmental conditions (*i.e.* pH, temperature, concentration). Some examples of potential applications involving copolymer materials containing β-CD and poly(acrylic acid) include the development of functional hydrogels as pharmaceutical excipients[33], controllable nano-assemblies for materials design[34], chemically responsive sol-gel materials[35], biomimetic agents with tunable rheology[36], and functional nano- to microscale coatings[37].

2.6. Acknowledgements

The authors wish to acknowledge the Natural Sciences and Engineering Research Council of Canada (NSERC), the Canada Foundation for Innovation (CFI), and the University of Saskatchewan for their kind support of this research.

2.7. References

(1) Sun, Y.; Chen, J. L.; Li, A. M.; Liu, F. Q.; Zhang, Q. X. *React Funct Polym* **2005**, *64*, 63-73.

(2) Yin, J.; Chen, R.; Ji, Y.; Zhao, C.; Zhao, G.; Zhang, H. *Chem. Eng. J.* **2010**, *157*, 466-474.

(3) Lanouette, K. H. *Chem. Eng.* **1977**, *84*, 99.

(4) End Poverty 2015: Millennium development goals. United nations website. http://www.un.org/milleungoals/environ.shtml (accessed September/27, 2008).

(5) Inoue, Y.; Harkushi, T. ; Liu, Y.; Tong, L. H.; Shen, B. J.; Jin, D. S. *J. Am. Chem. Soc.* **1993**, *115*, 475-481.

(6) van de Manakker, F.; Vermonden, T.; van Nostrum, C. F.; Hennink, W. E. *Biomacromolecules* **2009**, *10*, 3157-3175.

(7) Jang, J. S.; Bae, J. *Macromol. Rapid Commun.* **2005**, *26*, 1320-1324.

(8) Park, H.; Robinson, J. R. *Pharm. Res.* **1987**, *4*, 457-464.

(9) Bibby, D. C.; Davies, N. M.; Tucker, I. G. *Int. J. Pharm.* **1999**, *187*, 243-250.

(10) Bibby, D. C.; Davies, N. M.; Tucker, I. G. *Int. J. Pharm.* **1999**, *180*, 161-168.

(11) Emmett, P. H.; Brunauer, S. *J. Am. Chem. Soc.* **1937**, *59*, 1553-1564.

(12) Sing, K. S. W. *Chem. Ind.* **1967**, 829.

(13) Deboer, J. H.; Lippens, B. C.; Linsen, B. G.; Broekhof.Jc; Vandenhe.a; Osinga, T. J. *J. Colloid Interface Sci.* **1966**, *21*, 405.

(14) Barrett, E. P.; Joyner, L. G.; Halenda, P. P. *J. Am. Chem. Soc.* **1951**, *73*, 373-380.

(15) Huglin, M. B.; Liu, Y.; Velada, J. L. *Polymer* **1997**, *38*, 5785-5791.

(16) Mohamed, M. H.; Wilson, L. D.; Headley, J. V.; Peru, K. M. *Process Saf. Environ. Prot.* **2008**, *86*, 237-243.

(17) Dupuy, G.; Hilaire, G.; Aubry, C. *Clin. Chem.* **1987**, *33*, 524-528.

(18) Giles, C. H.; D' Silva, A. P.; Tridevi, A. S. *J. Appl. Chem.* **1970**, *20*.

(19) Freundlich, H. M. *Phys. Chem.* **1906**, *57A*, 385-470.

(20) Langmuir, I. *J. Am. Chem. Soc.* **1918**, *40*, 1361-1403.

(21) Brunauer, S.; Emmett, P. H.; Teller, E. I. *J. Am. Chem. Soc.* **1938**, *60*, 309.

(22) Sips, R. *J. Am. Chem. Soc.* **1948**, *125*, 6452.

(23) Pratt, D. Y.; Wilson, L. D.; Kozinski, J. A.; Mohart, A. M. *J. Appl. Polym. Sci.* **2010**, *116*, 2982-2989.

(24) Xu, W. L.; Liu, J. D.; Sun, Y. P. *Chinese Chemical Letters* **2003**, *14*, 767-770.

(25) Sing, K. S. W.; Everett, D. H.; Haul, R. A. W.; Moscou, L.; Pierotti, R. A.; Rouquerol, J.; Siemieniewska, T. *Pure Appl. Chem.* **1985**, *57*, 603-619.

(26) Yu, J. C.; Jiang, Z. T.; Liu, H. Y.; Yu, J. G.; Zhang, L. Z. *Anal. Chim. Acta* **2003**, *477*, 93-101.

(27) Mohamed, M. H.; Wilson, L. D.; Headley, J. V. *Carbohydr. Res.* **2011**, *346*, 219-229.

(28) Wilson, L. D.; Mohamed, M. H.; Headley, J. V. *J. Coll. Interface Sci.* **2011**, 357, 215-222.

(29) Li, J.; Meng, X.; Hu, C.; Du, J. *Biores. Tech.* **2009**, 100, 1168.

(30) Kwon, J. H.; Wilson, L. D. *J. Environ. Sci. Health. A.* **2010**, 45, 1793-1803.

(31) BlancoFuente, H.; AnguianoIgea, S.; OteroEspinar, F. J.; BlancoMendez, J. Biomat. **1996**, 17, 1667.

(32) Wilson, L. D.; Mohamed, M. H.; Berhaut, C. L. *Materials* **2011**, 4, 1528-1542.

(33) Zhu, W.; Li, Y.; Liu, L.; Chen, Y.; Wang, C.; Xi, F. *Biomacromol.* **2010**, 11, 3086-3092.

(34) Yan, Q.; Xin, Y.; Zhou, R.; Yin, Y.; Yuan, *J. Chem. Commun.* **2011**, 47, 9594-9596.

(35) Ogoshi, T.; Takashima, Y.; Yamaguchi, H.; Harada, A. *J. Am. Chem. Soc.* **2007**, 129, 4878-4879.

(36) Hashidzume**, A.;** Tomatsu**, I.;** Harada**, A.** *Polymer.* **2006**, 47, 6011-6027.

(37) Lefort, M.; Popa, G.; Seyrek, E.; Szamocki, R.; Felix, O.; Hemmerlé, J.; Vidal, L.; Voegel, J-C.; Boulmedais, F.; Decher, G.; Schaaf, P. *Angew. Chem. Int. Ed.* **2010**, 49, 10110-10113.

CHAPTER 3

Description

Chapter 3 includes a verbatim copy of an article published in December, 2012 in Journal of Colloid Interface Science (J. Colloid Interface Sci. **2012**, 387(1) 250-261.). The paper describes the systematic methods of synthesis and characterization of β-CD/TCl and β-CD /SCl copolymer materials.

Author's contribution

I carried out all the experimental work (*i.e.* synthesis and characterization of the copolymers). This work was principally supervised by Dr. Wilson. I wrote the first draft of the manuscript with assistance in the form of editing of the final manuscript from Dr. Wilson before submitting for publication. The co-authors grant permission of use of the published manuscript for this PhD thesis, and agree with the description of the roles and contributions of the authors.

Relationship of Chapter 3 to the overall objective of this project

As stated in the introduction, the first research objective was material design and characterization. This chapter reports the systematic design of a series of β-CD-based polyester copolymers by tuning of the synthetic conditions with various pre-polymer ratio and different types of cross-linkers (*e.g.* TCl and SCl). The physiochemical properties of the copolymers are anticipated to be engineered under control. A systematic characterization of the β-CD/TCl and β-CD/SCl copolymers was also described in this manuscript, including the surface characterization by gas and dye adsorption method.

Research highlight:

A series of β-CD-based polyester copolymer materials were synthesized using micro-emulsion- method to cross-link the functional unit β-CD and cross-linkers (*e.g.* TCl and SCl). The copolymers were prepared by varying the pre-polymer ratio and various types of cross-linkers during synthesis to achieve tunable physicochemical properties. Various characterization methods, such as, ^{1}H NMR, FT-IR, TGA, N_2 porosimetry, and dye adsorption method were involved to characterize the copolymers. The sorption isotherms were evaluated with Sips isotherm models to obtain the equilibrium sorption properties of polyester copolymers. The heterogeneous adsorption behaviour observed for grafted polyester and polyester copolymers using the dye adsorption method were further examined by ^{1}H NMR spectroscopy for polyester copolymers with low linker content (*e.g.*, SCl or TCl). The results provide support for two distinct types of sorption sites on the copolymer surface for PNP: β-CD inclusion sites and non-inclusion (*i.e*. interstitial) linker domains.

3. Preparation and Sorption Studies of Polyester Microsphere Copolymers Containing β-Cyclodextrin

Lee D. Wilson* and Rui Guo

Department of Chemistry, University of Saskatchewan, 110 Science Place, Saskatoon, Saskatchewan, S7N 5C9

*Corresponding author: Tel. 1-306-966-2961, Fax. 1-306-966-4730
Email: lee.wilson@usask.ca

3.1. Abstract

Polyester copolymer sorbent materials that incorporate β-Cyclodextrin (β-CD) were prepared using water-in-oil (w/o) micro-emulsion conditions at variable β-CD: cross linker mole ratios; where the cross linker units were sebacoyl chloride (SCl) and terephthaloyl chloride (TCl). The copolymers were characterized using TGA, nitrogen adsorption, and NMR/IR spectroscopy. The dye-based sorption properties of the copolymers with *p*-nitrophenol (PNP) in aqueous solution were evaluated at pH 4.6 and 295 K using UV-Vis spectrophotometry. The uptake of PNP varied from 0.221 to 0.352 mmol/g, according to the nature of the cross linker and the copolymer mole ratio. The sorption capacity of SCl-based copolymers exceed that for TCl-based copolymers, and correlate with the relative swelling properties and hydrated surface areas of the sorbent frameworks. ^{1}H NMR spectroscopy of copolymers with low levels of linker content (*i.e.* SCl or TCl) indicate dual sorption sites for PNP (*i.e.* β-CD inclusion sites and non-inclusion (interstitial) linker domains). The existence of dual sorption sites is similarly concluded for copolymers containing higher levels of cross linker. Inclusion complexes are firstly formed between PNP and the β-CD inclusion sites of the copolymer sorbent; thereafter, PNP is adsorbed onto the linker domains of the copolymer framework.

Keywords: Cyclodextrin, *p*-nitrophenol, sorption, copolymers, NMR spectroscopy, dual mode, and UV-Vis spectrophotometry

3.2. Introduction

Cyclodextrin-based copolymer materials represent a unique class of materials with tunable properties for a wide range of sorption-based applications ranging from chemical separations to contaminant removal from water[1-5]. The continued interest in cyclodextrins (CDs) and their copolymer materials are attributed, in part, to their ability to form stable complexes with a wide range of apolar inorganic and guest molecules[6-8]. β-CD is a cyclic oligosaccharide composed of seven glucopyranose units linked by α-1,4-glycosidic bonds which forms a torus-shaped macrocycle with a hydrophilic exterior and a lipophilic cavity (Scheme 3.1)[6]. In spite of the number of studies on CD-based copolymers, a detailed understanding of their heterogeneous sorption properties with simple guest compounds in aqueous solution is limited, as evidenced by a study reported by Ma and Li[9]. It was reported[9] that PNP forms 1:1 inclusion complexes with the β-CD inclusion sites of urethane copolymer materials ($K_{1:1} = 10^9$ M^{-1}), as compared with the 1:1 β-CD/PNP complex ($K_{1:1} = 197$ M^{-1})[9]. Wilson *et al*. concluded that the enhanced binding affinity between urethane copolymers and PNP[10] was an artifact, arising from an incomplete assessment of the non-inclusion (*i.e*. interstitial) binding sites (*cf.* Fig. 6 in [10]) of the copolymer framework. Recent studies[10-12] indicate that the sorption and host-guest recognition properties of β-CD copolymers are influenced by the surface area, pore structure, and the relative accessibility of the inclusion binding sites of the copolymer framework. Copolymers containing β-CD require favourable inclusion site accessibility in order to form well-defined inclusion complexes[8, 10]. Guo and Wilson[13] reported the synthesis of microsphere-based poly(acrylic acid) (PAA) copolymers containing β-CD to improve the surface accessibility of the sorption sites of such copolymer sorbents. These types of copolymer materials were shown to display tunable physicochemical properties that extended beyond the range of conventional cross linked sorbent materials because of their unique morphology and structure (*e.g*., inclusion and interstitial domains) and tunable hydrophile-lipophile balance (HLB)[8, 14]. Thus, rational sorbent design of CD-based copolymers should account for the inclusion site accessibility, role of the interstitial framework domains, cross link density, and the relative HLB of the sorbent framework[15].

The unique sorption properties of copolymers containing CDs are often attributed to the presence of inclusion binding sites; however, the role of the secondary adsorption sites (*i.e.* interstitial sites) are not well understood[10-12, 15-17]. The measurement of the concentration of the residual adsorbate (*i.e*. unbound species) does not adequately account for multiple binding sites.

In some cases, isotherm sorption parameters may provide indirect information about the sorption mechanism. Rossi *et al.*[18] reported an amphiphilic CD with multiple recognition sites; whereas, Mohamed *et al*.[11] reported two types of binding sites (*i.e*. inclusion and interstitial domains) for urethane-based copolymers. Yudiarto *et al.*[16] reported that ultrafiltration of *o*-, *m*-, and *p*-nitrophenol isomers by epichlorohydrin-based copolymers related to the presence of such secondary interstitial domains (*cf*. Figure 10 in [16]). Dual mode adsorption[17] due to the presence of multiple sorption sites in CD-based copolymers was evidenced by isotherm sorption parameters (*cf*. Scheme 2 in [17]). Thus, there is a need to carry out further research that complements equilibrium sorption studies to characterize the role of these sorption sites.

In this paper, we report the preparation and characterization of polyester copolymers formed between β-CD and two types of acid dichlorides: terephthaloyl and sebacoyl chloride, employing a water-in-oil (w/o) microemulsion-based synthesis (*cf*. Scheme 3.1)[13]. The sorption properties and structure of various copolymer/PNP complexes were studied in aqueous solution using UV-Vis and ^{1}H NMR spectroscopy. This study contributes to a significantly improved understanding of the interactions between PNP and polyester-based copolymer containing β-CD[19] which may be applied to a wide range of sorbent materials of this type.

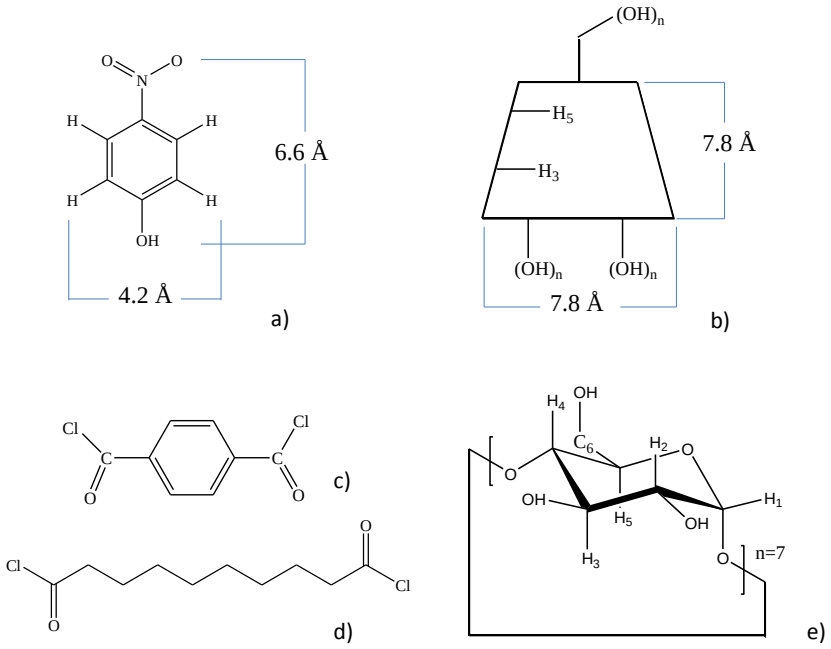

Scheme 3.1. Molecular structure of monomer units and adsorbate; a) *p*-nitrophenol, b) ^{1}H numbering scheme for the intracavity nuclei (H_3 and H_5) of β-CD, c) terephthaloyl chloride (TCl), d) sebacoyl chloride (SCl), and e) ^{1}H numbering scheme of the intracavity nuclei (H_3 and H_5) and extracavity nuclei (H_1, H_2, H_4 and H_6) of β-CD.

3.3. Materials and Methods

3.3.1. Materials

β-CD was purchased from VWR Canada Ltd. Terephthaloyl chloride (TCl), sebacoyl chloride (SCl), polyoxyethylene sorbitan monolaurate (Tween 20), *p*-nitrophenol (PNP), anhydrous ethyl ether, acetone, potassium bromide, deuterium oxide (D_2O), and 4Å (8-12 mesh) molecular sieves were purchased from Sigma-Aldrich Canada Ltd. Deuterated dimethyl sulfoxide (DMSO-d_6) and chloroform ($CDCl_3$) were purchased from Cambridge Isotope Laboratories, Inc. Cyclohexane, chloroform, and potassium phosphate monobasic were EMD products. All materials were used as received without further purification. Millipore water and medical grade nitrogen gas were used in the adsorption experiments.

3.3.2. Methods

3.3.2.1. Synthesis of copolymer materials

The synthesis of CD-based copolymer materials was adapted from an existing method, as outlined previously[20, 21]. To prepare the TCl-based copolymers, 0.6 g β-CD was dissolved in 6 mL 1 M NaOH solution and added drop-wise to 30 mL cyclohexane solution containing 5% (v/v) Tween 20. The solution was emulsified using magnetic stirring at a rate of 1,100 rpm for 30 min. The cross-linking solution was prepared by dissolving 5% (w/v) TCl in a 1:4 chloroform/cyclohexane mixture. The copolymers were formed by addition of the solution containing cross linker to the emulsion with stirring for 2 h at room temperature. The reaction was quenched by dilution of reaction mixture with 40 mL cyclohexane. The cyclohexane and water were removed using a rotary evaporator (pressure ~ 1 mbar). The crude product was washed with acetone in a Soxhlet extractor for 24 h to remove unreacted reagents and low molecular weight oligomers. The copolymer product was dried in a pistol dryer for 24 h, ground into a powder, and passed through a 40 mesh sieve to ensure a uniform particle size. A second cycle of washing in the Soxhlet extractor with anhydrous diethyl ether for 24 h was followed by drying, grinding, and sieving, as outlined above. SCl-based copolymers were prepared similar to the TCl-based copolymers, except that the SCl was in solution form and added directly into the emulsion mixture. The copolymers were prepared at 1:1, 1:5, and 1:10 β-CD: cross linker mole ratios.

The copolymer materials were characterized using NMR/FT-IR spectroscopy and TGA. The nomenclature of the copolymers is defined in accordance with the cross linker and a numeric value to indicate the relative mole quantity of cross linker; where the mole quantity of β-CD is unity. Hereafter, the copolymers are identified as TCl-1, TCl-5, TCl-10 for the β-CD: TCl copolymers; SCl-1, SCl-5, and SCl-10 for the β-CD: SCl copolymers to indicate the relative mole content of cross linker.

3.3.2.2. Characterization

FT-IR Spectroscopy

IR spectra were obtained with a Bio-RAD FTS-40 instrument and samples were analyzed in reflectance mode. Copolymer samples were prepared by grinding ~5 mg with pure spectroscopic grade KBr (~50 mg) with grinding in a small mortar and pestle. Diffuse Reflectance Infrared

Fourier Transform (DRIFT) spectra were recorded at room temperature with a resolution of 4 cm^{-1}, operating in the range of 400-4000 cm^{-1}. Multiple scans were recorded and corrected against a background spectrum of pure KBr. The intensity of the DRIFT spectra is reported in Kubelka-Munk units.

TGA

Thermal analyses of the copolymers were performed with a thermogravimetric analyzer, TGA (TA Instruments Q50). Samples were heated in open aluminum pans at 30 °C and allowed to equilibrate for 5 min prior to heating at a scan rate of 5 °C per min up to 500 °C.

Nitrogen Adsorption

Nitrogen adsorption measurements were obtained using a Micromeritics ASAP 2020 (Norcross, GA) to obtain the copolymer surface area and pore structure properties with an accuracy of ±5 % for the copolymers. In brief, ~ 1 g of sample was degassed at 550 μm Hg and ~ 70 ℃ for several hours in the sample chamber until the outgas rate became stabilized. Granular activated carbon (GAC), alumina, and silica-alumina sieves were used to check the calibration of the instrumental parameters. The BET surface area was calculated from the adsorption isotherm using 0.162 nm^2 as the surface area for nitrogen gas[22, 23]. The micropore surface area was obtained using a *t*-plot (de Boer method)[24]. The Barret-Joyner-Halenda (BJH) method[25] was used to estimate the pore volume and the pore diameter from the adsorption isotherm data. The BJH method used the Kelvin equation and the assumption of slit-shaped pores[22, 23].

^{1}H NMR Spectroscopy

All ^{1}H NMR experiments (1-D ^{1}H NMR, 2-D ROESY)[26, 27] were performed on a 3-channel Bruker Avance (DRX) spectrometer operating at a ^{1}H resonance frequency of 500.13 MHz at 298 K. Various solvents were used to dissolve the copolymers and the starting materials due to solubility: D_2O for TCl-1, SCl-1, and β-CD; $CDCl_3$ for TCl, and DMSO-d_6 for TCl-X and SCl-X (where X = 5, 10). To obtain information about copolymer sorption interactions with PNP, ^{1}H NMR samples were prepared in D_2O at pD ~ 5 to 6 for TCl-1/ and SCl-1/PNP systems at various relative mole ratios of PNP. All ^{1}H NMR spectra were referenced externally to tetramethylsilane (TMS, δ = 0 ppm) with a recycle delay (2 s) and a 90° pulse length (10 μs). 2-D NMR spectra were obtained using rotating-frame Overhauser effect spectroscopy (ROESY) [27b] using the following conditions; number of acquisitions (8), dummy scan time (8 s), and variable spin-lock

times (300 - 500 ms). 2D spectra were acquired with a spectral width of 12 ppm in 2k data points and the spin-lock power levels were set at 21.33 dB.

3.3.3. Sorption

The pore structure properties, surface area, and sorption properties were evaluated using a dye-based UV–Vis method reported previously[13] with PNP as the adsorbate dye. Fixed amounts (~20 mg) of the powdered and sieved copolymer materials were mixed with 7 mL of aqueous dye solution at variable concentration (0.1–10 mM) in 10 mM potassium phosphate monobasic buffer solution at pH 4.6. The samples were fully equilibrated on a horizontal shaker table for 24 h. The initial concentration (C_o) of PNP was determined before and after sorption (C_e) using the experimentally determined molar absorptivity of PNP (ε=9286.5 L mol^{-1} cm^{-1}; λ_{max}= 317 nm) at pH= 4.6, in agreement with reported values[11, 13, 28]. The sorption isotherms are depicted as plots of the amount of adsorbed PNP in the copolymer phase per mass of adsorbate (Q_e; mmol/g) versus the equilibrium residual concentration of unbound PNP in aqueous solution (C_e). The value of Q_e is defined by eqn. (3.1) where C_o is the initial PNP concentration, V is the volume of solution, and m is the mass of sorbent, described previously[11, 12].

$$Q_e = \frac{(C_0 - C_e)\times V}{m} \qquad (3.1)$$

The dye-based sorption method provides an independent estimate of the sorbent surface area (SA; m^2/g) according to eqn 3.2.

$$SA = \frac{A_m Q_m L}{Y} \qquad (3.2)$$

where A_m represents the cross-sectional area occupied by PNP (A_m for a "*coplanar*" orientation is 5.25×10^{-19} m^2/mol; whereas an "*orthogonal*" orientation is 2.5×10^{-19} m^2/mol), Q_m is the monolayer adsorption capacity per unit mass of sorbent, L is Avogadro's number (mol^{-1}), and Y is the coverage factor (Y = 1) for PNP[29].

The Sips isotherm is a versatile model with several adjustable parameters where the n_s term reflects the heterogeneity (*i.e.* when $n_s \neq 1$) of the sorbent, and a homogenous surface is inferred when n_s = 1. Langmuir isotherm behavior is predicted when n_s=1, whereas Freundlich behavior is described when $(K_s C_e)^{n_s} <<< 1$. The Sips model is defined by eqn. (3.3)[30].

$$Q_e = \frac{Q_m K_s C_e^{n_s}}{1 + K_s C_e^{n_s}} \qquad (3.3)$$

K_s is the Sips equilibrium constant, C_e is the residual equilibrium concentration of PNP in aqueous solution, and Q_m is defined by eqn. (3.2). The criteria of the "*best fit*" between the calculated isotherm and the experimental data are determined by the χ2-distribution (χ^2). The minimization of χ^2 denotes a "*best-fit*" for non-linear least squares fitting; χ^2 is defined by eqn. (3.4), according to the difference in the experimental ($Q_{e,i}$) and calculated ($Q_{c,i}$) values.

$$\chi^2 = \sum \sqrt{\frac{\left(Q_{e,i} - Q_{c,i}\right)^2}{N}} \qquad (3.4)$$

$Q_{c,i}$ is the calculated value of Q_e according to the Sips isotherm model (*cf.* eqn. 3.3) and N is the number of experimental data points.

3.4. Results and Discussion

3.4.1. Physicochemical Characterization of Copolymers

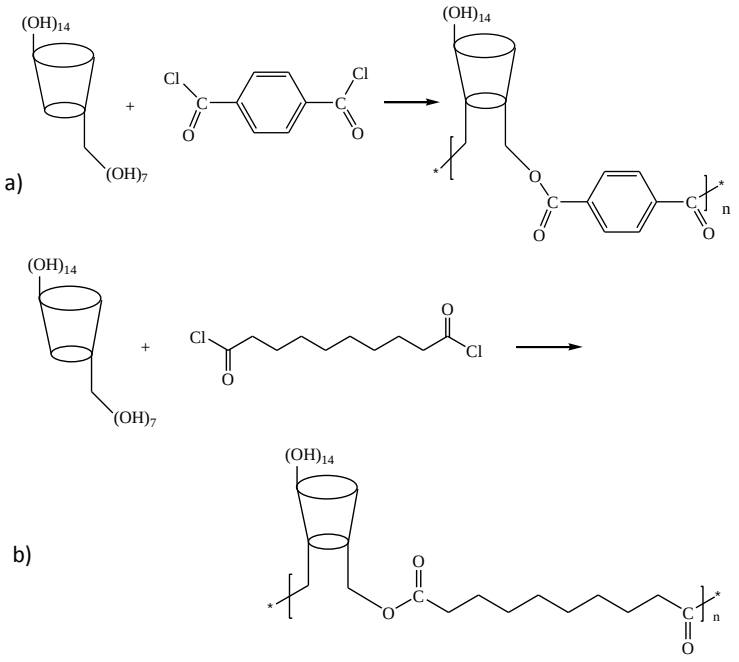

Scheme 3.2. Generalized copolymer formation between β-CD and the diacid chlorides at a 1:1 mole ratio; a) terephthaloyl chloride (TCl), and b) sebacoyl chloride (SCl).

Microsphere copolymers were prepared using variable mole ratios of β-CD and cross linkers (TCl or SCl) at 1:1, 1:5 and 1:10 using w/o (*i.e.* water/cyclohexane) microemulsion (*cf.* Scheme 3.2). The copolymers display variable physical characteristics (*e.g.*, thermal stability, morphology, and solubility) at different cross linker content. In contrast to the water soluble copolymers TCl-1 and SCl-1, copolymers prepared at higher cross linker content (*i.e.* > 1:1) and are generally insoluble in water but have good solubility in polar organic solvents such as DMSO[19]. Copolymers prepared using w/o microemulsion conditions relative to those prepared in organic solvents differ according to their morphology, as described previously[13].

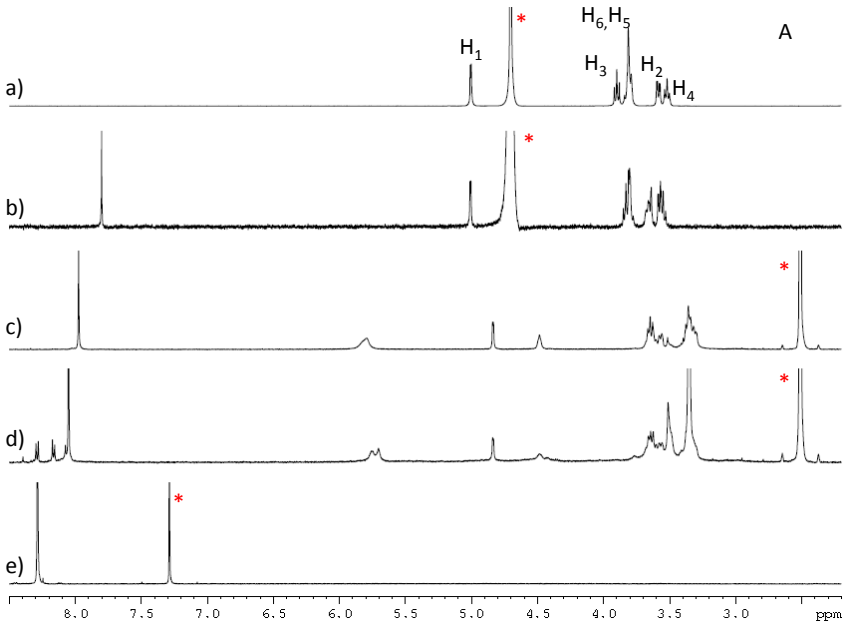

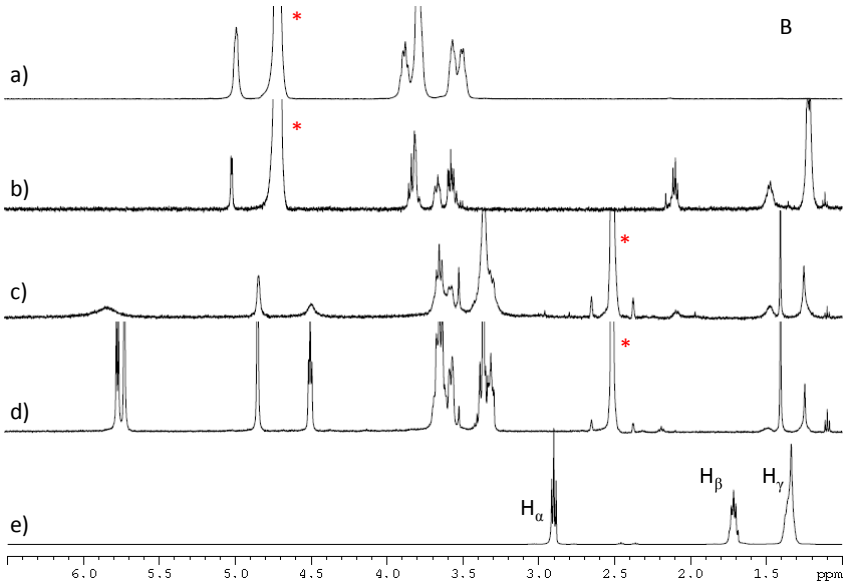

Figure 3.1. ^{1}H NMR spectra at 500 MHz and 298 K; A) β-CD, TCl, and TCl-X copolymers at variable levels of cross linker (X = 1, 5, 10), and B) β-CD, SCl, and SCl-based copolymers at variable levels of cross linker (X = 1, 5, 10). The asterisk (*) denotes NMR solvents (*i.e*. D_2O, DMSO and $CDCl_3$).

Figure 3.1 illustrates the ^{1}H NMR spectra at ambient pH and 295 K for the monomer species (*i.e*. β-CD, TCl, and SCl) and the respective copolymers at various composition ratios. The NMR spectra of the monomer species and the copolymers are similar; however, the copolymers show some line broadening and upfield shifts for the resonance lines of β-CD and the linker units. The ^{1}H-NMR spectra of the β-CD cavity nuclei (3.0-4.0 ppm) for the copolymers displayed chemical shift changes and line broadening in accordance to the level of cross linking and site of substitution of β-CD. The NMR results in Fig. 3.1 provide support that polyester linkages are formed and the molecular structure of the monomer species are preserved[31]. The resonance lines of TCl copolymers are relatively sharp and shifted upfield relative to the TCl monomer unit. The incremental Δδs values of the monomer units correspond to an increasing degree of substitution of the β-CD annulus due to cross linking for each type of linker unit. The NMR spectra of the water insoluble copolymers were obtained in DMSO-d_6, and compared with spectra for copolymers obtained in organic solvents[19, 33]. The spectra show some broad peaks at ~5.7 and 4.4

ppm for the hydroxyl groups on β-CD, as previously reported for β-CD in DMSO-d_6 by Schneider *et al.*[32] The relative composition of copolymers (*i.e.* β-CD : cross linker units) were calculated from integration of the ^{1}H NMR signals, as listed in Table 3.1. The cross linking efficiency of TCl is greater than SCl at these conditions, and may be due to differences in reactivity of the cross linkers in a w/o microemulsion. Differences in the reactivity of TCl and SCl were previously reported for SCl and TCl in dimethylacetamide[19]. For TCl-based copolymers, the monomer ratio was calculated from the integration ratios of the H_1 nuclei of β-CD (1/7 area) and the aromatic nuclei of TCl (1/4 area). The α-CH_2 groups of SCl (1/4 area) were evaluated for SCl-based copolymers relative to the H_1 nuclei of β-CD, as outlined above. The theoretical maximum number of ester linkages is 21 for β-CD. There are numerous hydroxyl groups in β-CD (*i.e.* seven primary and fourteen secondary hydroxyl groups) as shown in Scheme 3.1. Previous studies[12, 31] indicate that approximately 6 substituents can be grafted onto β-CD due to substituent steric effects in the annular hydroxyl region (*cf.* Scheme 3 in [12]). Even though a 1:10 mole ratio was used in the synthesis, the number of substituents grafted on TCl-10 is estimated to 6 TCl units.

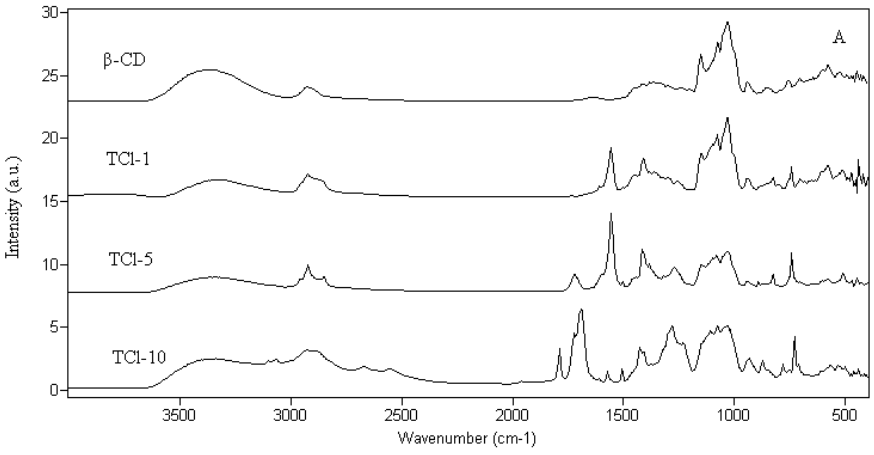

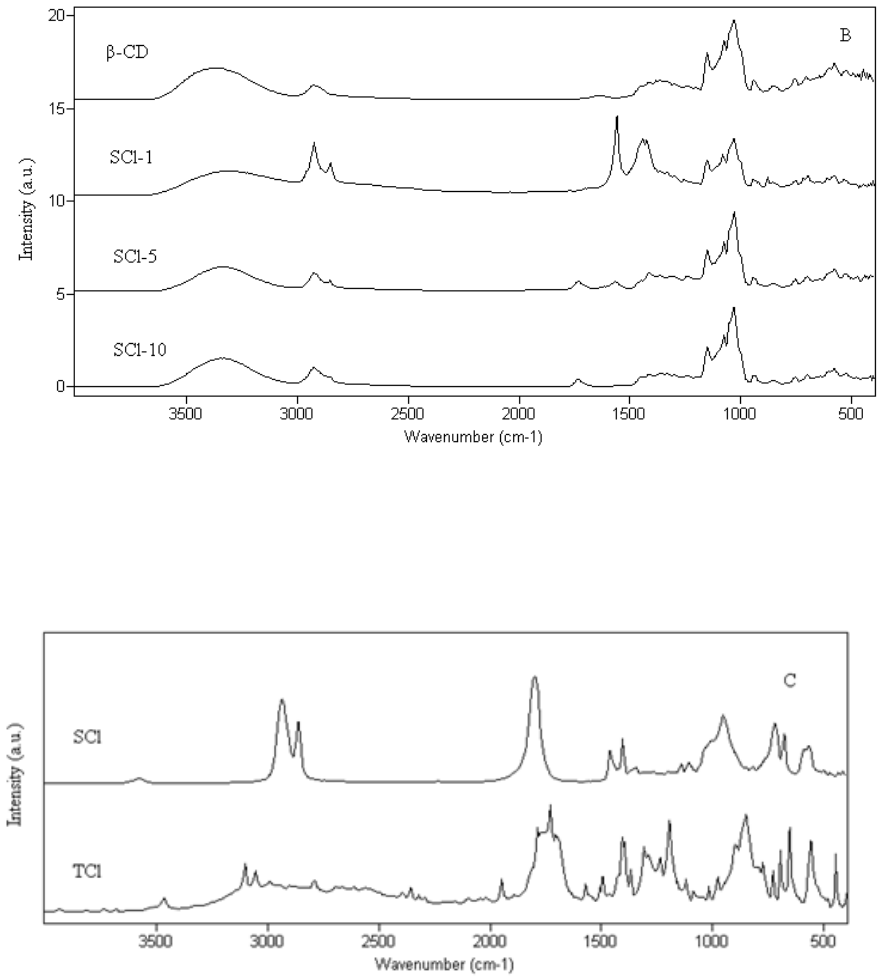

Figure 3.2. IR spectra (DRIFTS) obtained at 295 K: A) β-CD and TCl-X (X = 1, 5, and 10), and B) β-CD and SCl-X (X = 1, 5, and 10), and C) Diacid chloride cross linkers (SCl and TCl).

Table 3.1. Copolymer mole ratio composition **(**β-CD:cross linkcross linker) for TCl-/SCl-based copolymer materials containing β-CD according to ^{1}H NMR integration results.

Polymers	**Monomer Ratio β-CD : TCl**	**Polymers**	**Monomer Ratio β-CD : TCl**
TCl-1	1:1	**SCl-1**	1:2
TCl-5	1:3	**SCl-5**	1:3
TCl-10	1:6	**SCl-10**	1:2

DRIFT spectroscopy was used to assess the spectral signatures of the functional groups of the copolymers were prepared according to Scheme 3.2. The FT-IR spectra of the monomer units and the copolymer materials are shown in Figure 3.2a-b. The –OH stretching region (~3400 cm^{-1}), -CH stretching region (~2900 cm^{-1}) and C=O stretching region (~1700 cm^{-1}) are present in the copolymer products and confirm their molecular identity. The vibrational band of ν(C=O) is observed to vary between 1702-1666 cm^{-1} relative to that of the unreacted linker units (*i.e*. SCl and TCl). The intensity of the carbonyl signature increases for each copolymer as the linker content increases, in accordance with the relative mole ratio of β-CD and linker. The foregoing results are in agreement with those reported previously[19, 33] for polyester-based copolymers prepared in polar organic solvents (*i.e*. non-emulsion conditions).

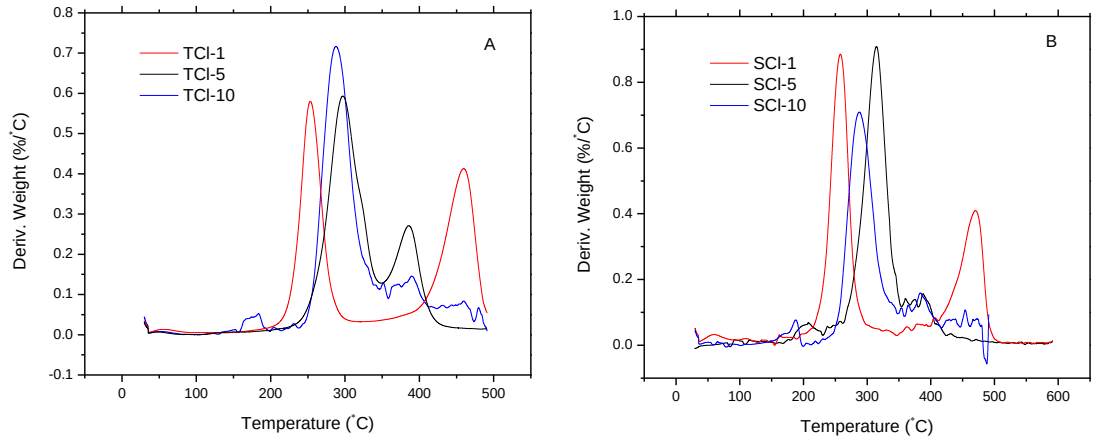

Figure 3.3. TGA of polyester copolymers containing β-CD; a) TCl-X (X = 1, 5, and 10), and b) SCl-X (X = 1, 5, and 10).

In Figure 3.3, the TGA results for the TCl- and SCl-based copolymers are presented as the derivative weight (mass loss/temperature) against temperature. There are two thermal events for each copolymer where the respective mass loss corresponds to the decomposition of the monomer units (*i.e.* β-CD, TCl, and SCl) at different temperatures. The relative peak area and temperature shift of the thermal events vary in accordance to the relative monomer ratio of the copolymer. In the case of TCl-1 and SCl-1, two thermal events are observed near 250 ℃ and 450 ℃. As the cross linker content increases, a convergence of the two thermal events occurs, and indicates that the increased amorphous character of the SCl-5, SCl-10, and TCl-10 copolymers. The mass loss ~ 275°C corresponds to the decomposition of β-CD; whereas, the higher transition temperatures are attributed to the cross linker units. The shift in temperature stability of the copolymers is related to the change in heat capacity, H-bonding effects, and the amorphous character of the copolymers as the linker content increases. Similar TGA results were reported for urethane-[31], epichlorohydrin-[34], and polyester-based copolymers[19] containing β-CD.

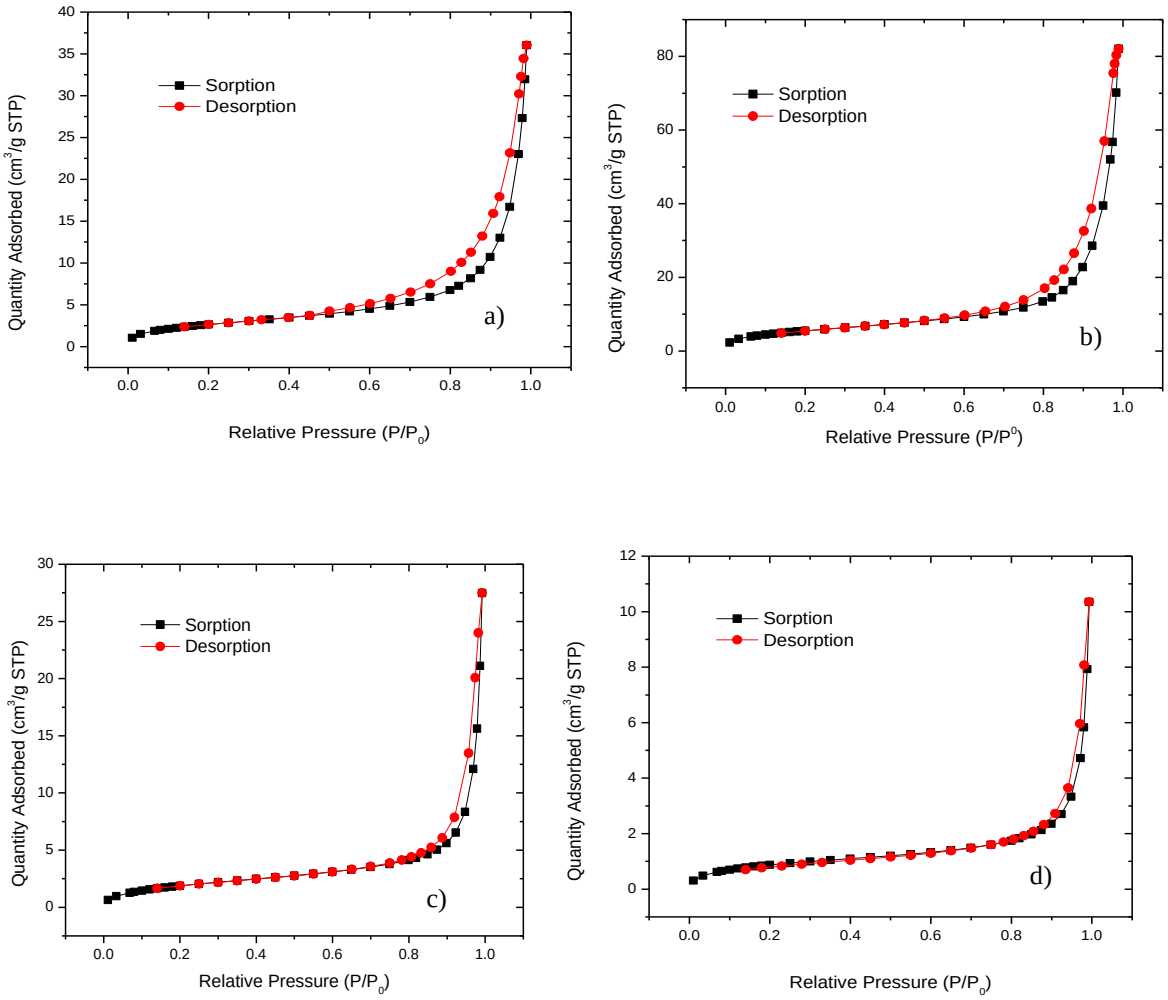

Figure 3.4. Nitrogen adsorption-desorption isotherms for the polyester copolymers; a) TCl-5, b) TCl-10, c) SCl-5, and d) SCl-10 at 77K.

Table 3.2. N_2 adsorption estimates of the surface area for the copolymer materials and β-CD at 77K.

Polymers	BET Surface Area (m^2/g)	Pore Width (Å)	Polymers	BET Surface Area (m^2/g)	Pore Width (Å)
TCl-1	11.5	119	SCl-1	12.1	118
TCl-5	9.99	142	SCl-5	7.42	101
TCl-10	20.7	156	SCl-10	3.35	87.2
β-CD	1.20	86.2			

As indicated above, the sorption properties of copolymer sorbents containing β-CD are unique, in part, due to their inclusion properties[4, 5, 15], and vary according to the relative sorbent surface area and inclusion site accessibility of β-CD. Nitrogen adsorption isotherms provide an estimate of the sorption characteristics and textural properties of copolymers in the "*dry*" state[10]. Figure 3.4 illustrates the nitrogen adsorption-desorption isotherms of the TCl- and SCl- based copolymers at intermediate and high linker contents. The copolymers display Type IV isotherms with hysteresis loops that vary according to their relative composition. Type IV isotherms generally describe the monolayer-multilayer adsorption of microporous adsorbents[35]. Type IV hysteresis loops feature parallel and almost horizontal branches (Type H1 and H3) attributed to adsorption-desorption in narrow slit-like pores that are often associated with narrow pore size distributions[35]. The results for β-CD (not shown) resemble the nitrogen adsorption results for SCl-10 and reveal features typical of a microporous material with a hysteresis loop which closes at $p/p_o \sim 0.9$. In contrast to "*soft materials*" such as PAA-β-CD copolymers[13], the reduced SA of the polyester copolymer materials is related to the high cross linking ratios employed and the use of w/o microemulsion conditions to produce a dense microporous framework. The TCl-based copolymers exhibit greater sorption toward nitrogen relative to the SCl-based copolymers, as evidenced by the textural properties in Table 3.2. The TCl-X copolymer framework is considered more rigid than SCl because of its aromatic linker units. Greater nitrogen adsorption is observed

for such highly cross linked copolymers, TCl-10 (20.7 m^2/g) relative to SCl-10 (3.35 m^2/g). The rigid framework and greater inclusion site accessibility of TCl-X materials was recently reported[19]. Thus, the differences in the BET surface areas for SCl-X and TCl-X sorbents indicate the influence of the cross linker rigidity and the relative composition. The SA estimates of polyester-based microspheres are slightly greater than those of the PAA-β-CD copolymers[13], and may be related to their greater β-CD content which contributes to the greater observed framework porosity.

3.4.2. Sorption

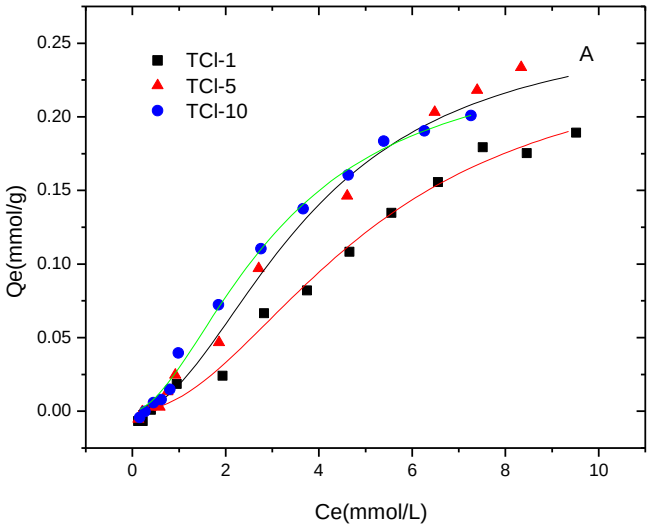

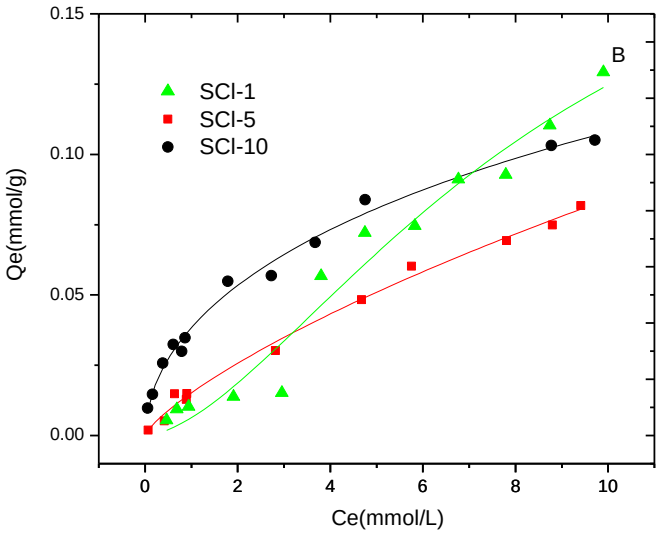

Figure 3.5. Sorption isotherms for β-CD-copolymers employing a fixed mass of sorbent (~20 mg) and variable concentration of PNP in buffer at pH 4.6 and 295 K; A) TCl-1, TCl-5, and TCl-10, and B) SCl-1, SCl-5, and SCl-10. The solid lines represent the best-fit according to the Sips isotherm.

Table 3.3. Dye-based method surface area (SA) estimates of copolymer materials obtained for the sorption of PNP at 295 K and pH 4.6, and the best fit Sips isotherm parameters (Q_m, K_{Sips} and n_s).

Copolymer	**pH**	**SA**[a]	**Q_m**[b]	**K_{Sips}**[c]	**n_s**	**χ^{2d}**
TCl-1	4.6	36.9	0.245	0.198	2.0	0.00005
TCl-5	4.6	39.6	0.263	0.268	2.0	0.00009
TCl-10	4.6	37.3	0.248	0.321	1.8	0.00003
SCl-1	4.6	33.3	0.221	0.117	1.6	0.00008
SCl-5	4.6	50.9	0.338	0.0280	0.87	0.00001
SCl-10	4.6	53.0	0.352	0.0393	0.65	0.00015

[a] surface area, (m^2/g)

[b] Q_m, (mmol/g)

[c] K_{Sips}, (L/mmol)

[d] χ^2, Chi-square distribution

Figure 3.5A-B illustrate the sorption isotherms (Q_e *vs.* C_e) of PNP with the TCl- and SCl-based copolymers at pH 4.6. In Fig. 5A, Q_e increases monotonically as C_e increases over the range of PNP concentrations investigated. The relative concentration dependence of Q_e observed for the TCl-based copolymers is TCl-10 ≈ TCl-5 > TCl-1. The ordering of the relative sorption capacity is understood in terms of the incremental contribution due to the linker domains. Similar trends were previously reported in a systematic study of urethane copolymers containing β-CD[11]. In Figure 3.5B, the sorption isotherms (Q_e vs. C_e) for SCl-5 and SCl-10 increase monotonically with increasing residual PNP (*i.e.* C_e) at pH 4.6 and 295 K. In contrast, the concentration dependence of Q_e is sigmoidal in nature for SCl-1. The latter effect is attributed, in part, to the partial solubility of SCl-1which contributes to a greater apparent value of Q_e over the range of C_e values studied. Notwithstanding the results for SCl-1, the Q_e values generally increase as the linker content increases, as shown by the relative ordering: SCl-10 ≈ SCl-5 > SCl-1. In general, the sorption capacity increases as the linker content increases for SCl-X and TCl-X, and indicates the importance of the linker domain sorption sites. TCl-10 and SCl-10 show similar sorption properties with TCl-5 and SCl-5, respectively. One possible reason might be due to the lower pore accessibility for the molecules with a molecular size similar to PNP at such levels of cross linking. TCl-10 has a fairly rigid porous network with a slightly decreased sorption capacity toward PNP, as compare with TCl-5.

The solid lines through the experimental data in Fig. 3.5 represent the *best-fit* according to the Sips model (*cf.* eqn 3.3). The isotherm parameters in Table 3.3 provide estimates of the monolayer sorption (Q_m), Sips equilibrium constant (K_{Sips}), and the exponential parameter (n_s). Monolayer adsorption behavior occurs when n_s=1; whereas, heterogeneous sorption occurs when $n_s \neq 1$. The latter is observed for each copolymer in Table 3.3 and provides support of multiple sorption sites for the inclusion and non-inclusion binding of PNP (*cf.* Scheme 3.2). Independent evidence is provided by the forthcoming 1-D and 2-D NMR spectroscopy results (*vide supra*). According to Table 3.3, the TCl copolymers have reduced sorption with PNP (Q_m = 0.245-0.263

mmol/g) while the SCl-based copolymers have greater sorption (Q_m = 0.221-0.352 mmol/g). The dye-based surface area (SA) estimates (*cf*. eqn. 3.3) of the copolymer materials were obtained using the Q_m values in Table 3.3, and generally exceed the BET estimates listed in Table 3.2. The difference in SA values (Tables 3.2 and 3.3) relate to the occurrence of copolymer swelling in aqueous solution. Swelling of "*soft materials*", such as PAA-based microsphere copolymers was previously reported[13], where the degree of swelling increased with increasing PAA content. Similarly, the greater swelling behaviour of SCl-based copolymers account for the offset in Q_m values. The Q_m values for intermediate and highly cross linked SCl- and TCl-X copolymers (X = 5 or 10) are comparable for a given linker; $Q_m \approx 0.25$ mmol/g (TCl-X) < $Q_m \approx 0.34$ mmol/g (SCl-X). The greater sorption capacity of the latter is attributed to its greater SA. Comparable differences in the SA due to swelling of aliphatic *vs*. aromatic containing copolymers are shown,, as previously reported for urethane copolymers[11,31].

3.4.3. Spectroscopic characterization of the PNP/Copolymer complexes

A detailed understanding of the sorption mechanism is limited without supporting spectroscopic studies. NMR spectroscopy has provided valuable insight concerning the formation of host-guest complexes[32, 36]. Therefore, ^{1}H NMR studies of the water soluble polyester copolymers (TCl-1/SCl-1) were measured in the presence of variable levels of PNP using 1-D and 2-D NMR methods in solution to characterize the nature of the copolymer/PNP complexes[37,38]. Thermodynamic sorption studies provide evidence for the existence of multiple sorption sites for copolymer-based β-CD sorbents[10, 15-19]. Figure 3.6 shows the ^{1}H NMR spectra for copolymer/PNP complexes formed in D_2O at ambient conditions (pD ~ 6). TCl-1 and SCl-1 were evaluated at variable copolymer/PNP ratios; TCl-1/PNP (*i.e*. 1:1, 1:2, 1:3, and 1:5) and SCl-1/PNP (1:1, 1:2, and 1:3). The chemical shift (δ) of the ortho- (H_o) and meta- (H_m) nuclei of PNP in the presence of copolymer are shifted upfield, consistent with observations for apolar binding processes[36]. The ^{1}H NMR complexation induced shift (CIS) values for H_o is more pronounced than H_m of PNP. The CIS values of PNP reach a maximum at the 1:2 copolymer/PNP ratio for TCl-1 and the 1:3 ratio for SCl-1 copolymers; thereafter, the CIS values (Δδ) are shifted downfield due to the fractional contribution of unbound PNP. The greater Δδ for H_o are anticipated because of the directional inclusion geometry of PNP within the cavity of β-CD[36-38], with additional H-bonding and van der Waals interactions between PNP and the

copolymer framework sites[11,17]. In addition to the observed Δδ for PNP, corresponding effects are observed for the β-CD nuclei (*i.e.* H_3 and H_5) of the SCl-1 and TCl-1 copolymers, and provide supporting evidence of inclusion binding[36-38]. In Fig. 3.6b, Δδis observed for the methylene groups of SCl-1, as evidenced by the interior methylene groups (*i.e.* γ- and δ-CH_2) of SCl. The results observed in Fig. 3.6 provide an indication that interactions may occur between PNP and the copolymer framework sites, both inclusion and linker domains[39]. However, the inclusion sites of β-CD are occupied firstly by PNP due to its pre-organized cavity and favourable complex stability; in agreement with the NMR results reported for the β-CD/PNP complex by Schneider *et al.*[32]. The interstitial sites (*i.e*. linker domains) are secondary in nature according to the sorption results, as described above. The occurrence of potential -CH-π and π-π interactions between PNP and the copolymer framework are anticipated[40] and the degree of sorption is well described by the Hansch parameter[41] of the copolymer framework.

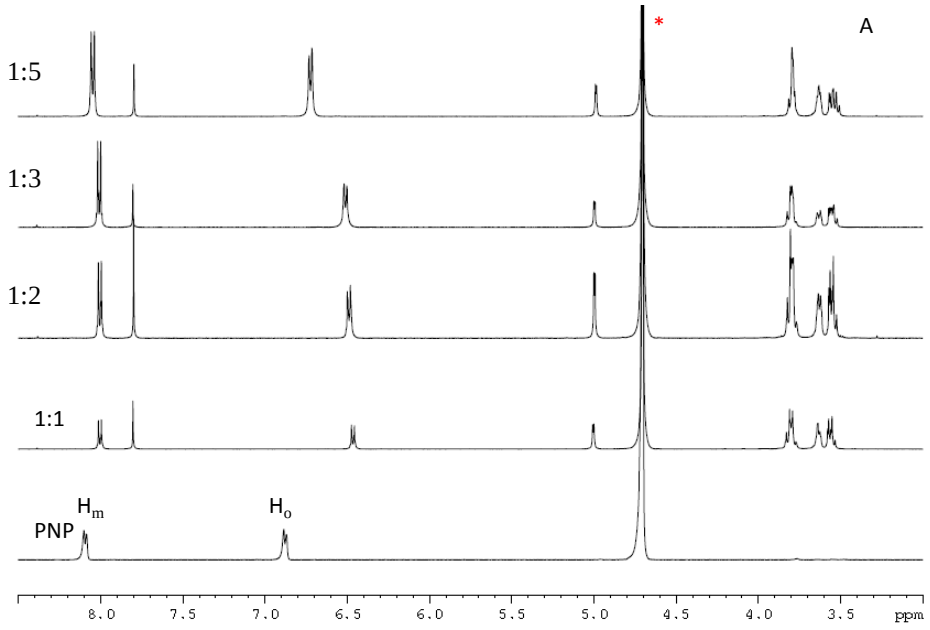

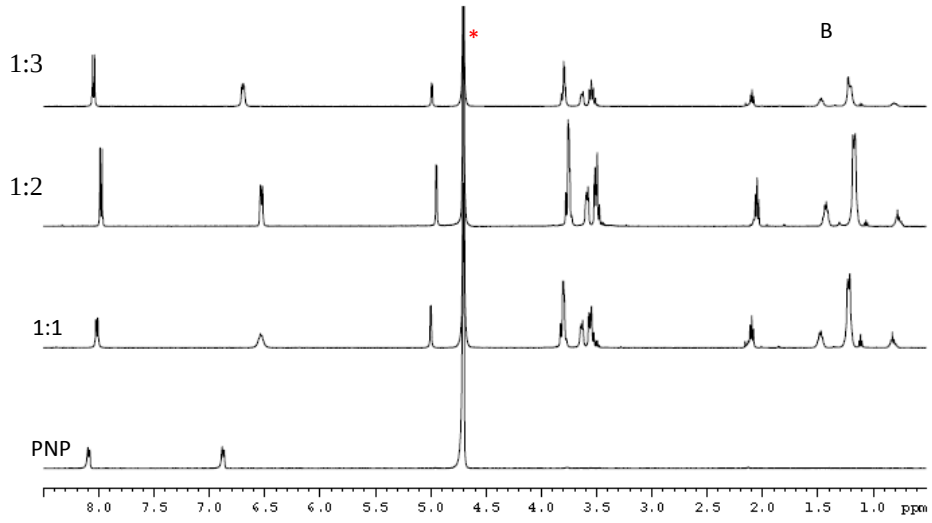

Figure 3.6. ^{1}H NMR spectra at 500 MHz and 298 K; A) TCl-1/PNP at the 1:1, 1:2, 1:3, and 1:5 copolymer/PNP ratios, and B) SCl-1/PNP for the 1:1, 1:2, and 1:3 copolymer/PNP systems. The asterisk (*) denotes the NMR solvent (D_2O).

Figure 3.7 and 3.8 illustrate the 2D-ROESY ^{1}H NMR spectra[26,27] for TCl-1 and SCl-1 with PNP at various copolymer/PNP mole ratios, analogous to the experimental conditions described for the 1-D spectra described in Fig. 3.5. In Fig. 3.7A, weak intermolecular nOe's are observed for the 1:1 TCl-1/PNP system between the ^{1}H nuclei of TCl with the *o*- and *m*-protons of PNP.

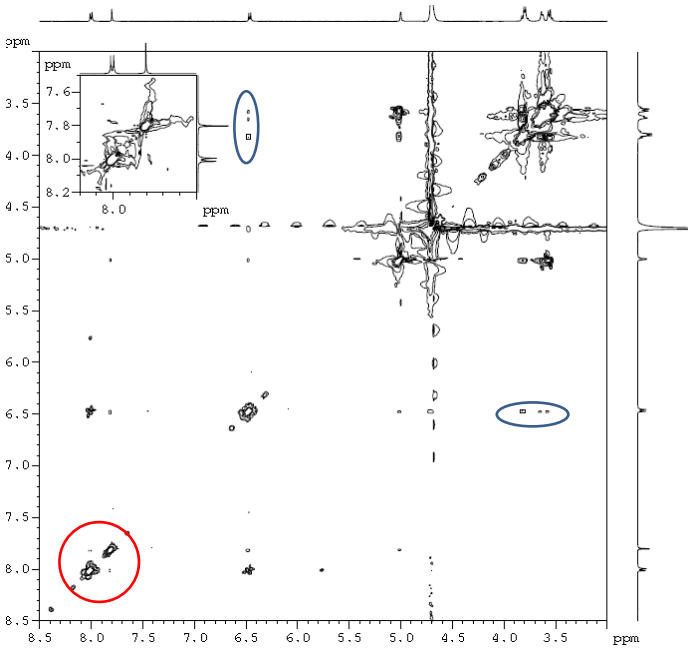

Figure 7A

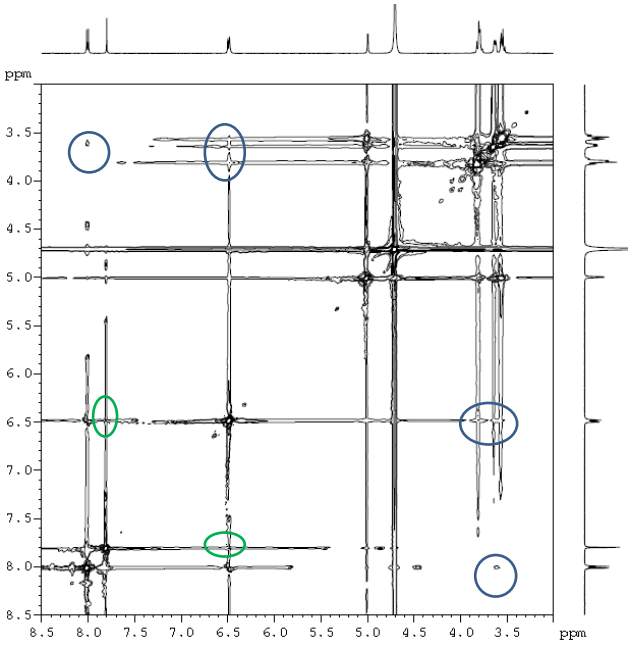

Figure 3.7B

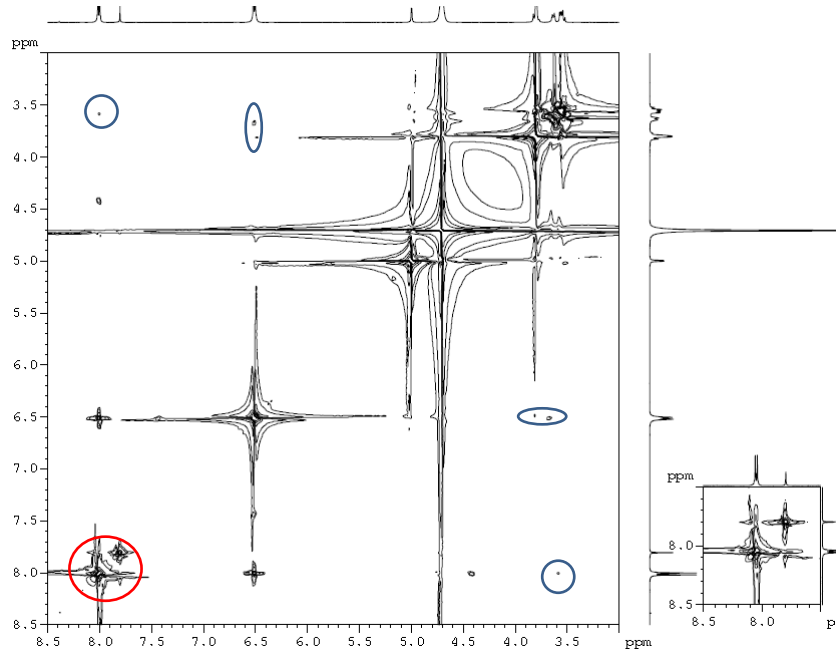

Figure 3.7C

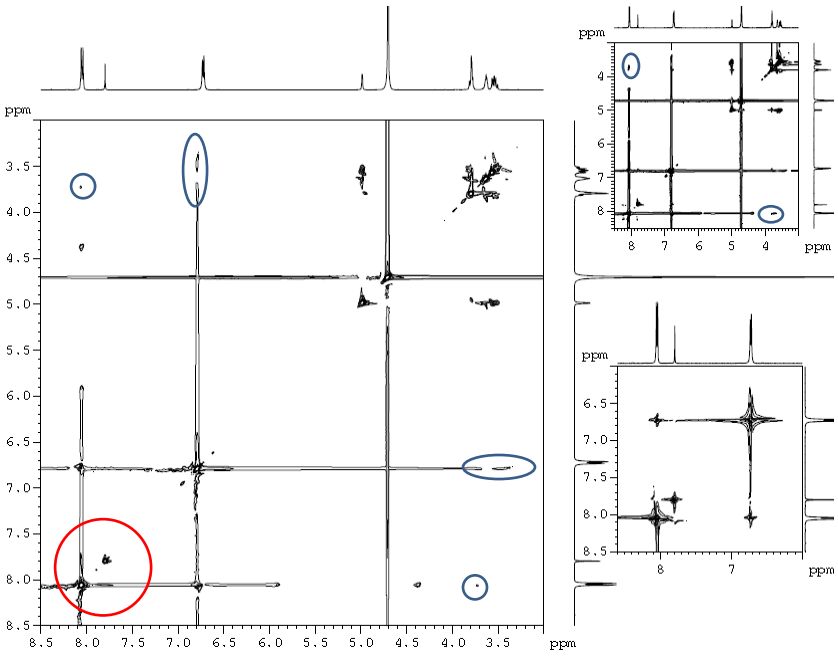

Figure 3.7D

Figure 3.7. 2-D ^{1}H NMR ROESY spectra in D_2O at 500 MHz and 298 K; A) 1:1 TCl-1/PNP, B) 2:1 TCl-1/PNP, C) 3:1 TCl-1/PNP, and D) 5:1 TCl-1/PNP systems.

Correlations are observed between the *o*-nuclei (H_o) of PNP and the interior cavity nuclei (*i.e*. H_3 and H_5) of β-CD. However, intermolecular correlations are not observed for the *m*-nuclei (H_m) of PNP with β-CD. The results observed herein are consistent with a previous report of complexes for β-CD/bisphenol A (*cf*. Fig. 3 in [42]). The inclusion geometry for the TCl-1 copolymer and β-CD are similar, and is attributed to cross linking of TCl at the primary hydroxyl groups of β-CD. Thus, the absence of steric effects in the annular region of the copolymer affords similar host-guest binding properties similar to β-CD (*cf*. Scheme 3.3), and these results are supported by an independent binding study of isostructural polyurethane copolymers with phenolphthalein (*cf.* Table 2 in [12]; β-CD:PDI *vs*. β-CD). The directional inclusion mode of the 1:1 β-CD/PNP complex (*cf*. Scheme 3.3) is consistent with the matching of the dipole moment of the host and the guest and the hydration characteristics of the system[6, 32, 36]. In Fig. 3.7B, nOe's are observed between H_o (PNP)/H_5 (β-CD) along with more pronounced correlations between the nuclei of PNP and the TCl unit. The ROESY spectrum in Fig. 3.7C is similar to Fig. 3.7B with the exception that a new nOe is observed for observed between H_m (PNP)/H_5 (β-CD). The increased intensity of the cross peaks between aromatic protons of PNP and TCl are consistent with the increased concentration of PNP. Fig. 3.7D resembles the general features noted in Fig. 3.7C where H_m (PNP) correlates with H_5 (β-CD); whereas, H_o (PNP) does not reveal any measureable correlation with the cavity nuclei of β-CD (*cf*. expanded spectra in the inset).

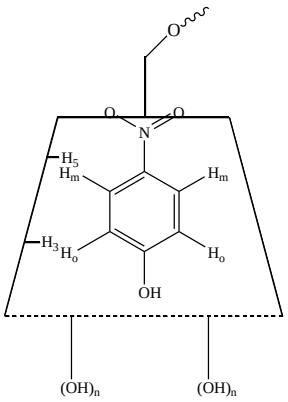

Scheme 3.3. Binding of PNP at the inclusion site of β-CD in the copolymer framework. The wavy line represents the cross linker (SCl or TCl) unit of the copolymer framework.

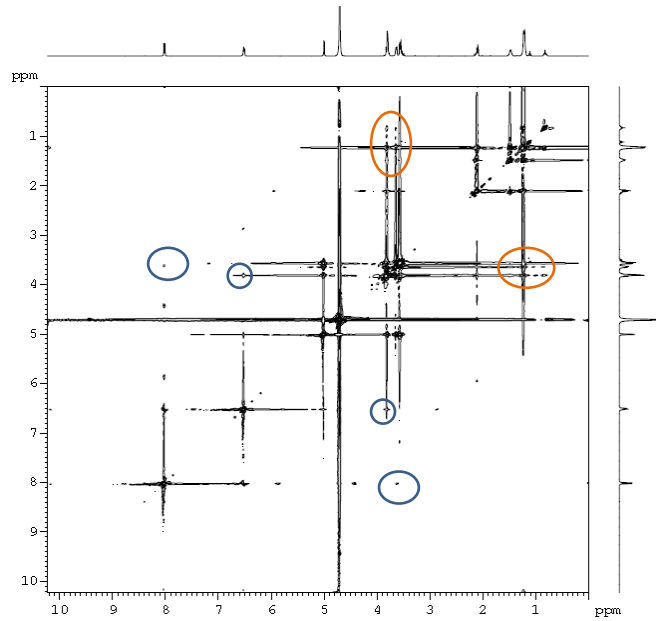

Figure 3.8A

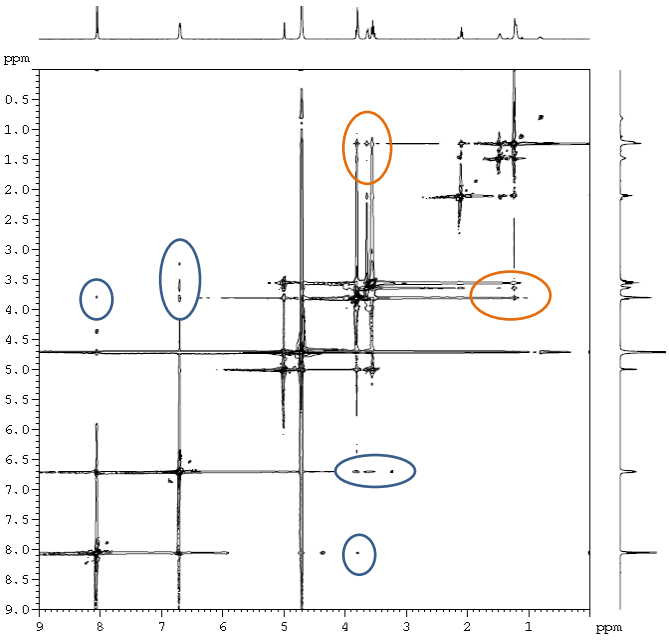

Figure 3.8B

Figure 3.8. 2-D ^{1}H NMR ROESY spectra obtained in D_2O at 500 MHz and 298 K; A) 1:1 SCl-1/PNP, and B) 3:1 SCl-1/PNP.

Figure 3.8 illustrates the ^{1}H NMR ROESY spectra for the SCl-1/PNP system at variable mole ratios (*i.e.* 1:1 and 1:3). In Fig. 3.8A, correlations are observed between H_o and H_m (PNP) with H_3 and H_5 (β-CD); however, there are no measurable nOe's between PNP with the methylene groups of SCl. Dipolar correlations are observed between the cavity nuclei of β-CD with the δ- and γ-CH_2 groups of SCl. The latter result may be due to coiling of the permethylene chain in the annular region of β-CD[43]. Self-inclusion of TCl in the interior of β-CD is unlikely because of the rigid aromatic TCl cross linker, as compared with SCl-1. In Fig. 3.8B, intermolecular correlations are observed between PNP and the interior nuclei of β-CD; however, no measureable correlations are evident between PNP and the various methylene units of SCl. Analysis of the dipolar correlations between the *o*- and *m*-protons of PNP with the cavity nuclei of β-CD of SCl-1 indicates that PNP forms an inclusion complex analogous to the TCl-1 copolymer. The sorption of PNP occurs at the inclusion and interstitial sites of the copolymer as illustrated in Scheme 3.4.

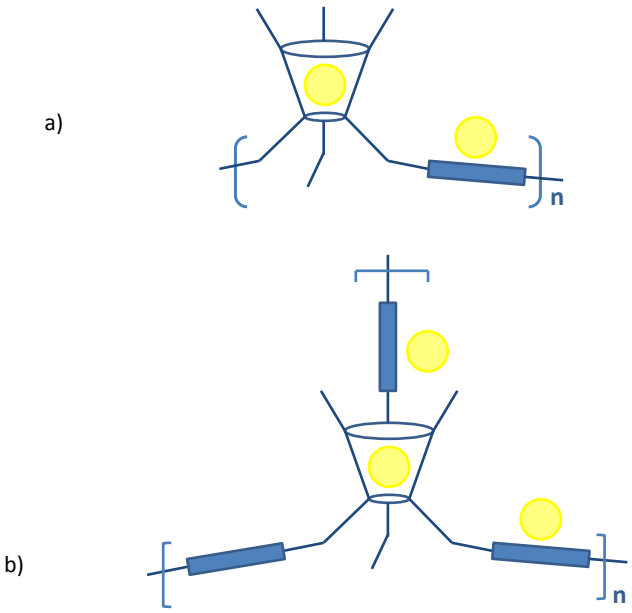

Scheme 3.4. The adsorption sites of cross linked polyester copolymers containing an adsorbate guest molecules (sphere represents PNP) at the β-CD inclusion sites (tori interior) and the non-

inclusion (interstitial) sites of the copolymer framework; a) low levels of cross linker (1:1 β-CD: linker) content, and b) moderate cross linker content (1:5 β-CD: linker). The straight line segments connecting the β-CD tori represent the cross linker units (TCl/SCl linker domains). The solvent has been omitted for clarity purposes.

The 1:1 copolymer/PNP systems favour the formation of β-CD inclusion complexes with PNP due to the favourable inclusion site accessibility. As the level of cross linker content increases, evidence of interactions between the cross linker domains with PNP are deduced according to the sorption results (*cf*. Fig. 3.5 and Scheme 3.4). Upfield Δδ values of the cross linker framework sites of SCl-1 and PNP (*cf*. Fig. 3.6) support this conclusion. ^{1}H NMR ROESY spectra for the TCl-1/PNP system provide unequivocal support for the association of PNP and the TCl linker units, as evidenced by the dipolar nOe correlations. In the case of the SCl-1/PNP system, such dipolar correlations were not observed between PNP and the SCl linker unit. This may be due, in part, to competitive inclusion of the permethylene chain of SCl in the β-CD cavity which attenuates the dipolar nOe's between the SCl framework and PNP, in agreement with the reduced sorption capacity of SCl-1 relative to TCl-1. The methylene chain of the SCl linker is sufficiently long to enable self-inclusion within the cavity of β-CD. The sorption results in Fig. 3.5b provide strong support that SCl-5 and -10 exhibit sorption of PNP with the linker domains of the copolymer framework; however, the relative insolubility of SCl-X or TCl-X (X = 5 and 10) in water precludes their NMR analysis in D_2O.

In a previous NMR study[44], complexes between an isostructural urethane copolymers (*i.e*. HDI-1) with PNP were investigated. The dipolar correlations between PNP and the hexamethylene linker unit of HDI-1 were observed using 1D ROESY experiments at variable temperatures, and corroborate the results of SCl-1 reported herein[45]. The absence of dipolar correlations between the linker domain of SCl-1 and PNP in Fig. 3.7 was attributed to competing equilibria such as the inter-conversion between the self-included and extended form of the linker unit. In the case of the self-included form of the SCl linker, the availability of potential sorption sites for PNP decrease accordingly; thereby, limiting the detection of dipolar correlations by 2D

NMR ROESY experiments, as observed herein. The sensitivity of 1D ROESY experiment depends not only on the optimization of the ROESY mixing time, but also on the selectivity of the shape of the excitation pulse, the duration and the power level. For example, the duration of the selective excitation presents one source of signal attenuation due to relaxation that is active during the shape selective pulse[46]. Optimization and/or modification of the standard 1-D selective ROESY pulse program may be necessary in future studies to unequivocally ascertain the suggested copolymer/guest correlations concluded herein for SCl-1/PNP (*cf.* Scheme 3.4). Notwithstanding the limited 2D NMR evidence of dipolar correlations between the linker domains of SCl-1 with PNP, additional support is presented for the sorption at multiple sites (*i.e.* inclusion and interstitial) for SCl-X and TCl-X copolymers. Various factors contribute to the limited dipolar interactions between the linker domains of SCl-1and PNP; competitive equilibria (*i.e.* self-inclusion of SCl by β-CD), motional dynamics of SCl, and hydration properties of SCl. Incremental sorption of PNP by linker sites with increasing linker content of the copolymer was concluded in this study. By contrast, TCl-1 cannot undergo self-inclusion and the occurrence of favourable π-π interactions contribute to enhanced complex stability between PNP and the linker domains of TCl, according to the 2D NMR results.

3.5. Conclusions

Microemulsion-based polyester sorbent materials containing β-CD exhibit favorable adsorption of PNP in aqueous solution at pH 4.6. Differences in the sorption properties were observed according to the nature of the linker (*i.e.* SCl *vs.* TCl) and the relative linker content of the copolymer materials. The sorption properties are well-described by the Sips isotherm. In general, the sorption capacity of SCl-X copolymers exceeds TCl-X copolymers, in accordance with swelling phenomena and the greater surface area of copolymers with aliphatic linkers. The sorption capacity toward PNP increases as the linker content of the copolymer increases. Inclusion complexes are formed between PNP and the β-CD sites of the copolymer; whereas, PNP is adsorbed at the cross link domains of the copolymer framework in a step-wise process with increasing adsorbate concentration (*cf.* Scheme 3.4). The results are strongly supported by the 1D- and 2D-NMR spectroscopic results. This study has contributed to a detailed understanding of the equilibrium thermodynamic sorption process between polyester copolymers containing β-CD and PNP. The results of this study will contribute to the further development of

copolymer materials with unique sorption and molecular recognition properties for contaminant species in aquatic environments and other sorption-based applications.

3.6. Acknowledgements

The authors wish to acknowledge the Natural Sciences and Engineering Research Council of Canada (NSERC), the Canada Foundation for Innovation (CFI), and the University of Saskatchewan for supporting this research. RG gratefully acknowledges NSERC for a PhD scholarship through the NSERC CREATE-HERA program.

3.7. References

(1) Sybilska, D.; Smolkova-Keulemansova, E. Ed. J. Atwood, L.; Davies, J. E. D.; MacNicol, D. D. *In Inclusion Compounds*; *Applications of inclusion compounds in chromatography* **1984**, 3, 173.

(2) Crini, G.; Morcellet, M. *J. Sep. Sci.* **2002**, 25, 789-813.

(3) Kozlowski, C. A.; Sliwa, W.; Nowik-Zajac, A. *Ed. J. Hu, Application of cyclodextrin derivatives and polymers in membrane separation From Cyclodextrins: Chemistry and Physics* **2010**, 141.

(4) Krause, R. W. M.; Mamba, B. B.; Bambo, F. M.; Malefetse, T. J. *Ed. J. Hu, Cyclodextrin polymers: synthesis and application in water treatment From Cyclodextrins: Chemistry and Physics* **2010**, 185.

(5) Penas, F.; Javier, I.; Jose, R.; Ed. Jose, S.; Jose, M. *Advances in Chemical Engineering* **2010**, 175.

(6) Bender, M. L.; Komiyama, M. Cyclodextrin *Chemistry. Berlin: Springer-Verlag*, **1978**.

(7) Wenz, G. *Angewandte Chemie Int. Ed. Engl.*, **1994**, 33, 803-822.

(8) van de Manakker, F.; Vermonden, T.; van Nostrum, C. F.; Hennink, W. E. *Biomacromol.* **2009**, 10, 3157-3175.

(9) Ma, M.; Li, D. *Chem. Mater.* **1999**, 11, 872-874.

(10)Wilson, L. D.; Mohamed, M. H.; Headley, J. V. *J. Colloid Interface Sci.* **2011**, 357, 215-222.

(11) Mohamed, M. H.; Wilson, L. D.; Headley, J. V. *J. Colloid Interface Sci*. **2011**, 356, 217-226.

(12) Mohamed, M. H.; Wilson, L. D.; Headley, J. V. *Carbohydr. Polym*. **2010**, 80, 186-196.

(13) Guo, R.; Wilson, L. D.; Appl, J. *Polym. Sci.* **2012**, 125, 1841-1854.

(14) Yuen, F.; Tam, K. C. *Soft Matter*. **2010**, 6, 4613-4630.

(15) Crini, G. *Prog. Polym. Sci*. **2005**, 30, 38-70.

(16) Yudiarto, A.; Kashiwabara, S.; Tashiro, Y.; Kokugan, T. *Sep. Purif. Tech*. **2001**, 24, 243-253.

(17) Garc á-Zubiri, I. X.; Gonz ález-Gaitano, G.; Isasi,J. R. J. *Colloid Interface Sci.* **2009,** 337, 11-18.

(18) Rossi, R. H.; Silva, O. F.; Vico, R. V.; Gonzalez, C. J. *Pure Appl. Chem.* **2009**, 81, 755.

(19) Poon, L.; Wilson, L. D.; Headley, J. V. J. *Appl. Polym. Sci.* **2012**.

(20) Bibby, D. C.; Davies N. M.; Tucker, I. G. *Int. J. Pharm.* **1999**, 180, 161-168.

(21) Pariot, N.; Edwards-Levy, F.; Andry M. C.; Levy, M. C. Int. *J. Pharm.* **2000**, 211, 19-27.

(22) Allen, T. *Particle Size Measurement: Surface Area and Pore Size Determination, fifth ed., Chapman & Hall, 2-6 Boundary Row, London, UK*, **1997**.

(23) Sing, K. *Coll. Surf. A.* **2001,** 3, 187–188.

(24) Broekhoff, J.C.P.; De Boer, J.H. *J. Catal.* **1968**, 10, 153-165.

(25) Barrett, E.P.; Joyner, L.G.; Halenda, P.P. *J. Am. Chem. Soc.* **1951**, 73, 373-380.

(26) Berger, S.; Braun, S. *In 200 and More NMR Experiments: A Practical Course, 3rd Ed.; Wiley-VCH: Weinheim, New York,* **2004**.

(27) a) Braunschweiler, L.; Ernst, R. R.; Mag, J. *Res. Chem.* 1983, 53, 521-528. b) Bax, A.D.; Davis, G. *J. Mag. Res. Chem.* **1985**, 65, 355-360. c) Bauer, C.; Freeman, R.; Frenkiel, T.; Keeler, J.; Shaka, A. *J. J. Mag. Res. Chem.* **1984**, 58, 442-457. d) Kessler, H.; Oschkihat, H.; Griesinger, C.; Bermel, W. *J. Mag. Res. Chem.***1986**, 70, 106.

(28) Dupuy, G.; Hilaire, G.; Aubry, C. *Clin. Chem.***1987**, 33, 524-528.

(29) Giles, C. H.; D' Silva, A. P.; Tridevi, A. S. *J. Appl. Chem.* **1970,** 20.

(30) Sips, R. *J. Am. Chem. Soc.* **1948**, 125, 6452.

(31) Mohamed, M. H.; Wilson, L. D.; *J. V. Carb. Res.* **2011**, 346, 219-229.

(32) Schneider, H-J.; Hacket, F.; Rüdiger, V. *Chem. Rev.* 1998, 98, 1755, and references cited therein.

(33) Bambo, M. F. *MSc Thesis, University of Johannesburg, South Africa,* **2007**.

34. Pratt, D. Y.; Wilson, L. D.; Kozinski, J. A.; Mohart, A. M. *J. Appl. Polym. Sci.* **2010**, 116, 2982.

(35) Sing, K. S. W.; Everett, D. H.; Haul, R. A.; Moscou, W. L.; Pierotti, R. A.; Rouquerol, J.; Siemieniewska, T. *Pure Appl. Chem.* 1985, 57, 603-619.

(36) Wood, D. J.; Hruska, F. E.; Saenger; W. *J. Am. Chem. Soc.* **1977**, 99, 1735-1740.

(37) Forgo, P.; D'Souza, V. T. *Mag. Res. Chem.* **1999**, 37, 48.

(38) a) Yamamoto, Y.; Onda, M.; Takahashi, Y.; Inoue, Y.; Chujo, R. *Carb. Res.* **1988**,182, 41, b) Inoue, Y.; Kanda, Y.; Yamamoto, Y.; Kobayashi, S. *Carb. Res.* **1992**, 226, 197.

(39) Domjan, A.; Geissler, E.; Laszlo, K. *Soft Matter* **2010**, 6, 247-251.

(40) a) Steed, J.W.; Atwood, J.L. *Supramolecular Chemistry, 2nd ed., John Wiley & Sons, Ltd., West Sussex, UK*, **2009**. b) Tewari, A. K.; Dubey, R. *Bioorg. Med. Chem.* **2008**, 16, 126-143.

(41) Hansch, C.; Kiehs, K.; Lawrence, G. L. *J. Am. Chem. Soc.*, **1965**, 87, 5770-5773.

(42) Yang, Z-X.; Chen, Y.; Liu, Y. *Carb. Res.* **2008**, 343, 2439-2442.

(43) Takahashi, K.; Narita, H.; Oh-Hashi, M.; Yokoyama, A.; Yokozawa, T. *J. Inclusion Phenom. Macrocycl. Chem.* **2004**, 50, 121-127.

(44) Karoyo, A. H.; Wilson, L. D. *Macromol.* **2012** *submitted*.

(45) Hasan, E. A.; Cosgrove, T.; Round, A. N. *Macromol.* **2008**, 41, 1393-1400.

(46) Furrer, J. J. *Nat. Prod.* **2009**, 72, 1437-1441.

CHAPTER 4

Description

Chapter 4 includes a verbatim copy of an article published in December, 2012 in Journal of Colloid Interface Science (J. Colloid Interface Sci. **2012**, 388, 1, 225-234.) The paper describes the systematic methods of synthesis and characterization of CS/PAA copolymer materials.

Author's contribution

I carried out all the experimental work including synthesis and characterization of the copolymers. This work was principally supervised by Dr. Wilson. I wrote the first draft of the manuscript with assistance in the form of editing of the final manuscript from Dr. Wilson before submitting for publication. The co-authors grant permission of use of the published manuscript for this PhD thesis, and agree with the description of the roles and contributions of the authors.

Relationship of Chapter 4 to the overall objective of this project

As stated in the introduction, the first research objective was material design and characterization. This chapter reports the systematic design of a series of CS based graft polyamide copolymers by tuning of the synthetic conditions (e.g. pre-polymer ratio). The physiochemical properties of the copolymers are anticipated to be engineered under control. A systematic characterization of the CS/PAA copolymers was also described in the manuscript, including the surface characterization by gas and dye adsorption method.

Research highlight:

A series of CS/PAA copolymer materials were synthesized using a dropping method to cross-link the polysaccharide, CS, and cross-linker PAA. The copolymers were prepared by varying the pre-polymer ratio during synthesis to achieve tunable physicochemical properties. Various characterization methods, such as, FT-IR, TGA, N_2 porosimetry, and dye adsorption method were carried out in this research. The Sips sorption isotherms were used to obtain the equilibrium sorption properties of CS/PAA copolymers. Heterogeneous adsorption was also observed for these CS-PAA copolymers with MB; the micropore domains of the copolymer framework and the numerous surface bound PAA sites ($-COO^-$). The tunable adsorption properties of these "*smart materials*" are observed upon external environmental changes as evidenced by the desorption of MB by altering the solution pH.

4. Synthetically Engineered Chitosan-Based Materials and their Sorption Properties with Methylene Blue in Aqueous Solution

Rui Guo and Lee D. Wilson*

Department of Chemistry, University of Saskatchewan, 110 Science Place, Saskatoon, Saskatchewan, S7N 5C9

*Corresponding author: Tel. 1-306-966-2961, Fax. 1-306-966-4730
e-mail: lee.wilson@usask.ca

4.1. Abstract

Chitosan (CS) and poly (acrylic acid) (PAA) were crosslinked by an ionic gelation method to form super absorbent polymers (SAPs). CS and PAA form amide bonds between the amino and carboxyl groups. The CS-PAA copolymers were synthetically engineered by varying the feed ratios of the prepolymer units. The copolymer materials possess tunable sorption and mucoadhesive properties with a backbone structure resembling proteinaceous materials. The sorption properties of the copolymers toward methylene blue (MB) in aqueous solution were studied using UV–Vis spectrophotometry at ambient pH and 295 K. The copolymers showed markedly varied interactions with MB, from *physisorption*- to *chemisorption-like* behavior, in accordance with their composition, surface area, and pore structure characteristics. The sorption isotherms were evaluated with the Sips model to provide estimates of the sorption properties. The sorbent surface area (271 and 943 m^2/g) and the sorption capacity (Q_m=1.03 and 3.59 mmol/g) were estimated for the CS-PAA copolymer/MB systems in aqueous solution.

Keywords: Chitosan; poly(acrylic acid); copolymers; sorbents; super absorbent polymers; sorption properties; methylene blue

4.2. Introduction

The removal of synthetic dyes from industrial effluents is a significant environmental issue of global concern due to the challenges in treating such industrial wastewater using conventional methods[1]. The presence of dyes in surface water environments, even at very low quantities, is aesthetically undesirable. Furthermore, these pigments can retard photosynthesis and limit the growth of aquatic biota by attenuating the transmission of sunlight in aquatic environments. Synthetic dyes are typically organic compounds which are recalcitrant in nature with variable toxicity. Remediation techniques have been recently reviewed and compared for the treatment of dye-containing wastewaters. These include electrochemical, coagulation and flocculation, chemical oxidation, solvent extraction, and adsorption based methods[1-3]. Among these techniques, adsorption is attractive because of its relatively low cost, technological simplicity, ease of operation, and good mechanical stability[3]. Methylene blue (MB; Fig. 4.1a) is a widely used organic dye in the chemical industry due to its high water solubility with various applications in coloring paper, temporary hair colorants, and dyeing of cottons, wools, and coatings for paper stock[4]. MB is hazardous when ingested through breathing, digestion, and dermal contact[4a]. Acute exposure to MB will cause increased heart rate, shock, Heinz body formation, vomiting, quadriplegia, cyanosis, jaundice, and tissue necrosis in humans[4a]. Activated carbon (AC) is a commonly used industrial adsorbent for MB removal due to its high adsorptive capacity, high surface area, microporous structure, and its high degree of surface reactivity[4]; however, commercial AC is generally expensive and difficult to regenerate after usage[4b]. In an effort to address the need of developing renewable biomaterial-based sorbents with improved dye sorption properties, synthetically engineered chitosan materials were prepared.

a)

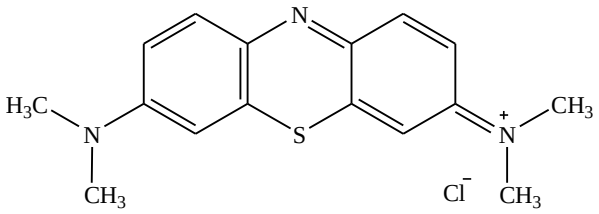

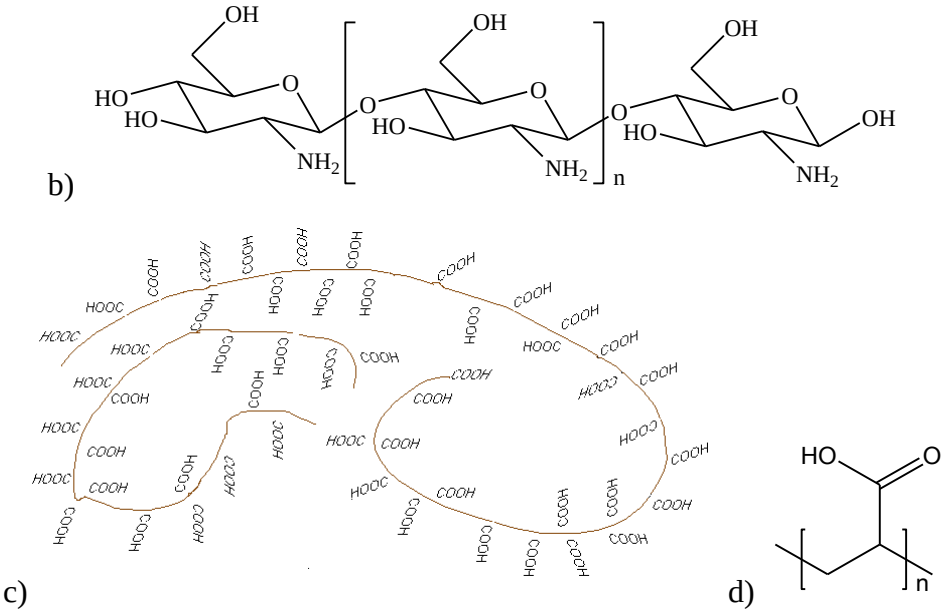

Figure 4.1. Molecular structure of a) Methylene blue, b) Chitosan, c) Schematic folded structure of poly (acrylic acid) (PAA), and d) PAA monomer, where n is the degree of polymerization.

Chitosan (CS; Fig. 4.1b) is produced industrially by the deacetylation of chitin derived from the exoskeletons of crustaceans or the cell walls of fungi, and widely used in various industries due to its biocompatibility, antibacterial properties, and low cost[5]. CS is a linear polysaccharide composed of randomly distributed β-(1→4)-linked D-glucosamine and N-acetyl-D-glucosamine units[5]. Polysaccharides such as chitosan are generally stiff molecules, due to the β-linkages and the stiffness leads to highly extended conformations of the polymer chains[5a]. CS serves as a rigid prepolymer back-bone component for the design of copolymer materials. In contrast, poly (acrylic acid) (PAA) is a soft and flexible polymer with numerous (56-68% w/w) carboxylic acid groups (*cf.* Figure 4.1c and d)[5f] which act as the crosslinker between the backbone units of CS. As the amino groups from CS are condensed together with the carboxylic groups of PAA via amide bonds, CS-PAA copolymers adopt a "*protein-like"* structure (*cf.* Scheme 4.1). The copolymers were prepared by self-assembly and complexation between oppositely charged polyelectrolytes (CS and PAA) through electrostatic interactions, referred to as the ionic gelation method.[6, 7] Ionic gelation

has the following advantages[6]: *i*) particles are formed under relatively mild conditions; *ii*) adjustable particle size; *iii*) favourable coulombic attractions; *iv*) tunable desorption properties; and *v*) relatively low toxicity. CS and PAA prepolymers are characterized as SAPs[8, 9], while the CS-PAA copolymers may serve as tunable SAPs for the removal of MB in aqueous solution. SAPs are characterized as networks of polymer chains, which can undergo swelling and entrap large amounts of water in the polymer framework[10-11]. Compared with conventional adsorbents[10], these CS-PAA copolymers are prepared with relative ease, biodegradability, and display low toxicity. These adsorbents possess super swelling capacity and are more versatile by virtue of their tunable pore structure and surface characteristics in aqueous solution.

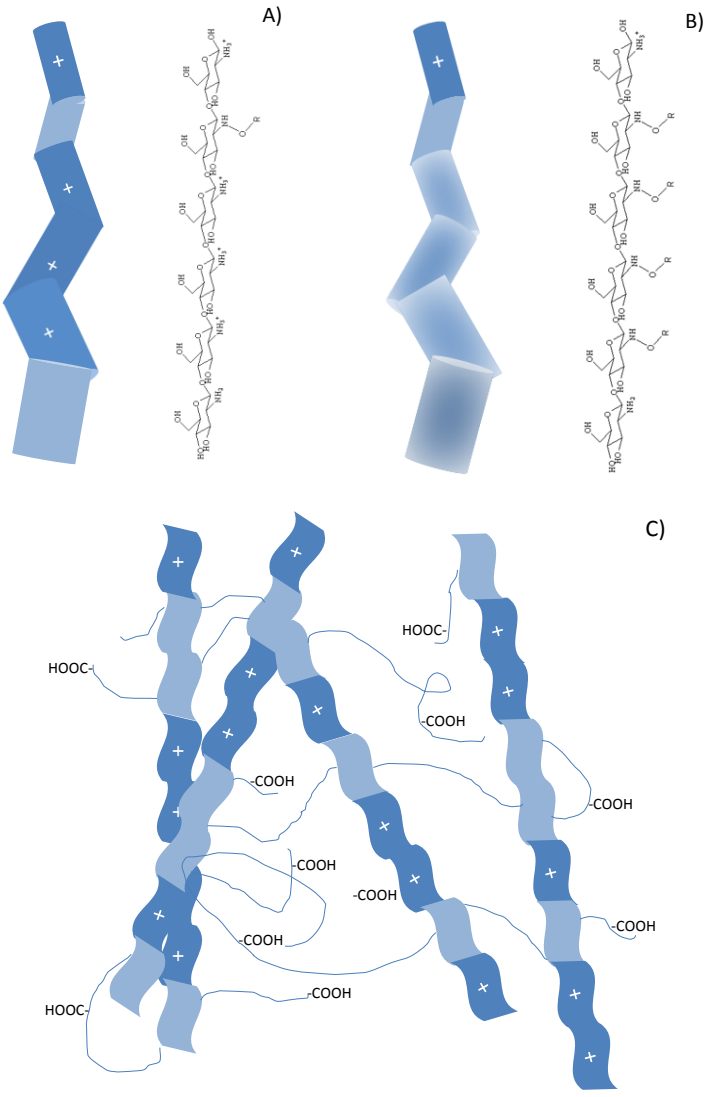

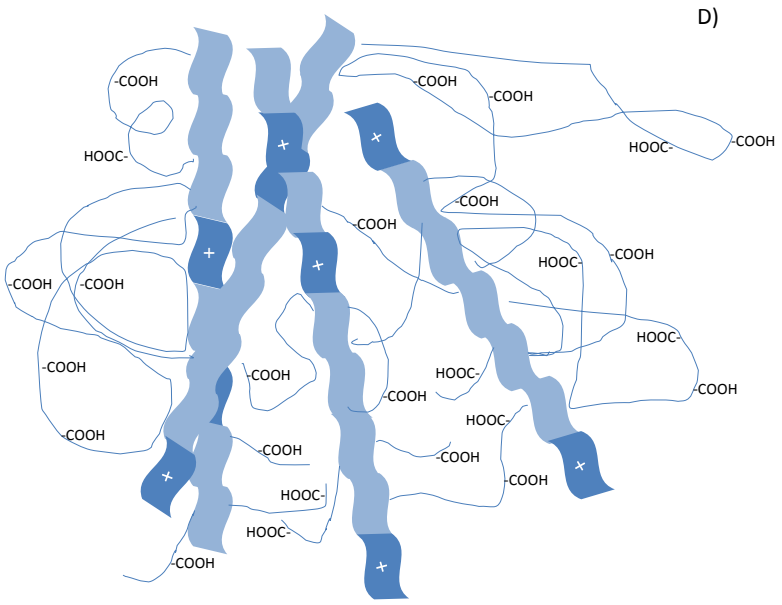

Scheme 4.1. Conceptual illustration of the crosslinked structure of CS-PAA copolymers in tits protonated form; a) single chain of CP-5, b) single chain of CP-1, c) multiple chains of CP-5, d) multiple chains of CP-1. Each ribbon represents one chitosan unit: light blue indicates neutral chitosan unit with amide bond after reacting with PAA and dark blue (with "+" symbols) indicates the protonated amine groups of chitosan.

CS and PAA have unique mucoadhesive properties due to the favorable dipolar and electrostatic interactions between the polar groups (*i.e.* ammonium and carboxylate) with mucosal surfaces[12-14]. Mucoadhesive materials are viscous in nature and well-known for their potential application as pharmaceutical excipients and controlled release properties[15, 16]. The CS-PAA copolymers were engineered with consideration of their tunable sorption and mucoadhesive properties by varying the synthetic feed ratios of CS and PAA. The objectives of this study were to synthesize the CS-PAA copolymers at various prepolymer ratios using an ionic gelation process and to examine their sorption properties with MB in aqueous solution at ambient conditions.

4.3. Experimental

4.3.1. Materials

Chitosan (CS, Mwt. ~ 50,000-190,000 g/mol) with an average degree of deacetylation of 75-85%, and poly (acrylic acid) (PAA, Mwt. ~ 250,000 g/mol) were obtained from Sigma-Aldrich Canada Ltd. Acetic acid and MB was obtained from EMD and Alfa Aesar, respectively. Medical grade nitrogen (Praxair) was used as the backfill gas for BET adsorption. All the reagents were used as received without any further purification.

4.3.2. Synthesis of the CS-PAA copolymers

CS and PAA with variable mole ratios of 5:1 and 1:1 were utilized in the synthetic preparations. Approximately 1g of CS was dissolved in 50 mL of 2% (w/v) acetic acid solution. An aqueous solution of 10% (w/v) PAA was added drop-wise to the CS solution with stirring at 1,100 rpm at room temperature using a Corning stirrer (PC320). The mixture was maintained at 1,100 rpm overnight. The aqueous solution containing the CS-PAA complex was then adjusted to pH 7 using 1M sodium hydroxide. The product and solvent were centrifuged at 9,000 rpm for 10 min., and the remaining supernatant solution and unreacted reagents decanted. The copolymers were rinsed extensively with distilled water to remove any sodium salts and subsequently freeze-dried at -55 ℃ for 24 hours. The copolymers were ground with a mortar and pestle and passed through a size 40 mesh (≤0.42 mm) sieve.

4.3.3. Copolymer Characterization

IR spectra were obtained with a Bio-RAD FTS-40 instrument with samples analyzed in reflectance mode. Solid samples were prepared by mixing copolymers (~5 mg) with pure spectroscopic grade KBr (~50 mg) with grinding in a mortar and pestle. The DRIFT (Diffuse Reflectance Infrared Fourier Transform) spectra were recorded at room temperature with a resolution of 4 cm^{-1} operating in the range of 400-4000 cm^{-1}. Sixteen scans were recorded and corrected against a background spectrum of pure KBr. The DRIFT spectra were recorded in reflectance mode (Kubelka-Munk intensity units). Thermal analyses of the copolymers were performed using thermogravimetry analysis, TGA (Q50 TA Instruments). Samples were

heated in open aluminum pans at 30 °C, and allowed to equilibrate for 5 min. prior to heating at a scan rate of 5 °C/min. up to 500 °C.

4.3.3.1. Nitrogen Adsorption

Nitrogen adsorption measurements were made on the copolymers using a Micromeritics ASAP 2020 (Norcross, GA) to obtain the surface area with an accuracy of ±5 %, as well as the pore structure properties. Approximately 1 g of sample was degassed at 550 μm Hg and ~ 70 ℃ for several hours in the sample chamber until the outgas rate was stabilized. Granular activated carbon (GAC), alumina, and silica-alumina sieves were used to check the calibration of the instrumental parameters. The BET surface area[17] was calculated from the adsorption isotherm using 0.162 nm^2 as the surface area for molecular nitrogen. The micropore surface area was obtained using a *t*-plot (de Boer method)[18, 19]. The Barret-Joyner-Halenda (BJH) method was used to estimate the pore volume and diameter from the adsorption isotherm data[20]. The BJH method uses the Kelvin equation and the assumption of slit-shaped pores[20].

4.3.3.2. Water swelling properties of copolymer materials

CS-PAA copolymers were placed in 3 dram glass vials containing pure Millipore water and allowed to equilibrate on a horizontal shaker table for 24 h. After the equilibration, the materials were centrifuged in a precision semi-micro centrifuge at 1,550 rpm for 30 min. and the supernatant aqueous solution was decanted. The copolymer materials were tamped dry using a Whatman filter paper to remove excess moisture, and the weight loss of the product was examined using TGA. The mass loss of hydrated sorbents and their swelling ratio (r) is described by Eqn. (4.1)[21],

$$r = \frac{m(swollen)}{m(dry)} \qquad (4.1)$$

where m (dry) and m (swollen) are the respective masses of the dry and hydrated copolymer, before and after equilibrating with water, respectively.

4.3.3.3. Adsorption Experiments

The pore structure properties, surface area, and sorption properties of CS-PAA copolymers with MB were evaluated using a previously reported UV–Vis method[22-24]. Fixed amounts (~10 mg) of the powdered and sieved copolymer materials were mixed with 7 mL of aqueous solution at variable dye concentrations (0.5–5 mM or 0.5–10 mM) in distilled water and equilibrated on a horizontal shaker table for 24 h. The concentrations of MB was determined before (C_o) and after sorption (C_e). The estimated molar absorptivity (ε) value for MB was determined (ε=70,25l $M^{-1}cm^{-1}$; λ_{max}= 664 nm), in agreement with a previous report[25]. The desorption experiments of MB from the copolymers were conducted at a fixed dye concentration (5 mM) with a fixed amount (10 mg) of polymer. After equilibration on a horizontal shaker in 3 dram glass vials for 24 h, the copolymers and MB solution were centrifuged and the UV-Vis spectra were obtained before and after adjusting pH of the solution from pH 6 to 2.

The sorption isotherms are depicted as plots of the adsorbed amount of MB in the copolymer phase per mass of adsorbate (Q_e; mmol/g) versus the equilibrium residual concentration of MB in aqueous solution (C_e). The value of Q_e is defined by eqn. (4.2) where C_o is the initial MB concentration, V is the volume of solution, and m is the mass of sorbent.

$$Q_e = \frac{(C_0 - C_e) \times V}{m} \qquad (4.2)$$

The dye sorption method[22] provides an independent estimate of the sorbent surface area (SA; m^2/g) in its hydrated state, according to eqn 4.3.

$$SA = \frac{A_m Q_m L}{Y} \qquad (4.3)$$

where A_m represents the cross-sectional area occupied by MB (A_m for a "*coplanar*" orientation is 8.72×10^{-19} m^2/mol, where the dimensions of the dye are 1.43 nm × 0.61 nm[26a]), Q_m is the monolayer adsorption capacity per unit mass of sorbent, L is Avogadro's number (mol^{-1}), and Y is the coverage factor (Y=2.0 for MB[26b]).

The Sips isotherm model[27] is a versatile and generalized isotherm that accounts for a distribution of adsorption energies on the sorbent surface with monolayer (Langmuir) to multi-layer (Freundlich) isotherms. The parameter (n_s) reflects the heterogeneity of the sorbent, where a value of n_s=1 infers a homogenous surface while $n_s \neq 1$ indicates a

heterogeneous surface. Langmuir behavior is predicted when n_s=1, and Freundlich behavior occurs when $K_s C_e^{n_s}$ <<<1. The Langmuir, BET, Freundlich, and Sips models are defined by eqn. 4.4[27].

$$Q_e = \frac{Q_m K_s C_e^{n_s}}{1 + K_s C_e^{n_s}} \qquad (4.4)$$

K_s is the Sips equilibrium constant and Q_m is defined by eqn. (4.2).

The criteria of the "best-fit" between the calculated isotherm and the experimental data are determined by the correlation coefficient (R^2) and the chi-square distribution (χ^2). The parameter $R^2 \sim 1$ denotes a "*best-fit*"; however, a more sensitive measure for non-linear least squares fitting involves the minimization of χ^2. χ^2 is defined by eqn. (4.5) according to the difference between the experimental ($Q_{e,i}$) and calculated ($Q_{c,i}$) sorption values with MB in aqueous solution.

$$\chi^2 = \sum \sqrt{\frac{(Q_{e,i} - Q_{c,i})^2}{N}} \qquad (4.5)$$

$Q_{c,i}$ is the calculated Q_e value with Sips isotherm model (*cf.* eqn 4.4), and N is the number of experimental data points.

4.4. Results and Discussion

4.4.1. Synthesis of copolymer materials

CS-PAA copolymers were prepared using molar ratios of CS:PAA at 5:1 and 1:1 using an ionic gelation method[7, 28]. The notation adopted for these copolymers is CP-5 and CP-1; respectively, the integer values correspond to the relative mole ratio of CS to PAA. The mole content of CS was estimated using a median value for the molecular weight range (*vide infra*). In contrast to the high viscosity of PAA, the copolymers containing PAA were formed as fine powders (semi-crystalline for CP-1) with greater ease of handling. Variation of the molar ratio of prepolymers resulted in copolymers with tunable properties (*e.g.*, surface chemistry, textural, and sorption properties). Both of the copolymers are insoluble in water, which is an important property which enables the study of their heterogeneous solid-solution sorption equilibria.

4.4.2. Characterization of copolymer materials

The FT-IR spectra for the starting materials (CS and PAA) and the CS-PAA copolymers (CP-5 and CP-1) are shown in Figure 4.2A. The –OH stretching region (~3400 cm^{-1}), -CH stretching region (~2900 cm^{-1}) and –C=O stretching region (~1710 cm^{-1}) are present in the copolymer products which supports their molecular identity. The IR spectra for the copolymers display additive features of functional groups present in the starting materials. The C=O stretch of each copolymer appears at ~1710 cm^{-1} as a result of the ester linkage between CS and PAA. The wavenumber for the copolymers are greater than the –C=O stretch of CS (~1680) for the N-acetyl groups. (*cf.* Fig. 4.2A). The C=O vibrational band is relatively broad for CP-1, and may be due to the overlap of the IR signatures for the unreacted carboxyl groups of PAA (-COOH) and the amide groups of CS-PAA copolymers, in agreement with Wang's results for CS-PAA hydrogel materials[5b]. The carbonyl band (1700 cm^{-1}) also shows a shift in frequency that varies according to the CS:PAA co-monomer ratio. Generally, the IR spectra of copolymer CP-5 tends to resemble the spectral features observed for CS whereas the CP-1 material tends to resemble the broad spectral features of PAA (~2900 cm^{-1}, ~1700 cm^{-1} and 1500-500 cm^{-1}). The broad spectral features may result from the polydisperse nature of PAA and its amorphous characteristics in proportion to the PAA content of the copolymer. The IR spectra were obtained in reflectance mode, so the higher degree of crystallinity of PAA and copolymers may also contribute to the broad signals. Fig 4.2B illustrates DRIFT spectra for the copolymer/MB complexes along with crystalline MB. The spectral features corresponding to the copolymer are broadened and of lower intensity than the IR signatures for MB. The broadened copolymer bands may be due to changes in morphology, due to swelling, and subsequent heat treatment to remove water. The greater intensity of the MB signatures may be related, in part, to its refractive character and the relatively high surface coverage (θ) of MB on the copolymer surface.

A.

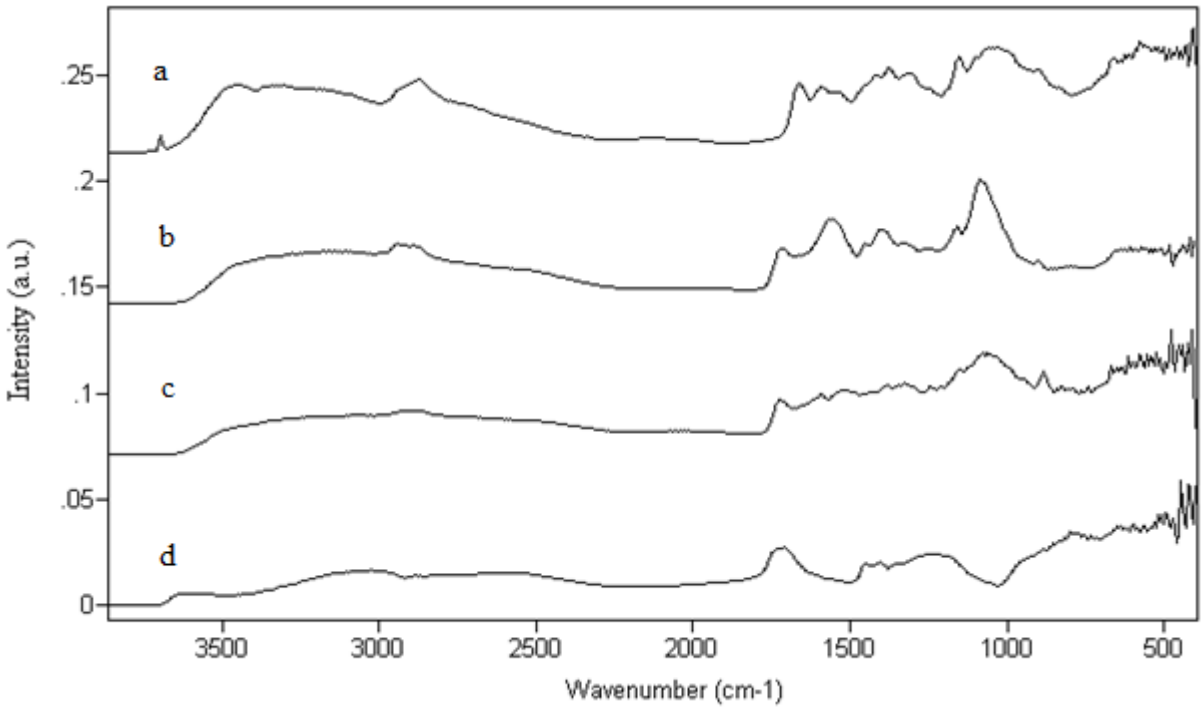

B.

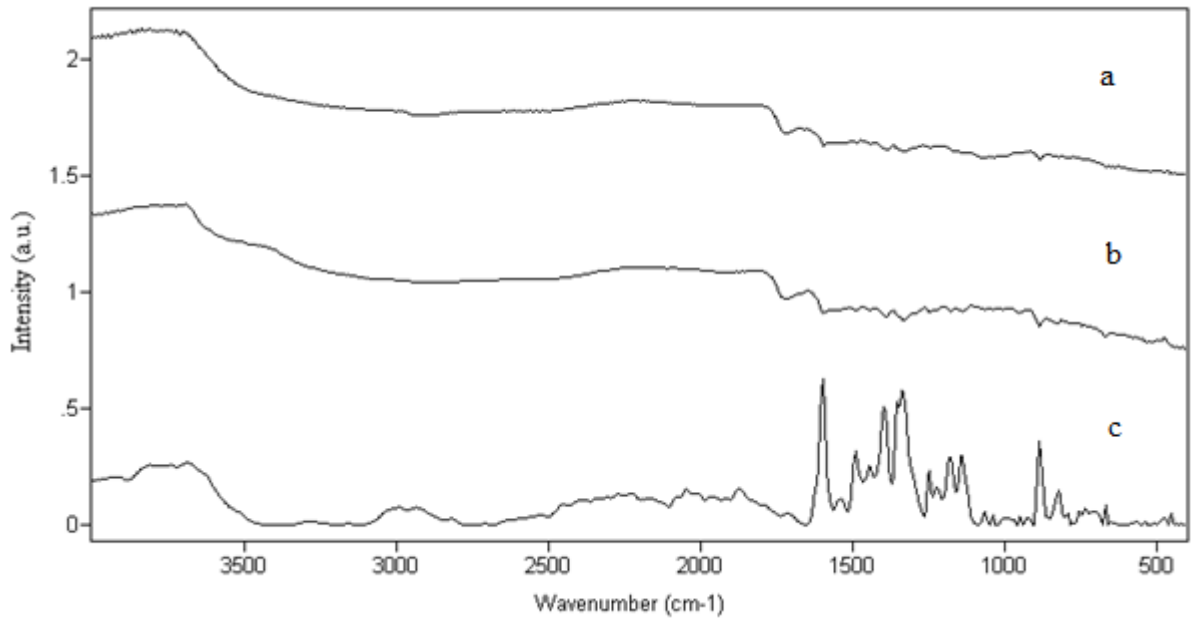

Figure 4.2. A. IR spectra (DRIFTS) for a) Chitosan, b) CP-5 copolymers, c) CP-1 copolymers, and d) PAA. B. IR spectra for the copolymers in the presence of adsorbed MB; a) CP-5 /MB, b) CP-1 /MB, and c) unbound crystalline MB.

In Fig. 4.3, the TGA results are presented as the derivative weight (mass loss/temperature) against temperature for the copolymers and prepolymers. Different thermal profiles are observed for the various copolymers relative to the prepolymers (*i.e.* CS and PAA) as the copolymer composition varies. Accordingly, the TGA results for the copolymers show two thermal events near 250 ℃/360 ℃ for CP-5 and 350 ℃/440 ℃ for CP-1, respectively. Comparable thermal behavior (two-step decomposition) has been reported by Wang[5b] and Chen for CS and PAA based materials[5c]. The copolymers show unique thermal stability relative to the prepolymer starting materials, as evidenced by a broadening of the thermal events and a lower onset temperature. The lower onset temperature (~225-275 ℃) relative to CS for the copolymers is related to changes in H-bonding, heat capacity, and morphology of the copolymer products. Similarly, a lower onset temperature is observed for the copolymers (~300-400 ℃) relative to PAA is attributed to the formation of amide linkages.

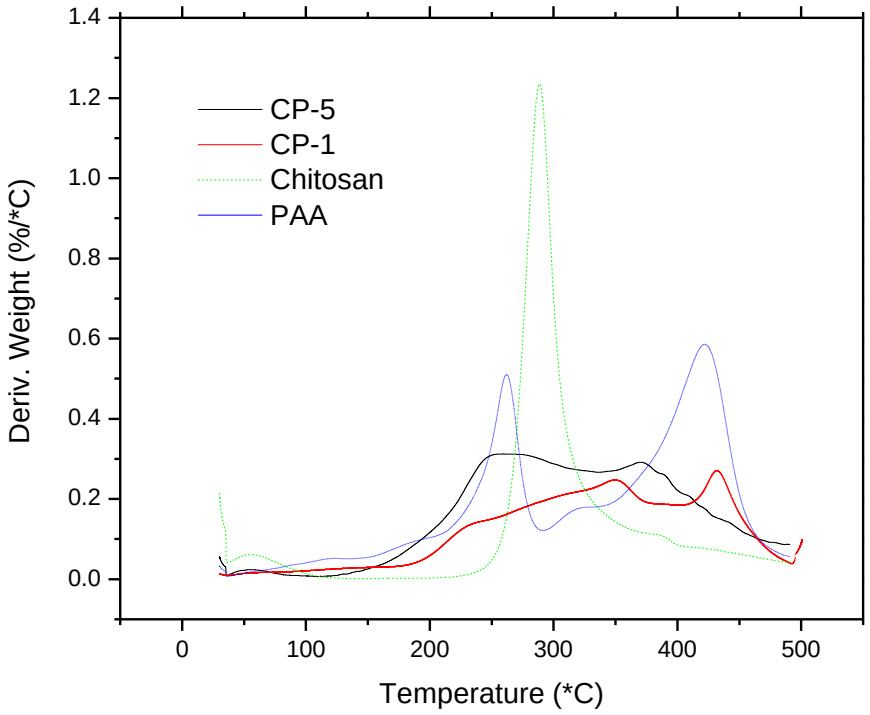

Figure 4.3. TGA results for Chitosan, PAA, and CS-PAA copolymers (CP-5 and CP-1).

4.4.2.1. Nitrogen Adsorption

The sorption properties of the copolymer materials in the solid state were evaluated using nitrogen adsorption (*cf.* Table 4.1). Figure 4.4A-D illustrates the nitrogen adsorption-desorption isotherms CS-PAA copolymers and the CS and PAA prepolymers. The copolymers show the hysteresis loops characteristic of Type IV isotherms which describe the monolayer-multilayer adsorption of such microporous adsorbents[29]. Type IV hysteresis loops feature parallel and almost horizontal branches (Type H1 and H3) that are associated with adsorption-desorption in narrow slit-like pores with narrow pore size distributions[29]. The BET surface area and pore volume estimates for the copolymers are as follows; CP-5 (18.5 m^2/g; with a pore volume of 0.060 cm^3/g) and CP-1 (0.719 m^2/g; 0.0012 cm^3/g). In general, copolymers such as CP-1 with high PAA content yield lower BET surface area relative to CP-5, in agreement with results reported for β-CD/PAA copolymers[24]. For example, SA values for β-CD/PAA 5:1 (1.63 m^2/g) are compared with β-CD/PAA 1:5 (0.275 m^2/g) and are related to differences in PAA content[24]. A contributing factor for the lower surface area of CP-1 may be related to the reduced porosity of the copolymer framework because of its disordered, folded arrangement in the anhydrous state. At low CS content, the PAA copolymers form more densely packed frameworks. In contrast, copolymers with greater CS content exhibit reduced packing density and greater porosity, as evidenced by the greater adsorption of N_2. PAA is considered a "*soft material*" with significant conformational motility of the polymer network. The lower BET surface area (0.376 m^2/g) for PAA is attributed to the collapsed pore structure of the polymer and its reduced surface area, as compared to its hydrated form in aqueous solution[22, 24].

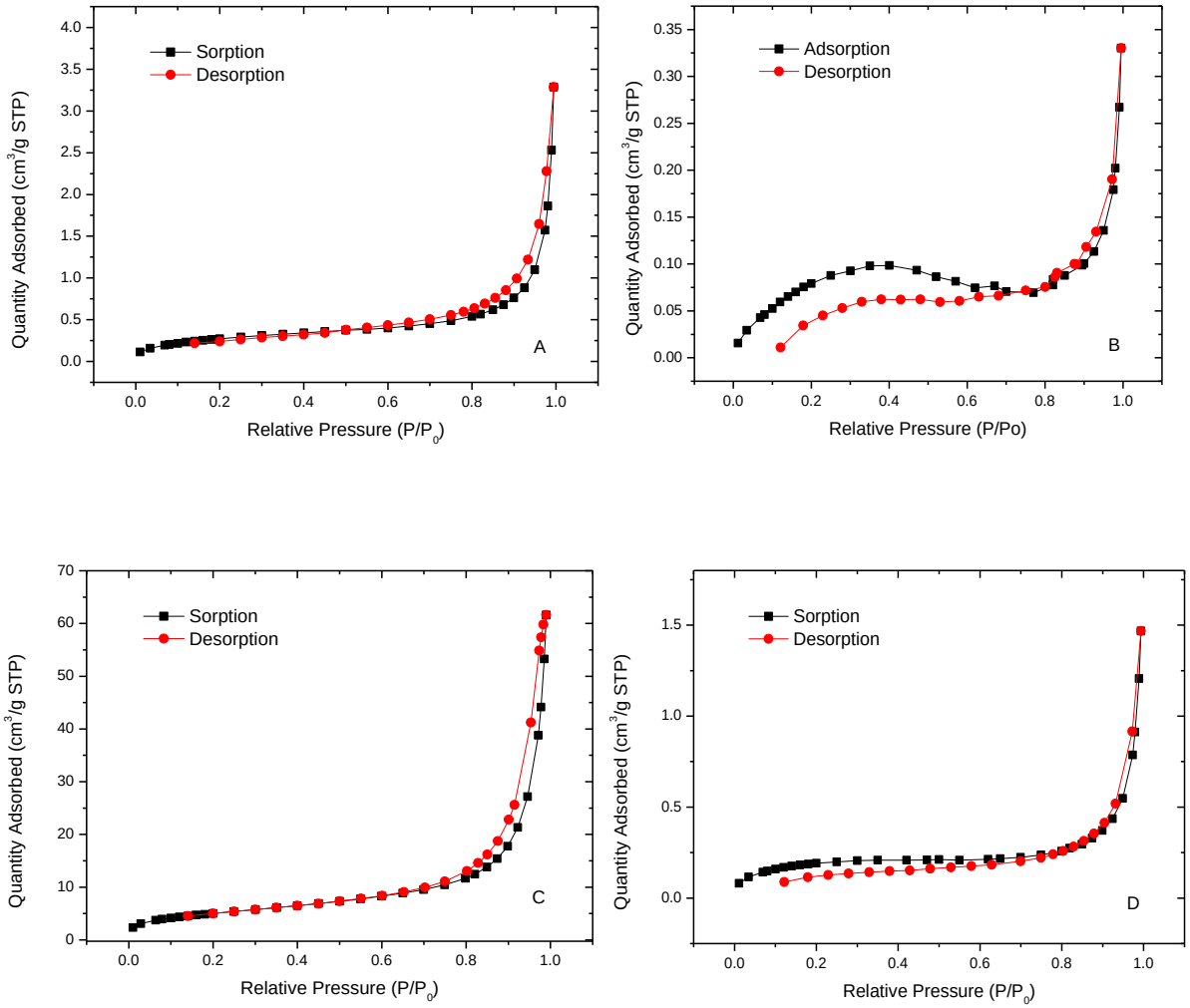

Figure 4.4. Nitrogen adsorption-desorption isotherms for chitosan/PAA copolymers and prepolymer materials at 77 K; A) Chitosan, B) PAA, C) CP-5, and D) CP-1.

Table 4.1. Textural properties of prepolymers and CS-PAA copolymers estimated from N_2 adsorption at 77K.

Polymers	BET Surface Area (m^2/g)	Pore Width (Å)	Pore Volume (cm^3/g)
CP-5	18.5469	129.5005	0.060046
CP-1	0.7186	67.6665	0.001216
Chitosan	1.0363	93.8318	0.002431
PAA	0.3755	29.5229	0.000277

4.4.2.2 Water Swelling Properties

The occurrence of swelling of the copolymer framework for the CS-PAA copolymers in aqueous solution are supported by the TGA results in Fig.4.5 A-B. Cooperative interactions such as electrostatic, H-bonding, and amide bonding of the copolymer network contribute to its high water swelling behaviour. The copolymer with greater PAA content (CP-1) displays greater swelling than CP-5. The enhanced swellability for CP-1 is attributed to the abundant -COOH groups and the ionized carboxylate groups on the polymer backbone. This results in electrostatic repulsions, local chain stiffening, and long-range excluded volume effects[9, 30]. The swelling ratio was calculated from the mass loss of water from the thermograms in Fig. 5 using eqn (4.1). After swelling for 24 h in deionized water, the hydrated CP-1 polymer has a swelling ratio r=22.6 and the CP-5 copolymer has a value of r=11.6. Thus, CP-1 absorbs ~22.6 times its mass in water; whereas, CP-5 absorbs ~11.6 times its mass. In Fig. 4.5A, the desorption temperature for water from CP-5 shows two types of mass loss events at ~100 and 120 ℃, where the greater fraction of water desorption occurs ~ 100 ℃. The hydrate water may be adsorbed at both the surface and micropore framework sites of CP-5. In contrast, CP-1, displays one continuous desorption profile over the range ~100-120 ℃ indicating that the presence of free -COOH groups promotes water swelling. CP-1 has a more extended network of hydration in aqueous solution, caused by the negatively charged carboxylic groups. The

observed differences in desorption temperatures of the hydrate water for CP-1 and CP-5 copolymers illustrate the effects of hydration of microporous and surface framework adsorption sites, in agreement with the composition of the copolymer materials. A recent report of hydration in nafion membranes illustrates that two types of hydration attributed to percolation structure and isolated cluster structure are evidenced by TGA and IR spectroscopy[31].

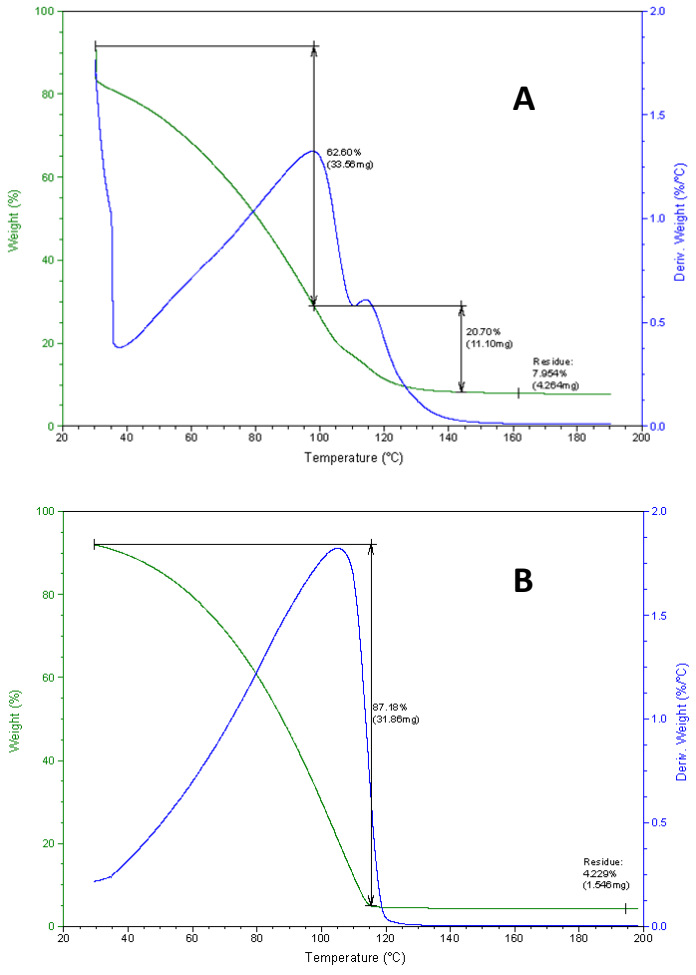

Figure 4.5. TGA of CS-PAA copolymers for evaluation of their water swelling properties; A) CP-5, and B) CP-1.

4.4.3. Copolymer Sorption Studies

The sorption properties of the copolymer materials were studied in aqueous solution using MB as a model adsorbate at ambient pH and 295 K. The MB solutions were significantly decoloured in the presence of the copolymers, illustrating their high sorption capacity toward MB. This was particularly evident with CP-1 where the dye solution changed from dark blue to a nearly transparent, even at the most concentrated solution of MB.

In Figures 4.6A-D, the sorption isotherms (Q_e versus C_e) are shown for the prepolymer materials (*i.e.* CS and PAA) and the corresponding copolymers (*i.e.* CP-5 and CP-1). In general, the magnitude of Q_e increases monotonically as C_e increases. In Figure 4.6C, CP-5 does not show saturation of the sorption sites when C_e reaches 5 mM. The dye solution used for CP-5 (5 mM) was lower in concentration than that studied for CP-1 (10 mM) due to the reduced sorption capacity of CP-5. Thus, a comparison of sorption properties is possible while maintaining good experimental accuracy and reasonable dilution factors.

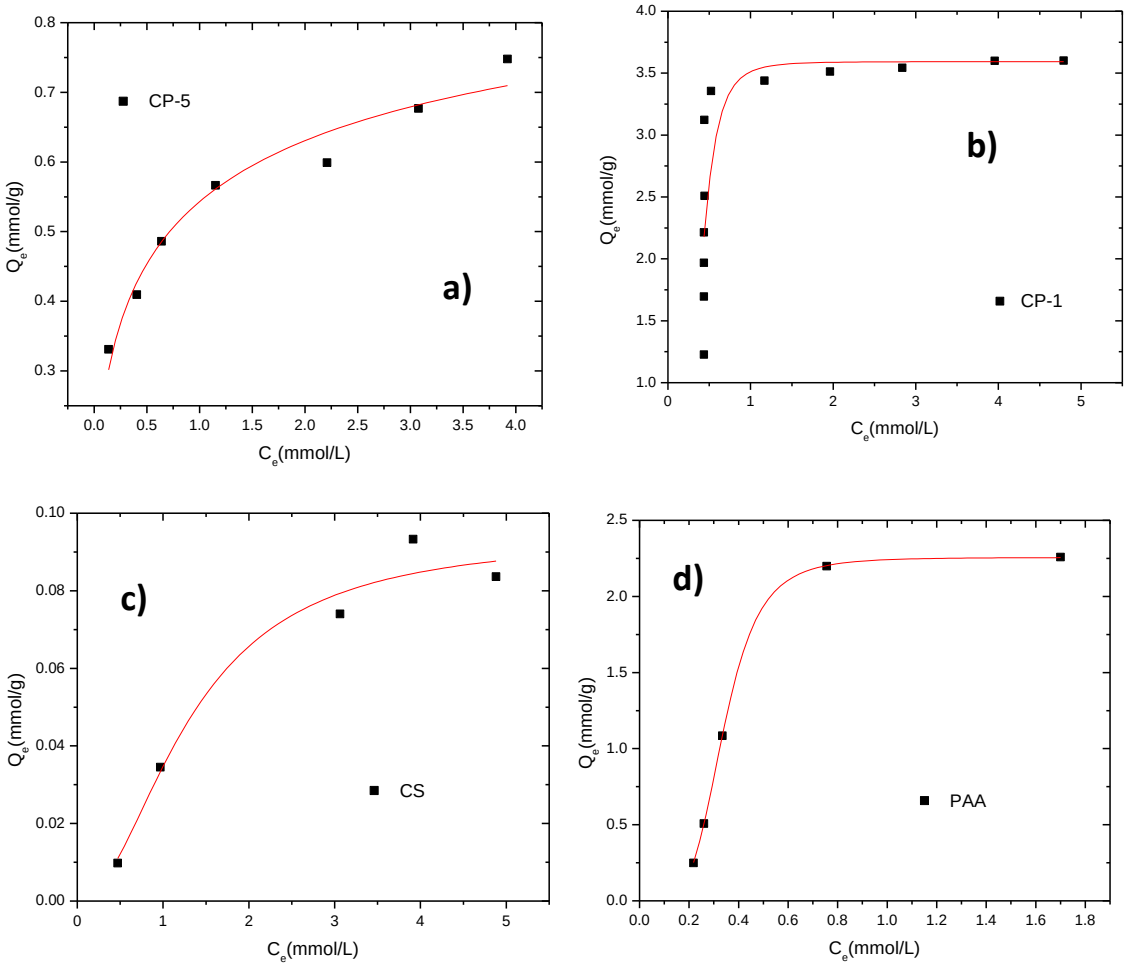

Figure 4.6. Sorption isotherms for Chitosan/PAA copolymers with MB at 22 ℃; a) CP-5, b) CP-1, c) CS, and d) PAA. The *best-fit* results were obtained using the Sips isotherm (*cf.* eqn 3).

The sorption results were analyzed using the Sips isotherm (*cf.* Eqn. 4.4) and the "best fit" sorption parameters are listed in Table 4.2. The Sips model provides a good general description of the sorption behavior of the copolymers. In Table 4.2, the dye-based estimates of the sorbent surface area (SA) were estimated using the Q_m values with eqn. 4.3. The SA values are as follows; CP-5 (271 m^2/g) and CP-1 (943 m^2/g). The values exceed the BET estimates in Table 4.1 by a substantial amount. The SA of CP-1 is similar to activated carbon (~10^3 m^2/g)[32], and further illustrates the remarkable tunability of these materials. The

difference in SA is attributed to the occurrence of swelling which was reported previously for PAA copolymers containing β-CD[24]. CP-1 and -5 display remarkably different sorption capacities toward MB according to the Q_m values for CP-5 (1.03 mmol/g) and CP-1 (3.59 mmol/g) for similar experimental conditions. The sorption properties are related to the preparative (prepolymer mole ratios) conditions of the copolymers and may be tuned accordingly. The Q_m values for the copolymers are unique when compared to various forms of activated carbon, and the Q_m values range from 0.00313-0.710 mmol/g[6, 33-35], as compared with CTS-g-PAA/APT hydrogel composites (~5.80 mmol/g)[36, 37].

Table 4.2. Dye-based method estimates of the sorbent surface area for the various prepolymer and copolymer materials obtained for the sorption of MB at 295 K and the best-fit parameters (Q_m, K_{Sips} and n_s) using Sips non-linear model.

Material	**SA**[a]	**Q_m**[b]	**K_{Sips}**[c]	**n_s**	**χ^{2d}**	**R^2**
CP-5	77.7	1.03	1.11	0.500	0.00093	0.964
CP-1	270	3.59	42.9	4.00	0.23094	0.710
CS	7.08	0.0941	0.584	1.98	0.00006	0.975
PAA	172	2.28	67.1	4.00	0.00203	0.998

[a] surface area, (m^2/g)

[b] Q_m, (mmol/g)

[c] K_{Sips}, (L/mmol)

[d] χ^2, Chi-square distribution

The Sips parameters for the copolymers (CP-1; n_s=4 and CP-5; n_s=0.5) indicate the presence of heterogeneous sorption sites and is consistent with the presence of multiple sorption sites. There are several potential sorption sites for MB in the copolymer framework; the micropore domains and the numerous surface bound PAA sites ($-COO^-$). Cooperative

binding sites are expected for such multi-functional copolymers. The sorption properties of CP-1 are related to its numerous -COOH groups; whereas, CP-5 is attributed to its micropore network structure. The greater Q_m value for CP-1 relative to CP-5 correlate with its greater PAA content. The PAA fraction of the copolymer plays an important role in the sorption process since PAA exhibits favourable sorption capacity toward MB (Q_m=2.28 mmol/g). In contrast, CS displays substantially lower sorption (Q_m=0.0941 mmol/g) with MB, and its Q_m value compares with that obtained for CS-based hydrogel beads (Q_m = 0.310 mmol/g)[37]. In addition to the heterogeneity parameter (n_s), the K_s term provides a relative measure of the sorption affinity for the sorbent/MB complexes. CP-1 and PAA show very large K_s values (42.9 L/mmol and 67.1 L/mmol respectively), as compared with CP-5 (1.11 L/mmol) and CS (0.584 L/mmol). The electrostatic interactions between anionic carboxylate groups of CP-1 and the MB cation is a driving force for the sorption process. Such ion-ion interactions contribute to the "*chemisorption-like"* behaviour observed for CP-1 and PAA. The two copolymers show markedly different sorption characteristics toward MB ranging from *physisorption* (CP-5) to *chemisorption-like* (CP-1) behaviour in accordance with their variable composition, structural morphology, surface area, and pore structure characteristics. The *"chemisorption-like"* behavior of CP-1 is considered as physisorption because there is no covalent bonding during sorption, as evidenced by the reversible binding observed in pH-switching (*vide supra*) experiments. The IR spectra in Fig. 4.2b for the complexes formed between MB with CP-5 or CP-1 show similar IR spectra with no apparent signatures of chemical bond formation. The absence of covalent bond formation is further supported by the UV-Vis spectra (Fig. 4.7 A and B) and images of the copolymer and MB illustrated at various pH conditions (Fig. 4.7 C and D). During desorption, the pH of the MB/copolymer solution is ~6 which is above the pK_a of PAA (4.6), the –COOH groups of CP-1 are deprotonated which result in strong coulombic attractions with MB. Below the pK_a of PAA (pH ~ 2) the COOH groups are protonated, resulting in desorption of MB from the sorbent phase (*cf*. Fig. 4.7C and D). MB solutions at variable pH (*i.e*. 2 and 6) display variable surface coverage indicating that PAA undergoes ionization and reversible binding with MB. A small quantity of CP-5 was recovered at low pH, which supports that the sorption properties of CP-5 depend on its pH, water swelling characteristics, and porous structure properties. CP-1 shows more

than 95% reversible desorption of bound MB by adjusting to pH ~2 (Fig. 4.7B). The adsorption of MB by CP-1 involves a combination of adsorption involving electrostatic interactions. The results also confirm that the sorption process for CP-1/MB is *"chemisorption-like"* in terms of its binding affinity. The sorption process is well described as highly cooperative, as evidenced by the reversible adsorption and desorption of MB, as follows: pH 2 (*low* θ) < pK_a (PAA) or pH 6 (*high* θ) > pK_a (PAA).

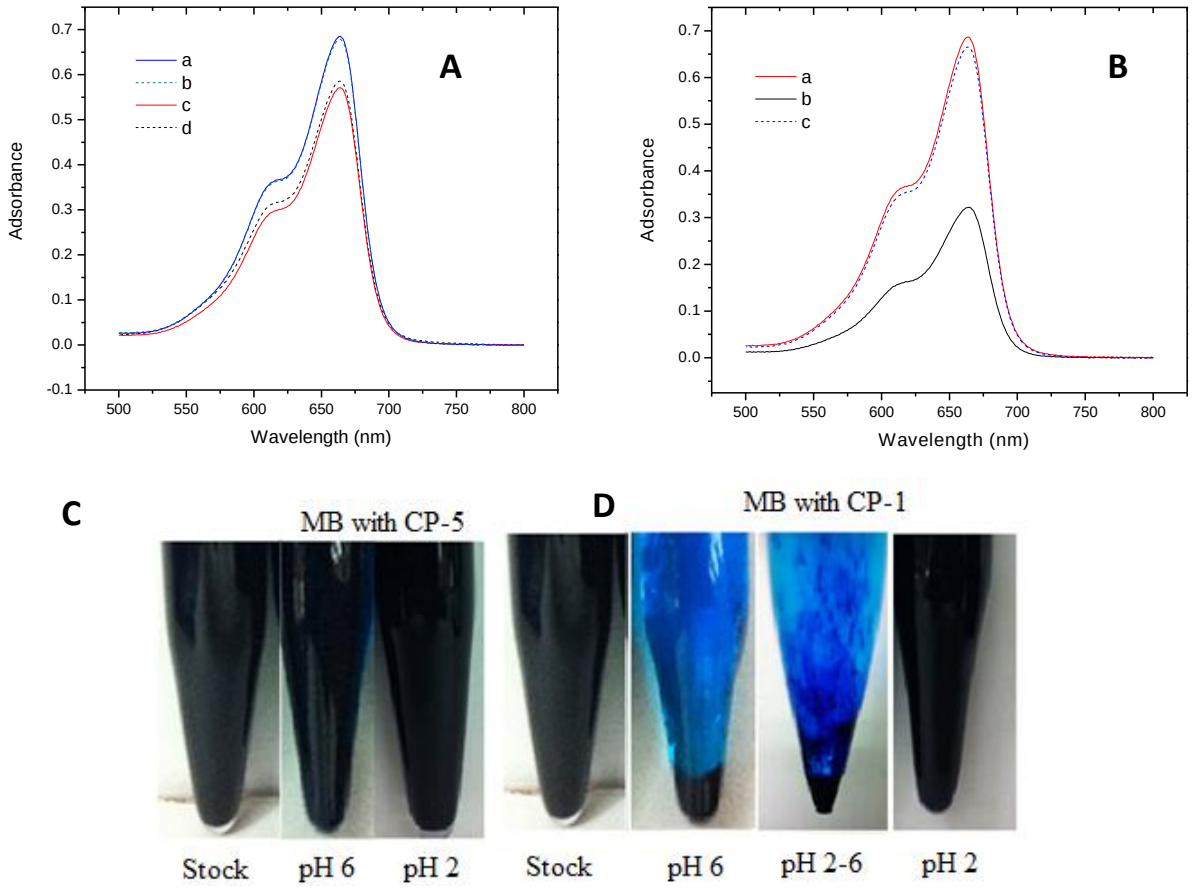

Figure 4.7. Adsorption and desorption of MB by CS-PAA copolymers as a function of solution pH: A) UV-Vis spectra of MB stock solutions; (a) pH 6, (b) pH 2.5 and MB solution after incubation with 10mg CP-5 for 24 h (c) pH 6, (d) pH 2.5, all samples with 500-fold dilution; B) UV-Vis spectra of MB solution after incubation with 10mg CP-1 for 24 h (a) pH 6 with 500-fold dilution (b) pH 6 with 10-fold dilution, (c) pH 2.5 with 500-fold dilution; C) Images of the sorption/desorption process of CP-1 (stock, 5mM MB solution); D) Images of the sorption/desorption process for CP-5 at 295 K.

4.5. Conclusions

In this work, we report the development of copolymers with *"protein-like"* characteristics based on CS and PAA prepolymers with variable composition. Tunable sorption properties of the SAP sorbents with methylene blue were observed in aqueous solution at 295 K, and in the solid state using nitrogen adsorption at 77 K. In aqueous solution, the copolymers display variable swelling and sorption behaviour according to their prepolymer ratios. The Sips model provided reliable estimates of the equilibrium sorption parameters of the copolymers in aqueous solution where the sorption capacity of MB varied from 1.03-3.59 mmol/g. The development of chitosan-based copolymer materials with tunable physicochemical properties represents a useful approach for the development of "*smart materials*" for the efficient immobilization of organic and inorganic contaminants in aqueous solution. The pH switchable materials developed herein have significant potential as pharmaceutical excipients, controllable nano-assemblies, and biomimetic agents. Further research is underway to understand the structure and sorption properties these remarkable materials.

4.6. Acknowledgements

The authors wish to acknowledge the Natural Sciences and Engineering Research Council of Canada (NSERC), the Canada Foundation for Innovation (CFI), and the University of Saskatchewan for the support of this research. Rui Guo gratefully acknowledges NSERC for a PhD scholarship through the NSERC CREATE-HERA program.

4.7. References

(1) Forgacs, E.; Cserháti, T.; Oros, G. *Environ Int.* **2004**, 30, 953-971.

(2) Tünay, O.; Kabdasli, I.; Eremektar, G.; Orhon, D. *Water Sci. Technol.* **1996**, 34. 9-16.

(3) Sanghi, R.; Bhattacharya, B. *Color Technol.* **2002**, 118, 256-269.

(4) a) Kumar, K.; Ramamurthi, V.; Sivanesan, S. *J. Colloid Interface Sci*. **2005,** 284, 14-21. b) Ozcan, A., *J. Colloid Interface Sci.* **2004**, 276, 39-46.

(5) a) Dumitriu, S. (Ed.), Polysaccharides: Structural Diversity and Functional Versatility, **2005**. 625-630. b) Liu, Y.; Zheng,Y.; Wang, A., *J. Environ. Sci. (China)*. **2010**, 22, 486-493. c) Chen,Y.; Tan, H. *Carbohydr Res.* **2006**, 341, 887-896. d) No, H.; Park, N.; Lee, S.; Meyers, S., *Int. J. Food Microbiol.* **2002**, 74, 65-72. e) Dutkiewicz, J.; Biomed. J., *Mater Res.* **2002**, 63, 373-381. f) Li, H.; Liu, B.; Zhang, X.; Gao, C.; Shen, J.; Zou, G., *Langmuir*. **1999**, 15, 2120-2124.

(6) Bernkop-Schnürch, A. (Ed.), Oral Delivery of Macromolecular Drugs: Barriers, Strategies and Future Trends, 2009. P.156

(7) Wang, J.; Y. Kuo, *J Appl Polym Sci.* **2008,** 107, 2333-2342.

(8) Gupta, K.C.; Jabrail, F.H. *Carbohydr Polym.* **2006**, 66, 43-54.

(9) Nge, T.; Hori, N.; Takemura, A.; Ono, H. *J Appl Polym Sci.* **2004**, 92, 2930-2940.

(10) Dhodapkar, R.; P. Borde, T. Nandy, Glob Nest J. 11 (2009) 223.

(11) Kabiri, K.; Omidian, H.; Hashemi, S.; Zohuriaan-Mehr, M. *Eur Polym J.* **2003**, 39, 1341-1348.

(12) Sogias, I. A.; Williams, A.C.; Khutoryanskiy, V.V. *Biomacromolecules.* **2008**, 9, 1837-1842

(13) Jain, A. K.; Chalasani, K. B.; Khar, R. K.; Ahmed, F. J.; Diwan, P. V. *J. Drug Target.* **2007**, 15, 417.

(14) Grabovac, V.; Guggi, D.; Bernkop-Schnurch, A. *Adv. Drug Deliv Rev.* **2005**, 57, 1713-1723.

(15) Serra, L.; Domenech, J.; Peppas, N.A. *Eur. J. Pharm. Biopharm*. **2009**, 71, 519-528.

(16) Shaikh, R.; Raj Singh, T. R.; Garland, M. J.; Woolfson,A. D.; Donnelly, R. F. *J. Pharm. Bioallied Sci.* **2011**, 3, 89-100.

(17) Emmett, P. H.; Brunauer, S. *J. Am. Chem. Soc.* **1937**, 59, 1553.

(18) Sing, K. S. W. *Chem Ind.* **1967**, 829-830.

(19) de Boer, J. H.; Lippens, B. C; Linsen, B.G.; Broekhoff, J.C.; van den Heuvel, P. A. T.; Osinga, J. *J. Colloid Interface Sci.* **1966**, 405-414.

(20) Brunauer, S.; Emmett, P.H.; Teller, E.I. *J. Am. Chem. Soc.* **1938**, 60, 309-319.

(21) Huglin, M.B.; Liu, Y.; Velada, J.L. *Polymer.* **1997**, 38, 5785-5791.

(22) Mohamed, M.H.; Wilson, L.D.; Headley, J.V. *Carbohydr. Res.* **2011**, 346, 219-229.

(23)Yu, J. C.; Jiang, Z.T.; Liu, H.Y.; Yu, J.G.; Zhang, L.Z. *Anal. Chim. Acta.* **2003**, 477, 93-101.

(24) a) Guo, R.; Wilson, L. D.; *J. Appl. Polym. Sci.* **2012**, 125, 1841-1854. b) Wilson, L. D.; Guo, R. *J. Colloid Interface Sci.* **2012**, *in press*.

(25) Hossain, M.; Kabir, A.; Kumar, G.S. *Dyes and Pigments.* **2012**, 92, 1376-1383.

(26) a) Pelekani, C.; Snoeyink, V.L. *Carbon.* **2000**, 38, 1423-1436. b) Inel,O.; Tumsek, F. *Turk. J. Chem.* **2000**, 24, 9-19.

(27) Sips, R. *J. Am. Chem. Soc.* **1948**, 125, 6452.

(28) Chang, T.; Wang, J.; Hon, M. *Macromol Bio.* **2004**, 4, 416.

(29) Sing, K. S. W.; Everett, D. H.; Haul, R. A. W.; Moscou, L.; Pierotti, R. A.; Rouquerol, J.; Siemieniewska, T. Pure. Appl. Chem. **1985**, 57, 603-619.

(30) Yin, Y.; Prudhomme, R.; Stanley, F. Relationship between Poly(Acrylic Acid) Gel

Structure and Synthesis, *ACS Symposium Series*, Vol. 480 Chapter 6, 91–113, Washington; Washington, **1992**.

(31)Wang, Y.; Kawano, Y.; Aubuchon, S. R.; Palmer, R. A. Macromol. **2003**, 36, 1138-1146.

(32) Kwon, J. H.; Wilson, L. D. *J. Env. Sci. & Health Part A*: **2010**, 45, 1793-1803.

(33) Aygun, A.; Yenisoy-Karakas, S.; Duman, I. *Microporous Mesoporous Mat.* **2003**, 66,189-195.

(34) Banat, F.; Al-Asheh, S.; Al-Makhadmeh, L. *Process Biochem*. **2003**, 39, 193-202.

(35) Blake, P.; Ralston, J. *Coll. Surf.* **1985**,15, 101-118.

(36) Wang, L.; Zhang, J.; Wang, A. *Desalination.* **2011,** 266, 33-39.

(37) Chatterjee, S.; Chatterjee, T.; Lim,S.R.; Woo, S.H. *Environ. Technol.* **2011**, 32, 1503-1514.

CHAPTER 5

Description

Chapter 5 includes a verbatim copy of a manuscript planned to submit to Industrial & Engineering Chemistry Research. The article describes the adsorption properties of a series of polysaccharide-based copolymers toward chloroform in aqueous solution.

Author's contribution

I carried out all of the experimental work from the synthesis to characterization of the copolymers. This work was principally supervised by Dr. Wilson and Dr. Bharadwaj. I wrote the first draft of the manuscript with assistance in the form of manuscript editing by Dr. Wilson and Dr. Bharadwaj. The co-authors grant permission of use of the manuscript for this PhD thesis, and agree with the description of the roles and contributions of the authors.

Relationship of Chapter 5 to the overall objective of this project

As stated in the introduction, the research objectives were to examine the sorptive properties of the synthesized copolymers toward THMs. As the most common of the various THMs in water, the sorption properties of the copolymers with chloroform are presented as a complete chapter. In this study, the copolymers that were prepared in chapters 2-4 were evaluated for their sorptive properties with chloroform in aqueous solutions. This study involved preliminary sorption study, kinetic studies and DAI sorption study to evaluate the sorption capacities of various adsorbents. The results provide an understanding of the sorption mechanism of copolymers with chloroform in aqueous solution.

Research highlight:

The copolymer adsorbents described in Chapters 2-4 were evaluated for their adsorption properties with chloroform in aqueous solution. The DAI method with GC-ECD detection was applied for quantitative detection of chloroform in water. A preliminary adsorption study and kinetic study of chloroform provide the information to establish the experimental protocol for the sorption study. The sorption parameters were evaluated using the Sips model. The sorption capacity (Q_m) values of chloroform for these synthetically engineered copolymers at similar conditions varied according to the tunable physicochemical properties of the copolymers.

5. Uptake of chloroform from aqueous solution with synthetically engineered copolymer materials

Rui Guo, Lee D. Wilson[*], and Lalita A. Bharadwaj

[a]Department of Chemistry, University of Saskatchewan, 110 Science Place, Saskatoon, Saskatchewan, S7N 5C9

[b]School of Public Health, University of Saskatchewan, Health Sciences Building, 107 Wiggins Road, Saskatchewan, S7N 5E5

[*]Corresponding author: Tel. 1-306-966-2961/ Fax. 1-306-966-4730
e-mail: lee.wilson@usask.ca

5.1. Abstract

To address the removal of chloroform from aquatic environments to levels consistent with regulatory requirements, a series of synthetically engineered copolymer sorbent materials were prepared and their sorption properties were evaluated. The copolymer sorbents were composed of polysaccharides (*i.e.* cyclodextrin or chitosan) and a cross-linker (*i.e.* poly (acrylic acid) or diacid chlorides) with variable mole composition. Gas chromatography (GC) employing a direct aqueous injection (DAI) method with an electron capture detector (ECD) enabled detection of chloroform in water. Sorption isotherms of the copolymer/chloroform systems in water were obtained at 295 K and ambient pH. The sorption parameters were evaluated using the Sips model. The sorption capacities of the copolymer sorbents with chloroform adopt the following relative order: β-CD/PAA 1:5 > SCl-5 > SCl-10 ~ CP-1 > β-CD/PAA 1:10 > CP-5 > AC > β-CD/PAA 1:5 at high speed. The copolymers showed markedly different sorption characteristics according to their variable composition, surface chemistry, and textural properties.

Keywords: *chloroform; sorption; β-CD; chitosan; copolymers; kinetics; thermodynamics; GC-EC;, direct injection method.*

5.2. Introduction

Trihalomethanes (THMs) are produced as disinfection by-products (DBPs) from drinking water chlorination processes involving gaseous chlorine or liquid sodium hypochlorite. Chlorine-based disinfection of drinking water is considered as a major public health achievement of the 20th century and remains the most widely used disinfection method in North America.[1] Chloroform (*cf.* Scheme 5.1a) is among one of the most common type of THMs formed in water due to the presence of available organic carbon species. The preparation of chloroform was first reported in 1831 by the French chemist Eugene Soubeiran, where it was produced from the reaction of acetone (2-propanone) and ethanol through the chlorination with leach powder (*i.e.* calcium hypochlorite)[2]. Similarly, Samuel Guthrie and Juetus von Liebig, also successfully and independently prepared the same compound[3]. Chloroform was chemically identified and characterized by Jean-Baptiste Dumas[4]. Chloroform is a commonly occurring solvent with relatively low chemical reactivity, miscibility with most organic liquids, and volatile. Chloroform is largely applied in pharmaceutical industries, rubber industry, and pesticide manufacturing. Its worldwide commercial production reached about 440,000 t in 1987 and domestic production in the United States was approximately 229,000 t in 1991,[5] and 216,000 t in 1993[6]. Chloroform is generally produced as a precursor to Teflon and various refrigerants; however, the use of Teflon as a refrigerant was phased out after the *Montreal Protocol on Substances that Deplete the Ozone Layer*[7].

Chloroform has been classified by the International Agency for Research on Cancer (IARC) as a potential carcinogen for human (Group 2B), which suggests limited evidence of carcinogenicity in humans but greater evidence in the case of animal studies. Epidemiology studies of human subjects indicate a greater incidence of bladder and colon cancers in areas where chlorinated drinking water is consumed[1, 8]. Further studies also show an association of waterborne chloroform in drinking water

with low birth weight, prematurity and intrauterine growth retardation[9]. The U. S. Environmental Protection Agency (EPA) has published the *Stage 1 disinfectants-Disinfection By-products Rule* to regulate the total THMs at a maximum average allowable annual level to 80 ppb[10]. In December 2001, this standard was increased to a 100-ppb maximum allowable limit for large surface water public systems[10]. The WHO guideline value of chloroform is set at 200 ppb. This guideline is considered relatively high; however, the WHO guideline sets a balance between microbiological water quality and toxicological levels. The increased guideline levels for DBPs adopted by the WHO are justified because water chlorination is essential for the removal of waterborne pathogens (microbes), which represent a real and immediate risk to health[11]. In Canada, 290 water systems serving a sampled population of 1,130,000 reported mean chloroform levels greater than 75 ppb, according to the data from water providers in 2003[12]. In a recent 2003 study for eight provinces in Canada during 1994-2000, the mean chloroform levels were lower than 50 ppb in drinking water systems, while some peak values were in the 400 ppb range[12], exceeding regulatory levels. As a result, the halomethane-based contaminants such as chloroform represent a concern in drinking water quality.

Three common removal methods in water purification of chlorine, chlorine by-products, and volatile organic carbons (VOCs) include filtration, reverse osmosis and distillation. Unlike the other two techniques, adsorption-based separation is not limited to the type or size of contaminants to be removed[13]. Adsorption can also selectively retain healthy trace minerals in drinking water by developing molecular selective adsorptive processes[13]. A recent example of adsorptive-based fractionation of complex chemical mixtures was reported by Mohamed et al. where synthetically engineered sorbent materials were used to fractionate naphthenic acids according to their variable physicochemical properties (*e.g.*, relative polarity, size, and lipophilic character)[14]. Adsorption-based removal of contaminants affords a relatively inexpensive and facile approach for water purification. Crini[15] has reviewed the use of polysaccharide-based sorbents for the adsorptive removal of contaminants. Commonly used industrial adsorbents include activated carbon and various types of

zeolite molecular sieves, and styrene-based polymeric materials. There is a need to develop improved sorbent materials with enhanced sorption capacity and molecular selectivity for the cost-efficient removal of chloroform and related THMs in contaminated water supplies.

The design of tunable sorbent materials for the controlled sorptive uptake of contaminants is feasible through a systematic materials design approach[14-18]. Tunable materials are possibly by varying the reaction conditions (*e.g.*, stirring rate and co-monomer ratios), the nature of the polysaccharide and the type of cross-linker[16-18]. In this study, we hypothesize that polysaccharide-based (*i.e.* β-CD and CS) copolymers may display tunable sorption with chloroform through control of cross-linking with suitable cross-linkers (*i.e.* PAA, SCl, and TCl) at variable composition. β-cyclodextrin (β-CD) is a torus-shaped macrocycle with a hydrophilic exterior and a lipophilic interior (*cf.* Scheme 5.1b) and can form stable noncovalent complexes with a variety of inorganic and organic compounds. The lipophilic cavities of β-CDs are suitably sized for the inclusion of low to medium sized lipophilic molecules such as chloroform[19]. Previous studies have reported that β-CD can be incorporated into copolymer frameworks by chemical cross-linking, grafting or non-covalent self-assembly[20, 21]. Although various guest molecules may favor complex formation with different CDs[22,23], β-CD is among the most widely studied host because of its suitable cavity dimensions and favourable thermodynamic complex stability with diverse guest molecules[19]. Chitosan (CS; Scheme 5.1c) is another polysaccharide material with interesting host-guest chemistry and suitable functional groups for copolymer preparation. Chitosan is produced industrially by the deacetylation of chitin obtained from the exoskeletons of crustaceans and the cell walls of fungi. CS is a linear polysaccharide composed of randomly distributed β-(1→4)-linked D-glucosamine and N-acetyl-D-glucosamine units[24] and it is widely used in various industries due to its biocompatibility, antibacterial properties, and relatively low cost. Chitosan possesses abundant amine and hydroxyl groups suitable for cross-linking reactions and potential adsorption sites for electrostatic and H-bonding interactions. Due to its structural rigidity, CS adopts extended chain

conformations and serves as a rigid prepolymer for the design of copolymer materials[18].

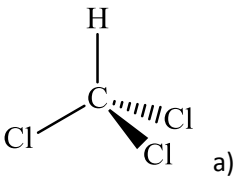

a)

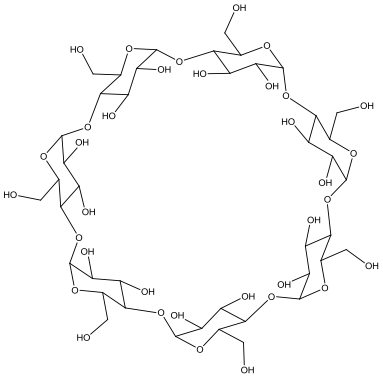

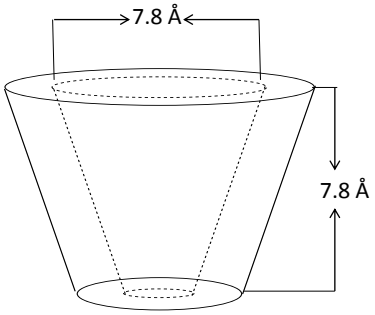

b)

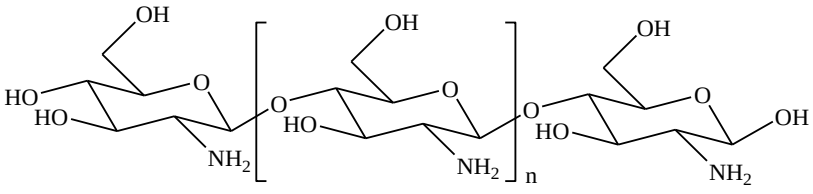

c)

Scheme 5.1. Molecular structure of a) chloroform, b) β-CD, and c) CS.

Gas chromatography (GC) with electron capture detection (ECD) is highly specific and sensitive for the analysis of halogen-containing compounds[8, 25, 26]. Solvent extraction[10, 27], head-space analysis[28, 29], and purge and trap[30] methods are commonly

used to detect these types of volatile organic compounds (VOCs). The direct aqueous injection (DAI) is very convenient and time-saving sampling method since no further handling or sample treatment requirements are required between collection and final analysis. In conjunction with GC-ECD, the DAI technique is considered reliable and provides good precision and analyte recovery[8, 25, 26]. The potential problems of the DAI method are as follows: *i*) water vapor may shorten the life of the ECD and the column; and *ii*) the method is more suitable for relatively clean samples (*i.e.* low turbidity levels) because there is no initial clean-up of samples required.

The objective of this study was to evaluate the removal of chloroform from spiked samples of water at 295 K and ambient pH using a series of synthetically engineered copolymers. The sorption capacities of a series of the copolymers (*cf.* Scheme 5.2a-d) were evaluated using solid-solution isotherms of copolymer/chloroform systems in water using the DAI method with GC-ECD quantitative analysis. The results were compared with commercially available sorbents such as chitosan and granular activated carbon.

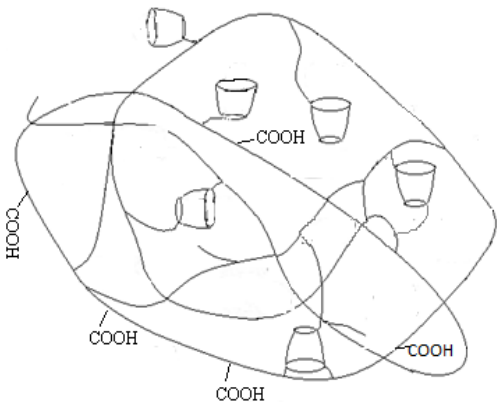

a)

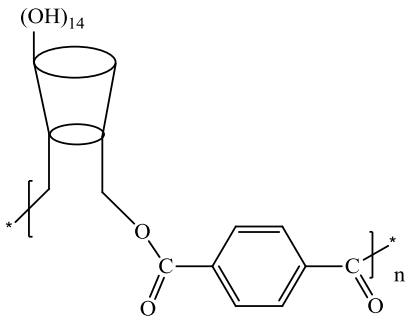

b)

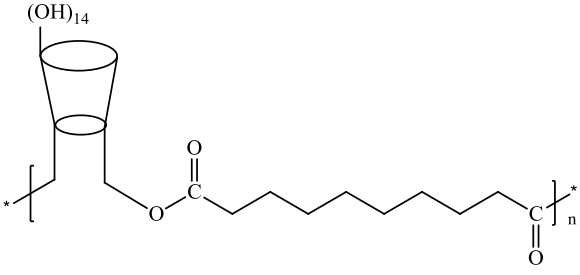

c)

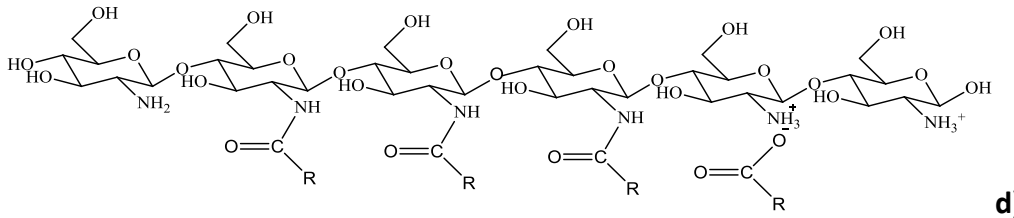

Scheme 5.2. Generalized molecular structure of sorbent materials: a) β-CD/PAA copolymer, where the toroidal-shaped represents β-CD and the straight line segments connecting the β-CD tori represent the ester linkage; b) β-CD/TCl copolymer; c) β-CD/SCl copolymer; and d) the CS/PAA copolymer.

5.3. Experimental Section

5.3.1. Reagents.

Methanol (HPLC grade) was obtained from Fisher Scientific. Chitosan (CS, Mwt. ~ 50,000-190,000 g/mol) with an average degree of deacetylation of 75-85% was obtained from Sigma-Aldrich Canada Ltd. Activated carbon (AC, Darco 20x40 LI) was purchased from Norit America and was treated with 2.0 M HCl using Soxhlet extractor for 48 h. All the water used in this work was distilled and deionized. All the solutions were freshly made for analysis.

5.3.1.1. Copolymer materials.

A series of polysaccharide based copolymers were prepared as described previously[16-18]. In particular, the following copolymers were studied herein: β-CD/PAA 5:1, β-CD/PAA 1:5, β-CD/PAA 1:5 at high speed, β-CD/PAA 1:10[16], β-CD/TCl 1:1 and 1:5[17], β-CD/SCl 1:1, 1:5 and 1:10[17], and CS/PAA copolymers, CP-1 and CP-5[18]. The synthetic protocol and characterization of the copolymers are described in detail elsewhere[14-16].

5.3.1.2. Internal standard.

The internal chromatography quantitative standard was a 1% (v/v) chlorobenzene

(Sigma-Aldrich) in methanol.

5.3.1.3. Stock standard solution.

A 100 ppm standard solution of chloroform was prepared by diluting chloroform (≥ 99.8%, EMD) in Millipore water in custom built gas-tight flasks (125 mL with screw caps lids and silicon/teflon liners to prevent loss of vapour upon dissolution. The solutions of chloroform in water were allowed to mix on a horizontal shaker table for 24 h to achieve equilibrium.

5.3.2. Apparatus

The vials (9 mL) with silicon/teflon inner lined caps were designed to achieve efficient gas-tight sealing of chloroform/water solutions. A 5890 Hewlett Packard gas chromatograph equipped with an electron-capture detector and a cool on-column injection system and a DV-1 column.

5.3.2.1. Operating conditions.

The helium carrier gas was maintained at a constant 10-kPa inlet pressure. The makeup gas was 5% (v/v) methane-argon mixture with a flow rate of 60.0 mL/min. The injector and detector temperature were set at 250 ° C. The maximum oven temperature was 300 ° C and the equilibrium time was 3.00 min. For chloroform, GC analysis, the operating conditions were as follows: the oven temperature and initial temperature were 50 ° C. The final temperature was 100 ° C. The initial time was 5.00 min. The heating rate was 10.0 ° C/min and the final time was 2.50 min.

5.3.3. Methods

The DAI method was used for the sampling of chloroform solutions without any extraction or pre-concentration steps. The aqueous solutions of chloroform/THMs were directly injected to the GC using a Hamilton microsyringe. 1 μL of analyte was injected with 1 μL of air into the injector for every injection.

5.3.3.1. Calibration of standard solutions.

A 25 mL (Quorpak N/M clear bottle) blank solution was made from a 100 ppm chloroform stock solution and mixed well after shaking on the horizontal shake table for 24 h. Approximately 15 data points ranging from 5-80 ppm were collected to obtain a calibration curve. An internal chlorobenzene standard (4% v/v) was added to the chloroform solutions for quantitative analysis.

The calibration curve was plotted by concentration versus area ratio which showed in eqn. (5.1).

$$area\ ratio = \frac{A_S}{A_I} \qquad (5.1)$$

A_S is the relative peak area of the respective analyte compound and A_I is peak area of the chlorobenzene internal standard.

5.3.3.2. Kinetic study

For the study of adsorption kinetics, fixed amounts of copolymers CP-1 and β-CD/PAA 1:5 (~10 mg) were mixed with 29 mL chloroform solution with an initial concentration of 100 ppm with continuous shaking for up to 24 h. The residual chloroform levels were measured at variable time intervals from 1 to 24 h.

A 4% (v/v) chlorobenzene internal standard was added 15 min. prior to each sample injection. The supernatant solution from each sample was sampled from each vial after complete settling of copolymer solid phase.

5.3.3.3. Sorption isotherms.

Fixed amounts (~1-2 mg) of the powdered and sieved copolymer materials were mixed with 8 mL of solution containing variable chloroform concentration (10-80 ppm) in gas-tight sealed glassware until fully equilibrated on a horizontal shaker table for 24 h.

A 4% chlorobenzene internal standard was added 15 min. ahead of each GC injection to the supernatant solution from the sample vial after fully settling of the solid phase copolymers.

The sorption isotherms are depicted as plots of the adsorbed level of chloroform in the copolymer phase per mass of adsorbate (Q_e; mmol/g) versus the equilibrium residual concentration of the unbound chloroform in aqueous solution (C_e). The value of Q_e is defined by eqn. (5.2) where C_0 is the initial concentration of chloroform, V is the volume of solution, and m is the mass of sorbent.

$$Q_e = \frac{(C_0 - C_e) \times V}{m} \qquad (5.2)$$

The Sips isotherm model[31] (eqn 5.3) is a versatile and generalized isotherm that accounts for a distribution of adsorption energies on the sorbent surface and also accounts for monolayer (Langmuir) and multi-layer (Freundlich) isotherm processes. The parameter (n_s) reflects the heterogeneity of the sorbent, where a value of n_s=1 infers a homogenous surface while $n_s \neq 1$ indicates a heterogeneous surface. Langmuir behavior is predicted when n_s=1, and Freundlich behavior is observed when $K_s C_e^{n_s}$ <<<1. The Sips model is defined by eqn. (5.3)[31].

$$Q_e = \frac{Q_m K_s C_e^{n_s}}{1 + K_s C_e^{n_s}} \qquad (5.3)$$

K_s is the Sips equilibrium constant and Q_m is the maximum monolayer adsorption capacity per unit mass of the sorbent.

The adsorption kinetics of chloroform adsorbed by copolymers is described by the pseudo-first-order (eqn. 5.4) and pseudo-second-order models (eqn. 5.5).

$$\ln(Q_e - Q_t) = \ln Q_e - k_1 t \qquad (5.4)$$

$$\frac{t}{Q_t} = \frac{1}{k_2 Q_e^2} + \frac{t}{Q_e} \qquad (5.5)$$

k_1 and k_2 are the rate constants for the pseudo-first-order and pseudo-second-order models, respectively. Q_t is the adsorbed amount of chloroform adsorbed per unit mass of adsorbent at time *t*. For the pseudo-second-order model, the initial adsorption rate (v_0) can be calculated as,

$$v_0 = k_2 Q_e^2 \qquad (5.6)$$

The criteria of the "best-fit" between the calculated isotherm and the experimental data are determined by the correlation coefficient (R^2) and the

chi-square distribution (χ^2). A unitary value of the correlation coefficient ($R^2 \sim 1$) denotes a suitable "*best-fit*"; however, a more sensitive measure for non-linear least squares fitting involves the minimization of χ^2. The chi-squared distribution is commonly used in the chi-squared tests for a goodness-of-fit between an observed and theoretical distribution. The independence of two criteria of classification of qualitative data, and a confidence interval estimation for a population standard deviation of a normal distribution from a sample standard deviation. χ^2 is defined by eqn. (5.7) according to the chi-squared distribution with k degrees of freedom.

$$\chi^2 = \sum_{i=1}^{k} \frac{(Q_{o,i} - Q_{e,i})^2}{Q_{e,i}} \qquad (5.7)$$

$Q_{o,i}$ represents the observed value and $Q_{e,i}$ is the expected value.

The intraparticle diffusion equation was used for the determination of the rate-limiting step to understand the sorption mechanism and is expressed by eqn. (5.8)[32],

$$Q_t = k_i t^{1/2} + C \qquad (5.8)$$

Where k_i is the intraparticle diffusion rate constant ($molg^{-1}min^{-1/2}$) and C is the intercept.

5.3.4. Error analysis.

The calculation of uncertainty for an arithmetic operation of several numbers associated with measurements, each of which has a random error is not simply the sum of individual errors. Based on eqn (5.2), the relationship between the parameters from instrument is multiplication and division, so the following eqn (5.9) was used for the error analysis[33],

$$\%e_4 = \sqrt{(\%e_1)^2 + (\%e_2)^2 + (\%e_3)^2} \qquad (5.9)$$

Where in the case of calculation of the error for Q_e, the uncertainties arise from, % e_1 calculated from calibration curves under the similar experimental condition; % e_2 calculated from the detection limit of analytical balance (10^{-5}) for mass measurement; % e_3 calculated from the detection limit of 10 mL Kimax-51 petite (0.06 mL) to obtain the volume of solution. % e_4 (6.41%) was implemented into the fitting program,

Origin 7.5 for the error bar evaluation.

5.4. Results and Discussion

Figure 5.1 shows that the GC-ECD chromatogram illustrates good separation of the chloroform standard, as evidenced by the distinct retention time of the major analyte peaks. The internal standard, chlorobenzene, exhibits suitable retention behaviour because it is partially soluble in water (0.05 g/mL) and well resolved in relation to the chloroform fraction. The ECD method is relatively selective and sensitive to haloform-containing organic species such as chloroform studied herein.

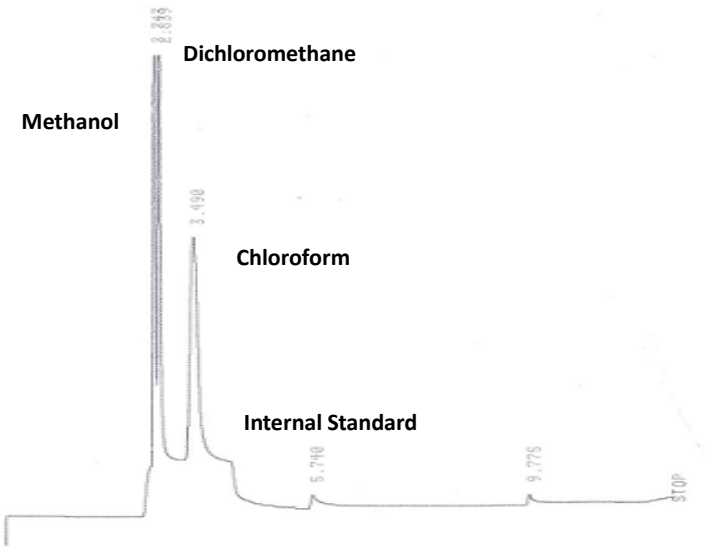

Figure 5.1. Gas chromatograph of chloroform (10 ppm) obtained using the DAI method with chlorobenzene as the internal standard.

5.4.1. A bench study

A bench study concerning the selection of suitable copolymer materials was carried out. An evaluation of their respective adsorption capacity with chloroform was estimated, along with a determination of the required experiment conditions (*e.g.* concentration of stock, detection limits, and the range of copolymer and solution doses, *etc.*). The results are shown in Table 5.1 where 29 mL of a 100 ppm chloroform solution with 10 mg copolymers were studied. Some of the copolymers were observed to have partial water solubility (*e.g.* SCl-1) or the formation of colloidal suspensions in solution (*e.g.* β-CD/PAA 5:1), and were therefore excluded from this study. The occurrence of residual copolymer components in sample solution may affect the quantitative results at trace levels. Recall that eqn. 5.2 assumes a heterogeneous equilibrium process where the sorbent and sorbate are phase separated according to copolymer insolubility. As well, chloroform is a VOC with relatively high vapor pressure at ambient conditions and is not amenable to normal workup procedures (*e.g.*, centrifugation or filtration) for separation of the copolymer and chloroform solution. The occurrence of dissolved and colloidal copolymers may result in contamination and were excluded in this study. The copolymers chosen in this study were selected according to the quality of data, ease of operation, and utility, as follows: β-CD/PAA 1:5, β-CD/PAA 1:5 at high speed, β-CD/PAA 1:10[16], β-CD/SCl 1:5 and 1:10[17], and CS/PAA copolymers, CP-1 and CP-5[18].

Table 5.1. Single-point sorption study for various copolymers.

Copolymers	Conc. (ppm)[a]	% removal[b]
CP-5	46.7	53.3
CP-1	30.6	69.4
β-CD/PAA 1:5	24.0	76.0
β-CD/PAA 1:5 at high speed	54.9	45.1
SCl-5	50.9	49.1
TCl-5	118	/
CD/PAA-5:1	110	/

[a] The residual concentration after sorption of 10 mg copolymers in 29 mL of 100 ppm chloroform solution for 24 h.

[b] Sorptive removal (%) of chloroform results for a single-point sorption study using 10 mg copolymers in 29 mL 100 ppm chloroform solution.

5.4.2. Sorption results

5.4.2.1. Adsorption kinetics

Non-equilibrium adsorption phenomena are time-dependent therefore; an understanding of the rate of adsorption is required for the rational design and evaluation of adsorbent properties at various conditions. The kinetic and equilibrium properties can be obtained from a temporal study of the adsorption process at variable time scales. Figure 5.2 shows the sorption of chloroform by copolymers CP-1 and β-CD/PAA 1:5 over a period of 0 to 24 h time intervals. Pseudo-first order and second order kinetic models were used to interpret the experimental data and evaluate the kinetics of the adsorption process (*cf.* Figure 5.3A and 5.3B); the parameters for pseudo-first order and second order kinetic models are shown in Table 5.2. The best-fit curves indicate that the pseudo-first order model is inappropriate as evidenced by the non-linear experimental data in a plot of $ln\ (Q_e\text{-}Q_t)$ *vs. t*. The pseudo second-order kinetic model shows an improved correlation coefficient (R^2) relative to

the first order model. Thus, the adsorption of chloroform by these two copolymer materials adopts pseudo-second order kinetics. Compared to the pseudo-first order model (Q_e equals to 0.647 mmol/g for CP-1 and 1.58 mmol/g for β-CD/PAA 1:5, respectively), the pseudo-second order fit shows a closer agreement with the sorption capacity determined independently at equilibrium (Q_e values of CP-1, 1.28 mmol/g compared to experimental measurement, 1.23 mmol/g; and β-CD/PAA 1:5, 1.78 to 1.70 mmol/g). The common usage of the empirical Lagergren pseudo-first order equation is for solid/liquid adsorption processes with a "one-site-occupancy" profile[34]. The mechanism is controlled by the interaction at the adsorbent surface where the adsorbing molecule occupies one adsorption site. On the other hand, the pseudo-second order model is proposed as a "two-site-occupancy" profile[34]. The kinetics of chloroform adsorbed onto the copolymer is more complicated than described by the first order Lagergren equation. Chloroform adsorption may involve various types of processes (*e.g.* transport to a solid surface, diffusion into pores, *etc*). According to Azizian[35], the pseudo-second order model shows a better fit than the first order model, particularly when the initial concentration of adsorbate is relatively low compared to the surface coverage factor, βθ. The initial concentration for chloroform used in the kinetic study is relatively low (~100 ppm) and may lead to a better fit using the pseudo-second order equation. However, one uncertainty of this explanation is the coverage factor changes significantly relative to the conditions of the sorption process[36]. As a result, the CD- and CS-based copolymers (CP-1 and β-CD/PAA 1:5) are well described by the pseudo-second order kinetic model.

The rate constant (K_2) for CP-1 is greater than that for β-CD/PAA 1:5, indicating a more rapid adsorption of chloroform with CP-1 compared to β-CD/PAA 1:5. However, the initial rate of adsorption (v_0) of CP-1 is less than β-CD/PAA 1:5, and may be due to its reduced adsorption capacity relative to the β-CD/PAA 1:5 copolymer.

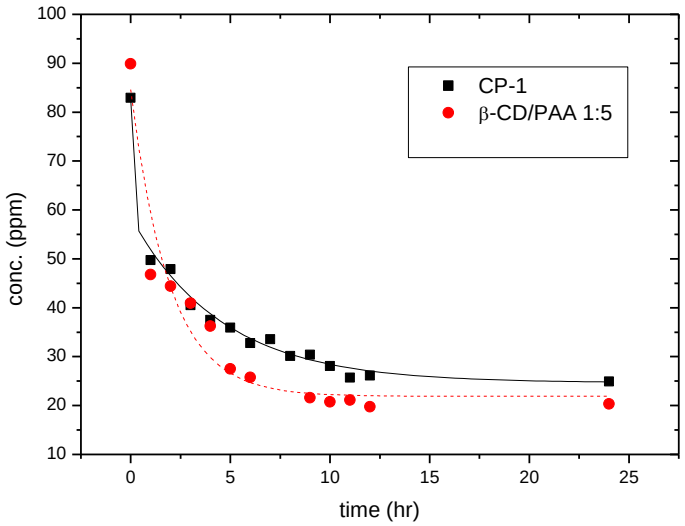

Figure 5.2. Chloroform uptake over a 24 h period by CP-1 and β-CD/PAA 1:5 at 295 K.

Table 5.2. Kinetic parameters of adsorption for CP-1 and β-CD/PAA 1:5 with chloroform at 295 K and ambient pH.

Adsorbate	**Pseudo 1st order**			**Pseudo 2nd order**			
	K_1 (h^{-1})	**Q_e ($mmolg^{-1}$)**	**R_1^2**	**K_2 (h^{-1})**	**Q_e ($mmolg^{-1}$)**	**R_2^2**	**v_0 ($mmolg^{-1}h^{-1}$)**
CP-1	0.372	0.647	0.935	0.923	1.28	0.995	1.51
β-CD/PAA 1:5	0.540	1.58	0.836	0.594	1.78	0.991	1.88

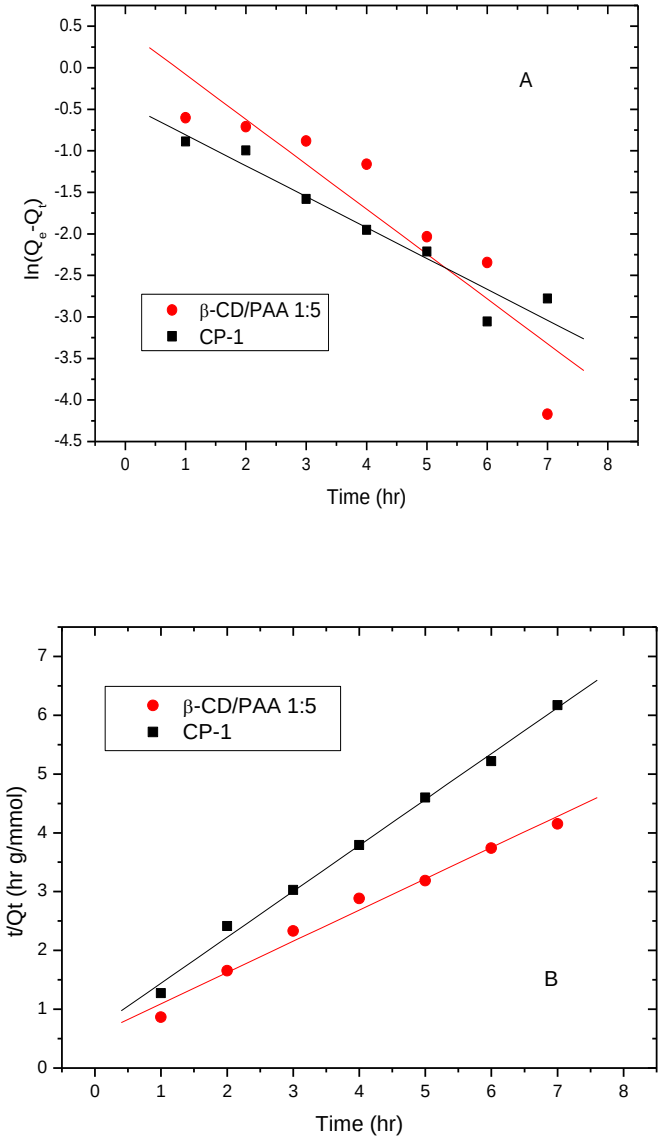

Figure 5.3. Kinetic of adsorption of chloroform: A) pseudo-first-order fit for CP-1 and β-CD/PAA 1:5, and B) pseudo-second-order fit for CP-1 and β-CD/PAA 1:5.

Since adsorption at the solid/liquid interface, an understanding of the diffusion process is important for obtaining a greater understanding of the adsorption mechanism. The copolymers display textural properties characteristic of porous materials at the meso- and micro-levels[16-18]. The solid/liquid adsorption process is generally described by three steps[37]: *i*) film or surface diffusion where adsorbates transport from the bulk solution to the external adsorbent surface; *ii*) intraparticle or

pore diffusion where adsorbates partition into the adsorbent interior; *iii*) absorption by the interior sites of adsorbents. The Weber-Morris intraparticle diffusion model is used to determine the rate-limiting step[37, 38] from plots of Q_t *vs* $t^{1/2}$ for the copolymers, CP-1 and β-CD/PAA 1:5 shown in Figure 5.5. The plot should yield a straight line where the intraparticle diffusion is the rate-limiting step, and when the plot intersects the origin, intraparticle diffusion is determined as the rate-limiting step. The multilinear plots shown in Figure 5.4 indicate three possible steps for the adsorption of chloroform at the copolymer surface. Based on the aforementioned results, intraparticle diffusion is not the rate-limiting step. The third step in the adsorption process is considered relatively rapid, therefore; surface diffusion or the intraparticle diffusion processes may be the rate-limiting steps.

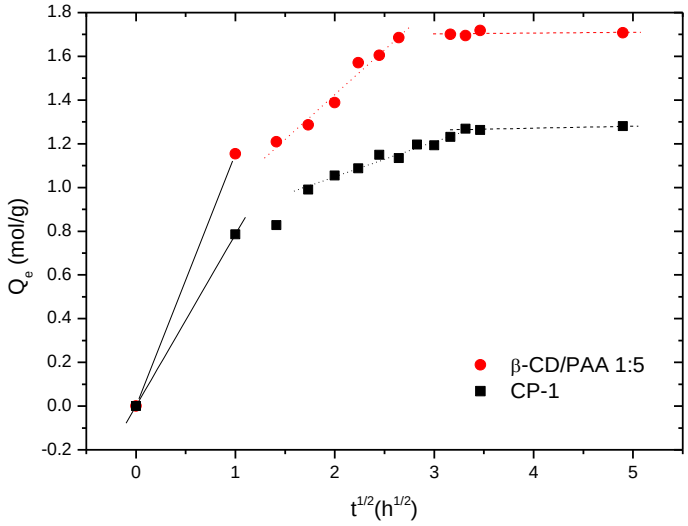

Figure 5.4. Weber-Morris intraparticle diffusion plots for chloroform adsorbed onto copolymers CP-1 and β-CD/PAA 1:5 at 295 K.

5.4.2.2. Sorption isotherms.

The sorption properties of the selected copolymer materials with chloroform were studied in aqueous solution using DAI method of GC-ECD at ambient pH and 295 K. A similar concentration range was used for the chloroform for the sorption isotherms to enable comparison among the various copolymers and to maintain good accuracy with suitable dilution factors. In Fig. 5.5A, the sorption isotherms (Q_e versus C_e) are compared for the prepolymer materials (*i.e.* CS) and the related cross-linked copolymers (*i.e.* CP-5 and CP-1). In Fig. 5.5B-C, the sorption isotherms (Q_e versus C_e) are shown for the β-CD-based copolymers (*i.e.* β-CD/PAA 1:5 and SCl-5) and are compared with the sorption results for AC. In general, the magnitude of Q_e increases monotonically as C_e increases. In some of the plots, the copolymers (*e.g.*, β-CD/PAA 1:5) do not show saturation of the sorption sites over the range of C_e values.

The sorption results were analyzed with the Sips isotherm (*cf.* Eqn. 5.4) which generally provides reliable results for the sorption capacities of copolymer dye-sorption[16-18]. The Sips model sorption parameters are listed in Table 5.3 and afford a good general description of the sorption properties of the copolymer/chloroform systems. The copolymer sorption capacities (Q_m; mmol/g) of chloroform are given in parentheses for similar experimental conditions adopt the following order: β-CD/PAA 1:5 (1.70) > SCl-5 (1.57) > SCl-10 (1.31) ~ CP-1 (1.23) > β-CD/PAA 1:10 (1.02) > CP-5 (0.785) > AC (0.593) > β-CD/PAA 1:5 at high speed (0.335). The copolymer sorption properties are related to the reagent ratios and reaction conditions and may be adjusted accordingly. The copolymers containing β-CD as the functional polysaccharide display good adsorption with chloroform relative to activated carbon. The β-CD/PAA 1:5 copolymer represents the greatest sorption among the materials studied for two reasons: *i*) β-CD forms stable complexes with small organic compounds; and *ii*) the cross-linking ratio is at a suitable level for chloroform to gain access the porous polymeric network. As a result, β-CD/PAA 1:10 contains a greater relative amount of cross-linker and may present a more impenetrable framework structure resulting in a reduced sorption capacity. Similarly, β-CD/PAA 1:5 at high speed was prepared at high mixing speeds under

micro-emulsion conditions. Higher mixing speeds generally result in smaller particles with more dense cross-linking and greater levels of β-CD grafting, affording higher sorption capacities[16]. In the case of the β-CD/PAA 1:5 copolymer prepared at high speed, the lowest sorption was observed among the copolymers studied. The observed result may be the denser framework structure of the copolymer with reduced chloroform accessibility to the micropore sites. In contrast, the CS copolymer materials have favourable sorption properties with chloroform, as compared to pristine chitosan which shows limited adsorption. CP-1 exhibits greater swelling behaviour than CP-5[18]. The increased swelling corresponds to a greater chloroform sorption capacity, in agreement with previously reported dye sorption properties[18]. The Q_m values of the copolymers are distinct when compared to macroporous Amberlite resins (XAD-4, ZH-00, and ZH-01), where the Q_m values (0.237-0.379 mmol/g)[39] are greater compared to activated carbon (Q_m ~0.00111-0.00470 mmol/g)[40].

The Sips exponent parameter for the copolymers deviates from unity and indicates the presence of heterogeneous or multiple sorption sites. In the case of β-CD- and CS-based copolymers, the accessibility of such sorption sites is variable due to the variable molecular structure of each polysaccharide platform. Multiple sorption sites for β-CD-based copolymers are attributed to the β-CD inclusion sites and the interstitial sites result from cross-linker domains. Indirect support is provided by systematic dye-sorption[16-18] and spectroscopic studies[17] of copolymers containing β-CD. Similarly, multiple sorption sites are available for CS copolymers according to the copolymer framework structure[18]; the cross-linked micropore domains of the copolymer framework and the numerous surface bound PAA sites ($-COO^-$). Hydrogen bond donor and acceptor sites are expected for such CS copolymers. Accordingly, hydrophobic effects, H-bonding, and electrostatic interactions are the driving forces for these physisorption processes, as evidenced by the reversibility of binding upon external stimuli, such as the change of temperature and pH[18].

Table 5.3. Best-fit equilibrium sorption parameters (Q_m, K_s and n_s) for the copolymer/chloroform systems at 295 K with the Sips model.

Material	Q_m [a]	K_s [b]	n_s	χ^2 [c]	R^2
CP-5	0.785	21.7	2.23	2.16×10^{-3}	0.962
CP-1	1.23	3.47	1.53	4.52×10^{-3}	0.961
β-CD/PAA 1:5	1.70	8.86	2.01	8.53×10^{-3}	0.950
β-CD/PAA 1:5 at high speed	0.335	11.1	0.984	2.70×10^{-4}	0.963
β-CD/PAA 1:10	1.02	1.70×10^{3}	3.98	8.00×10^{-4}	0.994
SCl-5	1.57	35.9	1.28	5.67×10^{-3}	0.976
SCl-10	1.31	1.61	0.624	4.32×10^{-3}	0.907
AC	0.593	2.55×10^{3}	4.89	5.90×10^{-4}	0.989

[a] Q_m, (mmol/g)

[b] K_{Sips}, (L/mmol)

[c] χ^2, Chi-square distribution

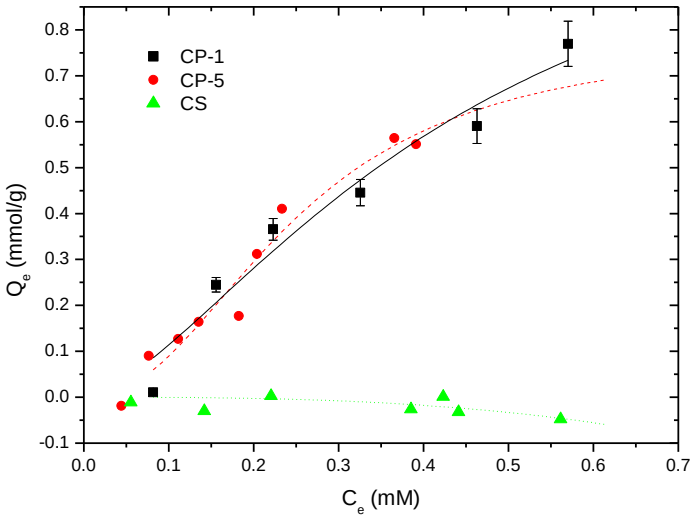

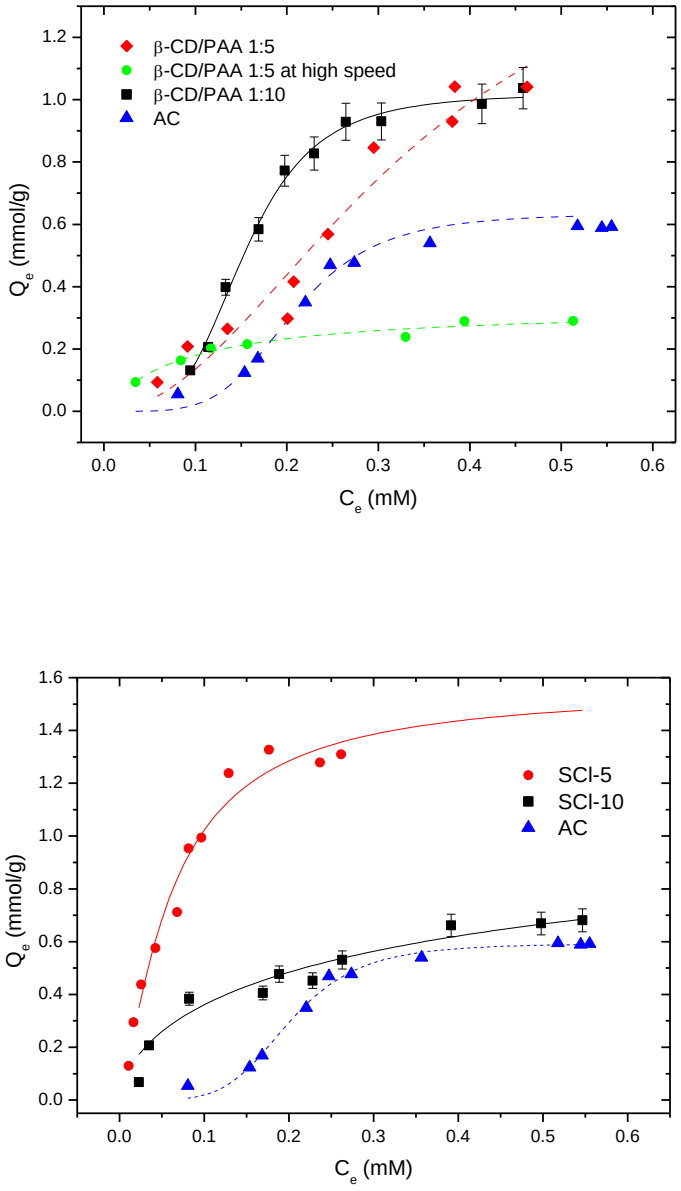

Figure 5.5. Sorption isotherms for the copolymer/chloroform systems at 295K: A) CP-5, CP-1, and CS, B) β-CD/PAA 1:5, β-CD/PAA 1:5 at high speed, β-CD/PAA 1:10 and CS, C) SCl-5, SCl-10, and AC. The *best-fit* results were obtained using the Sips isotherm (*cf*. eqn 5.3).

5.5. Conclusions

In this work, the sorption properties of copolymers containing either β-CD or CS with various cross-linkers and variable composition are reported using GC-ECD with a direct analysis injection method. The equilibrium and kinetic sorption properties of copolymer/chloroform systems were evaluated in aqueous solution at 295 K. The Sips model provided reliable estimates of the equilibrium sorption capacity (Q_m) of copolymers with chloroform varied from 0.00335-1.70 mmol/g. The development of versatile polysaccharide-based copolymer materials with tunable physicochemical properties represents a useful approach for the sorptive removal of chloroform in water environments. The synthetically engineered materials developed herein demonstrate their significant potential as sorbents for waterborne halomethanes such as chloroform and the significant improvement in water quality and public health. Further research is underway to understand the sorption properties of such copolymers sorbent with various other waterborne contaminants containing halogen functional groups. These copolymer materials can be use to improve water treatment technology, such as pre- and post-treatment to the existing treatment facilities. The materials can potentially replace some of the conventional adsorbents to provide more effective, cost-efficient and *"green"* contaminants removal.

5.6. Acknowledgements

The authors wish to acknowledge the Natural Sciences and Engineering Research Council of Canada (NSERC), the Canada Foundation for Innovation (CFI), and the University of Saskatchewan for the support of this research. Rui Guo gratefully acknowledges NSERC for a PhD scholarship through the NSERC CREATE-HERA program.

5.7. References

(1) Calderon, R. L. The epidemiology of chemical contaminants of drinking water. *Food and Chemical Toxicology* **2000**, *38, Supplement 1*, S13-S20.

(2) Soubeiran, E. *Ann. chim. phys.* **1831**, *48*, 157.

(3) Liebig, J. *Annalen der Pharmacie* **1832**, *1*, 182-283.

(4) Dumas, J. *Annalen der Pharmacie* **1834**, *107*, 650-656.

(5) National Toxicology Program (1991) NTP, Chemical Repository Data Sheet: Chloroform, Research Triangle Park, NC.

(6) International Trade Commission (1993), Synthetic Organic Chemicals, US Production and Sales, 77th Ed., Washington DC, US Government Printing Office, 3-18.

(7) Rossberg, M. In *Chlorinated Hydrocarbons;* Wiley-VCH Verlag GmbH & Co. KGaA: **2000**.

(8) Carpi, M.; Zufall, C. *Lc Gc N. Am.* **2003**, 88-91.

(9) Kramer, M. D.; Lynch, C. F.; Isaacson, P.; Hanson, J. W. *Epidemiology* **1992**, *3*, 407-413.

(10) Clesceri, L. S.; Greenberg, A. E.; Eaton, A. D. Trihalomethanes and Chlorinated Organic Solvents Standard Methods for the Examination of Water and Wastewater (APHA, AWWA and WEF) (U.S. EPA, Washington, D. C. Method 6232, 20th ed. 1998).

(11) WHO (1993), Ed.; In *Guidelines for drinking water quality. Volume 2: Health criteria and other supporting information.* World health organization: Geneva.

(12) Health Canada, 2011. Guidelines for Canadian Drinking Water Quality: Guideline Technical Document. (accessed 06/24, 2012).

(13) http://www.allaboutwater.org/filtration.html. (accessed 01/28, 2013).

(14) Mohamed, M. H.; Wilson, L. D.; Headley, J. V.; Peru, K. M. *Process Saf. Environ. Prot.* **2008**, *86*, 237-243.

(15) Crini, G. *Prog. Polym. Sci.* **2005**, *30*, 38-70.

(16) Guo, R.; Wilson, L. D. *J. Appl. Polym. Sci.* **2012**, *125*, 1841-1851.

(17) Wilson, L. D.; Guo, R. *J. Colloid Interface Sci.* **2012**, *387*, 250-261.

(18) Guo, R.; Wilson, L. D. *J. Colloid Interface Sci.* **2012**, *388*, 225-234.

(19) Inoue, Y.; Harkushi, T.; Liu, Y.; Tong, L. H.; Shen, B. J.; Jin, D. S. *J. Am. Chem. Soc.* **1993**, *115*, 475-481.

(20) Jang, J. S.; Bae, J. *Macromol. Rapid Commun.* **2005**, *26*, 1320-1324.

(21) van de Manakker, F.; Vermonden, T.; van Nostrum, C. F.; Hennink, W. E. *Biomacromol.* **2009**, *10*, 3157-3175.

(22) Graves, R.; Makoid, M.; Jonnalagadda, S. *J. Microencapsul.* **2005**, *22*, 661-670.

(23) Xiao, W.; Chen, W.; Zhang, J.; Li, C.; Zhuo, R.; Zhang, X. *J. Phys. Chem. B* **2011**, *115*, 13796-13802.

(24) Dumitriu, S., Ed.; In *Polysaccharides: Structural Diversity and Functional Versatility*. **2005**.

(25) Nicholson, A. A.; Meresz, O.; Lemyk, B. *Anal. Chem.* **1977**, *49*, 814-819.

(26) Pfaender, F. K.; Jonas, R. B.; Stevens, A. A.; Moore, L.; Hass, J. R. *Env. Sci. Tech.* **1978**, *12*, 438-441.

(27) Hodgeson, J. W.; Cohen, A. L. Determination of chlorination disinfection by-products and chlorinated solvents in drinking water by liquid-liquid extraction and gas chromatography with electron-capture detection. (U.S. EPA, Cincinnati, Ohio, USA, Method 551, 1990).

(28) Lovelock, J. E.; Maggs, R. J. *Nature* **1973**, *241*.

(29) Rook, J. J. *Water Treatment and Examination* **1972**, *21*.

(30) Eichelberger, J. W.; Budde, W. L. Measurement of purgeble organic compounds in water by capillary column gas chromatography mass spectrometry (environmental monitoring systems, U. S. EPA, Method 542.2, 1990).

(31) Sips, R. Structure of catalyst surface. *J. Am. Chem. Soc.* **1948**, *125*, 6452.

(32) Weber, W. J.; Morris, J. C. In *Advances in water pollution research: removal of biologically resistant pollutant from waste water by adsorption.* **1962**; Vol. 2, pp 231-266.

(33) Harrism, D. C., Ed.; In *Quantitative chemical analysis;* Freeman: United State, **2007**.

(34) Rudzinski, W.; Plazinski, W. *J. Phys. Chem. B* **2006**, *110*, 16514-16525.

(35) Azizian, S. *J. Colloid Interface Sci.* **2004**, *276*, 47-52.

(36) Liu, Y.; Shen, L. *Langmuir* **2008**, *24*, 11625-11630.

(37) Lazaridis, N.; Asouhidou, D. *Water Res.* **2003**, *37*, 2875-2882.

(38) Qiu, H.; Lv, L.; Pan, B.; Zhang, Q.; Zhang, W.; Zhang, Q. *J. Zhejiang Univ. -SCI A* **2009**, *10*, 716-724.

(39) Fei, Z. H.; Chen, J. L.; Gao, G. D.; Long, C. *Chin. J. Polym. Sci.* **2004**, *22*, 425-430.

(40) Abe, I.; Fukuhara, T.; Maruyama, J.; Tatsumoto, H.; Iwasaki, S. *Carbon* **2001**, *39*, 1069-1073.

CHAPTER 6

Description

Chapter 6 includes a verbatim copy of a manuscript planned to submit to & Engineering Chemistry Research. The article describes the adsorption properties of series of polysaccharide-based copolymers toward THMs in aqueous solution.

Author's contribution

I carried out all of the experimental work from the synthesis to characterization of the copolymers. This work was principally supervised by Dr. Wilson and Dr. Bharadwaj. I wrote the first draft of the manuscript with assistance in the form of manuscript editing by Dr. Wilson and Dr. Bharadwaj. The co-authors grant of use of the manuscript for this PhD thesis, and agree with the description of the and contributions of the authors.

Relationship of Chapter 6 to the overall objective of this project

As stated in the introduction, the research objective was to examine the sorptive properties of the synthesized copolymers toward THMs. This chapter is an extension the studies presented in Chapter 5 by examining the sorption properties of mixtures of THM components with copolymers. The sorption capacities of THMs with the copolymers were evaluated using the experimental protocol and analytical method developed in Chapter 5. Selective adsorption behaviours of the copolymers with individual THM component species from aqueous mixtures were observed due to the molecular selective nature of the copolymer materials.

Research highlight:

The DAI method with GC-ECD detection was utilized for the quantitative detection of THMs in water. A series of sorption isotherms of THMs with various copolymers were obtained at ambient temperature and pH; the sorption parameters were evaluated using the Sips model. The copolymers showed relatively high selectivity toward individual components of THMs due to nature of the copolymer materials and the variable molecule size and polarizability of THMs. The polymer adsorbents showed favorable adsorption come from both β-CD and CS-based copolymers (*e.g.*, β-CD/PAA 1:5 and CP-1).

6. Selective Removal of Tirhalomethanes (THMs) from Water by Synthetically

Engineered Copolymers Using a Direct Aqueous Injection (DAI) Method

Rui Guo[a], Lee D. Wilson[a*], and Lalita Bharadwaj[b]

[a]Department of Chemistry, University of Saskatchewan, 110 Science Place, Saskatoon, Saskatchewan, S7N 5C9

[b]School of Public Health, University of Saskatchewan, Health Sciences Building, 107 Wiggins Road, Saskatchewan, S7N 5E5

[*]Corresponding author: Tel. 1-306-966-2961, Fax. 1-306-966-4730
e-mail: lee.wilson@usask.ca

6.1. Abstract

The removal of trihalomethanes (THMs) from spiked water samples was evaluated with a series of synthetically engineered copolymer sorbent materials. The sorptive properties of synthetically engineered copolymers containing polysaccharides, such as, cyclodextrin and chitosan, respectively, were evaluated with THMs in aqueous solution. Gas chromatography (GC) employing a direct aqueous injection (DAI) method with electron capture or electrolytic conductivity detectors (ECD) was utilized for the detection of THMs in water at 295 K and ambient pH. The sorption isotherms of the copolymer/THM systems were evaluated using the Sips model. Depending on the nature of the copolymer, markedly different sorption characteristics were observed according to their composition and chemical surface characteristics. The copolymers showed relatively high selectivity toward individual components of THMs due to their various molecule size and polarizability.

Keywords: *THMs, sorption studies, β-CD, chitosan, copolymers, GC-ECD, DAI.*

6.2. Introduction

Drinking water quality is a significant issue for public health around the world. Chlorine disinfection of drinking water using gaseous chlorine or liquid sodium hypochlorite is often regarded as one of the major public health achievements of the 20th century[1]. Chlorination reduces the levels of microbial pathogens in water supplies thereby reducing the incidence of waterborne disease, however; the disinfection process results in the generation of disinfection by-product (DBPs) in water containing organic and inorganic matter[2, 3]. Trihalomethanes (THMs) are among the most common and important DBPs, and have become one of the greatest public health concerns in conventional water disinfection processes. THMs are halogen-substituted single-carbon compounds with a general molecular formula CHX_3, where X may represent fluorine, chlorine, bromine or iodine (*cf.* Scheme 6.1). The most important THMs in disinfected water supplies are chloroform, bromodichloromethane (BDCM), dibromochloromethane (DBCM) and bromoform. The formation of THMs is closely related to the specific conditions in the water environment, such as, chlorine dosage, contact time, pH, bromide ion concentration, and organic precursor concentration in the source water[2].

THMs are highly volatile organic compounds; their physical and chemical properties are listed in Table 6.1. Chloroform evaporates quickly when exposed to air and dissolves quickly in water. Both chloroform and brominated THMs remain in air and water for long periods and can partition to groundwater through soil[4]. Hydrolysis of brominated THMs in aqueous media is very slow; estimated half-lives of BDCM, DBCM, and bromoform are 1000, 274, and 686 years, respectively[4, 5].

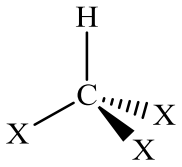

X represents either Cl, Br, or both
-Chloroform: $CHCl_3$
-Bromodichloromethane: $CHCl_2Br$
-Dibromochloromethane: $CHClBr_2$
-Bromoform: $CHBr_3$

Scheme 6.1. Molecular structure of THMs, where X represents halogen atom.

Table 6.1. Physical and chemical properties of THMs.

Properties	**Water solubility (g/L)**	**Vapor pressure (kPa)**	**Boiling point (℃)**	**Molecular weight (g/mol)**	**Molar volume (mL/mol)**	**K_H[a]**
Chloroform ($CHCl_3$)	7.50-9.30 (25 ℃)	21.3 (20 ℃)	61.3	119.4	80.5	0.0367 (24 ℃)
BDCM ($CHBrCl_2$)	3.32 (30 ℃)	6.67 (20 ℃)	90.0	163.8	82.7	0.00212
DBCM ($CHBr_2Cl$)	1.05 (30 ℃)	2.00 (30 ℃)	119	208.3	85.0	0.000783 (20 ℃)
Bromoform ($CHBr_3$)	3.19 (30 ℃)	2.90 (30 ℃)	150	252.7	89.0	0.000535

[a] Henry's law constant at 25 ℃, atm•m^3/mol[6]

The major routes of human exposure to THMs are ingestion, inhalation and dermal contact with chlorinated water. THMs can be ingested by direct ingestion of water and also through consumption of contaminated foods. Variable levels of THMs are found in food[7], such as, dairy products, vegetables, meat, *etc*. THMs, especially chloroform, can evaporate easily so they also may be absorbed into the human body

via inhalation of gaseous species during bathing and showers. The International Agency for Research on Cancer (IARC) has classified chloroform and BDCM as possible carcinogens for human (Group 2B) which means there is limited evidence of carcinogenicity in human but sufficient evidence in animal studies. DBCM and bromoform are assigned to Group 3 cancer potency because of inconclusive carcinogenicity in human and limited carcinogenicity in experimental animal studies[1, 8]; the IARC classification and U.S. Environmental Protection Agency (EPA) cancer potency factors are listed in Table 6.2. Besides carcinogenicity, animal studies indicate that chloroform in drinking water supplies may lead to low birth weight, prematurity and intrauterine growth retardation by a population-based case control analysis[1, 89]. THMs can cause acute and chronic ecological effects to aquatic life, *e.g.*, chloroform has moderate acute and chronic toxicity to aquatic organisms.

Table 6.2. IARC classification and U.S.EPA cancer potency factor of THMs.

Compounds	**Classification**	**Cancer potency factor (mg/kg/day)**
Chloroform	Group 2B	0.0061
BDCM	Group 2B	0.062
DBCM	Group 3	0
Bromoform	Group 3	0.0079

The U. S. Environmental Protection Agency (EPA) has published the disinfectants-Disinfection By-products Rule to regulate total THMs at a maximum allowable annual average level of 80 ppb in the Stage 1 and 40 ppb in Stage 2 for water treatment, respectively[10]. The maximum acceptable concentration (MAC) for

THMs in drinking water derived by Health Canada is 100 ppb. The MAC is based on a locational annual average of a minimum of quarterly samples taken at the point in the distribution system with the highest potential THM levels. As a result, the removal of THMs and the maintenance of their levels below the regulatory values is a significant drinking water quality issue.

Adsorption-based removal of THMs represents a relatively inexpensive and facile approach in water treatment technology. In comparison to reverse osmosis and distillation, filtration is limited to the type or size of contaminants they can be removed, whereas; adsorptive removal is a more versatile technology[11]. Commonly used adsorbents to remove THMs include activated carbons, which are considered generally expensive, variable chemical quality, and costly to regenerate after usage[12]. There is a need to develop improved synthetically sorbent materials with tunable sorptive properties to offset the aforementioned disadvantages noted for activated carbons.

The development of tunable sorbent copolymer materials was previously reported[14-16] for the controlled uptake of contaminants by variation of the synthetic conditions (*e.g.*, stirring rate and co-monomer ratios), the nature of the polysaccharide and cross-linkers[13-15]. Copolymer sorbents containing polysaccharides (*i.e.* β-CD and CS) were by cross-linked with suitable agents (*i.e.* PAA, SCl, and TCl) and variable reaction conditions. β-cyclodextrin (β-CD) is a macrocyclic oligosaccharide that with a internal depth of 7.8 Å and a internal diameter of 7.8 Å that is amphiphilic in nature and displays unique inclusion properties toward suitable sized lipophilic guest molecules (*cf.* Scheme 6.2a)[16]. Previous reports indicate demonstrated that β-CD can be used to construct copolymer frameworks by chemical cross-linking, grafting or non-covalent self-assembly[17, 18]. CS is a linear polysaccharide composed of randomly distributed β-(1→4)-linked D-glucosamine and N-acetyl-D-glucosamine units[19] and the relatively hydrophobic backbone of chitosan with amine groups is suitable for cross-linking reactions and potential active adsorption sites (*e.g.* electrostatic

interaction, H-bonding, *etc*.). The extended chain conformations of CS serve as a rigid prepolymer for the design of copolymer materials[15]. Similarly, chitosan (CS; Scheme 6.2b) represents a versatile polysaccharide material in materials design strategies because of its host-guest chemistry and accessible functional groups. Chitosan is a cost-effective biomaterial produced through the deacetylation of crustacean or fungi-derived chitin.

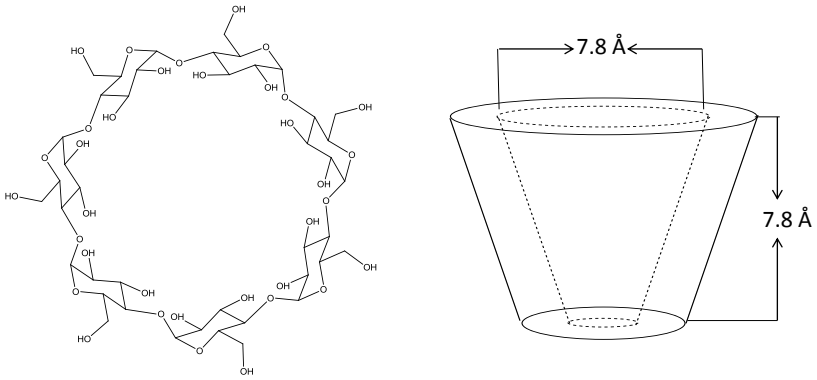

a)

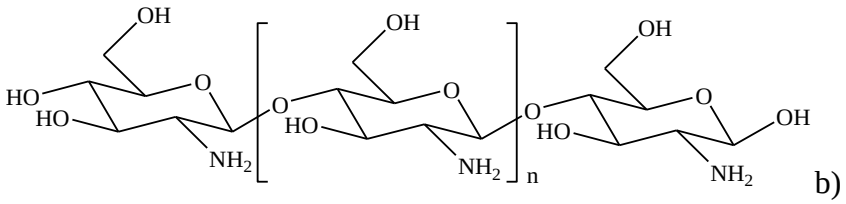

b)

Scheme 6.2. Molecular structure of a) β-CD and b) CS.

This study of the sorptive removal of THMs uses a series of synthetically

engineered copolymers. We hypothesized that synthetically engineered copolymers may be extended to the sorptive removal of THMs according to previous results obtained for chloroform in spiked water samples. The present study will be focused on THMs with a comparison of the sorption properties with chloroform. The sorption capacities of a series of synthetically engineered copolymers (*cf.* Scheme 6.3a-d[13-15]) were evaluated using solid-solution isotherms by directly measuring unbound THMs in water using the direct aqueous injection GC-DAI method with ECD detection. The DAI-GC method enabled quantitative detection of halomethanes in water[8, 20] and employed as one of the techniques for THMs detection by Health Canada[21]. The sorptive properties of the copolymers with THMs are anticipated to be variable in accordance with the textural and surface chemistry properties of the sorbents.

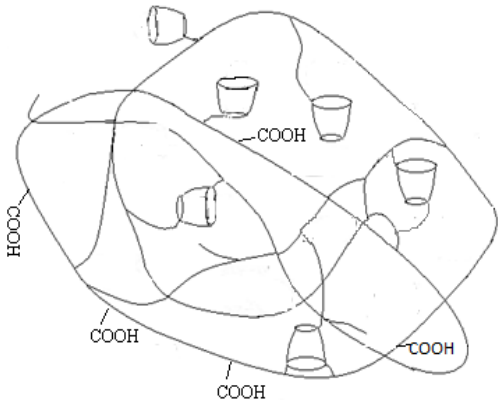

a)

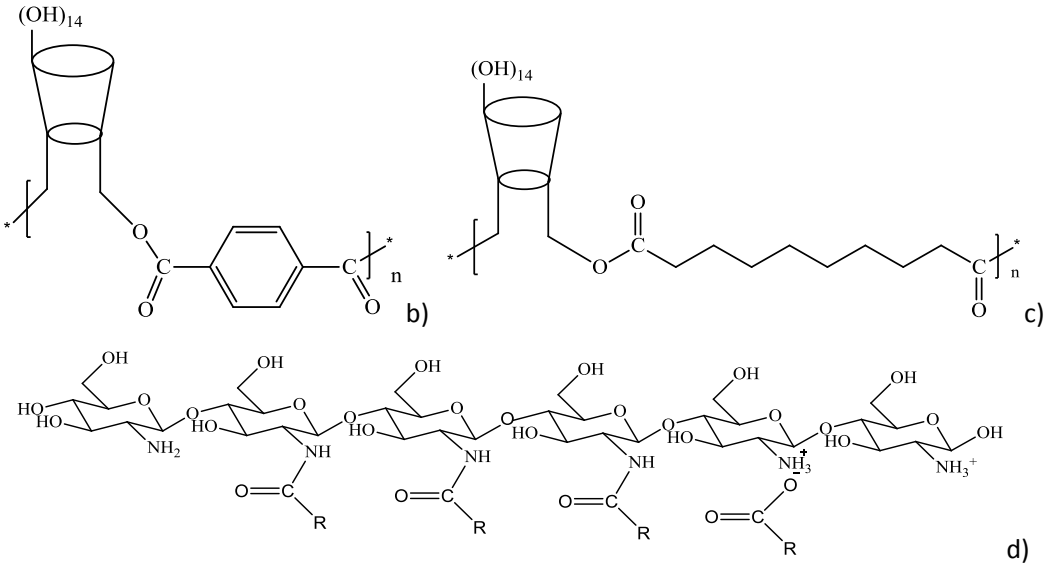

Scheme 6.3. Molecular structure of a) schematic representation of β-CD/PAA copolymer, where the toroidal-shaped represented CDs and the straight line segments connecting the β-CD tori represent the ester linkage; b) β-CD/TCl copolymer; c) β-CD/SCl copolymer; and d) CS/PAA copolymer.

6.2. Experimental Section

6.2.1. Reagents.

Methanol (HPLC grade) was obtained from Fisher Scientific. Activated carbon (AC, Darco 20x40 LI) was purchased from Norit America and was treated with 2.0 M HCl using Soxhlet extractor for 48 hours. All the water used in this work was distilled water. All the solutions were freshly made prior to analysis.

6.2.1.1.Copolymer materials.

Copolymers (β-CD/PAA 1:5, β-CD/PAA 1:5 at high speed, β-CD/PAA 1:10[13], β-CD/SCl 1:5 and 1:10[14], and chitosan/PAA copolymers, CP-1 and CP-5[15]; detailed synthetic methods and their materials characterization is reported previously.[13-15]

6.2.1.2. Internal standard.

The internal standard for GC analysis was a 1% (v/v) chlorobenzene solution (Sigma-Aldrich) in methanol.

6.2.1.3. Stock standard solution.

The THMs calibration standard is a mixture of chloroform, BDCM, DBCM and bromoform obtained from ULTRA Scientific as a 5,000 ppm (w/v) in methanol.

6.2.2. Apparatus.

Custom built 9 mL vials with Silicon/Teflon lined caps were designed for the sorption experiments to achieve efficient gas-tight seals. The gas chromatograph was a 5890 Hewlett Packard model equipped with an electron-capture detector (ECD) and

cool on-column (DV-1, 30m x 0.32mm ID x 25μm) injection system.

6.2.2.1. Operating conditions.

A helium carrier gas was maintained at a constant 10-kPa inlet pressure. The makeup gas was 5% (v/v) methane-argon mixture with a flow rate of 60.0 mL/min. The injector and detector temperature were set at 250 ° C. The maximum oven temperature was 300 ° C and the equilibrium time was set at 3.00 min. For chloroform/THMs, the GC operating conditions were as follows: oven temperature and initial temperature were 50 °C. The final temperature was 100 °C. The initial time was 5.00 min. The heating rate was 10.0 °C/min and the final time was 2.50 min.

6.2.3. Methods.

The direct injection method was used for the GC analysis without extraction or any pre-concentration steps. The aqueous solutions of THMs were directly injected to the GC using 1 μL of analyte with 1 μL of air into the injector for every analysis.

6.2.3.1. Calibration of standard solutions.

The standard solution of THMs was diluted to 50 ppm. 8 points ranged from 5-50 ppm were collected to construct a quantitative calibration curve.

The calibration curve was plotted by concentration versus area ratio according to eqn. (6.1).

$$area\ ratio = \frac{A_S}{A_I} \qquad (6.1)$$

A_S is the relative peak area of the respective THM compound and A_I is peak area of internal standard.

6.2.3.2. Sorption isotherms.

Fixed amounts (~5-6 mg) of the powdered and sieved copolymer materials were mixed with 7 mL of blank solution at variable concentration for each THM component (5-50 ppm) until fully equilibrated on a horizontal shaker table for 24 h.

A 4% (v/v) internal standard was added 15 min. ahead of each GC injection to the supernatant solution from the sample vial after completed gravity settling of the copolymers from the solution phase.

The sorption isotherms are depicted as plots of the adsorbed amount of THMs in the copolymer phase per mass of adsorbent (Q_e; mmol/g) versus the equilibrium residual concentration of unbound THMs (*i.e.* adsorbate) in aqueous solution (C_e). The value of Q_e is defined by eqn. (6.2) where C_0 is the initial concentration of THMs, V is the volume of solution, and m is the mass of adsorbent.

$$Q_e = \frac{(C_0 - C_e) \times V}{m} \qquad (6.2)$$

The Sips isotherm model is a versatile and generalized isotherm that accounts for a distribution of adsorption energies on the sorbent surface with behavior that may vary from monolayer (Langmuir) to multi-layer (Freundlich) adsorption. The parameter (n_s) reflects the heterogeneity of the sorbent, where a value of n_s=1 infers a homogenous surface while $n_s \neq 1$ indicates a heterogeneous surface. Langmuir behavior is predicted when n_s=1, and Freundlich behavior occurs when $K_s C_e^{n_s} <<< 1$. The Sips models is defined by eqn. (6.3)[22].

$$Q_e = \frac{Q_m K_s C_e^{n_s}}{1 + K_s C_e^{n_s}} \qquad (6.3)$$

K_s is the Sips equilibrium constant and Q_m is the maximum adsorption capacity per unit mass of sorbent.

The criteria of the "best-fit" between the calculated isotherm and the experimental data are determined by the correlation coefficient (R^2) and the chi-square distribution (χ^2). The parameter $R^2 \sim 1$ denotes a satisfactory "*best-fit*"; however, a more sensitive measure for non-linear least squares fitting involves the minimization of the χ^2 parameter. The chi-squared distribution is commonly used to test for the goodness of fit between an observed and a theoretical distribution, the independence of two criteria of classification of qualitative data, and in confidence interval estimation for a population standard deviation of a normal distribution from a

sample standard deviation. χ^2 is defined by eqn. (6.4) according to the chi-squared distribution with k degrees of freedom.

$$\chi^2 = \sum_{i=1}^{k} \frac{\left(Q_{o,i} - Q_{e,i}\right)^2}{Q_{e,i}} \qquad (6.4)$$

$Q_{o,i}$ represents the observed value and $Q_{e,I}$ is the expected value.

6.2.3.3. Error analysis.

The error analysis is based on an arithmetic operation on several parameters associated with measurements, each of which has a random error[23]. The most likely uncertainty for the result is not simply the sun of individual errors. Based on eqn (6.2), the relationship between the parameters from GC analysis is multiplication and division, so the error analysis is described by eqn (6.5) [23].

$$\%e_4 = \sqrt{(\%e_1)^2 + (\%e_2)^2 + (\%e_3)^2} \qquad \text{eqn. (6.5)}$$

In the case of the error calculation for Q_e, the uncertainties are attributed as follows: % e_1 calculated from calibration curves under the similar experimental condition; % e_2 calculated from the detection limit of analytical balance (10^{-5}) for mass measurement; % e_3 calculated from the detection limit of 10 mL Kimax-51 petite (0.06 mL) to obtain the volume of solution. % e_4 was implemented into the fitting program, Origin 7.5 for the error bar determination.

6.3. Results and Discussion

Figure 6.1 shows that GC-ECD chromatogram yields good separation of THMs standard according to the different retention times of the major analyte peaks. Chlorobenzene exhibits suitable retention behaviour as an internal standard because it is partially soluble in water (0.05 g/mL) and is well resolved relative to the four THM fractions. The DAI method provided reliable results for a previous quantitative study of chloroform (detection limit 0.1 ppb[8]). A similar methodology is employed herein for the quantitative determination of THMs and the adsorption capacity of copolymer sorbents (*cf.* eqns 6.2-6.3). The *in-situ* analysis of THMs avoids the extra step

required of solvent extraction and the isothermal GC operation reveals good chromatographic separation.

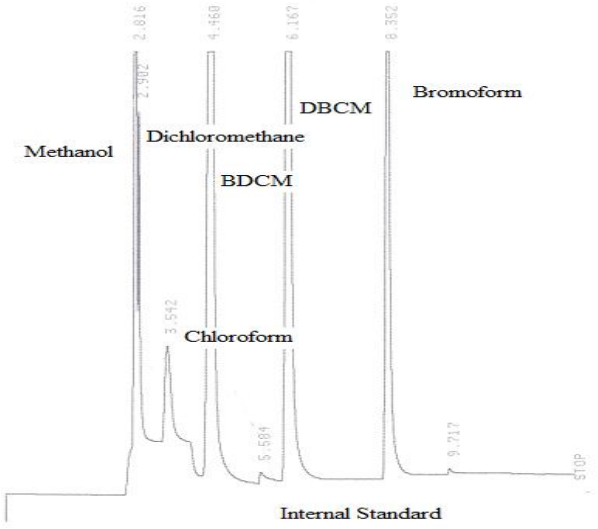

Figure 6.1. Gas chromatograph of THMs (10 ppm) obtained using the DAI method.

The calibration curves for THMs showed relatively good linearity with R^2 approaching unity (*cf.* Figure 6.2 and Table 6.3). The linearity check was performed by using standard solutions within 5-50 ppm for each component.

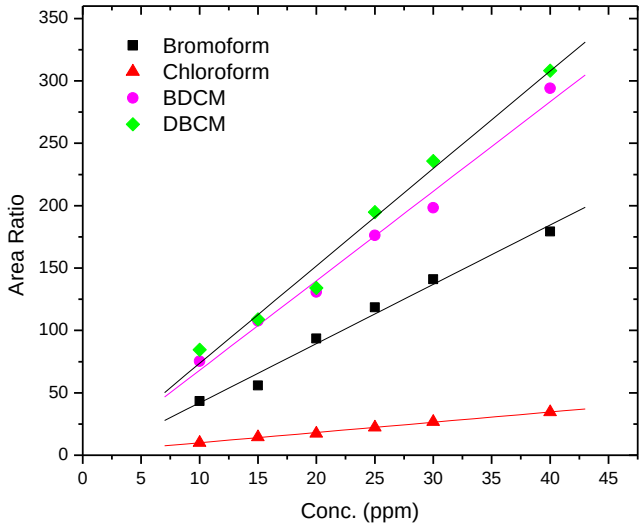

Figure 6.2. GC-based calibration curve of THMs in water at ambient pH and 295 K.

Table 6.3. R^2 values of calibration curves for THMs in water at ambient pH and 295 K using GC-ECD.

	Chloroform	BDCM	DBCM	Bromoform
R^2	0.998	0.993	0.993	0.993

Figures 6.3A-H illustrated the sorption isotherms (Q_e versus C_e) are shown for the copolymers materials and compared with activated carbon. The sorption properties of the selected copolymers that displayed favorable chloroform adsorption were selected for the sorption study with THMs in aqueous solution using the DAI method. In general, the magnitude of Q_e increases monotonically as C_e increases and significant differences in sorption affinity are observed amongst the various component THMs with the copolymers. In some cases, the copolymers do not show saturation of the sorption sites (*e.g.* bromoform adsorption on CP-1) in the range of experimental C_e values investigated. A similar concentration range was used for the THM stock solutions for the sorption isotherm study. The uniform concentration range provides a meaningful comparison among the various copolymers whilst maintaining good accuracy and suitable dilution factors.

The sorption results for THMs were evaluated with the Sips isotherm (*cf.* Eqn. 6.4) and the *"best fit"* sorption parameters are listed in Table 6.4. In previous studies[13-15], the Sips model provided reliable estimates of the copolymer-dye sorption capacity for various dye systems. The Sips model provides a good general description of the sorption behavior of copolymers to various THMs in aqueous solution. The sorption properties of copolymer materials are closely related to the synthetic conditions (*e.g.*, reagent mole ratios and mixing speeds) and type of cross-linker and polysaccharide. The THMs studied herein have similar molecular structure (*cf.*

Scheme 6.1) but variable physical and chemical properties (*e.g.*, sizes, polarizability, *etc.; refer to Table 6.1 and Table 6.5*), as evidenced by the remarkably different adsorption behaviour of the various copolymer materials. The CS based copolymers, CP-1 and CP-5, display distinct adsorption capacities to the various THMs. The THM species adsorbed on the copolymer CP-1 are in the order as follows: bromoform (0.440 mmol/g) > DBCM (0.415 mmol/g) > BDCM (0.387 mmol/g) > chloroform (0.0420 mmol/g), and adopt reverse order relative to CP-5 as follows: chloroform (0.141 mmol/g) > BDCM (0.119 mmol/g) > DBCM (0.0684 mmol/g) > bromoform (0.0522 mmol/g). Considering the relative binding affinity among various THM components, CP-1 shows a favorable adsorption to the brominated THMs and may be due to their greater hydrophobicity due to their greater molecular weight. Solvent effects and van der Waals interactions play the major role for the adsorption between CS copolymers and THMs possessing low solubility. Meanwhile, the overall adsorption capacity of CP-1 toward THMs is estimated by adding the Q_m values of chloroform and brominated THMs together is greater than CP-5 copolymer due to its greater surface accessibility in the swollen state (i.e. swelling ratio (r); r=22.6 for CP-1 and r=11.6 for CP-5, respectively[15]). The swelling parameters agree with the sorption behaviour reported previously for these copolymers with chloroform. CP-1 shows a better adsorption also because the greater PAA content compared with CP-5 results in a copolymer with more hydrophilic character and suitable for adsorption of THM molecules which are relatively polar molecules (*cf.* Table 6.5 lists the dipole moment of THMs calculated by Spartan'08 1.2.0). However, the adsorption of THMs on copolymers is a process that should consider several factors (*e.g.*, the surface characteristics of the copolymer, physiochemical properties of the adsorbates, *etc.*). Compared to more hydrophilic copolymers (*e.g.* CP-1), CP-5 represents a better adsorption of chloroform than other THMs possibly due to the surface accessibility of the copolymer and the molecular size of THMs (bromoform > BDCM > DBCM > bromoform) as discussed herein.

β-CD-based copolymers display remarkable sorption capacities toward THMs, in part, because β-CD provides a suitably sized lipophilic inclusion site for lipophilic

THMs (*cf.* Table 6.5). Relatively stable inclusion complexes of THM molecules within the β-CD cavity are also anticipated in water due to hydrophobic effects, which can be considered as an entropy-driven spontaneous process[24-26]. β-CD based copolymers also behave differently by varying the preparative techniques. For the β-CD/PAA copolymers, the preference to adsorb the various THM species is similar. The largest molecule, bromoform, is the most preferentially adsorbed onto β-CD/PAA copolymers followed by BDCM, DBCM, and finally chloroform due to their different molecular polarizability values. The more lipophilic THMs favorably enter into the β-CD lipophilic cavity due to unfavourable hydrophobic hydration. The β-CD/PAA 1:5 copolymer represents the greatest sorption among the β-CD/PAA copolymers because its moderate cross-linking ratio does not pose limitations for THMs to access the porous polymeric network. In contrast, β-CD/PAA 1:10 may have a more condensed framework structure because the greater amount of cross-linker[13] attenuates the sorption capacity. Similarly, β-CD/PAA 1:5 at high speed was prepared at high mixing speeds under micro-emulsion conditions which should result in smaller particles with greater cross-linking density as evidenced by greater β-CD grafting[13]. The β-CD/PAA 1:5 copolymer shows the lowest sorption amongst the copolymers studied herein. The sorption capacity may decrease because of the reduced pore accessibility on the surface of highly cross-linked copolymers toward THM molecules. The presence of micropore sites that result from intermediate cross-linked frameworks or accessible inclusion sites in the case of CD-based copolymers is anticipated to favour THM adsorption. Size-fit matching of THMs is evidenced by the β-CD/SCl based copolymers, SCl-5 and SCl-10 and show greater adsorption for the smallest THM molecules, chloroform and similar sorption capacities for the brominated THMs.

The adsorption capacity of Darco activated carbon is used to compare with the synthetic copolymer materials since AC is among the most wildly used adsorbent for removal of THMs. The adsorption isotherms of AC in Figure 6.3H are distinctive for chloroform and brominated THMs revealing differences in sorption affinity amongst the various THMs. The adsorption isotherm of chloroform onto AC displays a

standard Langmuir monolayer adsorption ($n_s \approx 1$), while the brominated THMs shows greater adsorption affinities which are attributed to their greater lipophilicity and through favourable van der Waals interaction with the AC surface[27]. The three THMs adsorption plateau at similar Q_e values may possibly due to the relative uniform surface of AC, as compared with copolymer sorbents. AC shows a high adsorption capacity toward chloroform (0.261 mmol/g) which is comparable with SCl-5 (0.287 mmol/g) and SCl-10 (0.248 mmol/g), however; AC adsorbs much less bromoform (0.141 mmol/g) than β-CD/PAA 1:5 (1.07 mmol/g) from the THM aqueous solution.

The relative sorption capacity of chloroform for these synthetically engineered copolymers according to the values of Q_m for similar experimental conditions adopts the following order: SCl-5 (0.287 mmol/g) > AC (0.261 mmol/g) > SCl-10 (0.248 mmol/g) > CP-5 (0.141 mmol/g) > β-CD/PAA 1:10 (0.111 mmol/g) > β-CD/PAA 1:5 (1.104 mmol/g) > β-CD/PAA 1:5 at high speed (0.0485 mmol/g) ~ CP-1 (0.0420 mmol/g). It is important to estimate the sorption capacities of copolymers with chloroform from water that involves various THMs because THMs always exist as a mixture in water treatment.

The Q_m values of various THMs are differ among the various copolymers. The overall sorption capacity of the copolymers are distinct when compared with carbonaceous materials such as powdered activated carbon (PAC), commercial carbon nanotubes (CNTs) to various activated carbon fibers (AC-10, AC-15, and AC-20)[28, 29] (*cf.* Table 6.4).

The Sips exponent parameter for the copolymers deviates from unity and indicates the presence of heterogeneous sorption sites, such as the presence of multiple sorption sites. For CD- and CS-based copolymers, the availability of multiple sorption sites is quite variable depending on the structural differences of the copolymer. The potential sorption sites on β-CD-based copolymers are given the inclusion sites provided by the macrocycle cavity of β-CD and the interstitial sites given by the polymeric network of copolymers, and is supported by systematic dye-sorption[13-15] and spectroscopic studies[14]. The available sorption sites for CS based copolymers include the micropore domains of the copolymer framework and the

numerous surface bound PAA sites (-COO^-)[15]. Hydrogen bond donor/ acceptor sites are anticipated for such cross-linked copolymers. The adsorption process is considered as a reversible physisorption process because the process is governed by the intermolecular forces.

Table 6.4. Best-fit Sips model parameters (Q_m, K_s and n_s) for the copolymer materials obtained for the sorption of THMs at ambient pH and 295 K.

CP-1	**Q_m[a]**	**K_S[b]**	**n_s**	**χ^{2}[c]**	**R^2**
Chloroform	0.0420	$2.95x10^3$	3.78	$8.32x10^{-6}$	0.979
BDCM	0.387	17.0	1.72	$6.00x10^{-5}$	0.994
DBCM	0.415	53.9	1.69	$1.40x10^{-5}$	0.990
Bromoform	0.440	375	2.04	$2.60x10^{-4}$	0.987
CP-5					
Chloroform	0.141	174	2.41	$4.00x10^{-5}$	0.988
BDCM	0.119	$3.46x10^3$	4.91	$6.00x10^{-5}$	0.982
DBCM	0.0684	144	1.95	$3.00x10^{-5}$	0.980
Bromoform	0.0522	$4.76x10^3$	2.77	$5.07x10^{-6}$	0.990
β-CD/PAA 1:5					
Chloroform	0.104	36.5	1.80	$1.54x10^{-7}$	1.00
BDCM	0.277	99.8	2.01	$6.31x10^{-6}$	0.999
DBCM	0.643	7.47	1.14	$1.10x10^{-4}$	0.994
Bromoform	1.07	6.33	1.09	$3.60x10^{-4}$	0.990
β-CD/PAA 1:5 at high speed					
Chloroform	0.0485	$2.23x10^3$	4.15	$2.00x10^{-5}$	0.974
BDCM	0.0712	94.0	1.47	$3.59x10^{-7}$	1.00
DBCM	0.0745	50.3	1.22	$8.13x10^{-6}$	0.994

Bromoform	0.0786	$2.71x10^{3}$	2.17	$3.69x10^{-6}$	0.999
β-CD/PAA 1:10					
Chloroform	0.111	2.63	0.515	$1.95x10^{-6}$	0.996
BDCM	0.184	6.83	1.29	$3.00x10^{-5}$	0.986
DBCM	0.116	81.8	1.78	$8.00x10^{-5}$	0.956
Bromoform	0.157	19.1	1.50	$5.00x10^{-5}$	0.985
SCl-5					
Chloroform	0.287	42.1	1.53	$3.10x10^{-4}$	0.971
BDCM	0.153	$6.19x10^{3}$	3.39	$7.00x10^{-5}$	0.990
DBCM	0.119	$5.56x10^{3}$	3.07	$1.19x10^{-6}$	0.991
Bromoform	0.0807	$6.78x10^{6}$	4.97	$2.00x10^{-5}$	0.986
SCl-10					
Chloroform	0.248	24.7	0.728	$2.80x10^{-4}$	0.951
BDCM	0.155	$5.84x10^{4}$	3.54	$1.10x10^{-4}$	0.983
DBCM	0.140	$9.64x10^{4}$	3.63	$4.00x10^{-5}$	0.990
Bromoform	0.116	$1.46x10^{6}$	4.40	$2.00x10^{-5}$	0.995
AC					
Chloroform	0.261	3.93	0.973	$6.00x10^{-5}$	0.978
BDCM	0.138	$2.39x10^{3}$	2.71	$5.00x10^{-5}$	0.982
DBCM	0.142	$1.45x10^{4}$	2.79	$3.00x10^{-5}$	0.991
Bromoform	0.141	$2.11x10^{3}$	3.35	$1.00x10^{-5}$	0.990
$Q_{m,L}$ [d]	PAC	CNTs	ACF A-10	ACF A-15	ACF A-20
Chloroform	0.0101	0.0202	0.0135	0.00804	0.00578
BDCM	0.0103	0.00751	0.00611	0.00391	0.00305
DBCM	0.0105	0.00518	0.0352	0.00184	0.0127
Bromoform	0.0109	0.00364	0.0380	0.0386	0.0255

[a] Q_m, (mmol/g)

[b] K_{Sips}, (L/mmol)

[c] χ^2, Chi-square distribution

[d] $Q_{m,L}$, Q_m values from literature[28, 29], converted to (mmol/g) for comparison

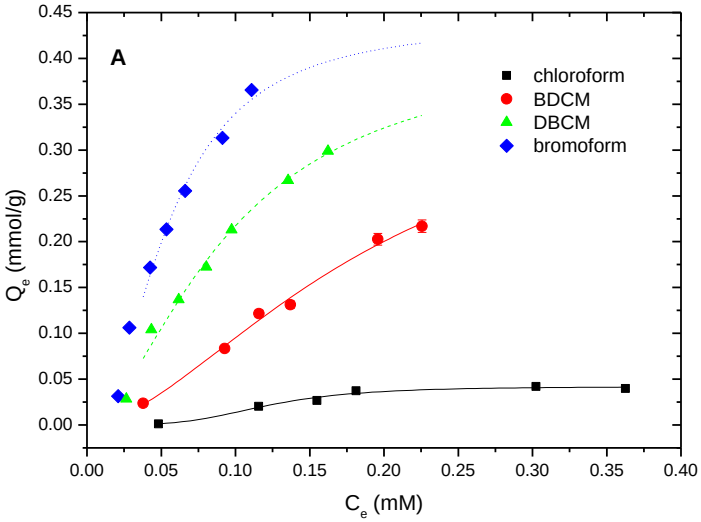

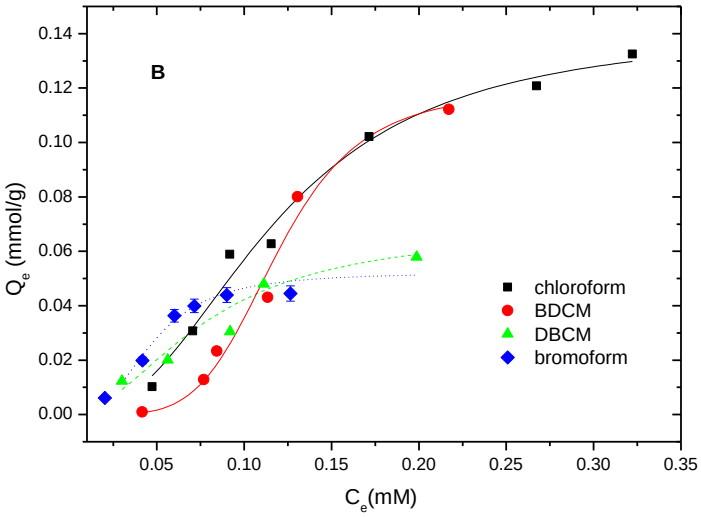

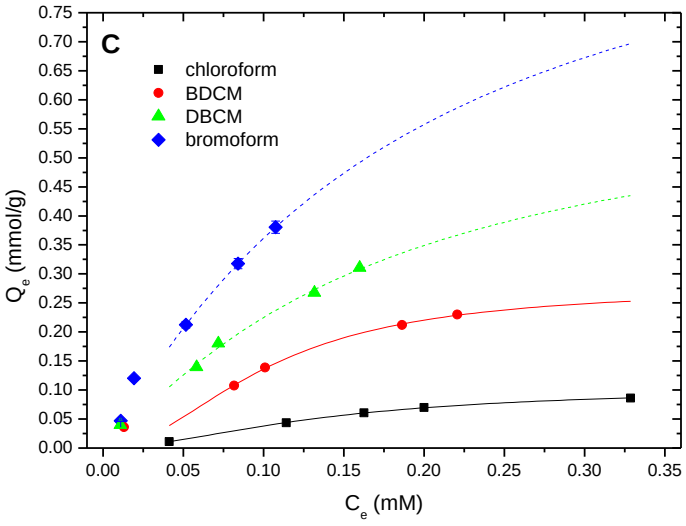
C
chloroform
BDCM
DBCM
bromoform
Qe (mmol/g)
Ce (mM)
0.00
0.05
0.10
0.15
0.20
0.25
0.30
0.35
0.40
0.45
0.50
0.55
0.60
0.65
0.70
0.75

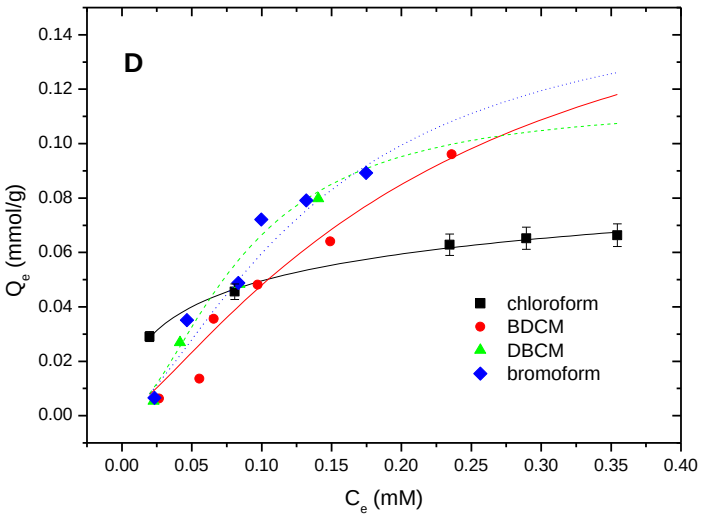
D
chloroform
BDCM
DBCM
bromoform
Qe (mmol/g)
Ce (mM)
0.00
0.02
0.04
0.06
0.08
0.10
0.12
0.14
0.35
0.40

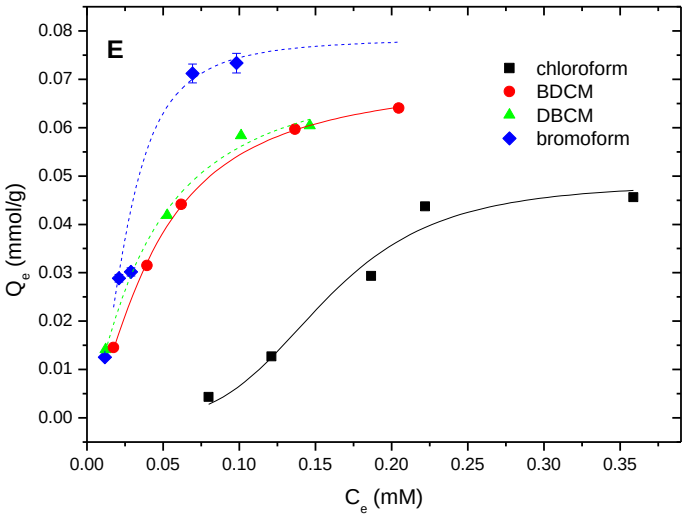
E
chloroform
BDCM
DBCM
bromoform
Qe (mmol/g)
Ce (mM)
0.00
0.01
0.02
0.03
0.04
0.05
0.06
0.07
0.08
0.00
0.05
0.10
0.15
0.20
0.25
0.30
0.35

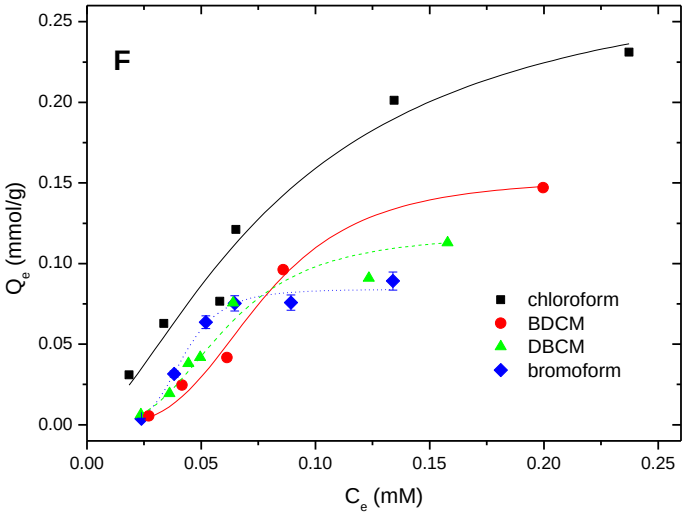
F
chloroform
BDCM
DBCM
bromoform
Qe (mmol/g)
Ce (mM)
0.00
0.05
0.10
0.15
0.20
0.25
0.00
0.05
0.10
0.15
0.20
0.25

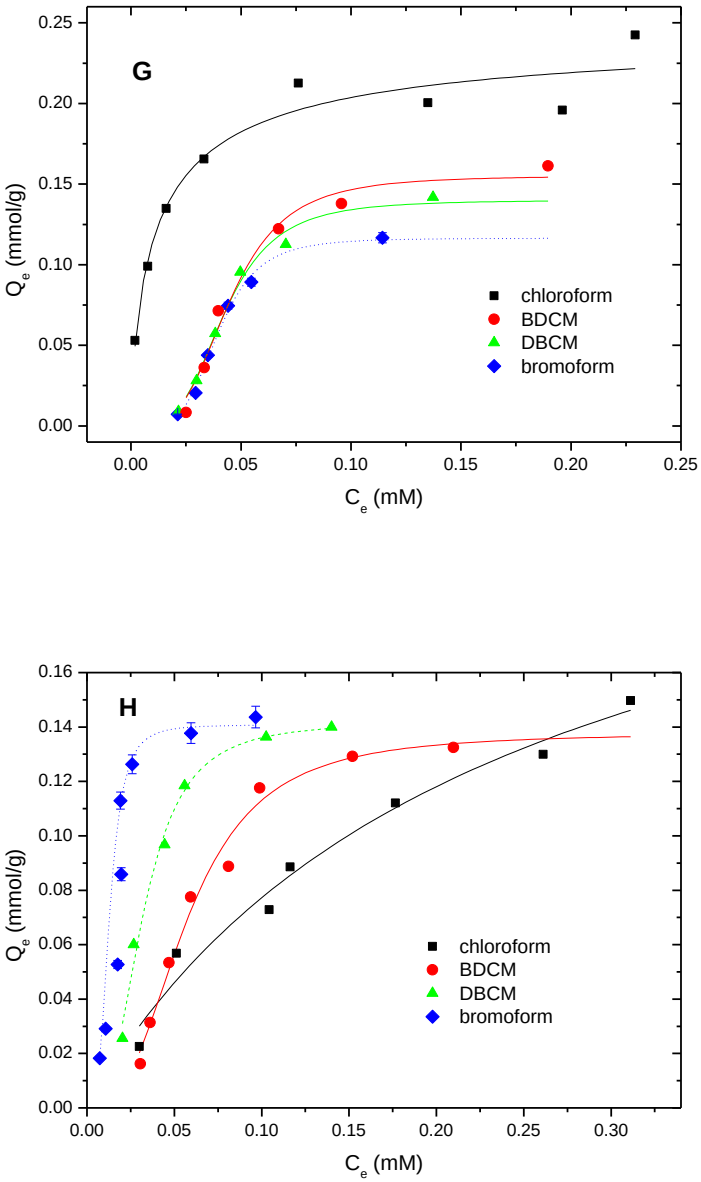

Figure 6.3. Sorption isotherms for copolymers with THMs at ambient pH and 295K; A) CP-1, B) CP-5, C) β-CD/PAA 1:5, D) β-CD /PAA 1:5 at high speed, E) β-CD/PAA 1:10, F) SCl-5, G) SCl-10, and H) AC. The *best-fit* results were obtained using the Sips model as shown by the lines through the data points (*cf*. eqn 6.3).

Table 6.5. Molecule properties of THMs calculated by Hartree-fock model (vacumm) using Spartan 08' v1.2.0.

THMs	Volume (Å)	d_s[a] (Å)	Dipole moment (Å)	V_m[b] (mL/mol)	d[c] (Å)
Chloroform	74.9	5.23	1.40	80.5	6.34
DBCM	79.4	5.33	1.35	82.7	6.40
BDCM	83.9	5.43	1.23	85.0	6.46
Bromoform	88.3	5.53	1.03	89.0	6.56

[a] d_s, van der Waals diameters calculated by Spartan.

[b] Molar volume, calculated by $V_m=M_w/\rho$, where M_w is molecular weight and ρ is density.

[c] Molecule diameter, the radius if molecule was calculated by V_m and $V=V_m/N_A=4/3\pi r^3$, assuming THM molecules in a shape of sphere (where $\pi=3.14$, $N_A=6.02214x10^{23}$).

6.4. Conclusion

In this work, a systematic sorption study of THMs in spiked water samples with synthetically engineered copolymers is reported. The sorption properties of these tunable copolymer sorbents containing either β-CD or CS were evaluated with a mixture of in aqueous solution at ambient pH and 295K using GC-ECD using a direct analysis injection method. The Sips model provided reliable estimates of the monolayer sorption capacity of the copolymers with chloroform (0.0485-0.287 mmol/g); DBCM (0.0712-0.277 mmol/g); BDCM (0.0684-0.387mmol/g); and bromoform (0.0522-1.07 mmol/g). The copolymers show highly relative uptake selectivity with various THMs due to the distinct physiochemical properties of the synthetically engineered adsorbents. The development of carbohydrate-based copolymer materials with tunable physicochemical properties represents a novel and versatile approach to controllably remove THMs from contaminated water supplies. The materials described herein have significant potential as sorbents for the removal of halomethane-based contaminants. Further research is to understand the molecular

selectivity of such copolymers sorbent with real water samples. These materials can be further employed in the rural remote areas for drinking water treatment as a sorbent material. According the type of halomethane contaminants, a single copolymer or a mixture of copolymers can be applied as a filter-system to upgrade the level of the water treatment.

6.5. Acknowledgments

The authors wish to acknowledge the Natural Sciences and Engineering Research Council of Canada (NSERC), the Canada Foundation for Innovation (CFI), and the University of Saskatchewan for the support of this research. Rui Guo gratefully acknowledges NSERC for a PhD scholarship through the NSERC CREATE-HERA program.

6.6. References.

(1) Calderon, R. L. *Food and Chemical Toxicology* **2000**, *38, Supplement 1*, S13-S20.

(2) Rook, J. J. *Water Treatment and Examination* **1974**, *23*, 234-243.

(3) Christman, R.; Norwood, D.; Millington, D.; Johnson, J.; Stevens, A. *Environ. Sci. Technol.* **1983**, *17*, 625-628.

(4) WHO (1998), Trihalomethanes in Drinking-water: Background document for development of WHO Guidelines for Drinking-water Quality.

(5) Mabey, D. M. Aquatic fate process data for organic priority pollutants. **1982**, *(EPA 4014-81-PB87-16909).*

(6) SRC (2008), Physprop Database. Syracuse Research Corporation. Available from http://www.syrres.com/esc/physdemo.htm.

(7) Health Canada，2011. Guidelines for Canadian Drinking Water Quality: Guildline Technical Document. (accessed 06/24, 2012) .

(8) Carpi, M.; Zufall, C. *Lc Gc N. Am.* **2003**, 88-91.

(9) Kramer, M.; Lynch, C.; Isacson, P.; Hanson, J. *Epidemiology* **1992**, *3*, 407-413.

(10) Clesceri, L. S.; Greenberg, A. E.; Eaton, A. D. Trihalomethanes and Chlorinated Organic Solvents Standard Methods for the Examination of Water and Wastewater (APHA, AWWA and WEF) (U.S. EPA, Washiington, D. C. Method 6232, 20th ed. 1998).

(11) http://www.allaboutwater.org/filtration.html. (accessed 01/28, 2013).

(12) Ozcan, A.; Ozcan, A. *J. Colloid Interface Sci.* **2004**, *276*, 39-46.

(13) Guo, R.; Wilson, L. D. *J. Appl. Polym. Sci.* **2012**, *125*, 1841-1851.

(14) Wilson, L. D.; Guo, R. *J. Colloid Interface Sci.* **2012**, *387*, 250-261.

(15) Guo, R.; Wilson, L. D. *J. Colloid Interface Sci.* **2012**, *388*, 225-234.

(16) Bender, M. L.; Komi yam, M. In *Cyclodextrin Chemistry;* Springer verlag.: New York, 1977.

(17) Jang, J. S.; Bae, J. *Macromol. Rapid Commun.* **2005**, *26*, 1320-1324.

(18) van de Manakker, F.; Vermonden, T.; van Nostrum, C. F.; Hennink, W. E. *Biomacromolecules* **2009**, *10*, 3157-3175.

(19) Dumitriu, S., Ed.; In *Polysaccharides: Structural Diversity and Functional Versatility.* 2005.

(20) Pfaender, F. K.; Jonas, R. B.; Stevens, A. A.; Moore, L.; Hass, J. R. *Environ. Sci. Technol.* **1978**, *12*, 438-441.

(21) Health Canada **1995**, Environmental and work place health: Trihalomethane.

(22) Sips, R. *J. Am. Chem. Soc.* **1948**, *125*, 6452.

(23) Harrism, D. C., Ed.; In *Quantitative chemical analysis;* Freeman: United State, 2007 .

(24) Gelb, R. I.; Schwartz, L. M.; Cardelino, B.; Fuhrman, H. S.; Johnson, R. F.; Laufer, D. A. *J. Am. Chem. Soc.* **1981**, *103*, 1750-1757.

(25) Gerasimowicz, W. V.; Wojcik, J. F. *Bioorg. Chem.* **1982**, *11*, 420-427.

(26) Connors, K. A. *Chem. Rev.* **1997**, *97*, 1325-1358.

(27) Akesson, J.; Sundborg, O.; Wahlstrom, O.; Schroder, E. *J. Chem. Phys.* **2012**, *137*, 174702.

(28) Lu, C.; Chung, Y.; Chang, K. *Water Res.* **2005**, *39*, 1183-1189.

(29) Nakamura, T.; Kawasaki, N.; Araki, M.; Yoshimura, K.; Tanada, S. *J. Environ. Sci. Health Part A-Toxic/Hazard. Subst. Environ. Eng.* **2001**, *36*, 1303-1310.

CHAPTER 7

7. Conclusions and Future Work

7.1. Conclusions

The objectives of the research were successfully achieved by the preparation of a series of synthetically engineered polysaccharide-based (*e.g.*, β-CD or CS) copolymers. The materials are considered as "*green adsorbents*" suitable for water filtration as evidenced by their remarkable and selective adsorption properties with THMs in aqueous solution. The chapters included in this thesis are arranged based on the logical division between each sub-project from published studies and the overall objectives of research (*cf.* Scheme 7.1).

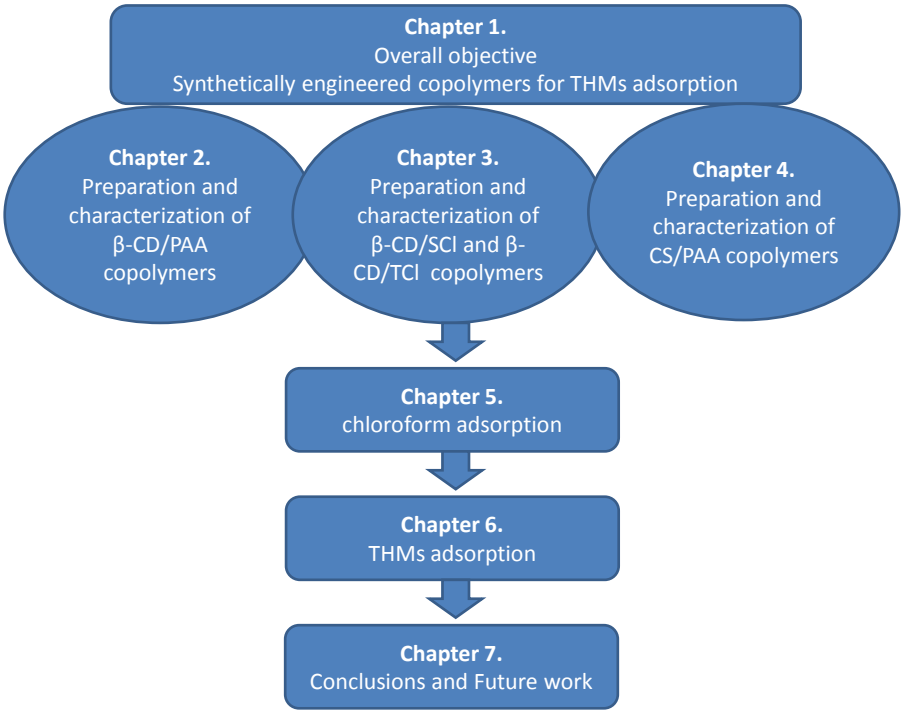

Scheme 7.1. Organization of the content of the PhD thesis.

The synthesis and characterization of copolymers were introduced in Chapters 2-4. The physiochemical properties of copolymers are unique and tunable for particular molecular adsorbates by controlled synthetic conditions (*e.g.*, type of polysaccharide, cross-linker, reagent ratios, solvent, and mixing speeds). For example, β-CD/PAA copolymers required w/o micro-emulsion-evaporation methods and CS/PAA copolymers involved the use of an ionic gelation method. A dropping method employed a drop-wise addition of reagents (cross-linkers) into the solution of polysaccharides to yield products with smaller particle size and larger surface area. Various polymerization methods were studied for copolymer preparation: a conventional "*bottom-up*" method for polyester materials and a "*grafted on*" method for grafted polyester and grafted polyamide copolymers.

The use of various techniques, such as, FT-IR, TGA, DSC, SEM, elemental (C and H) analyses, NMR spectroscopy, and gas/dye adsorption methods, provided structural and physicochemical characterization of the copolymer materials. Nitrogen adsorption provided information on the surface area and pore structure characteristics of the copolymer and the polysaccharide starting materials in solid state. The sorption properties of the copolymers in aqueous solution were studied using various dye probes (*e.g.*, PNP and MB) by UV–Vis spectrophotometry. The copolymers showed markedly different sorptive uptake properties with dye probes in accordance with their composition, surface area, and pore structure characteristics. Variable surface properties of the copolymer adsorbents were observed for their solid-gas and solid-solution isotherms due to the different surface chemistry of the copolymers. The sorption isotherm parameters were evaluated with various models (*e.g.*, Langmuir, BET, Freundlich and Sips); where the Sips isotherm showed the most favourable agreement with the experimental results.

The sorbent SA values (12.0-331 m^2/g) and the sorption capacity (Q_m=0.359-2.20 mmol/g at pH=4.6; Q_m=0.0701-0.191 mmol/g at pH=10.3) were estimated for the β-CD/PAA copolymers with PNP in aqueous solution. The uptake of PNP (Q_m) by the polyester copolymers (*e.g.*, β-CD/SCl and β-CD/TCl copolymers) in aqueous solution varied from 0.221 to 0.352 mmol/g and the estimated SA values in aqueous solution

ranged from 50.9 to 33.3 m^2/g. The heterogeneous adsorption behaviour observed for grafted polyester and polyester copolymers using the dye adsorption method were further examined by ^1H NMR spectroscopy for polyester copolymers with low linker content (*e.g.*, SCl or TCl). The results provide support for two distinct types of sorption sites on the copolymer surface for PNP: β-CD inclusion sites and non-inclusion (*i.e*. interstitial) linker domains. Inclusion complexes are firstly formed between PNP and the β-CD inclusion sites of the copolymer sorbent; thereafter, PNP is adsorbed onto the linker domains in the polymeric framework. The sorbent SA values (271 and 943 m^2/g) and the sorption capacity (Q_m=1.03 and 3.59 mmol/g) were estimated for the CS-PAA copolymer/MB systems in aqueous solution. The proteinaceous CS-PAA copolymers showed diverse interactions with MB that range from *physisorption-like* to *chemisorption-like* behaviour, in accordance with the composition, surface area, and pore structure characteristics of the sorbent materials. Heterogeneous adsorption was also observed for these CS-PAA copolymers with MB where the micropore domains of the copolymer framework and the numerous surface bound PAA sites ($-COO^-$) represent two of the main sorption sites. The switchable adsorption properties of these "*smart materials*" are observed upon external environmental changes as evidenced by the "*pH switchable*" desorption of dye species by altering the pH of the solution.

The synthetically engineered copolymer sorbent materials described in Chapters 2-4 were evaluated for their adsorption properties with chloroform in aqueous solution. The DAI method with GC-ECD detection enabled quantitative detection of chloroform in water. A preliminary adsorption study and kinetic study of chloroform provided the information to establish the experimental protocol for the sorption study. The sorption parameters were evaluated using the Sips model. The sorption capacity (Q_m) values of chloroform for these synthetically engineered copolymers for similar conditions ranged from 0.00335-1.70 mmol/g. The relative ordering of the Q_m values was observed: β-CD/PAA 1:5 > SCl-5 > SCl-10 ~ CP-1 > β-CD/PAA 1:10 > CP-5 > AC > β-CD/PAA 1:5 at high speed.

Chapter 6 describes an extension of the sorption study presented in Chapter 5 and

outlines the sorption properties of mixtures of THMs in water with copolymers. The copolymers showed distinct adsorption capacities to THMs: chloroform (0.0485-0.287 mmol/g); DBCM (0.0712-0.277 mmol/g); BDCM (0.0684-0.387mmol/g); and bromoform (0.0522-1.07 mmol/g). The copolymers showed relatively high selectivity toward individual components of THMs due to their variable molecular size and polarizaliby. The copolymers showed favorable adsorption (*e.g.*, β-CD/PAA 1:5, CP-1) and each type of polysaccharide (*e.g.*, β-CD and CS) copolymers displays great potential for the removal of halomethane-based contaminants. The development of carbohydrate-based copolymer materials with tunable physicochemical properties represents a novel and versatile approach for the controlled removal of THMs from contaminated water supplies and this research is anticipated to contribute further to improved sorbent technology that addresses water quality and public health concerns with safe drinking water. These synthetically engineered copolymer materials are anticipated to be employed in the rural or remote areas where such point-of-use drinking water treatment is required. According to the type of halomethane contaminants, a single copolymer or a mixture of copolymers may be applied as a multi-component filter-system for advanced water treatment systems.

As a summary of the sorption behaviour displayed by the copolymers with THMs, the Q_m value is a soprtion parameter dependent on several variables: Q_m=f (x, y, z, z'), where x represents the nature of polysaccharide component (*e.g.*, CS or β-CD); y represents the nature of cross-linker; z represents the cross-linking density controlled by synthesis conditions, such as, the ratio between polysaccharides and cross-linkers and mixing speed of w/o micro-emulsion; z' represents the nature of the target guest molecule, (*e.g.*, size and polarizability). Each of the various terms (*i.e.* x, y, z, z') plays a role in the overall sorption properties, so the rationale design of synthetically engineered copolymers toward target guest molecule is essential in adsorption-based contaminant removal.

7.2. Future Work

These novel carbohydrate-based copolymers with tunable physicochemical properties represent significant potential as adsorbent materials for the removal of halomethane-based contaminants; however, there are knowledge gaps which need to be addressed for their practical usage. Further research on aspects of the kinetic and thermodynamic studies, surface chemistry studies, and desorption studies are required to understand the factors that control the sorption process. Moreover, there is a need to test the sorptive properties of the materials described in this study toward different types of targeted contaminants.

7.2.1. Kinetic and Thermodynamic Studies

The objectives of the proposed research are to investigate the thermodynamic sorption properties and some aspects of the kinetics of adsorption between copolymer/THMs in aqueous solution. A detailed study of the sorption mechanism can help to address the factors governing the adsorption process and the energetics of the sorption process.

The THMs showed favorable adsorption with both β-CD- and CS-based copolymers, such as, β-CD/PAA 1:5 and CP-1. The classical sorption studies at various temperatures may provide further thermodynamic insight of the sorption process; the isosteric heat (ΔH_{ads}) of adsorption[1] is suggested for future research. ΔH_{ads} can be estimated by assuming that the equilibrium constant (K) is dependent on temperature (T) according to the van't Hoff equation shown in Eqn. 7.1, where θ represents a well-defined surface coverage value shown in Eqn. 7.2.

$$\left(\frac{\partial \ln K}{\partial T}\right)_{\theta} = \frac{\Delta H_{ads}}{RT^2} \qquad (7.1)$$

$$\theta = \frac{Q_e}{Q_m} \qquad (7.2)$$

ΔH_{ads} enables the determination of ΔS and ΔG according to Eqn. 7.3:

$$\Delta G = -RT \ln K = \Delta H - T\Delta S \qquad (7.3)$$

The adsorption process is governed by numerous factors such as solute-solute and

solute-solvent interactions. Molecular recognition which relates to the specific interaction between two or more molecules through noncovalent bonding, such as, H-bonding, metal coordination, hydrophobic effects, van der Waals forces, π-π interactions, electrostatic interactions is an important consideration for the development of materials with molecular selective adsorption properties[2]. The thermodynamic contributions for the adsorption process between copolymers and adsorbates can be expressed by Eqn. 7.4[3, 4].

$$\Delta G_{bind} = \Delta G_{t+r} + \Delta G_{vib} + \Delta G_r + \Delta G_h + \Delta G_{vdw} + \sum \Delta G_p \quad (7.4)$$

Where, the Gibbs energy changes are determined by: ΔG_{t+r}, translational and rotational; ΔG_{vib}, residual soft vibration modes; ΔG_r, restriction of rotors upon complexation; ΔG_h, hydrophobic interaction; ΔG_{vdW}, the van der Waals interaction; $\sum \Delta G_p$, the sum of interacting polar group contributions. The ΔG_{t+r}, ΔG_r and ΔG_{vib} are functions of adsorbate and temperature, which are inherent to the adsorption process of copolymer/THMs systems. ΔG_{vdW} is dependent on a composite of the nature of adsorbates (*e.g.*, molecular weight, polarizability, *etc*.) and the degree of solvation effects.

Generally, hydrophobic interactions between two apolar molecules at room temperature are described as entropy-driven processes[5]; while the other interactions are considered as more enthalpy-driven in nature. As a result, if $|\Delta H| < |T\Delta S|$, the thermodynamic process may be more entropy-driven and suggests that the hydrophobic effect is a dominant mechanism. Alternatively, the electrostatic interaction and other non-covalent interactions may be the driving force for the adsorption process. Furthermore, the value of ΔG for the adsorption process may reveal which copolymers favour sorption of the component THMs; contributing to a further understanding of molecular selective behaviour of such sorbent materials.

Preliminary kinetic studies of the adsorption of chloroform were carried out (*cf*. Chapter 5) using β-CD/PAA 1:5 and CP-1 copolymers at room temperature. More detailed kinetic studies at various temperatures with various THMs (*e.g.*, bromoform or BDCM) are recommended. This will contribute to a further understanding of the

adsorption mechanism of THMs and for the practical use of such copolymer adsorbents in real water environments. Variable temperature sorption studies would contribute to a further understanding of the adsorption mechanism and this could be accomplished using a GC-MS based head-space analysis method[6]. This is suggested since THMs are VOCs and the experimental operation at higher temperatures requires precautions to maintain the accuracy of the experiment.

7.2.2. Surface Chemistry Study

Adsorption happens at the copolymer surface where the nature of the surface (*e.g.*, hydrophilic and hydrophobic sites) is important to understand the adsorption mechanism. The surface tension and/or flotation experiments[7, 8] of the copolymers in water are recommended as further mechanism studies.

7.2.3. Desorption Experiment

The adsorption process for the carbohydrate copolymer/THM systems represents a reversible physisorption process. In order to successfully design *"smart materials"* for THMs removal as reusable adsorbents, desorption experiments are required. An understanding of the process will contribute to the practical application of the copolymers for water treatment industrial processes.

Since the THMs are VOCs, a temperature-dependent desorption is a potentially feasible and efficient method. The design of a simplified experimental set-up is shown in Scheme 7.2. The apparatus is similar to a vacuum dryer. Because the copolymers are relatively stable according to their TGA data, the copolymers can be heated at particular pressure conditions to cause separation of THMs from adsorbents. The experimental temperature and pressure used for desorption can be determined by various methods, such as, temperature programmed desorption (TPD) and TGA. In addition, the temperature and pressure required for the desorption experiment are also closely related to the thermodynamic properties of the copolymers and can be estimated from the thermodynamic results. A mixture of THMs will be collected after desorption experiment; further distillation can be conducted to isolate the individual

halomethane fractions. There are several reasons to carry out this temperature-dependent desorption experiment as a future study; 1) determine the desorption efficiency for application as reusable adsorbents; 2) collect THMs to prevent the chemicals from atmospheric contamination, minimize losses, and recycle the chemicals for future value-added processes.

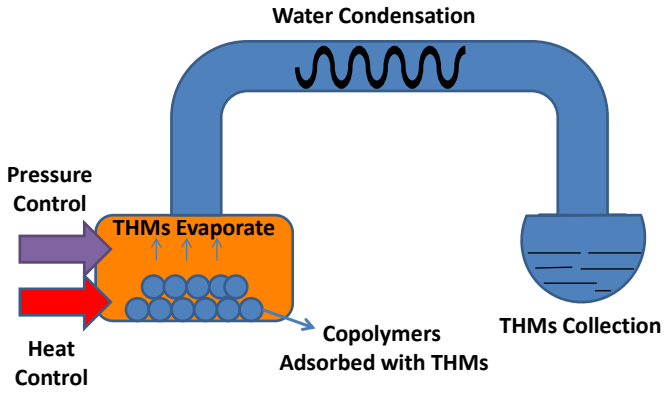

Scheme 7.2. A schematic outline of the design of a simplified experimental set-up for the time-based desorption experiment.

7.2.4. Further Sorption Experiments

As good adsorbent materials, the copolymers are expected to have great adsorption capacities toward various types of contaminants in water environments. The organic precursors of THMs (*e.g.*, haloacetic acids (HAAs)[9, 10] and dissolved organic carbons (DOCs)[9, 11, 12]) represent an additional category of adsorbates that could be studied in future adsorption studies.

7.3. References

(1) Garcia-Zubiri, I. X.; Gonzalez-Gaitano, G.; Isasi, J. R. *J. Colloid Interface Sci.* **2007**, *307*, 64-70.

(2) Baron, R.; Setny, P.; McCammon, J. A. *J. Am. Chem. Soc.* **2010**, *132*, 12091-12097.

(3) Nicholls, I. A. *Chem. Lett.* **1995**, 1035-1036.

(4) Nicholls, I. A.; Adbo, K.; Andersson, H. S.; Andersson, P. O.; Ankarloo, J.; Hedin-Dahlstrom, J.; Jokela, P.; Karlsson, J. G.; Olofsson, L.; Rosengren, J.; Shoravi, S.; Svenson, J.; Wikman, S. *Anal. Chim. Acta* **2001**, *435*, 9-18.

(5) Tadashi, M., Ed.; In *Application of Thermodynamics to Biological and Materials Science. Chapter 4. Thermodynamics of Supramolecular Structure Formation in Water;* InTech: 2011.

(6) Rook, J. J. *Water Treatment and Examination* **1974**, *23*, 234-243.

(7) Gutierrez-Rodriguez, J. A.; Aplan, F. F. *Colloids and Surfaces* **1984**, *12*, 27-51.

(8) Peng, F. *Energy Fuels* **1996**, *10*, 1202-1207.

(9) Babi, K. G.; Koumenides, K. M.; Nikolaou, A. D.; Mihopoulos, N. S.; Tzoumerkas, F. K.; Makri, C. A.; Lekkas, T. D. *Proceedings of the 8th International Conference on Environmental Science and Technology, Vol A, Oral Presentations* **2003**, 52-63.

(10) Nikolaou, A.; Golfinopoulos, S.; Kostopoulou, M.; Lekkas, T. *Water Res.* **2002**, *36*, 1089-1094.

(11) Black, B.; Harrington, G.; Singer, P. *J. Am. Water Work Assoc.* **1996**, *88*, 40-52.

(12) Edzwald, J.; Becher, W.; Wattier, K. *J. Am. Water Work Assoc.* **1985**, *77*, 122-132.